

ISSN 1854-6250

APEM
journal

Advances in Production Engineering & Management

Volume 16 | Number 4 | December 2021




University of Maribor

Published by CPE
apem-journal.org

Advances in Production Engineering & Management

Identification Statement

| | |
|---|---|
|  | ISSN 1854-6250 Abbreviated key title: Adv produc engineer manag Start year: 2006 ISSN 1855-6531 (on-line) |
|  | Published quarterly by Chair of Production Engineering (CPE), University of Maribor Smetanova ulica 17, SI – 2000 Maribor, Slovenia, European Union (EU) Phone: 00386 2 2207522, Fax: 00386 2 2207990 Language of text: English |
| | APEM homepage: apem-journal.org University homepage: www.um.si |

APEM Editorial

Editor-in-Chief

Miran Brezocnik

editor@apem-journal.org, info@apem-journal.org
University of Maribor, Faculty of Mechanical Engineering Smetanova ulica 17, SI – 2000 Maribor, Slovenia, EU

Desk Editor

Martina Meh

desk1@apem-journal.org

Janez Gotlih

desk2@apem-journal.org

Website Technical Editor

Lucija Brezocnik

desk3@apem-journal.org

Editorial Board Members

Eberhard Abele, Technical University of Darmstadt, Germany
Bojan Acko, University of Maribor, Slovenia
Joze Balic, University of Maribor, Slovenia
Agostino Bruzzone, University of Genoa, Italy
Borut Buchmeister, University of Maribor, Slovenia
Ludwig Cardon, Ghent University, Belgium
Nirupam Chakraborti, Indian Institute of Technology, Kharagpur, India
Edward Chlebus, Wroclaw University of Technology, Poland
Igor Drstvensek, University of Maribor, Slovenia
Illes Dudas, University of Miskolc, Hungary
Mirko Ficko, University of Maribor, Slovenia
Vlatka Hlupic, University of Westminster, UK
David Hui, University of New Orleans, USA
Pramod K. Jain, Indian Institute of Technology Roorkee, India
Isak Karabegović, University of Bihać, Bosnia and Herzegovina

Janez Kopac, University of Ljubljana, Slovenia
Qingliang Meng, Jiangsu University of Science and Technology, China
Lanndon A. Ocampo, Cebu Technological University, Philippines
Iztok Palcic, University of Maribor, Slovenia
Krsto Pandza, University of Leeds, UK
Andrej Polajnar, University of Maribor, Slovenia
Antonio Pouzada, University of Minho, Portugal
R. Venkata Rao, Sardar Vallabhbhai National Inst. of Technology, India
Rajiv Kumar Sharma, National Institute of Technology, India
Katica Simunovic, J. J. Strossmayer University of Osijek, Croatia
Daizhong Su, Nottingham Trent University, UK
Soemon Takakuwa, Nagoya University, Japan
Nikos Tsourveloudis, Technical University of Crete, Greece
Tomo Udiljak, University of Zagreb, Croatia
Ivica Veza, University of Split, Croatia



Subsidizer: The journal is subsidized by Slovenian Research Agency



Creative Commons Licence (CC): Content from published paper in the APEM journal may be used under the terms of the Creative Commons Attribution 4.0 International Licence (CC BY 4.0). Any further distribution of this work must maintain attribution to the author(s) and the title of the work, journal citation and DOI.

Statements and opinions expressed in the articles and communications are those of the individual contributors and not necessarily those of the editors or the publisher. No responsibility is accepted for the accuracy of information contained in the text, illustrations or advertisements. Chair of Production Engineering assumes no responsibility or liability for any damage or injury to persons or property arising from the use of any materials, instructions, methods or ideas contained herein.

Published by CPE, University of Maribor.

Advances in Production Engineering & Management is indexed and abstracted in the **WEB OF SCIENCE** (maintained by **Clarivate Analytics**): **Science Citation Index Expanded**, **Journal Citation Reports** – Science Edition, **Current Contents** – Engineering, Computing and Technology • **Scopus** (maintained by **Elsevier**) • **Inspec** • **EBSCO**: Academic Search Alumni Edition, Academic Search Complete, Academic Search Elite, Academic Search Premier, Engineering Source, Sales & Marketing Source, TOC Premier • **ProQuest**: CSA Engineering Research Database – Cambridge Scientific Abstracts, Materials Business File, Materials Research Database, Mechanical & Transportation Engineering Abstracts, ProQuest SciTech Collection • **TEMA (DOMA)** • The journal is listed in **Ulrich's** Periodicals Directory and **Cabell's** Directory



University of Maribor
Chair of Production Engineering (CPE)

Advances in Production Engineering & Management

Volume 16 | Number 4 | December 2021 | pp 389–518

Contents

| | |
|--|------------|
| Scope and topics | 392 |
| A deep learning-based worker assistance system for error prevention: Case study in a real-world manual assembly | 393 |
| Riedel, A.; Gerlach, J.; Dietsch, M.; Herbst, S.; Engelmann, F.; Brehm, N.; Pfeifroth, T. | |
| Optimal path planning of a disinfection mobile robot against COVID-19 in a ROS-based research platform | 405 |
| Banjanovic-Mehmedovic, L.; Karabegovic, I.; Jahic, J.; Omercic, M. | |
| Using augmented reality devices for remote support in manufacturing: A case study and analysis | 418 |
| Buń, P.; Grajewski, D.; Górski, F. | |
| The impact of the collaborative workplace on the production system capacity: Simulation modelling vs. real-world application approach | 431 |
| Ojstersek, R.; Javernik, A.; Buchmeister, B. | |
| A multi-criteria decision-making in turning process using the MAIRCA, EAMR, MARCOS and TOPSIS methods: A comparative study | 443 |
| Trung, D.D.; Thinh, H.X. | |
| Molecular-dynamics study of multi-pulsed ultrafast laser interaction with copper | 457 |
| Yin, C.P.; Zhang, S.T.; Dong, Y.W.; Ye, Q.W.; Li, Q. | |
| A comparative study of different pull control strategies in multi-product manufacturing systems using discrete event simulation | 473 |
| Xanthopoulos, A.S.; Koulouriotis, D.E. | |
| Latent class analysis for identification of occupational accident casualty profiles in the selected Polish manufacturing sector | 485 |
| Nowakowska, M.; Pajęcki, M. | |
| Impact of Industry 4.0 on decision-making in an operational context | 500 |
| Rosin, F.; Forget, P.; Lamouri, S.; Pellerin, R. | |
| Calendar of events | 515 |
| Notes for contributors | 517 |

Journal homepage: apem-journal.org

ISSN 1854-6250 (print)

ISSN 1855-6531 (on-line)

Published by CPE, University of Maribor.

Scope and topics

Advances in Production Engineering & Management (APEM journal) is an interdisciplinary refereed international academic journal published quarterly by the *Chair of Production Engineering* at the *University of Maribor*. The main goal of the *APEM journal* is to present original, high quality, theoretical and application-oriented research developments in all areas of production engineering and production management to a broad audience of academics and practitioners. In order to bridge the gap between theory and practice, applications based on advanced theory and case studies are particularly welcome. For theoretical papers, their originality and research contributions are the main factors in the evaluation process. General approaches, formalisms, algorithms or techniques should be illustrated with significant applications that demonstrate their applicability to real-world problems. Although the *APEM journal* main goal is to publish original research papers, review articles and professional papers are occasionally published.

Fields of interest include, but are not limited to:

| | |
|--|---|
| Additive Manufacturing Processes | Machine Learning in Production |
| Advanced Production Technologies | Machine-to-Machine Economy |
| Artificial Intelligence in Production | Machine Tools |
| Assembly Systems | Machining Systems |
| Automation | Manufacturing Systems |
| Big Data in Production | Materials Science, Multidisciplinary |
| Block Chain in Manufacturing | Mechanical Engineering |
| Computer-Integrated Manufacturing | Mechatronics |
| Cutting and Forming Processes | Metrology in Production |
| Decision Support Systems | Modelling and Simulation |
| Deep Learning in Manufacturing | Numerical Techniques |
| Discrete Systems and Methodology | Operations Research |
| e-Manufacturing | Operations Planning, Scheduling and Control |
| Evolutionary Computation in Production | Optimisation Techniques |
| Fuzzy Systems | Project Management |
| Human Factor Engineering, Ergonomics | Quality Management |
| Industrial Engineering | Risk and Uncertainty |
| Industrial Processes | Self-Organizing Systems |
| Industrial Robotics | Smart Manufacturing |
| Intelligent Manufacturing Systems | Statistical Methods |
| Joining Processes | Supply Chain Management |
| Knowledge Management | Virtual Reality in Production |
| Logistics in Production | |

A deep learning-based worker assistance system for error prevention: Case study in a real-world manual assembly

Riedel, A.^{a,*}, Gerlach, J.^a, Dietsch, M.^a, Herbst, S.^a, Engelmann, F.^a, Brehm, N.^a, Pfeifroth, T.^a

^aDepartment of Industrial Engineering, Ernst-Abbe University of Applied Sciences, Jena, Germany

ABSTRACT

Modern assembly systems adapt to the requirements of customised and short-lived products. As assembly tasks become increasingly complex and change rapidly, the cognitive load on employees increases. This leads to the use of assistance systems for manual assembly to detect and avoid human errors and thus ensure consistent product quality. Most of these systems promise to improve the production environment but have hardly been studied quantitatively so far. Recent advances in deep learning-based computer vision have also not yet been fully exploited. This study aims to provide architectural, and implementational details of a state-of-the-art assembly assistance system based on an object detection model. The proposed architecture is intended to be representative of modern assistance systems. The error prevention potential is determined in a case study in which test subjects manually assemble a complex explosion-proof tubular lamp. The results show 51 % fewer assembly errors compared to a control group without assistance. Three of the four considered types of error classes have been reduced by at least 42 %. In particular, errors by omission are most likely to be prevented by the system. The reduction in the error rate is observed over the entire period of 30 consecutive product assemblies, comparing assisted and unassisted assembly. Furthermore, the recorded assembly data are found to be valuable regarding traceability and production improvement processes.

ARTICLE INFO

Keywords:

Deep learning;
Machine learning;
Industry 4.0;
Smart manufacturing;
Manual assembly;
Assistance system;
Error prevention;
Object detection

*Corresponding author:

alexander.riedel@eah-jena.de
(Riedel, A.)

Article history:

Received 14 October 2021
Revised 3 December 2021
Accepted 4 December 2021



Content from this work may be used under the terms of the Creative Commons Attribution 4.0 International Licence (CC BY 4.0). Any further distribution of this work must maintain attribution to the author(s) and the title of the work, journal citation and DOI.

1. Introduction

The continuing global trend towards highly customized products, small batch sizes and short product life cycles is leading to a variety of challenges that manufacturing companies have to face [1, 2]. To meet these challenges, manufacturing systems must be designed more flexible both in terms of the production process and the product itself, as well as the deployment of employees. In practice, a flexible product and production means rapidly changing processes to which workers must adapt. However, flexible deployment of employees and tasks reduces the available training time per employee.

For economic and technological reasons, complex products with small batch sizes are preferably produced in a manual assembly environment [3]. However, in this type of production, product quality and assembly time depend heavily on the characteristics of the workers, such as their qualifications, working conditions and experience. The constraints of flexibility can counteract these desired characteristics, as, for example, a short-term temporary worker is not able to acquire many years of experience. At the level of the production process, high product com-

plexity and variance lead to higher cognitive demands on each worker [4]. The resulting combination of limited worker skills and complex tasks causes the need for error preventing assembly assistance systems. These systems, also referred to as Cyber-Physical-Systems (CPS) [5], use sensors to collect data of the assembly, process them and provide visual instructions to the worker [6]. Generally, assembly assistance systems have shown to both reduce the error rate [7] and increase the workers productivity [8]. Methods for analysing worker motions in motion time systems have been recently advanced [9] and might be suitable to give assistance during assembly processes.

Like the workplaces they are used at, these systems need to be flexible and adaptable to a variety of products, processes, and workers. A modular architecture with a central unit and one or more plug-and-play cyber-physical units would meet the requirement for flexibility and adaptability of such systems. The use of deep learning object detection is crucial to the proposed method, as it allows to detect visible assembly errors and the visually observable assembly status at a high accuracy in contrast to traditional computer vision methods [10]. Thus, the accurate detection of every assembly part's position and status at all times can be considered as a crucial task and information source for other assembly assistance modules to work.

In this paper we propose a modular assembly assistance system combining various modules, applied to a complex real-world product on a manual assembly workstation. The system is driven by a deep learning object detection model to detect the assembly status and potential assembly errors from RGB video. The information derived from the object detection unit are used to display the current work instruction, errors, warnings and guarantee full traceability of each work step. The information about the current work step provided by the object detection unit is also used by a pick-by-light module and an electric screwdriver. Additionally, any type of worker assistance module that works on information which can be visually retrieved from the assembly process is attachable to the system. The system architecture is displayed in Fig. 1.

To validate the assumed error prevention potential, we conducted experiments in which test subjects carried out the manual assembly of an explosion-proof tube lamp with and without assembly assistance. The assembly product was provided by the internationally operating company R. Stahl AG for this investigation. Especially in safety-critical areas such as explosion-proof product manufacturing, the risk of assembly errors must be reduced to near zero.

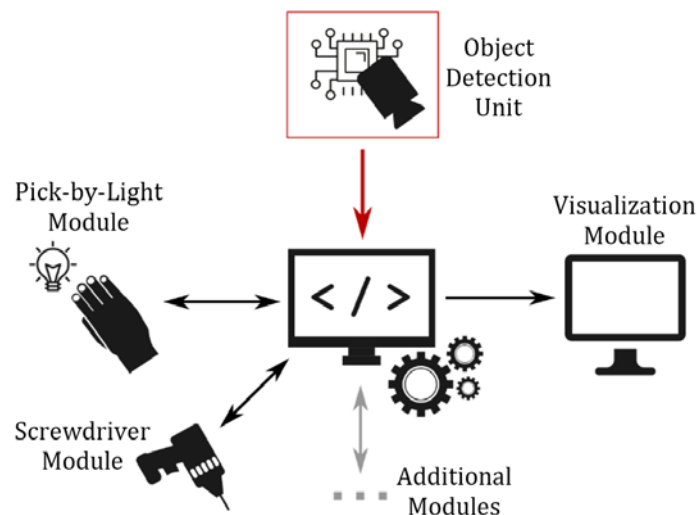


Fig. 1 Schematic architecture of the proposed error preventing assembly assistance system.

The use of object detection in manual assembly and modular assembly assistance systems has been described in literature [11-14]. However, the combination of both, their implementation effort and, most importantly, their quantitative effect on a real-world assembly task, remains mostly unclear. To address this lack of knowledge about modern assembly assistance systems, this work aims to provide:

- Architectural details of a modular assembly assistance system powered by state-of-the-art deep learning-based object detection technologies
- Implementational details of the proposed assistance system
- A quantitative analysis of the error prevention potential based on experiments conducted with test subjects

Related work

The proposed assembly assistance system characterized in Fig. 1 mainly relies on (1) deep learning object detection and (2) a modular approach. Both aspects will be considered and compared to existing methods in literature.

The application of deep learning-based object detection in manual assembly has been widely investigated in terms of feasibility and regarding how the acquired information can be used in the assembly process. The use cases include e.g., counting assembly parts to support the handling process [12], detecting small electrical parts during assembly [15] or recognizing work steps in a virtual reality environment [16]. These approaches underline the purpose and the importance of using advanced object detection in manual assembly, however they are not implementing the method in a productive assembly assistance system or evaluate its benefit. In a real-world scenario, the final goal of applying object detecting in manual assembly tasks would be to increase productivity by reducing the error rate or assembly time. This case study acts as a logical follow-up for many object detection assistance system concept studies by determining the productivity impact of this method.

Fraunhofer IPA propose a multi-modal worker assistance system “MonSiKo” combining 3D object detection, acoustic detection, and motion tracking, collecting data to operate a pick-by-light system and work step detection [17]. The sensor-fusion approach of vision, acoustics and inertial sensing is a reliable source of data but brings an expensive installation and high workplace invasiveness. A qualitative or quantitative analysis of the manual assembly process improvements was not carried out.

Oestreich *et al.* show the quantitative effect of a basic assembly assistance system on the assembly duration during the training period [18]. The proposed system includes digital instruction visualization and a proximity sensor for detecting workpieces. Each completed work step is manually confirmed by the user with the proximity sensor being the only source of indirect sanity checking the assembly process. Although a quantitative user study is conducted, the effect on assembly errors is not evaluated as they can hardly be directly assessed without the use of an object detection method.

Kaczmarek *et al.* present a vision-only approach to monitor the progress in a manual assembly task [19]. By using an RGB-depth camera, different height layers and areas can be defined as regions, where a located object is either assembled or not assembled. The method prevents assembly errors caused by unassembled parts, however the use of hard-coded areas and layers instead of machine learned features raises doubts about the universal and flexible use in a real-world use case.

A study conducted by Faccio *et al.* proposes a more advanced vision-only approach to error and progress monitoring [20]. Here, the workers hand positions are compared to virtual pre-defined three-dimensional control volumes to determine correct or wrong hand positions. The assistance system provides visual feedback based on the hand reaching into the control volumes. In a follow-up work, the authors conduct user studies to compare the assembly durations with and without the assistance system [21]. The proposed system shortens the average assembly duration by 22 %. However, the error reduction rate using the system is not provided. The use of pre-defined control volumes is inflexible in the case of various workers having different types of hand movements. Deep learning object detection methods could provide a sufficient way to directly observe the object status and potential errors.

The case study provided by Rocha *et al.* presents a vision-based assembly assistance system, based on detecting hand movements over control points [22]. The system follows a modular approach, using the collected movement data to determine the components status. Rocha *et al.*

focus on implementational details and data collection rather than on determining error or assembly duration reduction.

The literature review underlines the current research situation, where deep learning-based object detection is underrepresented in assembly assistance systems and their impact on key performance indicators like error rate has hardly been studied. Due to the large variety of assistance systems described in literature, our proposed method will act as a meta-approach of the most advanced and lightweight systems.

2. Materials and methods

To comprehensively perceive the assembly process and simultaneously provide aid to the worker, we chose a vision-only approach. Based on the assembly part's state, a pick-by-light module, an electric screwdriver and an according work instruction is triggered during the assembly process. The product to be assembled is a complex explosion-proof tube lamp which require 34 work steps including plugging, clicking, screwing, and testing operations. To carry out the quantitative error analysis, two groups of 10 participants each assembled the product with and without the assistance system.

2.1 System architecture

The systems individual modules are interconnected via the MQTT network protocol. The key information shared in the Broker/Client architecture is the currently observed workpiece status. This status might be the presence of the workpiece, the absence of a workpiece or a potential faulty assembly. Based on this information, the current work step is derived to present the associated instruction via the visualization module. When detecting a faulty assembly, the visualization module will also present warning messages to the worker. Both the pick-by-light module and the electric screwdriver are activated based on the current work step. For traceability purposes, the grab status and tightening status of the pick-by-light and screwdriver module are published as MQTT messages and stored in a database. Assembly part status messages are stored in a database as well. The complete MQTT messaging scheme is displayed in **Napaka! Vira sklicevanja ni bilo mogoče najti.**

To derive the work step from assembly parts, each work step is mapped to the presence or absence of certain key objects for this respective step. This approach guarantees flexibility in case of changing workflows.

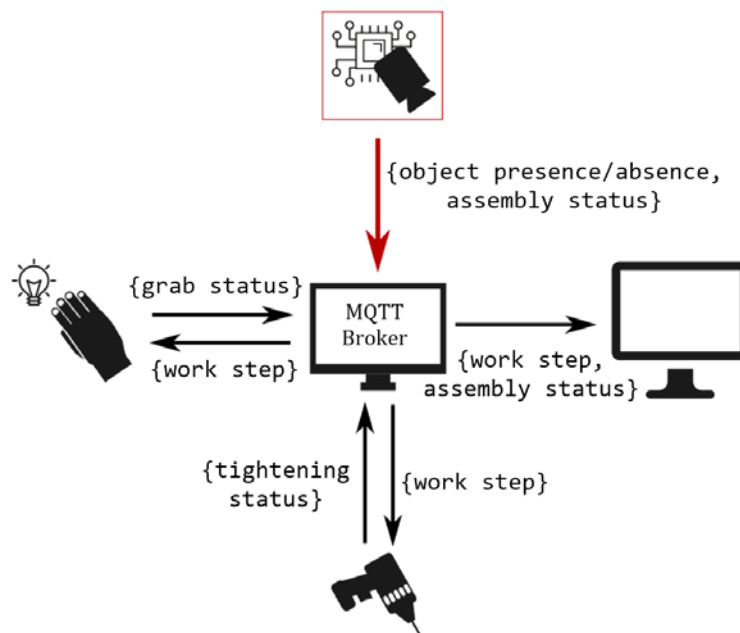


Fig. 2 MQTT messaging scheme of the proposed assembly assistance system. The figure pictures the information flow and content between the modules

The single modules run on edge devices such as Raspberry Pi (pick-by-light module, screw-driver module, MQTT broker), Nvidia Jetson AGX Xavier (object detection unit) or a capacitive industrial panel PC (visualization module). The use of individual devices for each module allows the easy extension or reduction of the proposed assistance system.

2.2 Deep learning-based object detection

The workpiece status (presence, absence, faulty) is acquired via the state-of-the-art single shot object detection model YOLOv4 [23]. The model was chosen because it is capable of delivering real-time results at a high accuracy on GPU edge devices such as the Nvidia Jetson AGX Xavier. To maximize the inference speed, the trained model was optimized using Nvidia's TensorRT runtime. The SDK applies a variety of optimization techniques such as precision calibration, layer fusion, or multi-stream execution [24].

In total, 1512 training images containing 5485 object instances and 790 validation images containing 1468 object instances were used for training the model. The training data consists of 41 individual object classes, so each class is represented by 134 training instances on average. The small training set size is reasonable due to the low intra-class and high inter-class variance of the assembly parts. The training was conducted on a Nvidia GeForce 1650 Super GPU using the Darknet Framework [25]. The mean average precision at 50 % intersection over union (mAP@.50) reached 99.81 % after 6 training epochs for the validation data set. This evaluation metrics gives proof that the model is capable of predicting all classes at a satisfactory level.

Object and error detection can be difficult with small parts or parts that change their appearance only slightly after assembly. The chosen camera perspective (aerial view, see Fig. 2) makes it impossible, for example, to detect the correct vertical engagement of a part in a holder. Identifying the correct torque value by vision can be considered very difficult, so bolts are only checked for their presence. It has been shown that parts that can appear in many different shapes, e.g. thin wires, require a larger number of training data to achieve an accurate detection result.

Collecting the training and validation data and annotating all object instances took a workload of roughly 10 hours for a single person. Given the high complexity of the product with 34 work steps and 41 object classes to annotate, this temporal expenditure seems reasonable, as it can also be performed by untrained personnel. The inference is performed on a Nvidia Jetson AGX Xavier, publishing the detected objects in real-time via MQTT messages. For collecting the training data as well as inferencing, an IMX 178 image sensor was used, mounted above the working area. An example of the inference for a single frame is displayed in Fig. 2.



Fig. 2 Inference of a single frame by the trained YOLOv4 model. The inference results are published via MQTT and the corresponding work step or assembly faults are derived based on the detected objects.

2.3 Pick-by-light module

As pick-by-light is one of the most widespread assembly assistance systems used in industry [26], the proposed meta-assistance-system was equipped with such system. The module operates based on the published current work step derived by the object detection unit. All 21 boxes of material needed in the assembly process are provided with LED lights to guide the worker in finding and picking. Photoelectric barriers are used to detect the successful grabbing process, that is also stored in a database for traceability reasons.

2.4 Electric screwdriver module

The electric screwdriver is a required tool in the assembly process of the studied explosion-proof tube lamp. The required parameters such as torque and speed are set according to the current work step. Also, the screwdriver is only active during the relevant work steps to preserve the correct working sequence. For traceability purposes, the tightening parameters angle, torque, and speed are published and stored in a database. As the electrical screwdriver is necessary in the assembly of the tube lamp, it is used for both the assisted and unassisted assembly workplace. In case of the unassisted assembly, the activation and the correct torque value are set according to the number of screwing processes. In case of a faulty screwing, it has to be set manually for the following screws.

2.5 Visualization module

The work instruction is visualized on a 15" touch screen panel PC. According to the current work step, the respective instruction is presented. After completion and detection by the object detection unit, the next work step instruction is moved on to automatically. For each assembly task, a meaningful image as well as a clear text instruction is presented. Additionally, workers can watch a short video sequence of the assembly at the touch of a button.

3. Experimental setting

The experimental setup refers to the assembly process of a complex tube lamp with support of the proposed assembly assistance system (experimental group) and a control group without said system. Two physically identical workstations are set up for the assembly experiments as shown in Fig. 3. The work instructions for both groups are identical content-wise but paper-based in the control group and screen-based in the experimental group.

The assembly process takes 34 individual work steps including, among other tasks, 21 steps of plugging parts, 5 cable connections, 3 screwing processes, and 2 functionality tests. The assembly parts are made of materials such as plastic, aluminium, steel, glass, and electrical components. Their sizes range from 1 mm cable wires to a 50 cm long tube housing. The large variety of assembly processes, materials, and part sizes ensures the relevance of the assembly error data composition for different kinds of products. In addition, the assembly process diversity makes the results transferable to other products and modern assistance systems.

In both the experimental group and the control group 10 test subjects assembled tube lamps for a duration of 8 hours. During this period, at least 30 tube lamps could be assembled by each test person. The subjects have never assembled the exact lamp before but might have different general knowledge in manual assembly. They were not given any further information on the assembly process except for their work instructions. The whole process was led and supervised by experienced engineers in manufacturing. During the assembly process, the supervisors manually recorded every occurring assembly error.



Fig. 3 The workstation on the left is set up without the proposed assistance system and relies on the paper based work instruction on the far left of the picture. The workstation on the right side is equipped with a pick-by-light system and a work instruction visualization. Those are operated with the data supplied by the object detection unit.

Error assessment

To determine error modes for each work task, an error assessment was performed. As a basis for subsequent analyses, the tasks are described according to the hierarchical task analysis (HTA) method [27]. HTA shows all possible ways of interaction with a system as each task is divided into sub-tasks until no further sub-divisions can be done. Based on the possible assembly states, a human reliability analysis such as THERP (technique for human error-rate prediction) [28] is used to map the states to relevant error categories. As the aim of this work is a comparative error reduction study rather than an error analysis, so THERP was used to identify errors. Due to the high complexity of the assembly product, only safety- and functionality-relevant error modes are taken into further consideration. In total, the study supervisor team identified 70 potential error states. Errors made by the test subjects are counted as such if no error recovery takes place within the next work step. This approach respects the real-world scenario the study is aiming for. Workers typically fix errors but should not reverse too many steps due to time constraints.

According to guideline VDI 4006-2 [29], the identified errors were classified into the four categories described in Table 1. Using error categories provides the results at a higher interpretability level. The difference in error composition between the experimental and control group might be due to specific assistance modules, so each module’s influence can be discussed.

Comparing the 70 relevant error states, 18 (25 %) are considered errors by omission, 27 (39 %) execution errors, 9 (13 %) errors by confusion, and 16 (23 %) quantitative errors. The following analysis is intended to compare the error occurrence for the assisted and unassisted assembly lines.

Table 1 Selection of error categories according to VDI 4006-2, that occurred during the assembly process of the explosion-proof tube lamp

| Type (Abbreviation) | Description | Example |
|-------------------------|---|--|
| Error by omission (OM) | Some action was not carried out | - Worker forgot to plug in two cable wires - Worker forgot to perform functionality test |
| Execution error (EX) | Something is wrongly set or selected | - Worker chose a wrong plastic cap - Worker sets wrong torque value for screwing |
| Error by confusion (CE) | Something is done instead of something else | - Worker reverses positive and negative pole connections - Worker confuses two similar looking plastic parts |
| Quantitative error (QE) | Something is too much or too little | - Worker applies two layers of insulating film instead of one - Worker only screws 7 of the 8 required screws |

4. Results and discussion

To analyse the occurrence of assembly errors, different metrics were determined. The following evaluation considers the first 30 assemblies of the test subjects, as each person was able to complete at least this number of full assemblies during the execution of the experiment.

4.1 Error prevention analysis

To track the test subject's training process over the course of the assemblies, the errors were accumulated for every five assemblies. For the case of this analysis, the errors are counted total without being classified into error types. For both the assisted assembly group (AA) as well as the unassisted assembly (UA) group, the number of errors decreases over the number of performed assemblies (Fig. 5). The AA group records a decrease from an average of 5.0 errors in assemblies 1-5 to an average of 0.20 in assemblies 26-30, which is a decline of 95 %. The UA control group shows 8.5 errors in assemblies 1-5 and 1.3 errors in assemblies 26-30, resulting in a decline of 85 %. While both groups show a training progress in terms of error reduction, the assisted assembly group produces fewer error states at each point in the assembly process. During the first 15 assembly operations the number of errors steadily decreases in both groups. In the following 15 assemblies, the number of assembly errors remains relatively constant at a lower level. This leads to the assumption that there is an initial training phase followed by a skilled work phase.

The total number of errors in 30 individual assemblies decreases from an average of 17.4 in the unassisted assembly group to 9.2 when using the proposed assistance system, which corresponds to an error reduction of 51 %. The results apply to both the initial training phase and the following skilled phase.

The generally smaller interquartile range in the assisted assembly group indicates a smaller statistical dispersion of the number of errors in this group. The lower spread over the number of test subjects signals a more stable assembly environment. The general error reduction effect provided by the assembly assistance system brings a variety of positive effects in the studied use case. First, the required amount of supervision during the training period can be reduced. Second, the number of rejects due to errors is reduced. Third, the assembly time is reduced due to less rework caused by faulty assemblies. Since these positive effects are difficult to quantify, we assume a linear correlation of each factor with the number of total errors.

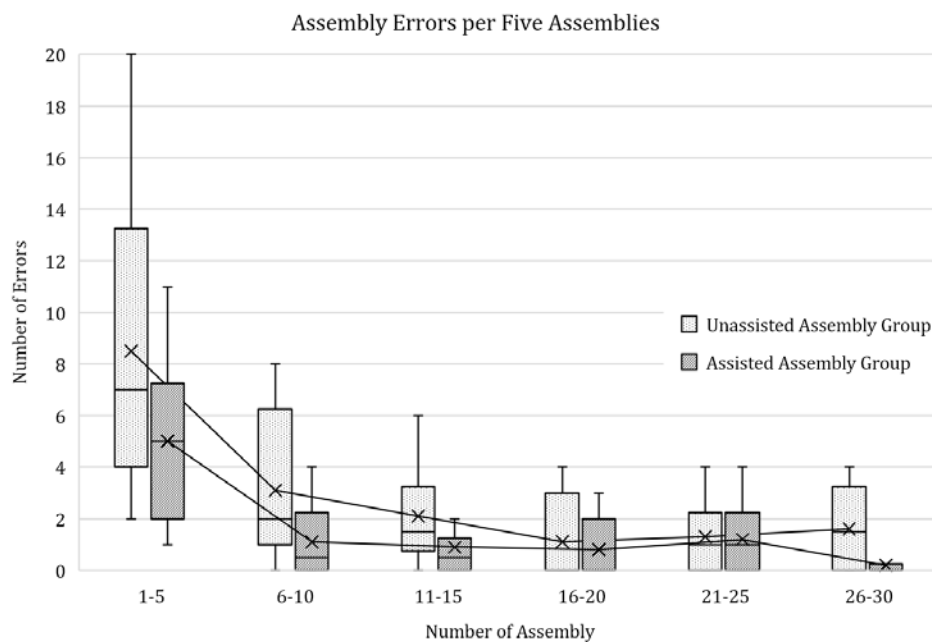


Fig. 4 Number of assembly errors encountered in assembly using the assistance system and without using the assistance system. The errors are accumulated for five assemblies to show the potential training effect during assembly.

To track the assistance system's ability to prevent certain types or error modes, the number of errors per category (Table 1) are analysed. The results show that the AA group produces fewer errors for each of the four error types (Fig. 6). Especially errors by omission (59 % error reduction), quantitative errors (50 % error reduction) and execution errors (42 % error reduction) are effectively prevented by the assembly assistance system. As the system allows the execution of the following work step only if the current work step is visually detectable, errors by omission are actively prevented. Additionally, the pick-by-light system is likely to prevent several types of errors by reducing the cognitive load and the risk of assembling incorrect parts. The control of the electric screwdriver by the assistance system prevents incorrectly set torques and the forgetting of screwdriving operations. The qualitative analysis of the error prevention potential for each assistance module coincides with the quantitative results previously explained.

In the underlying use case, it is important not to trade error prevention for additional assembly time. For this reason, the workplace invasiveness of the system was kept as low as possible. Comparing the assembly times of both groups, AA group is able to assemble even faster on the first runs. After the initial training period, both groups show similar assembly times. The detailed analysis of the assembly times should not be part of this work, but the results indicate that the proposed assembly assistance system does not affect the worker in any undesirable way.

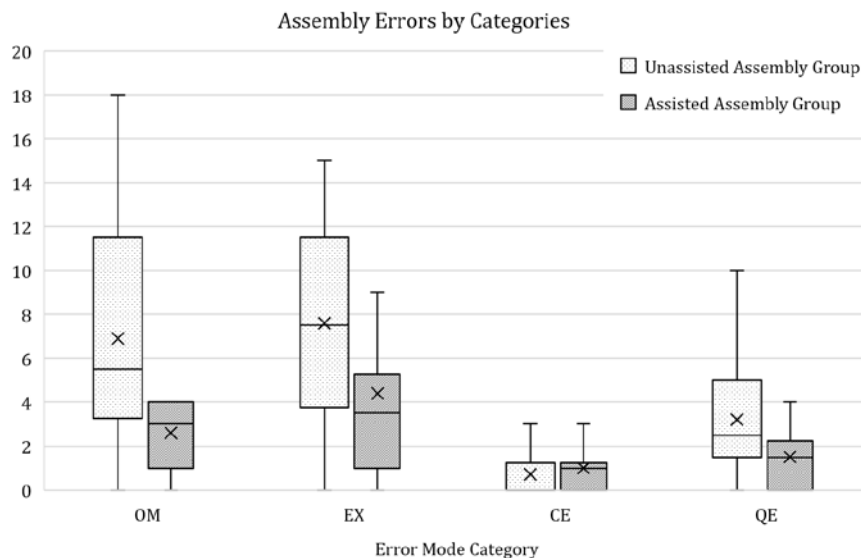


Fig. 6 Number of assembly errors per category summed for all 30 assemblies per test person. The four categories are errors by omission (OM), execution errors (EX), errors by confusion (CE) and quantitative errors (QE).

4.2 Additional insights

In addition to the error prevention aspect, the system's ability to provide traceability should also be discussed. During the execution of the conducted experiments, assembly data of 10 workdays were recorded. In this period, about 600 tube lamps were assembled in a total of 11,000 work steps. The traceability data include the relative position of every visible component at every time in the assembly process. This information provided by the object detection unit can be very valuable in tracing individual assembly errors or providing evidence of critical assembly steps. Especially in safety-critical assembly environments like the presented explosion-proof use case product, this high grade of traceability might be a competitive advantage. In addition to storing the acquired assembly data, it can also be processed to gain meaningful insights into the production process and further increase the production efficiency. Unsupervised-learning methods might be used to cluster the data and find irregularities that could lead to the identification of additional errors.

The economic value of the proposed system is highly dependent on the product, labour costs and whether other measures have already been taken to avoid production errors. The cost per error also depends on the industry and potential threat. This external failure cost like warranty expenses, legal costs associated with claims or recall costs are also highly sector and product

dependent. Generally, the proposed assistance system will be amortised faster in high-priced product manufacturing and safety regulated sectors like explosion-proof manufacturing. A detailed estimate of the economic value is likely to be the subject of follow-up research. To give a rough estimate for the costs of the proposed assistance system we can say that the hardware equipment (worker display, cameras, GPU, edge computers, etc.) used in our experiments is currently available for about 5,000€. In practice the implementation of such a system will be comparable to a software project including all phases (requirements analysis, implementation, test), which is by far the largest cost factor. Currently, such a project must be considered as an individual software development project because there is no standard software product existing. However, as described above, there are open-source software components available for the training and application of neural networks that can accelerate the development enormously.

5. Conclusion

This research paper studies a real-world manual assembly use case to determine the error prevention potential of a state-of-the-art assembly assistance system. The chosen approach is a combination of the most recent advances in assembly assistance systems and deep learning. Our proposed system relies on a deep learning object detection model to accurately identify the state of each assembly part in real-time. The object detection module supplies data to other assistance modules such as pick-by-light or the electrical screwdriver which are used within the system. In order to analyse the system's error prevention ability, a complex manual assembly product was provided by the company R. Stahl AG. The explosion-proof tube lamp is assembled in 34 work steps using different assembly techniques. Since the product is used in safety-critical environments, finding methods to avoid assembly errors is highly relevant. In experiments with test subjects, it was found that the proposed assistance system can prevent 51 % of the assembly errors compared to a control group without the use of assistance. Especially errors by omission are effectively prevented, as the system supervises the assembly process and notices the non-assembly of components. Due to the number of test persons, the number of individual assemblies and the variety of assembly techniques, this case study can also be representative for other comparable assistance systems and complex products. Additionally, it is discussed how the collected data can further be used as valuable sources of information.

Despite the high error prevention capability, the economic value of implementing the proposed assistance systems remains unclear. In order to determine this value, case-dependent analysis have to be carried out that include the cost of individual errors, labour costs and the value of additional traceability. Although the test subjects did not express any concerns, the acceptance and applicability of the system in a production environment needs to be intensively studied. In addition to the implementation details for the use in a company's production ecosystem, legal aspects also need to be clarified depending on local legislation.

In follow-up studies, the time-saving potential of the assembly assistance system could be investigated, and ways found to quantify its economic benefits. The potential of the recorded assembly data should also be further investigated using machine learning methods.

Acknowledgement

The authors would like to thank the Carl-Zeiss-Foundation for their support within the research project "Smart Assembly". Acknowledgements also go to our industrial partners for providing assembly products and exchange of knowledge.

References

- [1] Koren, Y. (2010). *The global manufacturing revolution: Product-process-business integration and reconfigurable systems*, John Wiley & Sons, New Jersey, USA, doi: [10.1002/9780470618813](https://doi.org/10.1002/9780470618813).
- [2] Zhou, F., Ji, Y., Jiao, R.J. (2013). Affective and cognitive design for mass personalization: Status and prospect, *Journal of Intelligent Manufacturing*, Vol. 24, No. 5, 1047-1069, doi: [10.1007/s10845-012-0673-2](https://doi.org/10.1007/s10845-012-0673-2).

- [3] Metzmacher, A.I., Hellebrandt, T., Ruessmann, M., Heine, I., Schmitt, R.H. (2019). Aligning the social perspective with the technical vision of the smart factory, In: Schmitt, R., Schuh, G. (eds.), *Advances in Production Research*, WGP 2018, Springer, Cham, Switzerland, 715-729, doi: [10.1007/978-3-030-03451-1_69](https://doi.org/10.1007/978-3-030-03451-1_69).
- [4] Merkel, L., Atug, J., Berger, C., Braunreuther, S., Reinhart, G. (2018). Mass customization and paperless assembly in the learning factory for cyber-physical-production systems: Learning module 'from paperbased to paperless assembly', In: *Proceedings of 2018 IEEE 18th International Conference on Advanced Learning Technologies (ICALT)*, Mumbai, India, 270-271, doi: [10.1109/ICALT.2018.00130](https://doi.org/10.1109/ICALT.2018.00130).
- [5] Villani, V., Sabattini, L., Czerniaki, J.N., Mertens, A., Vogel-Heuser, B., Fantuzzi, C. (2017). Towards modern inclusive factories: A methodology for the development of smart adaptive human-machine interfaces, In: *Proceedings of 2017 22nd IEEE International Conference on Emerging Technologies and Factory Automation (ETFA)*, 1-7, doi: [10.1109/ETFA.2017.8247634](https://doi.org/10.1109/ETFA.2017.8247634).
- [6] Quint, F., Loch, F., Orfgen, M., Zuehlke, D. (2016). A system architecture for assistance in manual tasks, In: Novais, P., Konomi, S. (eds.), *Ambient intelligence and smart environments, Volume 21: Intelligent Environments*, IOS Press BV, Amsterdam, The Netherlands, 43-52, doi: [10.3233/978-1-61499-690-3-43](https://doi.org/10.3233/978-1-61499-690-3-43).
- [7] Fast-Berglund, Å., Fässberg, T., Hellman, F., Davidsson, A., Stahre, J. (2013). Relations between complexity, quality and cognitive automation in mixed-model assembly, *Journal of Manufacturing Systems*, Vol. 32, No. 3, 449-455, doi: [10.1016/j.jmsy.2013.04.011](https://doi.org/10.1016/j.jmsy.2013.04.011).
- [8] Hinrichsen, S., Bendzioch, S. (2019). How digital assistance systems improve work productivity in assembly, In: Nunes, I.L. (ed.), *Advances in Human Factors and Systems Interaction*, Springer International Publishing, 332-342, doi: [10.1007/978-3-319-94334-3_33](https://doi.org/10.1007/978-3-319-94334-3_33).
- [9] Turk, M., Pipan, M., Šimic, M., Herakovič, N. (2020). Simulation-based time evaluation of basic manual assembly tasks, *Advances in Production Engineering & Management*, Vol. 15, No. 3, 331-344, doi: [10.14743/apem2020.3.369](https://doi.org/10.14743/apem2020.3.369).
- [10] Zamora-Hernández, M.-A., Castro-Vargas, J.A., Azorin-Lopez, J., Garcia-Rodriguez, J. (2021). Deep learning-based visual control assistant for assembly in Industry 4.0, *Computers in Industry*, Vol. 131, Article No. 103485, doi: [10.1016/j.compind.2021.103485](https://doi.org/10.1016/j.compind.2021.103485).
- [11] Min, Y., Zhang, Y., Chai, X., Chen, X. (2020). An efficient pointLSTM for point clouds based gesture recognition, In: *Proceedings of 2020 IEEE/CVF Conference on Computer Vision and Pattern Recognition (CVPR)*, Seattle, USA, 5760-5769, doi: [10.1109/CVPR42600.2020.00580](https://doi.org/10.1109/CVPR42600.2020.00580).
- [12] Börold, A., Teucke, M., Rust, A., Freitag, M. (2020). Deep learning-based object recognition for counting car components to support handling and packing processes in automotive supply chains, *IFAC-PapersOnLine*, Vol. 53, No. 2, 10645-10650, doi: [10.1016/j.ifacol.2020.12.2828](https://doi.org/10.1016/j.ifacol.2020.12.2828).
- [13] Ozdemir, R., Koc, M. (2019). A quality control application on a smart factory prototype using deep learning methods, In: *Proceedings of 2019 IEEE 14th International Conference on Computer Sciences and Information Technologies (CSIT)*, Lviv, Ukraine, 46-49, doi: [10.1109/STC-CSIT.2019.8929734](https://doi.org/10.1109/STC-CSIT.2019.8929734).
- [14] Pierleoni, P., Belli, A., Palma, L., Palmucci, M., Sabbatini, L. (2020). A machine vision system for manual assembly line monitoring, In: *Proceedings of 2020 International Conference on Intelligent Engineering and Management (ICIEM)*, London, United Kingdom, 33-38, doi: [10.1109/ICIEM48762.2020.9160011](https://doi.org/10.1109/ICIEM48762.2020.9160011).
- [15] Tavakoli, H., Walunj, S., Pahlevannejad, P., Plociennik, C., Ruskowski, M. (2021). Small object detection for near real-time egocentric perception in a manual assembly scenario, *Computer Science, Computer Vision and Pattern Recognition*, Cornell University, from <https://arxiv.org/abs/2106.06403>, accessed October 17, 2021.
- [16] Eversberg, L., Grosenick, P., Meusel, M., Lambrecht, J. (2021). An industrial assistance system with manual assembly step recognition in virtual reality, In: *Proceedings of 2021 International Conference on Applied Artificial Intelligence (ICAPAI)*, Halden, Norway, 1-6, doi: [10.1109/ICAPAI49758.2021.9462061](https://doi.org/10.1109/ICAPAI49758.2021.9462061).
- [17] Egeler, R., Wimpff, D.-P., Jauch, C., Wiedenroth, S.J., Wolf, A., Ruck, M., Wohlfeld, D. (2017). MonSiKo – Adaptives Montageassistentz- und Interaktionssystem mittels 3D-Szenenanalyse und intuitiver Mensch-Technik Kommunikation, Schlussbericht, Stuttgart, Germany, from <http://publica.fraunhofer.de/dokumente/N-590407.html>, accessed October 14, 2021.
- [18] Oestreich, H., Töniges, T., Wojtynek, M., Wrede, S. (2019). Interactive learning of assembly processes using digital assistance, *Procedia Manufacturing*, Vol. 31, 14-19, doi: [10.1016/j.promfg.2019.03.003](https://doi.org/10.1016/j.promfg.2019.03.003).
- [19] Kaczmarek, S., Hogreve, S., Tracht, K. (2015). Progress monitoring and gesture control in manual assembly systems using 3D-image sensors, *Procedia CIRP*, Vol. 37, 1-6, doi: [10.1016/j.procir.2015.08.006](https://doi.org/10.1016/j.procir.2015.08.006).
- [20] Faccio, M., Ferrari, E., Galizia, F.G., Gamberi, M., Pilati, F. (2019). Real-time assistance to manual assembly through depth camera and visual feedback, *Procedia CIRP*, Vol. 81, 1254-1259, doi: [10.1016/j.procir.2019.03.303](https://doi.org/10.1016/j.procir.2019.03.303).
- [21] Pilati, F., Faccio, M., Gamberi, M., Regattieri, A. (2020). Learning manual assembly through real-time motion capture for operator training with augmented reality, *Procedia Manufacturing*, Vol. 45, 189-195, doi: [10.1016/j.promfg.2020.04.093](https://doi.org/10.1016/j.promfg.2020.04.093).
- [22] Rocha, C.A.P., Rauch, E., Vaimel, T., Garcia, M.A.R., Vidoni, R. (2021). Implementation of a vision-based worker assistance system in assembly: A case study, *Procedia CIRP*, Vol. 96, 295-300, doi: [10.1016/j.procir.2021.01.090](https://doi.org/10.1016/j.procir.2021.01.090).
- [23] Bochkovskiy, A., Wang, C.-Y., Liao, H.-Y.M. (2020). YOLOv4: Optimal speed and accuracy of object detection, *Computer Science, Computer Vision and Pattern Recognition*, Cornell University, from <http://arxiv.org/abs/2004.10934>, accessed October 14, 2021.
- [24] NVIDIA deep learning TensorRT documentation, from <https://docs.nvidia.com/deeplearning/tensorrt/developer-guide/index.html>, accessed October 14, 2021.
- [25] Redmon, J., Darknet: Open Source Neural Networks in C, from <http://pjreddie.com/darknet/>, accessed October 14, 2021.

- [26] Stockinger, C., Steinebach, T., Petrat, D., Bruns, R., Zöller, I. (2020). The effect of pick-by-light-systems on situation awareness in order picking activities, *Procedia Manufacturing*, Vol. 45, 96-101, [doi: 10.1016/j.promfg.2020.04.078](https://doi.org/10.1016/j.promfg.2020.04.078).
- [27] Annett, J. (2003). Hierarchical task analysis, In: Hollnagel, E. (ed.), *Handbook of cognitive task design*, Vol. 2, Lawrence Erlbaum Associates, Mahwah, New Jersey, USA, 17-35.
- [28] Kirwan, B. (1994). *A guide to practical human reliability assessment*, First edition, CRC Press, London, United Kingdom.
- [29] VDI. VDI 4006 Blatt 2:2017-11, Human reliability – Methods for quantitative assessment of human reliability. (2017), from <https://www.vdi.de/>, accessed October 14, 2021.
- [30] Jiang, C., Xi, J.T. (2019). Dynamic scheduling in the engineer-to-order (ETO) assembly process by the combined immune algorithm and simulated annealing method, *Advances in Production Engineering & Management*, Vol. 14, No. 3, 271-283, [doi: 10.14743/apem2019.3.327](https://doi.org/10.14743/apem2019.3.327).

Optimal path planning of a disinfection mobile robot against COVID-19 in a ROS-based research platform

Banjanovic-Mehmedovic, L.^a, Karabegovic, I.^{b,*}, Jahic, J.^c, Omercic, M.^d

^aUniversity of Tuzla, Faculty of Electrical Engineering, Tuzla, Bosnia and Herzegovina

^bAcademy of Sciences and Arts of Bosnia and Herzegovina, Sarajevo, Bosnia and Herzegovina

^cUniversity of Cambridge, Cambridge, United Kingdom

^diLogs GmbH, Klagenfurt, Austria

ABSTRACT

Due to COVID-19 pandemic, there is an increasing demand for mobile robots to substitute human in disinfection tasks. New generations of disinfection robots could be developed to navigate in high-risk, high-touch areas. Public spaces, such as airports, schools, malls, hospitals, workplaces and factories could benefit from robotic disinfection in terms of task accuracy, cost, and execution time. The aim of this work is to integrate and analyse the performance of Particle Swarm Optimization (PSO) algorithm, as global path planner, coupled with Dynamic Window Approach (DWA) for reactive collision avoidance using a ROS-based software prototyping tool. This paper introduces our solution – a SLAM (Simultaneous Localization and Mapping) and optimal path planning-based approach for performing autonomous indoor disinfection work. This ROS-based solution could be easily transferred to different hardware platforms to substitute human to conduct disinfection work in different real contaminated environments.

ARTICLE INFO

Keywords:

Disinfection mobile robot;
COVID-19;
Optimal path planning;
Particle Swarm Optimization (PSO);
Simultaneous localization and mapping (SLAM);
Dynamic Window Approach (DWA);
Robot Operating System (ROS);
ROS-based platform

**Corresponding author:*
isak1910@hotmail.com
(Karabegovic, I.)

Article history:

Received 19 November 2021
Revised 27 November 2021
Accepted 28 November 2021



Content from this work may be used under the terms of the Creative Commons Attribution 4.0 International Licence (CC BY 4.0). Any further distribution of this work must maintain attribution to the author(s) and the title of the work, journal citation and DOI.

1. Introduction

Service mobile robots provide task services at different public places, e.g., in factories, airports, malls or hospitals. Because of similarities between operational environments in hospitals and manufacturing facilities, many service tasks are adapted in both environments [1]. We are currently witnessing a pandemic caused by the COVID-19 virus, so disinfection is a necessary task in many institutions. Using service disinfection robots is very attractive and advantageous for highly effective treatments, highly effective pathogen elimination, whole area treatment, disinfection of all surfaces in the area, higher productivity, etc.

Numerous design solutions for disinfection robots have been developed. Shen *et al.* [2], during the COVID-19 pandemic, compared over 200 robotic systems that could assist with Covid-related issues. The study concludes that robotics systems are overall suitable for dealing with COVID-19 related challenges, including disinfection. Robots for disinfection are mainly categorized [3] into UV light based and liquid agent spray solutions. Considering their mobility, they are often categorized [4] as mobile based, drones or semi-autonomous. After comparing several robots for disinfection, the survey concludes that liquid agent spray robots have a great advantage of being able to function 24/7, performing disinfection of target areas following a specific path. However, the survey notices that these robots may not be useful in areas with gaps or holes where is hard to reach by the liquid. According to the previously mentioned categorization, our solution fits into a category of mobile robots based on UV light disinfection. Even before the COVID 19 pandemic started, research conducted in robotics investigated questions that robotics solutions need to address to "effectively deploy robots in infectious diseases outbreaks" [5]. One of the three main research questions, relevant to our work, focuses on the interaction between robots and patients.

Recent research in the field of mobile robotics focusing on disinfection tackles problem related to planning and execution of navigation path, especially on optimization of the path considering navigation and disinfection target constraints. Shi *et al.* [6] approach the challenge of making mistakes in the path planning. They transform the collaborative scheduling problem of intelligent disinfection use to the distributed constraint optimization problem.

Tan *et al.* [7] introduced Aimi-Robot UVC robot that uses a graph-optimized SLAM algorithm to enable localization and map creation in the unknown environments. Aimi-Robot uses lidar sensors, gyroscopes, and odometers to obtain environmental information, and with the aforementioned SLAM algorithm it is able to increase real-time localization accuracy. Conte, Leamy, and Furukawa [8] presented an unmanned ground vehicle robot with map-based teleoperation that disinfects in complex indoor environments. The main contribution of this work is the two-stage mapping technique enabling teleoperation and allowing a human to operate the robot beyond the line-of-sight. The map dynamically constructs the map of 3D surfaces. To get a detailed map, Sayed *et al.* [9] presented a robot controlled by a joystick, which uses the Microsoft Kinect Xbox360 sensor. The navigation challenge is approached by using ROS navigation algorithms, SLAM, and machine vision. Marques *et al.* [10] suggest how to optimize a trajectory of a robot by building a probabilistic roadmap in the robot's configuration space. To deal with the fact that it is an NP-hard Mixed-Integer Linear Programming, they employ a two-stage solver that combines a Linear Program (LP) and a Travelling Salesman Problem (TSP). Conroy *et al.* [11] present a low-cost robotic platform for ultraviolet light disinfection, with off-the-shelf components and ROS navigation stack (standard mapping, control, and odometer packages), and use simulation to verify their concept. Ruan *et al.* [12] introduced a low-cost robot that combines the Hydrogen Peroxide Vaporous and SLAM for automated disinfection operation in the complex indoor environment. The robot builds a map of the environment using SLAM, powered by the ROS navigation stack, and then it follows a prescribed path. UltraBot robot [13] created for UV disinfection combines SLAM, Monte Carlo localization, and autonomous navigation in known environments for localization and path planning. This platform is a partially 3D printed and uses standard the ROS packages. These factors combined enable it to achieve high accuracy in localization.

Compared to the discussed robots, our solution combines Particle Swarm Optimization (PSO) algorithm with Dynamic Window Approach (DWA) for optimal path planning and obstacle avoidance. In addition, the suggested solution relies on ROS components. Instead of presenting a concrete solution, we present a concept that is easy to transfer to different hardware platform as a non-expensive and practical solution, and which is adjustable for specific applications in this domain.

The rest of this paper is organized as follows: Section 2 describes current planning methods used in the autonomous vehicles research field, with focus on the PSO-based optimization method; Section 3 introduces the ROS-based research platform and its modules related to the navigation; Section 4 introduces our solution- SLAM and path planning based approach for performing

disinfection, which are implemented in ROS, while Section 5 describes the simulation setup and discussion. Finally, the last section contains the conclusions and future work.

2. Path planning methods

Service robots are supposed to navigate in crowded environments in a way that requires methods for motion planning and obstacle avoidance. The main problem in robot path planning is the capability of creating collision-free waypoints in the path to reach the destination point regarding to some optimization criteria such as the shortest distance or minimum time. Usually, the path planning module is divided into the global planner, which uses a priori information of the environment to create the best possible path and the local planner, which recalculates the initial plan to avoid possible dynamic obstacles [14].

Path planning can be classified into initial practical planners, grid-based algorithms, sampling-based planning (SBP) approaches, algorithms based on optimization and machine learning based algorithms [15].

Initial complete practical planners such as Road Map (RM), Potential Fields, and Cell Decomposition (CD) techniques are unable to deal with dynamic and complex high dimension problems [16].

Grid-based algorithms transform the environment in a grid-mesh. Dijkstra's algorithm is always able to find the shortest path between two points, but it has very high computational complexity. Many algorithms have been created which are able to find the shortest path with the lowest computational cost: A*, Bi A*, Breadth-first, Best-First path planning [17]. The A* uses heuristics to be faster. The Bidirectional A* algorithm is a graph search algorithm that finds the shortest path from an initial vertex to a goal vertex in a directed graph running two simultaneous searches. The Breadth-first Search is a classic graph search algorithm, which works by expanding and systematically exploring a given node and progressively redoing the same procedure for all its neighbours. The Best-First algorithm is one of the most popular in the literature. The Best-First algorithm uses the given heuristic function, which is applied equally through the search space, to quantify the value of each candidate exploited during the process and, thus, continues the exploration until reaches the point of interest. These algorithms, however, become extremely costly when applied to large environments or environments with dynamic objects [17].

Sampling Based Planning (SBP) approaches are the most influential approaches in path planning. SBPs are probabilistically complete, i.e., it finds a solution, if one exists, provided with infinite run time. The most popular SBP algorithms are Probabilistic Roadmap (PRM), Rapidly-exploring Random Tree (RRT) and Rapidly-exploring Random Tree Star (RRT*). PRM based methods are mostly used in highly structured static environments such as factory floors. RRT and RRT* based approaches extend non-holonomic constraints and support dynamic environment as well. The major advantages of SBP algorithms are low computational cost, applicability to high dimensional and complex problems [18].

Evolutionary Algorithms (EA) are based on the principle of natural evolution, where randomly select a candidate set of solutions and apply the quality function as an abstract fitness measure. The evolutionary algorithms tend to find an optimal solution by converging from the initial state to the global optimal using a fitness function. A few of optimization techniques based on nature-inspired optimization heuristics are Genetic Algorithm (GA), Particle Swarm Optimization (PSO), Ant Colony Optimization Algorithm (ACO), Artificial Bee Colony (ABC), Cuckoo Search (CS). The Genetic algorithm is based on a direct analogy to Darwinian natural selection and mutations in biological reproduction. ACO is inspired by the behaviour of real ant colonies and PSO is used for optimizing continuous nonlinear functions and performs a parallel search in a space of solutions. The PSO has many advantages compared to other evolutionary methods: it has few parameters, small population and fast convergence [19].

Recently, many researchers have tried to solve path planning problems using machine learning [15]. The classical Q-Learning algorithm is improved using deep learning and this combination gives very good results.

PSO algorithm

The PSO is inspired by the social behaviour of a flock of migrating birds trying to reach an unknown destination [20]. In the PSO algorithm, a candidate solution is presented as a particle. The algorithm utilizes a collection of flying particles in a search space (current and possible solutions) and moves towards a promising area to get to a global optimum [21]. A given number of state space vectors (particles) are initialized randomly. Particles fly through the search space at predefined velocities, which are dynamically adjusted according to its own previous best value $pbest_i$ and its previous best group's $gbest$ [22-25]. The performance of each particle is measured according to a known fitness function, which is related to the problem to be solved.

The best solutions are evolved through several generations. Each particle updates its position and velocity as follows:

$$X_i^t = X_i^t + V_i^{t+1} \quad (1)$$

$$V_i^{t+1} = \omega V_i^{t+1} + c_1 r_1 (pbest_i - X_i^t) + c_2 r_2 (gbest - X_i^t) \quad (2)$$

where V_i^{t+1} is the velocity of the i -th particle at time $t + 1$, X_i^t is the position of particle at time t ; c_1 and c_2 are acceleration coefficients, which denote the cognitive and social parameters, respectively and are usually set to a value of 2, although good results have been also produced with $c_1 = c_2 = 4$; r_1 and r_2 are two random functions in the range $[0,1]$. The inertial weight ω is used for regulating the global exploration and local exploration abilities. It presents the global search behaviour, set to a large value in the beginning of the searching process and dynamically reduced during the optimization (which emulates a more local search behaviour). Its range is suggested to be $0.2 \leq \omega \leq 0.4$. All particles move to the global best solution to finish the search process [24].

3. ROS-based research platform

3.1 General information about ROS

Robot Operating System (ROS) [26] is a framework that facilitates development of robotic applications. It is organised around the idea of common data structures for standard robotic operations, and it comprises a large database of libraries and tools. In its current version ROS2, it supports a significant number of robots through abstractions usually expected from an operating system (e.g., support with abstraction of hardware to software). However, ROS is a meta operating system as it runs on top of a real operating system (Linux, macOS, or Windows 10). ROS relies on distributed communication between nodes and is hence suitable for controlling larger robotics environments, involving other robots and large number of sensors on-robot and off-robot sensors. Projects of ROS are organised into stacks, where the ROS navigation stack [33] is one of the most prominent projects.

ROS2, officially released in 2017, in addition to features supported in ROS1, also supports C++17 standard and works with Python version 3.5 (where ROS1 supports C++03 and C++11 and works with Python 2). In addition to these, ROS2 provides various Quality of Service policies which improve communication over different networks.

One of the most used simulators with ROS is the Gazebo simulator [27, 34]. The focus of Gazebo is to simulate physics of robotics, support rendering, offer communication interfaces and a user interface. The simulator offers possibilities for both indoor and outdoor navigation modelling and supports robot models with different level of details (from simple platforms to robots with full sensor suite). Some of the dynamic operations that the simulator supports include motion, constraints, collision, and contact friction. It also has support for various sensors, including cameras, Kinect, lasers, RFID, etc. The Gazebo ROS package provides interface between the Gazebo and ROS framework.

Another simulator often used with ROS is SVL Simulator [35]. It is a simulation platform used for autonomous vehicles. Applications of the SVL simulator include warehouse robotics, autonomous racing, sensor/sensor systems development and marketing, real-time embedded systems

for automotive, etc. Commonly supported scenarios are complex traffic scenarios, testing localization module in new Digital Twin environments, testing autonomous vehicle stack in real, etc. SVL supports running ROS2 simulations with its ROS navigation stack.

Rviz [36] is a 3D visualization tool commonly used in ROS. It enables visualisation of data, and is most commonly used to show sensor data and dynamic states of different processes. Typical examples of data visualisation using Rviz include data from laser sensors, camera, odometry, etc. It has several built-in data types including camera, image, map, point, path, etc.

3.2 ROS navigation stack and Nav2

ROS navigation [37] stack performs 2D navigation operations. As input, it takes odometry, sensor streams, and a goal pose. It outputs velocity commands that are sent to a mobile base.

Nav2 project [33] is a successor of the ROS navigation stack to be used in ROS2. Nav2, among others, contains tools to load, serve, and store maps (Map Server), localize the robot on the map (AMCL), plan a path from A to B around obstacles (Nav2 Planner), control the robot as it follows the path (Nav2 Controller), convert sensor data into a Costmap representation of the world (Nav2 Costmap 2D), compute recovery behaviours in case of failure (Nav2 Recoveries), follow sequential waypoints (Nav2 Waypoint Follower), and plugins to enable custom algorithms and behaviours (Nav2 Core), Fig. 1.

4. SLAM and path planning in ROS

The disinfection mobile robot first builds the map of the designated environment based on Simultaneous localization and mapping (SLAM). Then, it accomplishes the disinfection mission of the environment according to the selected path avoiding obstacles during this process. Our solution combines Particle Swarm Optimization (PSO) algorithm with Dynamic Window Approach (DWA) for global path planning and obstacle avoidance, respectively. The suggested concept of our approach is presented in Fig. 2.

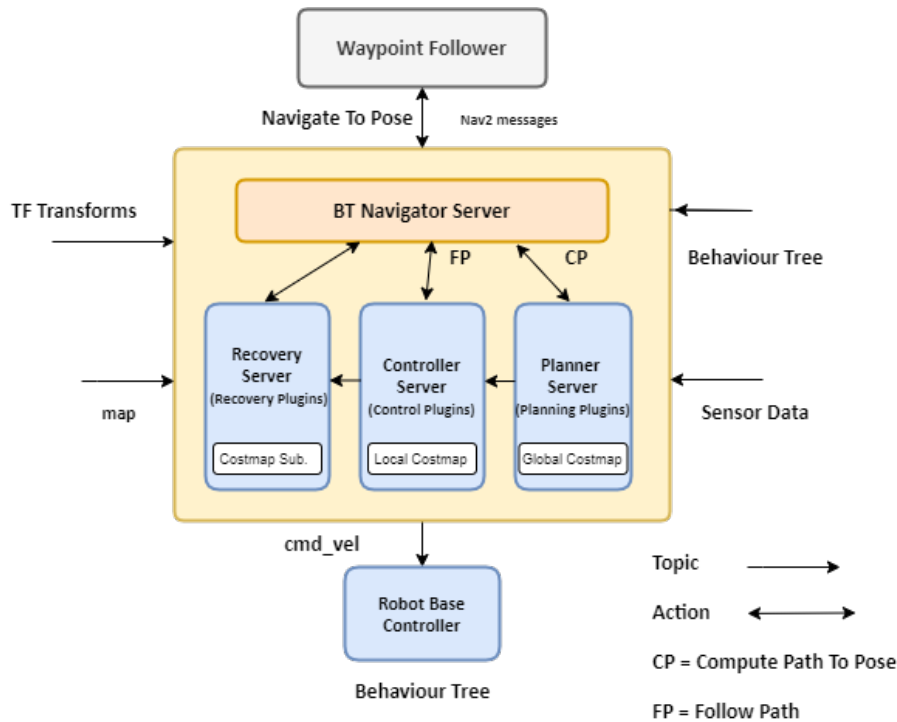


Fig. 1 ROS Nav2 stack

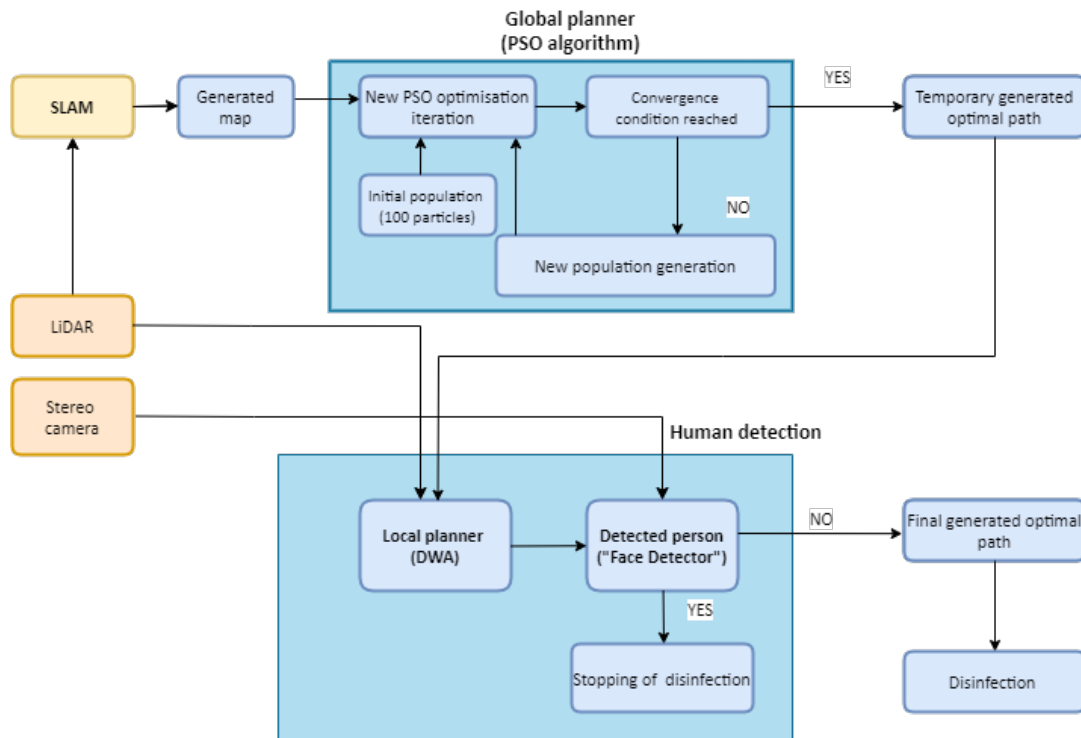


Fig. 2 The suggested concept of the disinfection mobile robot relies on ROS components

4.1 SLAM implementation in ROS

For the proposed concept of Optimal path planning of the disinfection mobile robot, we used the Gmapping SLAM algorithm due to its robustness in indoor environments and limited computational burden.

Simultaneous localization and mapping (SLAM) is a concept concerned with the problem of building a map of an unknown environment by a mobile robot while at the same time enables localization and navigation through the environment using the map [28]. The main function of SLAM is to analyze the input data to determine the pose of the robot and build an environment map in order for the robot to move autonomously.

The SLAM problem could be solved using filtering or smoothing approaches. The main filtering SLAM techniques are Kalman filters (EKF, UKF) and particle filters, and they are designed as on-line approaches. The smoothing approaches like the graph SLAM, estimate the full robot trajectory by processing the full set of the sensor measurements and they are classified as the full SLAM problem.

The SLAM could also be classified into 2D and 3D SLAM. The most common 2D-lidar SLAM algorithms in ROS include Gmapping, Cartographer, Hector, Core, Lago. Gmapping is a SLAM algorithm based on 2D-lidar using Rao-Blackwellized Particle Filters (RBPF) to build the 2D grid map. It decomposes the SLAM problem into two parts: localization and mapping through the conditional joint distribution [29].

In recent years, the machine learning and deep learning techniques have been involved in research regarding SLAM to effectively reduce the positioning error, achieve high-precision tracking detection, and improve the accuracy of robot target detection [28, 30].

4.2 PSO based global path planner

After building the map, it is necessary to solve the path planning problem to enable the robot to perform multi-point disinfection at a specified location in the generated 2D map. The path planner could be classified into two categories: the global path planner and the local planner. We selected the PSO algorithm as the global path planner in our approach.

The PSO algorithm searches for the best values by performing a simulation for each particle in the population at the given environmental data. The number of particles is generated around

the robot's initial position and within its sensing range. Each particle takes a new velocity and position based on the constantly updated PSO equations. A candidate for the robot's next position is determined by the position of the best particle, i.e., the one nearest to the goal. When the criteria for the PSO exiting are satisfied, a raw trajectory is obtained and postprocessed to generate the optimized trajectory.

In case of obstacles, which are suddenly appearing on the pre-planned path, the local path planner performs partial secondary path planning to avoid obstacles and to come to the target position and the disinfection process is done, Fig. 2. In case of people detection, where the ROS package for face recognition "Face Detector" from a stereo camera data is used, the robot must stop its disinfection process, Fig. 3. The face detector employs the OpenCV face detector, based on a cascade of Haar-like features to obtain an initial set of detections [38].

To disinfect the space as efficiently as possible, it is necessary to select points in the space from which the largest possible area of the room could be covered, Fig. 4.

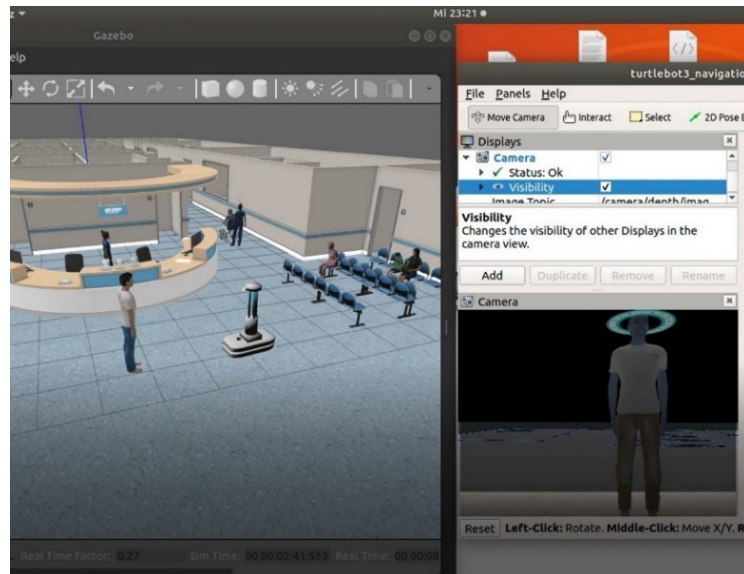


Fig. 3 ROS package "Face Detector" for people detection

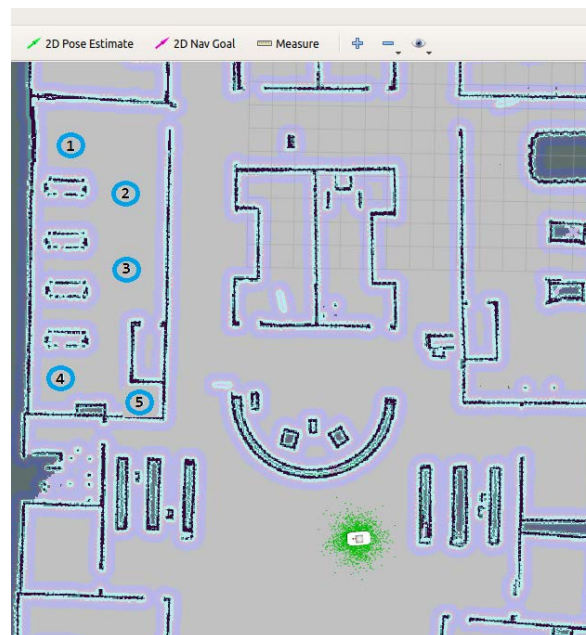


Fig. 4 Selected points in the mapped robot environment

Most path planners aim to generate an optimal path considering a single objective like path length or path travel time. However, in practice, path planning in dynamic environments emphasizes the necessity of considering multiple objects in path planning [21]. The used fitness function is generated as the weighted sum of the three objectives: the path shortness fitness function F_{sh} , the path smoothness fitness function F_{sm} . The shortest path is defined as the Euclidean distance between each newly generated particle and the goal in each iteration, and the smoothest path is defined as the robot moving angle in two successive iterations.

$$F = \alpha_1 \cdot F_{sh} + \alpha_2 \cdot F_{sm} \quad (3)$$

$$F_{sh} = \sqrt{(px_i^t - x_G)^2 + (py_i^t - y_G)^2} \quad (4)$$

$$F_{sh} = \cos^{-1} \frac{((px_i^t - x_G) \cdot (x_B - x_G)) + ((py_i^t - y_G) \cdot (y_B - y_G))}{\sqrt{((px_i^t - x_G)^2 + (py_i^t - y_G)^2)} \cdot \sqrt{((x_B - x_G)^2 + (y_B - y_G)^2)}} \quad (5)$$

where (px_i^t, py_i^t) is the position of i -th particle in iteration t , (x_G, y_G) is the goal position and (x_B, y_B) is the best position for the swarm. The weights of the shortest and smoothest fitness functions, α_1 and α_2 respectively, are in interval $0 \leq \alpha_1 + \alpha_2 \leq 1$.

The suitable path is obtained by minimizing this function F according to the assigned weights of each criterion.

4.3 DWA local planner

Dynamic Window Approach (DWA) to reactive collision avoidance which exists as ROS robot local navigation packet employed as the local planner in our research. Using a map, the planner creates a kinematic trajectory for the robot to get from a start to a goal location. The advantage of this approach is that reduces the search space to the dynamic window, which consists of the velocities reachable within a short time interval and which yield a trajectory on which the robot is able to stop safely [31]. Each simulated trajectory can be evaluated using an objective function that incorporates characteristics such as: proximity to obstacles, proximity to the goal, proximity to the global path:

$$F = \alpha_1 \cdot F_{ep} + \alpha_2 \cdot F_{lg} + \alpha_3 \cdot F_{oc} \quad (6)$$

where, F_{ep} denotes the distance to the path from the endpoint of the trajectory in meters, F_{lg} denotes the distance to the local goal from the endpoint of the trajectory in meters, and F_{oc} denotes the maximum obstacle cost along the trajectory [32]. α_i are the weighted coefficients of the related terms.

This ROS controller serves to connect the path planner to the robot and send the velocity value gained by maximizing an objective function. DWA is used here because its calculation time is short, the local path can be updated in real time and there is no dead angle obstacle or local optimization in the disinfection scenes [12].

5. Simulation and results

To analyse the function of the proposed PSO path planner algorithm, we ran several simulations in the ROS environment. The number of iterations, the particle number and the particle velocity are important factors influencing the performance of the PSO algorithm. The approach used in this simulation is varies those parameters and compares mobile robot trajectories and fitness function values. The same start and goal coordinates are used for all parameter values and the generated trajectories. Based on the results from these simulations, we tuned the algorithm parameters to optimal values.

The weights α_1 and α_2 are tuned through extensive simulation and try and errors, with the best-found values $\alpha_1 = 0.2$ and $\alpha_2 = 0.8$. As a competing method for comparing the PSO based global path planner using different weights α_1 and α_2 , the efficient standard Dijkstra's and Astar algorithms were selected, Fig. 5. and Fig. 6, respectively.

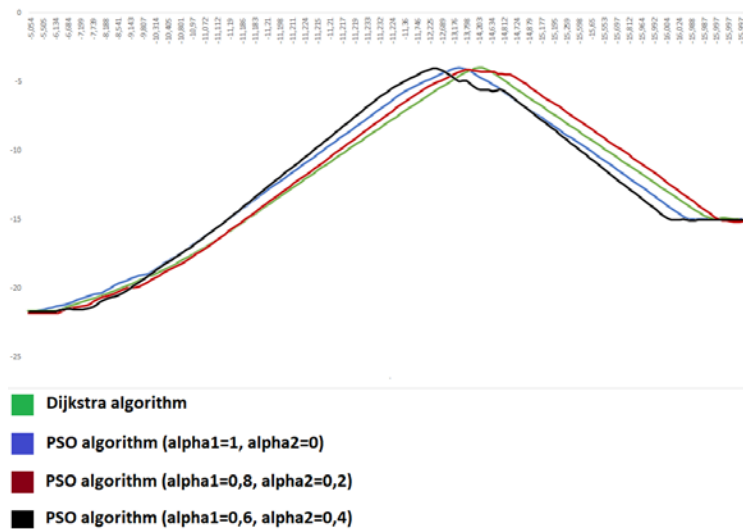


Fig. 5 Comparison of PSO global path planner of the mobile robot using different weights α_1 and α_2 , with the efficient standard Dijkstra's algorithm

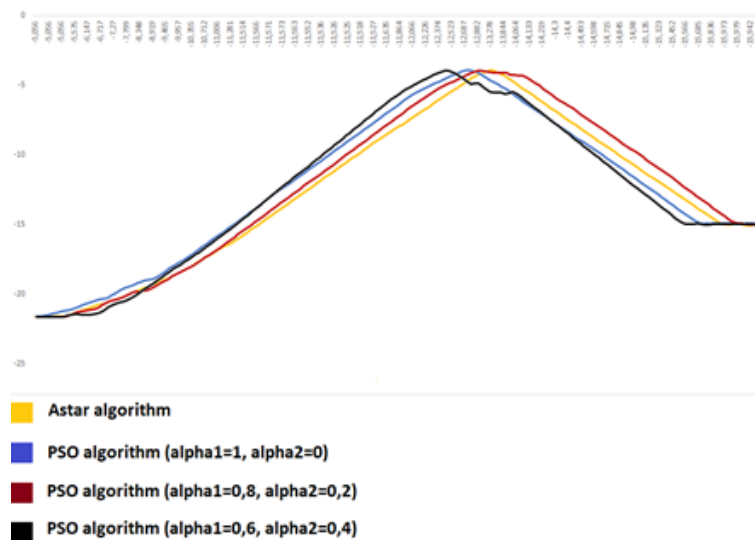


Fig. 6 Comparison of PSO global path planner of the mobile robot using different weights α_1 and α_2 , with the efficient standard Astar method

The results show that Dijkstra's and Astar algorithms generate almost identical paths. The PSO based path planner with weights $\alpha_1 = 0.2$ and $\alpha_2 = 0.8$ is the closest to the path generated by the Dijkstra's or the Astar algorithm. This is the path that is closest to the ideal path of the robot from the start to the end point, so this choice of coefficients is the best in those experiments. Variations can be made by reducing/increasing the number of iterations per calculation. In this experiment, the number of iterations was initially set to 25. Since the global planner performs a new plan calculation every 2 seconds, the 25-iteration PSO algorithm could not give up-to-date results and forward to the global planner, so it often happened that the robot deviated from the calculated path. Increasing the number of iterations results in greater accuracy in calculating the ideal path but requires more computing resources at the same time and results in a slower calculation. Fig. 7 presents the robot path with 2 iterations per calculation and the path with 5 iterations per calculation, compared to the path generated with the Astar algorithm. Both PSO paths have an initial variation in motion, because the robot loses the path for a short period of time until the calculation is performed. The deviation is larger when moving with 5 iterations per calculation because more time is required for the calculation. Therefore, the number of iterations was reduced to 2 iterations. The Fig. 8 presents comparison of path planning results, where the number of particles for the PSO algorithm was changed from 100 particles to 50 particles.

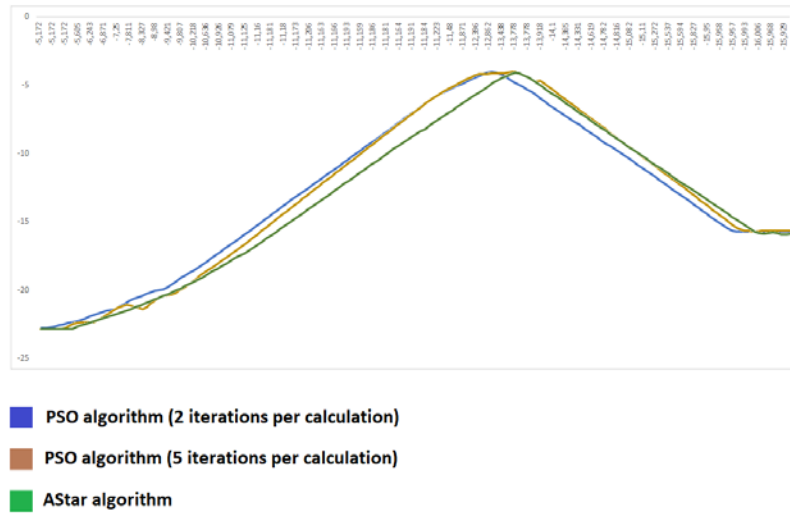


Fig. 7 Comparison of PSO path planning from the start to the end point for different values of the number of iterations with the Astar method

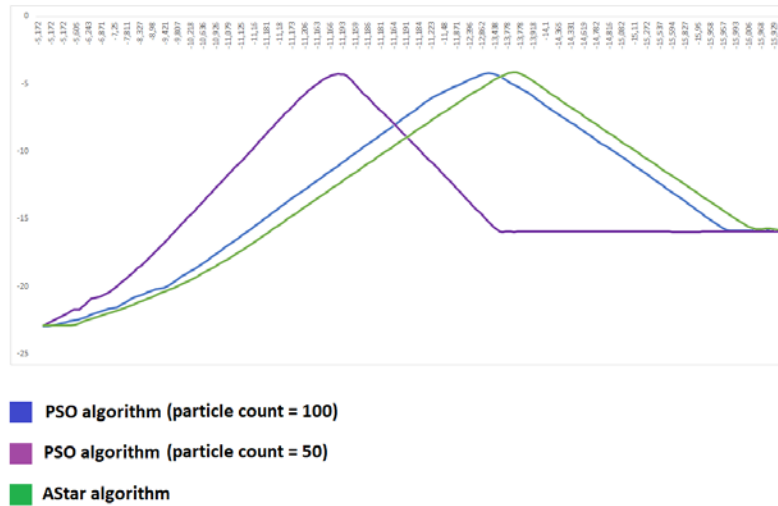


Fig. 8 Comparison of path planning produced by PSO algorithm for different values of the number of particles and the Astar method

A few graphical results of running DWA as the local path planner and PSO as the global path planner on problems with and without people as obstacles are illustrated consecutively in Figs. 9 and 10. Implementation of the PSO path planner with disinfection in the selected environment is presented in Fig. 9. A scenario where the mobile robot enters the room but recognizes people in the room and interrupts the disinfection process is presented in Fig. 10.

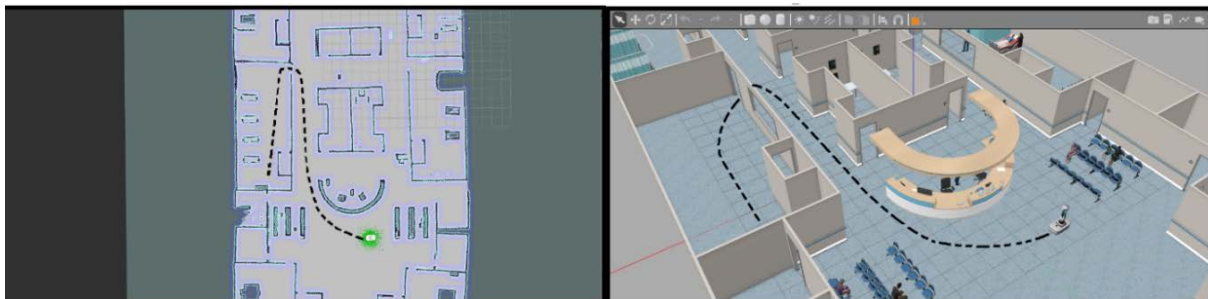


Fig. 9 Optimal path planning based on PSO with the finished disinfection task.

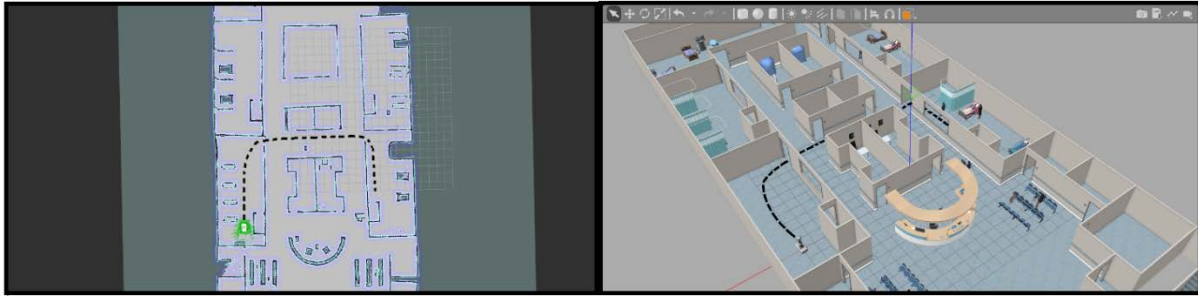


Fig. 10 Optimal path planning based on PSO with the cancelled disinfection task

6. Conclusion

In this paper, we present the DWA and PSO based path planning of an autonomous mobile disinfection robot based on Gmapping SLAM. The optimal path planning of the disinfection robot system was tested in the ROS indoor environment. By comparing PSO with the Dijkstra's and the Astar algorithms, it can be concluded that it is possible to easily improve path planning performance using PSO by adjusting parameters such as particle number, number of iterations, or fitness function coefficients. The simulation results show that the proposed method is effective as optimal path planner in combating COVID-19. In the future, more detailed work needs to be done in multi-criteria optimization of path planning combined with a disinfection model and people detection using deep learning. We are also planning to design and implement a disinfection mobile robot structure based on the discussed concepts.

Acknowledgement

This research is supported in scope of „Project Investigation of the optimal path of a mobile robot for Corona virus space disinfection“, funded by Ministry of Education, Science and Youth of Sarajevo Canton, Bosnia and Herzegovina, 2020-2021.

References

- [1] Ozkil, A.G., Fan, Z., Dawids, S., Aanes, H., Kristensen, J.K., Christensen, K.H. (2009). Service robots for hospitals: A case study of transportation tasks in a hospital, In: *Proceedings of 2009 IEEE International Conference on Automation and Logistics*, Shenyang, China, 289-294, doi: [10.1109/ICAL.2009.5262912](https://doi.org/10.1109/ICAL.2009.5262912).
- [2] Shen, Y., Guo, D., Long, F., Mateos, L.A., Ding, H., Xiu, Z., Hellman, R.B., King, A., Chen, S., Zhang, C., Tan, H. (2021). Robots under COVID-19 pandemic: A comprehensive survey, *IEEE Access*, Vol. 9, 1590-1615, doi: [10.1109/ACCESS.2020.3045792](https://doi.org/10.1109/ACCESS.2020.3045792).
- [3] Marsh, A. (2020). We've been killing deadly germs with UV light for more than a century, *IEEE Spectrum*, from <https://spectrum.ieee.org/tech-history/dawn-of-electronics/weve-been-killing-deadly-germs-with-uv-light-for-more-than-a-century>, accessed November 11, 2021.
- [4] Moore, K.S. (2020). Flight of the GermFalcon: How a potential coronavirus-killing airplane sterilizer was born, *IEEE Spectrum*, from <https://spectrum.ieee.org/germfalcon-coronavirus-airplane-ultraviolet-sterilizer-news>, accessed November 11, 2021.
- [5] Kraft, K. (2016). Robots against infectious diseases, In: *Proceedings of 2016 11th ACM/IEEE International Conference on Human-Robot Interaction (HRI)*, Christchurch, New Zealand, 627-628, doi: [10.1109/HRI.2016.7451889](https://doi.org/10.1109/HRI.2016.7451889).
- [6] Shi, M., Yang, H., Liao, X., Chen, Y., Xiao, S., Wu, J. (2021). Research on strategy of intelligent disinfection robot based on distributed constraint optimization, In: *Proceedings of 2021 IEEE International Conference on Artificial Intelligence and Computer Applications (ICAICA)*, Dalian, China, 82-85, doi: [10.1109/ICAICA52286.2021.9497927](https://doi.org/10.1109/ICAICA52286.2021.9497927).
- [7] Tan, X., Zhang, H., Zhou, X., Zhong, H., Liu, L. (2021). Research on graph-based SLAM for UVC disinfection robot, In: *Proceedings of 2021 IEEE International Conference on Real-time Computing and Robotics (RCAR)*, Xining, China, 1064-1069, doi: [10.1109/RCAR52367.2021.9517506](https://doi.org/10.1109/RCAR52367.2021.9517506).
- [8] Conte, D., Leamy, S., Furukawa, T. (2020). Design and map-based teleoperation of a robot for disinfection of COVID-19 in complex indoor environments, In: *Proceedings of 2020 IEEE International Symposium on Safety, Security, and Rescue Robotics (SSRR)*, Virtual event, 276-282, doi: [10.1109/SSRR50563.2020.9292625](https://doi.org/10.1109/SSRR50563.2020.9292625).
- [9] Sayed, A.S., Ammar, H.H., Shalaby, R. (2020). Centralized multi-agent mobile robots SLAM and navigation for COVID-19 field hospitals, In: *Proceedings of 2nd Novel Intelligent and Leading Emerging Sciences Conference (NILES)*, Giza, Egypt, 444-449, doi: [10.1109/NILES50944.2020.9257919](https://doi.org/10.1109/NILES50944.2020.9257919).

- [10] Correia Marques, J.M., Ramalingam, R., Pan, Z., Hauser, K. (2021). Optimized coverage planning for UV surface disinfection, In: *Proceedings of 2021 IEEE International Conference on Robotics and Automation (ICRA)*, Xi'an, China, 9731-9737, doi: [10.1109/ICRA48506.2021.9561032](https://doi.org/10.1109/ICRA48506.2021.9561032).
- [11] Conroy, J., Thierauf, C., Rule, P., Krause, E., Akitaya, H., Gonczi, A., Korman, M., Scheutz, M. (2021). Robot development and path planning for indoor ultraviolet light disinfection, In: *Proceedings of 2021 IEEE International Conference on Robotics and Automation (ICRA)*, Xi'an, China, 7795-7801, doi: [10.1109/ICRA48506.2021.9561405](https://doi.org/10.1109/ICRA48506.2021.9561405).
- [12] Ruan, K., Wu, Z., Chio, I., Zhang, Y., Xu, Q. (2021). Design and development of a new autonomous disinfection robot combating COVID-19 pandemic, In: *Proceedings of 2021 6th IEEE International Conference on Advanced Robotics and Mechatronics (ICARM)*, Chongqing, China, 803-808, doi: [10.1109/ICARM52023.2021.9536167](https://doi.org/10.1109/ICARM52023.2021.9536167).
- [13] Perminov, S., Mikhailovskiy, N., Sedunin, A., Okunevich, I., Kalinov, I., Kurenkov, M., Tsetserukou, D. (2021). UltraBot: Autonomous mobile robot for indoor UV-C disinfection, In: *Proceedings of 2021 IEEE 17th International Conference on Automation Science and Engineering (CASE)*, Lyon, France, 2147-2152, doi: [10.1109/CASE49439.2021.9551413](https://doi.org/10.1109/CASE49439.2021.9551413).
- [14] Marin-Plaza, P., Hussein, A., Martin, D., De la Escalera, A. (2018). Global and local path planning study in a ROS-based research platform for autonomous vehicles, *Journal of Advanced Transportation*, Vol. 2018, Article ID 6392697, doi: [10.1155/2018/6392697](https://doi.org/10.1155/2018/6392697).
- [15] Gao, P., Liu, Z., Wu, Z., Wang, D. (2019). A global path planning algorithm for robots using reinforcement learning, In: *Proceeding of 2019 IEEE International Conference on Robotics and Biomimetics (ROBIO)*, Dali, China, 1693-1698, doi: [10.1109/ROBIO49542.2019.8961753](https://doi.org/10.1109/ROBIO49542.2019.8961753).
- [16] Khan, A., Noreen, I., Habib, Z. (2017). On complete coverage path planning algorithms for non-holonomic mobile robots: Survey and challenges, *Journal of Information Science and Engineering*, Vol. 33, 101-121, doi: [10.6688/IJSE.2017.33.1.7](https://doi.org/10.6688/IJSE.2017.33.1.7).
- [17] Ferreira, J., Júnior, A.A.F., Galvão, Y.M., Barros, P., Fernandes, S.M.M., Fernandes, B.J.T. (2020). Performance improvement of path planning algorithms with deep learning encoder model, In: *Proceedings of 2020 Joint IEEE 10th International Conference on Development and Learning and Epigenetic Robotics (ICDL-EpiRob)*, Valparaiso, Chile, 1-6, doi: [10.1109/ICDL-EpiRob48136.2020.9278050](https://doi.org/10.1109/ICDL-EpiRob48136.2020.9278050).
- [18] Noreen, I., Khan, A., Habib, Z. (2017). Optimal path planning using RRT* based approaches: A survey and future directions, *International Journal of Advanced Computer Science and Applications*, Vol. 7, No. 11, 97-107, doi: [10.14569/IJACSA.2016.071114](https://doi.org/10.14569/IJACSA.2016.071114).
- [19] Robinson, J., Sinton, S., Rahmat-Samii, Y. (2002). Particle swarm, genetic algorithm, and their hybrids: Optimization of a profiled corrugated horn antenna, In: *Proceedings of IEEE Antennas and Propagation Society International Symposium (IEEE Cat. No.02CH37313)*, San Antonio, USA, 314-317.
- [20] Sulistijono, I.A., Kubota, N. (2006). A comparison of particle swarm optimization and genetic algorithm for human head tracking, In: *Proceedings of Joint 3rd International Conference on Soft Computing and Intelligent Systems and 7th International Symposium on advanced Intelligent Systems*, 2204-2209. doi: [10.14864/softscis.2006.0.2204.0](https://doi.org/10.14864/softscis.2006.0.2204.0).
- [21] Masehian, E., Sedighzadeh, D. (2010). A multi-objective PSO-based algorithm for robot path planning, In: *Proceedings of 2010 IEEE International Conference on Industrial Technology*, Via del Mar, Chile, 465-470, doi: [10.1109/ICIT.2010.5472755](https://doi.org/10.1109/ICIT.2010.5472755).
- [22] Xu, W., Yin, Y. (2018). Functional objectives decision-making of discrete manufacturing system based on integrated ant colony optimization and particle swarm optimization approach, *Advances in Production Engineering & Management*, Vol. 13, No. 4, 389-404, doi: [10.14743/apem2018.4.298](https://doi.org/10.14743/apem2018.4.298).
- [23] Banjanovic-Mehmedovic, L., Baluković, A. (2020). PSO optimized fuzzy controller for mobile robot path tracking, In: Karabegović, I. (ed.), *New technologies, development and application III, NT 2020, Lecture notes in networks and systems*, Springer, Switzerland AG, Vol. 128, 413-421, doi: [10.1007/978-3-030-46817-0_47](https://doi.org/10.1007/978-3-030-46817-0_47).
- [24] Yu, M.R., Yang, B., Chen, Y. (2018). Dynamic integration of process planning and scheduling using a discrete particle swarm optimization algorithm, *Advances in Production Engineering & Management*, Vol. 13, No. 3, 279-296, doi: [10.14743/apem2018.3.290](https://doi.org/10.14743/apem2018.3.290).
- [25] Wang, J.F., Kang, W.L., Zhao, J.L., Chu, K.Y. (2016). A simulation approach to the process planning problem using a modified particle swarm optimization, *Advances in Production Engineering & Management*, Vol. 11, No. 2, 77-92, doi: [10.14743/apem2016.2.211](https://doi.org/10.14743/apem2016.2.211).
- [26] Quigley, M., Gerkey, B., Conley, K., Faust, J., Foote, T., Leibs, J., Wheeler, R., Ng, A. (2009). ROS: An open-source robot operating system, *Proceedings of ICRA Workshop on Open Source Software*, Kobe, Japan.
- [27] Koenig, N., Howard, A. (2004). Design and use paradigms for Gazebo, an open-source multi-robot simulator, In: *Proceedings of 2004 IEEE/RSJ International Conference on Intelligent Robots and Systems (IROS) (IEEE Cat. No.04CH37566)*, Vol. 3, Sendai, Japan, 2149-2154, doi: [10.1109/IROS.2004.1389727](https://doi.org/10.1109/IROS.2004.1389727).
- [28] Alsadik, B., Karam, S. (2021). The simultaneous localization and mapping (SLAM) – An overview, *Surveying and Geospatial Engineering Journal*, Vol. 2, No. 1, 1-12, doi: [10.38094/sgej1027](https://doi.org/10.38094/sgej1027).
- [29] Grisetti, G., Stachniss, C., Burgard, W. (2007). Improved techniques for grid mapping with Rao-Blackwellized particle filters, *IEEE Transactions on Robotics*, Vol. 23, No. 1, 34-46, doi: [10.1109/TRO.2006.889486](https://doi.org/10.1109/TRO.2006.889486).
- [30] Wang, D., Tan, K., Dong, Y., Yuan, G., Du, X. (2020). Estimating the position and orientation of a mobile robot using neural network framework based on combined square-root cubature Kalman filter and simultaneous localization and mapping, *Advances in Production Engineering & Management*, Vol. 15, No. 1, 31-43, doi: [10.14743/apem2020.1.347](https://doi.org/10.14743/apem2020.1.347).

- [31] Fox, D., Burgard, W., Thrun, S. (1997). The dynamic window approach to collision avoidance, *IEEE Robotics & Automation Magazine*, Vol. 4, No. 1, 23-33, doi: [10.1109/100.580977](https://doi.org/10.1109/100.580977).
- [32] Chen, D., Lin, H. Zhao, C., Lei, J., Zou, J., Huang, L. (2021). Train carriage disinfection robot based on visual SLAM, *Journal of Computers*, Vol. 32, No. 3, 210-221, doi: [10.3966/199115992021063203015](https://doi.org/10.3966/199115992021063203015).
- [33] The Nav2 project, from <https://navigation.ros.org>, accessed November 11, 2021.
- [34] Gazebo robot simulator, from <http://gazebo.org/>, accessed November 11, 2021.
- [35] SVL Simulator, from <https://www.svl simulator.com/docs/tutorials/robotics-ros2/>, accessed November 11, 2021.
- [36] 3D visualization tool for ROS, from <http://wiki.ros.org/rviz>, accessed November 11, 2021.
- [37] ROS Navigation Stack, from <https://github.com/ros-planning/navigation>, accessed November 11, 2021.
- [38] ROS face detector, from http://wiki.ros.org/face_detector, accessed November 11, 2021.

Using augmented reality devices for remote support in manufacturing: A case study and analysis

Buń, P.^{a,*}, Grajewski, D.^a, Górski, F.^a

^aPoznan University of Technology, Poznań, Poland

ABSTRACT

Industry 4.0 forces increased digitization, production flexibility, improvement of employee competences and integration of employees and IT systems within an enterprise. To this end, state-of-the-art systems and IT solutions, such as the Virtual Reality (VR) and Augmented Reality (AR), are implemented. New systems must be integrated with the existing IT architecture, and their implementation forces the enterprise to provide network access with sufficient bandwidth to fully benefit from the capabilities of new technologies. The paper discusses the practical application of modern AR solutions in the industry, with a special focus on remote support for maintenance operations and training of production employees. Two experiments aimed determining the impact of various environmental conditions on the possibility of using the AR Remote Support are described. Basing on those experiments it is possible to determine the environmental conditions required to use HoloLens 2 AR goggles in two dedicated remote support applications.

ARTICLE INFO

Keywords:

Smart manufacturing;
Industry 4.0;
Remote support;
Augmented reality (AR);
Virtual reality;
HoloLens 2;
Ambient noise;
Wi-Fi networks

*Corresponding author:

pawel.bun@put.poznan.pl
(Buń, P.)

Article history:

Received 4 October 2021
Revised 10 December 2021
Accepted 11 December 2021



Content from this work may be used under the terms of the Creative Commons Attribution 4.0 International Licence (CC BY 4.0). Any further distribution of this work must maintain attribution to the author(s) and the title of the work, journal citation and DOI.

1. Introduction

In Industry 4.0 [1], which forces increasing digitization and automation of the manufacturing environment [2], workers' capabilities can be enhanced and augmented with new systems, machines, tools and advanced human-machine interaction technologies [3]. One of them is the Augmented Reality (AR), which, alongside the Virtual Reality [4], is one of the keys and most promising technologies for Industry 4.0 that can be used to support both factory workers and engineers at the workplace [5, 6]. The AR can be achieved by overlaying the information space, containing real-time task-relevant information, on top of the physical space [7]. AR applications remotely support new as well as experienced workers in task performance and with interactive repair instructions [8]. Despite all its advantages, the AR technology has not been used widely so far in real contexts of various complex industrial operations [9]. The reasons are complex, including the high cost [10] and inconvenient use of the AR equipment [11, 12], and the need for the enterprise to ensure adequate network capacity and IT infrastructure (including digitalization of products, processes and services [13]).

Even at the beginning of the 21st century, obtaining technical assistance or expert support required the physical presence of an expert who had the necessary knowledge and could solve the problem or instruct the employee [14]. This solution works well for small production companies where most of the activities are concentrated in one hall. In the case of larger enterprises, where production is distributed among many plants, the need to provide expert support in each of them may generate additional costs.

Remote support can help reduce costs by eliminating the physical presence of experts on the factory floor [15]. Unfortunately, voice communication may be insufficient if the problem is serious or difficult to describe, or the employee who is physically on site does not have sufficient competence to describe the problem. One way to solve the problem is to take a photo of the faulty resource and send it for expert assessment using email or cloud storage service. If the photo quality is good enough to provide the expert with necessary information, it can be annotated and sent back, or voice communication can be established to explain how to remedy the problem.

An AR remote support app which supports direct video and audio transmission can streamline the process by providing the expert with a better insight into the problem. Several of such applications have been developed so far; however, they all leave room for improvement. For example, the stabilization of annotations requires further enhancement [16]. Implementation of the AR technology, still under development, is very difficult in the industry due to technical limitations and ergonomics of devices. Nevertheless, its potential is widely recognized [17].

There are several solutions that support remote collaboration that use AR goggles, such as Microsoft Dynamics 365 (Remote Assist) or AR4vision. Although the applications can be used on tablets and smartphones, the software manufacturer recommends that the employee be equipped with AR goggles to have their hands free, what speeds up the operations significantly [18]. The remote expert runs the app on a PC, Mac or other mobile device. Both solutions provide audio and video communication for remote expert support in the field of:

- maintenance and servicing of machines,
- monitoring and inspection tasks.

The use of AR4vision helps to achieve savings resulting from the reduction of repair time, travel and machine downtime. The benefits include [19]:

- reduced time of reaction and task completion by 40 %,
- reduced travel costs by up to 70 %,
- remote training of staff,
- remote control and operation of machines and devices,
- owing to a quick response operators or service technicians, 30 % of failures and problems does not generate costs related to downtime or damage to the machine.

However, reliance on these data should be limited, as the data are not confirmed by the results of the study results published in peer-reviewed scientific journals. Most of the AR solutions described in scientific publications are evaluated in laboratory conditions, whilst data from hands-on implementations are scarce. Nevertheless, there are many examples of laboratory tests and prototype systems described in the literature, which use the AR to support operators during assembly/disassembly [20-22], maintenance [23, 24], welding operations [25], or inspection activities [26].

The AR technology can facilitate the implementation of new, innovative processes in industrial plants and improvement of the efficiency of existing ones. In particular, it enables the access to resources and knowledge bases, which in large enterprises and organizations combine hundreds of thousands of data and information sources [27]. Mobile AR technologies provide employees with easier access to resources, manuals, and user guides to solve everyday problems. They support remote work with specialists, even in geographically remote locations making it possible to quickly upload photos or videos to current reports. Additionally, they streamline communication among team members [28] and, in conjunction with other innovative technologies such as the Internet of Things and additive manufacturing, can affect supply chain management [29].

The AR has enabled an innovative approach to inspections, servicing and maintenance in the industry. Online data exchange and communication with other team members streamlines the

process of problem solving by non-experts in each field. Supported by the AR solutions, service technicians are able to perform less complex repairs with virtually no need for prior training. For example, Bosch offers technologies that combine the Augmented Reality and live streaming in the production and servicing of machines. Digital information received by employees (e.g., data sheets, technical data) is supplemented by live recordings [30].

A widespread introduction of the 5G technology is bound to support the AR in terms of remote access to enterprise knowledge bases. The manufacturers of AR solutions predict that the full potential of AR applications will only be achieved only owing to the 5G network (characterized by low latency and very high bandwidth [31]). Thus, the AR will have an even greater impact on efficiency, cost reduction, safety and speed of manufacturing processes [32].

The authors carried out a number of activities aimed at setting recommendations for the developed solutions and the conditions under which those solutions can be effectively implemented, in cooperation with an enterprise developing modern solutions for companies implementing the Industry 4.0 concept. The paper presents results of research undertaken to determine the environmental conditions required to be able to use remote support for the HoloLens 2 device. Two experiments have been conducted to determine the impact of ambient noise and Wi-Fi network quality on the applicability of the solution. The first experiment aimed to determine how environmental conditions, such as distance, walls, and other Wi-Fi networks, affect the quality of audio and video transmission through a remote support app. The second one was conducted to check how ambient noise affects the understanding of expert's instruction during a remote support call.

The paper describes results of studies made in cooperation with an external software development company, whose clients are production companies operating in the automotive sector. The two conditions (noise and Wi-Fi) were marked as the most relevant (i.e. problematic) during the course of previous factory floor implementations. That is why particular attention were paid to them.

2. Materials and methods

2.1 Research concept and plan

Two experiments were carried out to determine the impact of various environmental conditions on the possibility of using the AR Remote Support. The first experiment examined the quality of the impact of the Wi-Fi signal quality on the reception of audio/video content in AR Remote Support applications. The second experiment was aimed at assessing how noise affected the understanding of expert's instructions when using HoloLens 2. A simplified plan of experiments is presented in Fig. 1.

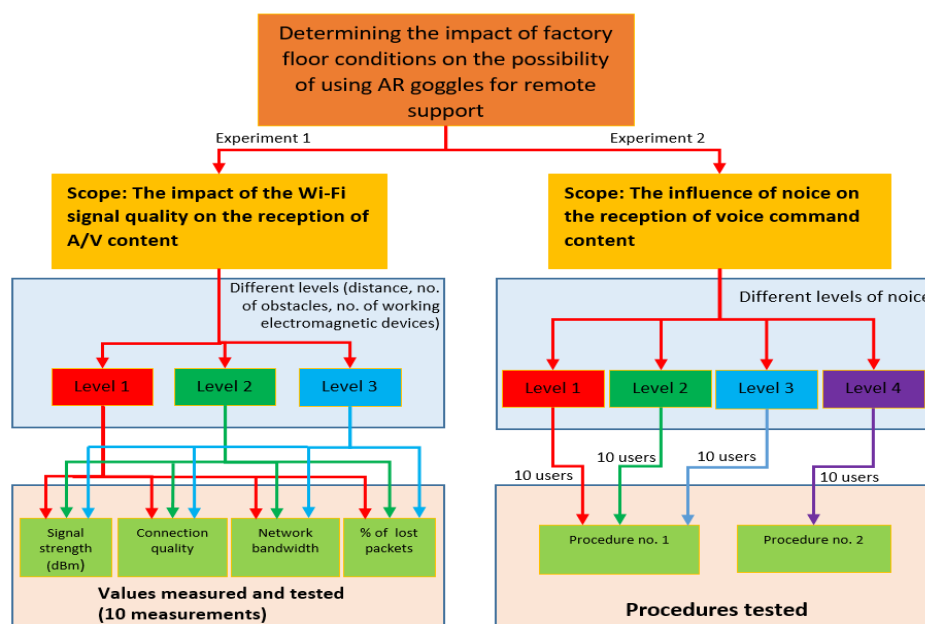


Fig. 1 Plan of experiments

2.2 Software and hardware used

Experiments were conducted using Microsoft HoloLens2 which is a standalone mixed reality device, that enables hands free interaction with displayed content. That type of interaction is possible with the help of voice commands, eye tracking, hand tracking and gesture recognition. This is made possible by a number of sensors, which are shown in the Table 1 that lists the device specifications.

Table 1 Microsoft HoloLens 2 specification [33]

| Parameter group | Parameter type | Parameter value |
|--------------------------|---------------------------------|---|
| Display | Optics | See-through holographic lenses (waveguides) |
| | Eye-based rendering | Display optimization for 3D eye position |
| Sensors | Head tracking | 4 visible light cameras |
| | Eye tracking | 2 Infrared (IR) cameras |
| | Depth | 1-MP Time-of-Flight depth sensor |
| | Inertial measurement unit (IMU) | Accelerometer, gyroscope, magnetometer |
| Audio and speech | Camera | 8-MP stills, 1080p30 video |
| | Microphone array | 5 channels |
| | Speakers | Built-in spatial sound |
| Compute and connectivity | Wi-Fi | 802.11ac 2x2 |
| | Bluetooth | 5 |
| | USB | USB Type-C DRP |
| Fit | Weight | 566 grams |

Two different software for AR remote support were used in experiments:

- Microsoft Dynamics 365 Remote Assist,
- Apzumi Spatial.

Microsoft Dynamics 365 Remote Assist allows the user to transfer visual instructions in the form of:

- files (graphic formats and PDF) containing digital machine documentation or operating / repair instructions,
- graphically applied comments on photos (screenshots) made by a service technician equipped with the AR goggles,
- annotations in the form of arrows (they can be anchored in the AR user space) to refer to specific parts of the machine or resource.

The Dynamics 365 platform also offers the Dynamics 365 Guide solution. It is a tool dedicated to the AR goggles, which enables employees to learn while working or in a training session by enabling access to holographic, interactive instructions. The app lets the user scan QR codes for procedures, located in the place where the job should be done. The database contains graphic files, movies, and 3D models for the operators to see what to do and where. It can be used as a learning tool as well as to support the performance of daily tasks and reduce the number of errors.

The solution includes easy-to-use forms for creating training content (step-by-step instructions, procedures illustrated with images, videos, and 3D models). The user equipped with HoloLens 2 can change the location of instructions / procedures in his workspace (move them to specific places, near a given machine or production line), or the instructions can move with the user. Extensive procedures feature prompts pointing to tools and parts that will be needed, as well as instructional data (e.g., presentations of how and where a given tool should be used).

Apzumi Spatial, developed by Apzumi, is an AR application designed to support production workers as well as maintenance and repair staff. The application also offers support in the training of new employees and the implementation of new products [34].

The application allows to display product visualizations, training procedures, production and operating procedures assistance, as well as connect with other users using the AR goggles and the Internet platform. The content of the platform can be created by the employees. It can be created by users themselves; however, most users will not have the right competences required. The content posted on the platform is typically multimedia (text, images, videos) and interactive animated

3D models. 3D models can be prepared by designers and 3D graphic designers, and the substantive content (the content of the manual) by trainers responsible for training, as well as specialists and experts. To access the platform content, the user needs to scan a QR code, generated for each 3D model or procedure in the phase of content creation.

The remote support module supports connection with specialists / experts in the given field, which facilitates remote service. Due to the high requirements for wireless connectivity, the module is treated as a separate layer of the system with specific requirements.

2.3 Wi-Fi requirements for video and audio transmission

In wireless communication, the dynamically changing network conditions (including link bandwidth, latency, packet loss, etc.) may affect the quality of audio and video connections, especially if devices such as AR goggles are used. Connections are also possible in environments with reduced link capacity; however, the quality of operation of selected functions may be severely deteriorated.

To effectively use the developed solution dedicated to the HoloLens 2 goggles at a satisfactory level, a minimum link bandwidth of 1.5 Mb / s (upload / download) is required. It applies to:

- peer-to-peer (P2P) video calls in Full HD resolution (1080p at 30 frames per second),
- reception of content and high-quality sound (15 fps).

However, an analysis of results of the first practical tests of the HoloLens 2 goggles, available on industry portals, shows that to obtain the optimal quality of video connections (i.e., without interruptions in the reception of video content), a bandwidth of at least 4-5 Mb should be provided [35]. However, even such wireless link parameters do not guarantee video connections with the expected / required image quality.

The minimum requirements for the Wi-Fi bandwidth for selected scenarios performed with the use of HoloLens 2 goggles (assuming that the device is located within the optimal range of the access point) are shown in Table 2.

Table 2 Minimum Wi-Fi bandwidth requirements for selected scenarios [36]

| Bandwidth (minimum) | Scenarios |
|---------------------|-------------------------------|
| 30 kb/s | audio P2P |
| 130 kb/s | audio P2P with screen sharing |
| 500 kb/s | video P2P, 360p at 30 fps |
| 1.2 Mb/s | video P2P, 720p at 30 fps |
| 1.5 Mb/s | video P2P, 1080p at 30 fps |

2.4 Experiment No. 1 – Influence of Wi-Fi quality on the AR remote support

The scope of experiment No. 1 was to investigate the impact of Wi-Fi signal quality on the reception of audio / video content. It was assumed that the tests were to be carried out at three levels, corresponding to three different distances from the access point and three different numbers of electronic devices up and running, affecting the electromagnetic interference generated:

- Level 1 (place: Smart Factory (SF) laboratory of an area of approx. 35 sq. m)
 - distance from the access point: 2-4 m (obstacles: no),
 - number of running electromagnetic devices: 4 (one notebook running in the active Wi-Fi connection mode, one Wi-Fi router – access point used, two smartphones in the active Wi-Fi connection mode).
- Level 2 (place: Virtual Reality (VR) laboratory of an area of approx. 60 sq. m)
 - distance from the access point: 6-10 m (obstacles: 1 partition wall),
 - number of running electromagnetic devices: 11 (three PC monitors, two PC base stations, two laptops, one Wi-Fi router, three smartphones in the active Wi-Fi connection mode).
- Level 3 (place: Rapid Prototyping (RP) Laboratory of an area of approximately 80 sq. m)
 - distance from the access point: 16-22 m (obstacles: 2 reinforced concrete walls + 1 partition wall),

- number of running electromagnetic devices: 16 (one notebook running in the active Wi-Fi connection mode, one Wi-Fi router, seven wireless Wi-Fi cameras, five devices for 3D printing, two smartphones in the active Wi-Fi connection mode).

The experiments were carried out within the range of several local wireless network access points available in the building of the Faculty of Mechanical Engineering, the Poznań University of Technology (Fig. 2):

1. SF laboratory (level 1) – 9 local networks.
2. VR laboratory (level 2) – 9 local networks.
3. RP laboratory (level 3) – 11 local networks.

The variables in the experiment were therefore the distance from the target point (different Wi-Fi signal strengths) and the electromagnetic disturbance.

The tested values were:

1. Signal strength (dBm).
2. Connection quality (assessed on a scale of 1-5).
3. Network bandwidth (measured in Mb/s when transferring a file of 500 MB).
4. Percentage number of packet errors in relation to the number of packets received (%).

For each level, ten attempts were made to download a file located on an external server using the Dropbox application. During the data download process, the bandwidth and signal strength of the Wi-Fi network were measured, and the number of communication errors was counted (a ping application was used to calculate the percentage number of erroneous packets in relation to the number of packets received).

Then, based on the obtained measurements, the connection quality was assessed on a Likert scale of 1-5.



Fig. 2 Interference of various Wi-Fi networks – view in the Wi-Fi Analyzer application

2.5 Experiment No. 2 – Impact of noise level on the quality of conversation

To determine the impact of noise level on the quality of conversation, tests were planned and then carried out at four levels:

- Level 1 (place: SF laboratory) – silence; no devices turned on (approx. 30 dB on average),
- Level 2 (place: SF laboratory) – presence of two interviewers (approx. 50 dB on average),
- Level 3 (place: SF laboratory) – presence of two interviewers and the production line switched on (approx. 70 dB on average),
- Level 4 (place: RP laboratory, presented in Fig. 3.) – conversation with an expert, accompanied by the Airpress HL155/25 compressor (1.1 kW) switched on (approx. 85 dB).



Fig. 3 Rapid Prototyping Laboratory containing multiple additive manufacturing devices and IP cameras

To determine the impact of noise level on the quality of conversation, tests were planned and then carried out at four levels:

Two remote support procedures were prepared for the experiment:

1. Procedure No. 1 (purpose: control of the control box elements, place of implementation; Smart Factory Lab – SF).
2. Procedure No. 2 (purpose: test activation of a selected device for additive manufacturing and change of selected settings, place of implementation; Rapid Manufacturing Laboratory – RP).

Both procedures are presented in the Fig. 4. Both procedures were performed by users wearing HoloLens 2 glasses and using Apzumi Spatial Call application (Fig. 5) and Dynamics 365 Remote Assist (Fig. 6).

The values tested were the reception of the content of audio commands as part of the procedures performed (%) and the fluency of the conversation and video transmission assessed by an expert who connected with the user of the AR goggles.

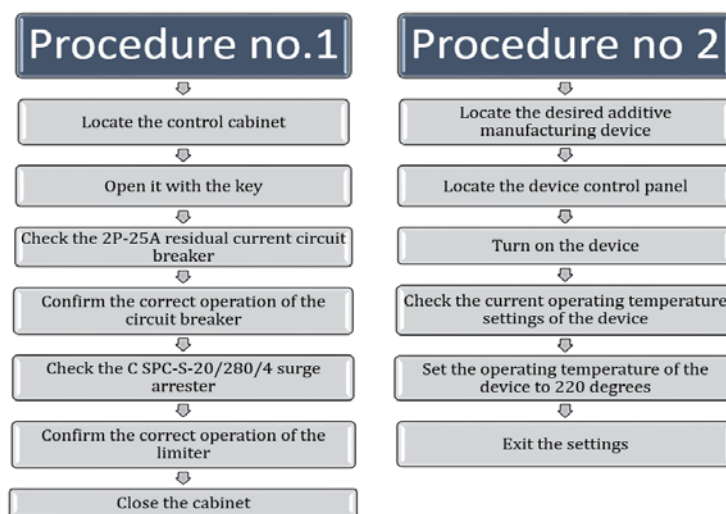


Fig. 4 Procedures carried out in the experiment No. 2

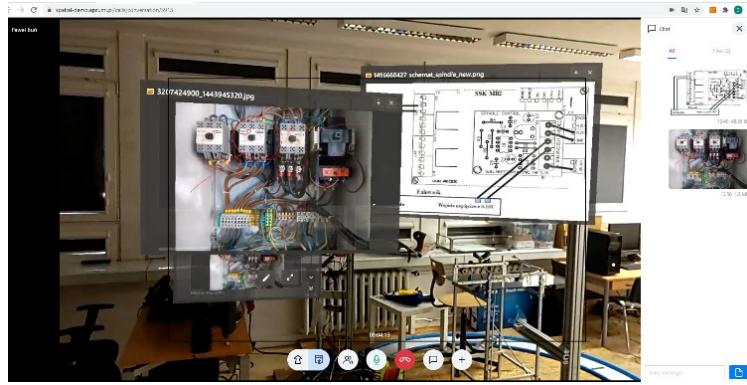


Fig. 5 Expert view in remote mode – Apzumi Spatial Call application (VR Laboratory)



Fig. 6 Expert View in Remote Mode – Dynamics 365 Remote Assist App (SF Laboratory)

3. Results and discussion

3.1 Experiment No. 1

The experiment examining the impact of the Wi-Fi signal quality consisted in 10 attempts, for each of the three levels defined above, to download a file located on an external server using the Dropbox application. During the data download process, the bandwidth and signal strength of the Wi-Fi network were measured, and the number of communication errors was counted (a ping application was used to calculate the percentage number of erroneous packets in relation to the number of packets received). Based on the obtained measurements, a subjective assessment of the connection quality made (on a scale of 1-5).

The results of the experiment are shown in Fig. 7. Interference levels are based on distance from access point (4/10/20 m), obstacles (no obstacles/ partition wall/ 2 reinforced walls, 1 partition wall), number of electronic devices up and running (4/11/16) and number of local Wi-Fi networks (9/9/11).

In addition, the maximum distances from the target point were set to ensure the reception of content at a satisfactory level:

1. in the absence of obstacles – 20 m,
2. with one obstacle (a partition wall) – 12 m,
3. more than one obstacle (a reinforced concrete wall + a partition wall) – 6 m.

Exceeding the maximum distances resulted in a significant decrease in the quality of the connection, as expected. A person wearing the AR goggles reported problems with receiving the data sent by the expert, while the expert noted a decrease in the quality of the A/V signal (Fig. 8).

A decrease in the video transmission quality and disturbances in the audio transmission impeded the conversation and made it impossible to understand the instructions given by an expert in the Remote Support application. Therefore, further in the study, this Wi-Fi network configuration was abandoned.

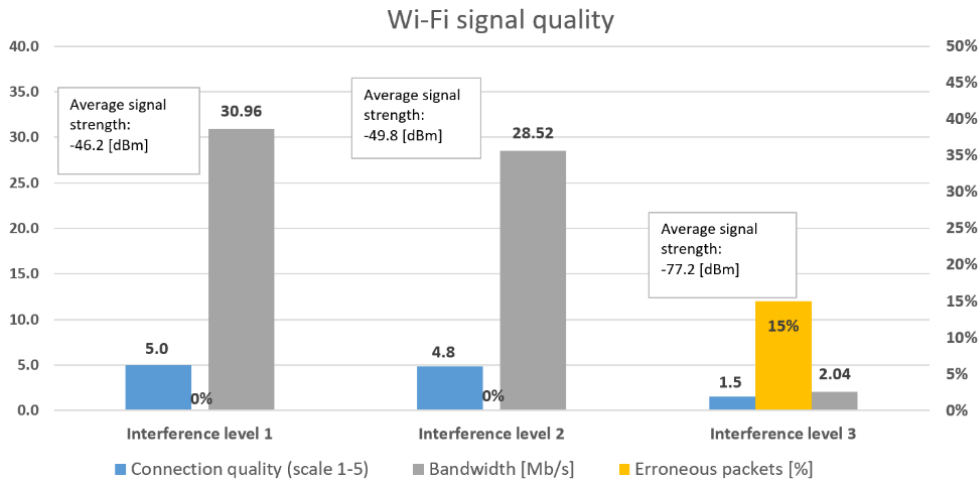


Fig. 7 Wi-Fi signal quality at selected interference levels

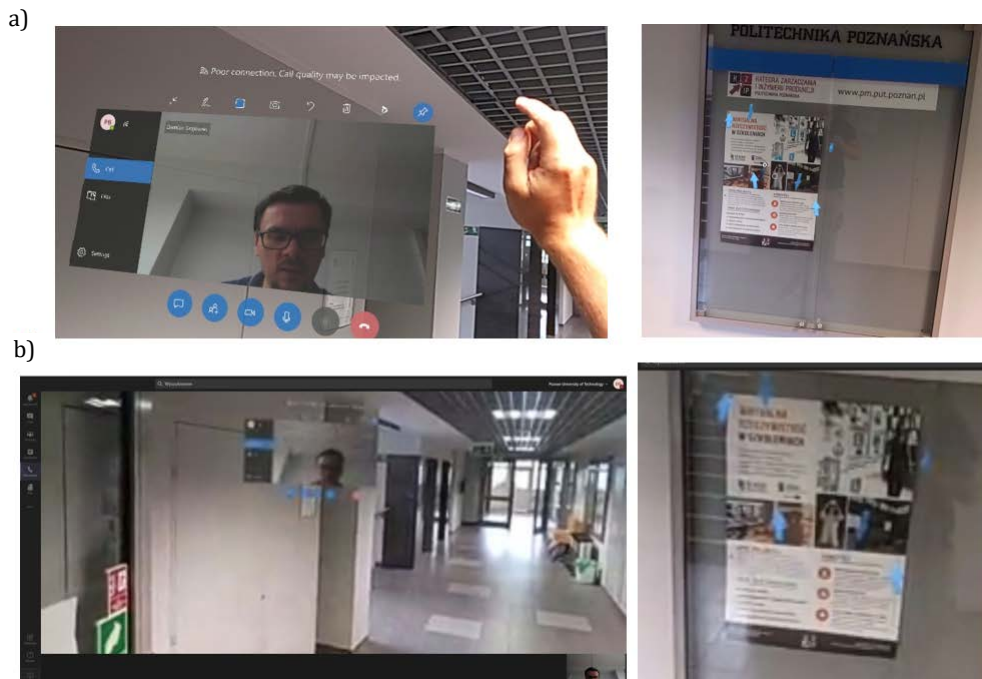


Fig. 8 View of the user of the AR goggles (a) and the expert in remote mode (b) in the case of exceeding the allowable distance from the access point

3.3 Experiment No. 2

Experiment consisted in examining the impact of noise on the ability to conduct a conversation and effectively implement the developed procedures using the HoloLens 2 glasses with the Apzumi Spatial Call application and the Dynamics 365 Remote Assist.

The values tested were the reception of audio commands, as part of the procedures performed (%), and the fluency of conversation and video transmission, assessed by an expert who connected with the user of the AR goggles. A total of 40 people took part in the study, testing both applications by implementing remote service procedures at four different noise levels (10 people for each noise level). The results and the average ratings are shown in Tables 3 and 4.

Based on a subjective assessment of the quality of conversation (reception of commands by the service technician and understanding of questions/answers by the expert) and video transmission (expert assessment in the remote mode), the functionality of both applications in terms of remote support of a production worker was compared.

Table 3 Results of experiment 2 (Apzumi Spatial Call application). ACC – Audio command comprehension, QA – Quality of audio, QV – Quality of video, AV – Average

| Attempt No. | Level 1 (lab SF) ca. 30 dB | | | Level 2 (lab SF) ca. 50 dB | | | Level 3 (lab SF) ca. 70 dB | | | Level 4 (lab RP) ca. 85 dB | | |
|-------------|----------------------------|----------|----------|----------------------------|----------|----------|----------------------------|----------|----------|----------------------------|----------|----------|
| | ACC (%) | QA [1-5] | QV [1-5] | ACC (%) | QA [1-5] | QV [1-5] | ACC (%) | QA [1-5] | QV [1-5] | ACC (%) | QA [1-5] | QV [1-5] |
| 1 | 100 | 5 | 5 | 100 | 5 | 5 | 100 | 4 | 5 | 0 | 1 | 1 |
| 2 | 100 | 5 | 5 | 100 | 5 | 5 | 100 | 5 | 5 | 0 | 1 | 1 |
| 3 | 100 | 5 | 5 | 100 | 5 | 5 | 100 | 4 | 5 | 0 | 1 | 2 |
| 4 | 100 | 5 | 5 | 100 | 5 | 5 | 100 | 3 | 4 | 0 | 1 | 1 |
| 5 | 100 | 5 | 5 | 100 | 4 | 5 | 100 | 5 | 5 | 0 | 1 | 1 |
| 6 | 100 | 5 | 5 | 100 | 5 | 5 | 50 | 3 | 5 | 0 | 1 | 1 |
| 7 | 100 | 5 | 4 | 100 | 5 | 5 | 100 | 3 | 4 | 0 | 1 | 2 |
| 8 | 100 | 5 | 5 | 100 | 5 | 5 | 50 | 5 | 5 | 0 | 1 | 1 |
| 9 | 100 | 5 | 5 | 100 | 5 | 5 | 100 | 4 | 5 | 0 | 1 | 1 |
| 10 | 100 | 5 | 5 | 100 | 5 | 5 | 100 | 4 | 5 | 0 | 1 | 2 |
| AV | 100 | 5.0 | 4.9 | 100 | 4.9 | 5.0 | 90 | 4.0 | 4.8 | 0 | 1.0 | 1.3 |

Table 4 Results of experiment 2 (Dynamics Remote Assist App).. ACC – Audio command comprehension, QA – Quality of audio, QV – Quality of video, AV – Average

| Attempt No. | Level 1 (lab SF) ca. 30 dB | | | Level 2 (lab SF) ca. 50 dB | | | Level 3 (lab SF) ca. 70 dB | | | Level 4 (lab RP) ca. 85 dB | | |
|-------------|----------------------------|----------|----------|----------------------------|----------|----------|----------------------------|----------|----------|----------------------------|----------|----------|
| | ACC (%) | QA [1-5] | QV [1-5] | ACC (%) | QA [1-5] | QV [1-5] | ACC (%) | QA [1-5] | QV [1-5] | ACC (%) | QA [1-5] | QV [1-5] |
| 1 | 100 | 5 | 5 | 100 | 5 | 5 | 100 | 4 | 5 | 0 | 1 | 1 |
| 2 | 100 | 5 | 5 | 100 | 5 | 5 | 100 | 3 | 5 | 0 | 1 | 1 |
| 3 | 100 | 4 | 4 | 100 | 4 | 5 | 50 | 4 | 4 | 0 | 1 | 1 |
| 4 | 100 | 5 | 5 | 100 | 5 | 4 | 100 | 3 | 3 | 0 | 1 | 1 |
| 5 | 100 | 5 | 5 | 100 | 4 | 5 | 50 | 3 | 4 | 0 | 1 | 1 |
| 6 | 100 | 5 | 5 | 100 | 4 | 5 | 50 | 4 | 5 | 0 | 1 | 1 |
| 7 | 100 | 5 | 4 | 100 | 5 | 5 | 100 | 3 | 4 | 0 | 1 | 1 |
| 8 | 100 | 5 | 5 | 100 | 5 | 5 | 50 | 4 | 5 | 0 | 1 | 1 |
| 9 | 100 | 5 | 5 | 100 | 5 | 5 | 100 | 2 | 5 | 0 | 1 | 1 |
| 10 | 100 | 5 | 5 | 100 | 5 | 5 | 100 | 4 | 5 | 0 | 1 | 1 |
| AV | 100 | 4.9 | 4.8 | 100 | 4.7 | 4.9 | 80 | 3.4 | 4.5 | 0 | 1.0 | 1.0 |

The most important observation concerning usability of the Apzumi Spatial Call solution dedicated to HoloLens 2 goggles in difficult industrial conditions is that at a noise level of approx. 50 dB, remote service can be provided conveniently. All the messages issued by an expert were understood without any problems by the users of goggles, thus it was possible to carry out the procedure. Neither the experts reported any problems with understanding the audio content. The situation changed at a noise level of 70 dB, where a decrease was observed in the comprehension of instructions and commands issued by an expert. Nonetheless, once repeated, the messages were understood, and the procedure performed. Additionally, a test was carried out at a noise level of 75 dB, which resulted in a significant decrease in the quality of audio content reception (down to 40 %). With the compressor running and the sound intensity exceeding 85 dB (level 4), it was practically impossible to talk. An additional difficulty was the distant location of the room (RP lab) where the compressor noise was emitted, which also led to a drop in ratings in the perception of video content. Slightly worse results were obtained from the tests of the Dynamics 365 Remote Assist application.

3.3 Discussion

Based on an analysis of the results, the following observations can be drawn:

- Terrain obstacles in buildings (walls, windows and doors) cause high attenuation and deterioration of the Wi-Fi signal quality.
- The presence of turned-on electronic devices generating electromagnetic field negatively affects the signal strength and connection bandwidth (decrease by ca. 10 %).
- Operation of other wireless networks causes interference; a large number of devices operating in particular bands causes the interference phenomenon.
- Low bandwidth when downloading 500 MB of data (the problem occurred at level 3). During the tests there were problems with the Wi-Fi connection on the HoloLens 2 device.

The studies were made in cooperation with an industrial company, which develops innovative industrial-grade MR platform, for automotive companies. Results of the described studies were directly implemented in the platform operation – a set of recommendations for the production companies was formulated, basing on the above-mentioned observations, and it was considered in future implementations.

4. Conclusion

The authors believe that the AR is a promising technology for remote employee support and expert consultation. With continuous access to database resources such as materials, device diagrams, 3D models and multimedia files, the employee is able to get an insight into the problem and figure out what repairs or maintenance works should be performed. However, both access to databases and expert consultation require Web access with sufficient bandwidth connectivity and appropriate network architecture. Applications such as Dynamics 365 Remote Assist and Apzumi Spatial facilitate the development of the IT layer, easy creation of databases and uploading of files containing all the necessary materials. Both support audio and video connections of production workers with field experts. However, their use in the industrial conditions is difficult due to certain environmental circumstances which affect the network capacity, as well as the noise generated by machines, which can reduce the audibility of expert instructions.

The research into the use of an AR application dedicated to the HoloLens 2 device shows that communication with experts is possible at a noise level of up to 75-80 dB. Extensive operation of industrial machines also affects the quality of AV transmission, verified based on both the measurements of signal strength and a subjective assessment of employees. Therefore, applied in an industrial environment, the applications may require the use of Wi-Fi signal amplifiers [37].

Despite the above-mentioned limitations, users expressed a very positive opinion on both solutions and emphasized how valuable for them were the functions related to remote expert support, annotation and the possibility of sending photos, diagrams and other multimedia content.

The obtained results are new – the scientific contribution is clear determination of Wi-Fi and ambient noise conditions, under which a Mixed Reality application can function in the factory floor, which was not fully known in earlier literature. The results were implemented in selected industrial companies.

Further research planned by the authors will include, among others, tests in real conditions – in a factory floor, and a study of the impact of using Wi-Fi signal amplifiers on the audibility, file transmission and ability to carry out machine repairs or inspections using the described AR remote support applications. Another factor to consider is the use of a headphones and microphone, connected to an MR device, with active background noise suppression. Before implementing AR Remote support technology, managers who want to modernize manufacturing process should examine the factory floor conditions and consider the implementation of the above-mentioned solutions. However, until we carry out the research, we are not able to assess their effectiveness.

Acknowledgement

The research work was done as a part of a project with Apzumi company and was partially supported by the Ministry of Education and Science, Republic of Poland, under the project 0613/SBAD/4677.

References

- [1] Sari, T., Güleş, H.K., Yiğitöl, B. (2020). Awareness and readiness of Industry 4.0: The case of Turkish manufacturing industry, *Advances in Production Engineering & Management*, Vol. 15, No.1, 57-68, doi: [10.14743/apem.2020.1.349](https://doi.org/10.14743/apem.2020.1.349).
- [2] Oesterreich, T.D., Teuteberg, F. (2016). Understanding the implications of digitisation and automation in the context of industry 4.0: A triangulation approach and elements of a research agenda for the construction industry, *Computers in Industry*, Vol. 83, 121-139, doi: [10.1016/j.compind.2016.09.006](https://doi.org/10.1016/j.compind.2016.09.006).
- [3] Romero, D., Stahre, J., Taisch, M. (2020). The Operator 4.0: Towards socially sustainable factories of the future, *Computers & Industrial Engineering*, Vol. 139, Article No. 106128, doi: [10.1016/j.cie.2019.106128](https://doi.org/10.1016/j.cie.2019.106128).

- [4] Żywicki, K., Zawadzki, P., Górski, F. (2018). Virtual reality production training system in the scope of intelligent factory, *Advances in Intelligent Systems and Computing*, Vol. 637, 450-458, doi: [10.1007/978-3-319-64465-3_43](https://doi.org/10.1007/978-3-319-64465-3_43).
- [5] Marino, E., Barbieri, L., Colacino, B., Fleri, A.K., Bruno, F. (2021). An Augmented Reality inspection tool to support workers in Industry 4.0 environments, *Computers in Industry*, Vol. 127, Article No. 103412, doi: [10.1016/j.compeind.2021.103412](https://doi.org/10.1016/j.compeind.2021.103412).
- [6] Urbas, U., Ariansyah, D., Erkoyuncu, J.A., Vukašinić, N. (2021). Augmented reality aided inspection of gears, *Tehnički Vjesnik – Technical Gazette*, Vol. 28, No. 3, 1032-1037, doi: [10.17559/TV-20200728151912](https://doi.org/10.17559/TV-20200728151912).
- [7] Uva, A.E., Gattullo, M., Manghisi, V.M., Spagnulo, D., Cascella, G.L., Fiorentino, M. (2018). Evaluating the effectiveness of spatial augmented reality in smart manufacturing: A solution for manual working stations, *The International Journal of Advanced Manufacturing Technology*, Vol. 94, 509-521, doi: [10.1007/s00170-017-0846-4](https://doi.org/10.1007/s00170-017-0846-4).
- [8] Castellanos, M.J., Navarro-Newball, A.A. (2019). Prototyping an augmented reality maintenance and repairing system for a deep well vertical turbine pump, In: *2019 International Conference on Electronics, Communications and Computers (CONIELECOMP)*, 36-40, doi: [10.1109/CONIELECOMP.2019.8673254](https://doi.org/10.1109/CONIELECOMP.2019.8673254).
- [9] Bottani, E., Vignali, G. (2019). Augmented reality technology in the manufacturing industry: A review of the last decade, *IISE Transactions*, Vol. 51, No. 3, 284-310, doi: [10.1080/24725854.2018.1493244](https://doi.org/10.1080/24725854.2018.1493244).
- [10] Kulkov, I., Berggren, B., Hellström, M., Wikström, K. (2021). Navigating uncharted waters: Designing business models for virtual and augmented reality companies in the medical industry, *Journal of Engineering and Technology Management*, Vol. 59, Article No. 101614, doi: [10.1016/j.jengtecman.2021.101614](https://doi.org/10.1016/j.jengtecman.2021.101614).
- [11] Palmarini, R., Erkoyuncu, J.A., Roy, R., Torabmostaedi, H. (2018). A systematic review of augmented reality applications in maintenance, *Robotics and Computer-Integrated Manufacturing*, Vol. 49, 215-228, doi: [10.1016/j.rcim.2017.06.002](https://doi.org/10.1016/j.rcim.2017.06.002).
- [12] Vujica Herzog, N., Buchmeister, B., Beharic, A., Gajsek, B. (2018). Visual and optometric issues with smart glasses in Industry 4.0 working environment, *Advances in Production Engineering & Management*, Vol. 13, No. 4, 417-428, doi: [10.14743/apem2018.4.300](https://doi.org/10.14743/apem2018.4.300).
- [13] Ellingsen, O., Aasland, K.E. (2019). Digitalizing the maritime industry: A case study of technology acquisition and enabling advanced manufacturing technology, *Journal of Engineering and Technology Management*, Vol. 54, 12-27, doi: [10.1016/j.jengtecman.2019.06.001](https://doi.org/10.1016/j.jengtecman.2019.06.001).
- [14] Ludwig, T., Stickel, O., Tolmie, P., Sellmer, M. (2021). shARe-IT: Ad hoc remote troubleshooting through augmented reality, *Computer Supported Cooperative Work (CSCW)*, Vol. 30, 119-167, doi: [10.1007/s10606-021-09393-5](https://doi.org/10.1007/s10606-021-09393-5).
- [15] Obermair, F., Althaler, J., Seiler, U., Zeilinger, P., Lechner, A., Pfaffeneder, L., Richter M., Wolfartsberger, J. (2020). Maintenance with augmented reality remote support in comparison to paper-based instructions: Experiment and analysis, In: *2020 IEEE 7th International Conference on Industrial Engineering and Applications (ICIEA)*, 942-947, doi: [10.1109/ICIEA49774.2020.9102078](https://doi.org/10.1109/ICIEA49774.2020.9102078).
- [16] Chang, Y.S., Nuernberger, B., Luan, B., Höllerer, T. (2017). Evaluating gesture-based augmented reality annotation, In: *2017 IEEE Symposium on 3D User Interfaces (3DUI)*, 182-185, doi: [10.1109/3DUI.2017.7893337](https://doi.org/10.1109/3DUI.2017.7893337).
- [17] Egger, J., Masood, T. (2020). Augmented reality in support of intelligent manufacturing – A systematic literature review, *Computers & Industrial Engineering*, Vol. 140, Article No. 106195, doi: [10.1016/j.cie.2019.106195](https://doi.org/10.1016/j.cie.2019.106195).
- [18] Syberfeldt, A., Holm, M., Danielsson, O., Wang, L., Brewster, R.L. (2016). Support systems on the industrial shop-floors of the future – Operators' perspective on augmented reality, *Procedia CIRP*, Vol. 44, 108-113, doi: [10.1016/j.procir.2016.02.017](https://doi.org/10.1016/j.procir.2016.02.017).
- [19] AR4vision. Benefits of Augment Reality, from <https://ar4vision.pl/#korzyzsci>, accessed September 7, 2021.
- [20] Ojer, M., Alvarez, H., Serrano, I., Saiz, F.A., Barandiaran, I., Aguinaga, D., Querejeta, L., Alejandro, D. (2020). Projection-based augmented reality assistance for manual electronic component assembly processes, *Applied Sciences*, Vol 10, No. 3, 796, doi: [10.3390/app10030796](https://doi.org/10.3390/app10030796).
- [21] Blattgerste, J., Renner, P., Strenge, B., Pfeiffer, T. (2018). In-situ instructions exceed side-by-side instructions in augmented reality assisted assembly, In: *Proceedings of the 11th Pervasive Technologies Related to Assistive Environments Conference*, 133-140, doi: [10.1145/3197768.3197778](https://doi.org/10.1145/3197768.3197778).
- [22] Kranzer, S., Prill, D., Aghajanpour, D., Merz, R., Strasser, R., Mayr, R., Zoerrler, H., Plasch, M., Steringer, R. (2017). An intelligent maintenance planning framework prototype for production systems, In: *2017 IEEE International Conference on Industrial Technology (ICIT)*, doi: [10.1109/ICIT.2017.7915520](https://doi.org/10.1109/ICIT.2017.7915520).
- [23] Del Amo, I.F., Erkoyuncu, J.A., Roy, R., Wilding, S. (2018). Augmented reality in maintenance: An information-centred design framework, *Procedia Manufacturing*, Vol. 19, 148-155, doi: [10.1016/j.promfg.2018.01.021](https://doi.org/10.1016/j.promfg.2018.01.021).
- [24] Palmarini, R., Erkoyuncu, J.A., Roy, R., Torabmostaedi, H. (2018). A systematic review of augmented reality applications in maintenance, *Robotics and Computer-Integrated Manufacturing*, Vol. 49, 215-228, doi: [10.1016/j.rcim.2017.06.002](https://doi.org/10.1016/j.rcim.2017.06.002).
- [25] Antonelli, D., Astanin, S. (2015). Enhancing the quality of manual spot welding through augmented reality assisted guidance, *Procedia CIRP*, Vol. 33, 556-561, doi: [10.1016/j.procir.2015.06.076](https://doi.org/10.1016/j.procir.2015.06.076).
- [26] Ramakrishna, P., Hassan, E., Hebbalaguppe, R., Sharma, M., Gupta, G., Vig, L., Sharma, G., Shroff, G. (2016). An AR inspection framework: Feasibility study with multiple ar devices. In: *2016 IEEE International Symposium on Mixed and Augmented Reality (ISMAR-Adjunct)*, 221-226, doi: [10.1109/ISMAR-Adjunct.2016.0080](https://doi.org/10.1109/ISMAR-Adjunct.2016.0080).
- [27] Galkin, M., Auer, S., Scerri, S. (2016). Enterprise knowledge graphs: A backbone of linked enterprise data, In: *2016 IEEE/WIC/ACM International Conference on Web Intelligence (WI)*, 497-502, doi: [10.1109/WI.2016.0083](https://doi.org/10.1109/WI.2016.0083).
- [28] Fraga-Lamas, P., Fernandez-Carames, T.M., Blanco-Novoa, O., Vilar-Montesinos, M.A. (2018). A review on industrial augmented reality systems for the industry 4.0 shipyard, *IEEE Access*, Vol. 6, 13358-13375, doi: [10.1109/ACCESS.2018.2808326](https://doi.org/10.1109/ACCESS.2018.2808326).

- [29] Sabri, Y., Micheli, G.J.L., Nuur, C. (2018). Exploring the impact of innovation implementation on supply chain configuration, *Journal of Engineering and Technology Management*, Vol. 49, 60-75, doi: [10.1016/j.jengtecman.2018.06.001](https://doi.org/10.1016/j.jengtecman.2018.06.001).
- [30] BOSCH. Augmented Reality applied within Bosch technical service trainings, from: <https://www.boschautomotiveservicesolutions.com/examples-augmented-reality-applications>, accessed August 30, 2021.
- [31] Parvez, I., Rahmati, A., Guvenc, I., Sarwat, A.I., Dai, H. (2018). A survey on low latency towards 5G: RAN, core network and caching solutions. *IEEE Communications Surveys & Tutorials*, Vol. 20, No. 4, 3098-3130 doi: [10.1109/COMST.2018.2841349](https://doi.org/10.1109/COMST.2018.2841349).
- [32] Siriwardhana, Y., Porambage, P., Liyanage, M., Ylianttila, M. (2021). A survey on mobile augmented reality with 5G mobile edge computing: Architectures, applications and technical aspects, *Communications Surveys & Tutorials*, Vol. 23, No. 2, 1160-1192, doi: [10.1109/COMST.2021.3061981](https://doi.org/10.1109/COMST.2021.3061981).
- [33] Microsoft. HoloLens2 specification, from <https://docs.microsoft.com/en-us/hololens/hololens2-hardware>, accessed August 30, 2021.
- [34] Apzumi. Apzumi Spatial, from <https://spatial.apzumi.com/>, accessed March 30, 2021.
- [35] Microsoft. Technical requirements for deploying and using Dynamics 365 Remote Assist, from <https://docs.microsoft.com/en-us/dynamics365/mixed-reality/remote-assist/requirements>, accessed March 22, 2021.
- [36] Microsoft. Prepare your organization's network for Microsoft Teams, from <https://docs.microsoft.com/en-us/MicrosoftTeams/prepare-network#best-practice-monitor-your-network-using-cq-d-and-call-analytics>, accessed August 22, 2021.
- [37] Batalla, J.M. (2020). On analyzing video transmission over wireless Wi-Fi and 5G C-band in harsh IIoT environments, *IEEE Access*, Vol. 8, 118534-118541, doi: [10.1109/ACCESS.2020.3005641](https://doi.org/10.1109/ACCESS.2020.3005641).

The impact of the collaborative workplace on the production system capacity: Simulation modelling vs. real-world application approach

Ojstersek, R.^{a,*}, Javernik, A.^a, Buchmeister, B.^a

^aUniversity of Maribor, Faculty of Mechanical Engineering, Maribor, Slovenia

ABSTRACT

In recent years, there have been more and more collaborative workplaces in different types of manufacturing systems. Although the introduction of collaborative workplaces can be cost-effective, there is still much uncertainty about how such workplaces affect the capacity of the rest of production system. The article presents the importance of introducing collaborative workplaces in manual assembly operations where the production capacities are already limited. With the simulation modelling method, the evaluation of the introduction impact of collaborative workplaces on manual assembly operations that represent bottlenecks in the production process is presented. The research presents two approaches to workplace performance evaluation, both simulation modelling and a real-world collaborative workplace example, as a basis of a detailed time study. The main findings are comparisons of simulation modelling results and a study of a real-world collaborative workplace, with graphically and numerically presented parameters describing the utilization of production capacities, their efficiency and financial justification. The research confirms the expediency of the collaborative workplaces use and emphasise the importance of further research in the field of their technological and sociological impacts.

ARTICLE INFO

Keywords:
Simulation modelling;
Production system capacity;
Industry 5.0;
Assembly line;
Human-robot collaboration;
Collaborative workplace

**Corresponding author:*
robert.ojstersek@um.si
(Ojstersek, R.)

Article history:
Received 7 September 2021
Revised 11 December 2021
Accepted 13 December 2021



Content from this work may be used under the terms of the Creative Commons Attribution 4.0 International Licence (CC BY 4.0). Any further distribution of this work must maintain attribution to the author(s) and the title of the work, journal citation and DOI.

1. Introduction

Optimization of production systems has been an attractive research field for many decades. Researchers are constantly wondering how to improve production system capacity or use it as efficiently as possible. In recent years, there have been an increasing number of collaborative machines that, together with workers, form high flexible, economically justified collaborative workplaces. Collaborative machines are to some extent already well studied, but their impact on the collaborative workplace, on workers and more broadly on the manufactured system is often unknown. Where is the turning point when a collaborative workplace is economically, socially and from a capacity standpoint justified? We want to answer this complex research question.

Researchers have been asking for years who is working with whom (human with robot, or vice versa) [1]. This issue, given the complexity of the social dimensions of the collaborative workplace and the security parameters, raises a lot of unanswered questions from the worker's point of view [2]. The findings show that we are talking about a hybrid research area, associated with a concept of Industry 5.0 [3, 4], where safety meets ergonomics, technological efficiency, and the unanswered

question of the integrated impact of collaborative workplaces on the production system [5]. As we know, proper ergonomic analysis of workplaces significantly improves their productivity [6], but this is only proven in manual assembly workplaces; how different production parameters can affect the collaborative workplace is not known. Only general guidelines for the preparation and arrangement of the collaborative workplaces are given [7], where the authors still draw parallels with the manual assembly workplaces [8]. The shortcomings of such research are highlighted when we want to analyse in detail the impact of collaborative workplaces on the sustainable justification of the production system [9]. The authors cite limitations in terms of different time, cost and technological suitability of collaborative workplace parameters. Determining the appropriate "collaborative" parameters [10] is crucial in the use of efficient and safe (for worker and robot) workplaces [11]. Research work presents that states of safe parameters of speed and acceleration of collaborator robots in a common workspace [12], but how the change of parameters affects the efficiency of the collaborative workplace and other production capacities is hard to define [13]. Due to these limitations, researchers want to provide a general methodology for the introduction of collaborative workplaces [14], but when one of the general advantages is high flexibility of collaborative machines and associated production systems [15] in which we include them, the implementation is very demanding, most often made individually [16]. The answers to the questions about the feasibility of introducing collaborative workplaces must thus respond to an appropriate investment strategy [17] and the sustainable justification of such workplaces and their wider impact [9]. Correlations between these parameters [18] can be well represented by simulation modelling methods [19], where an integrated approach to planning and deployment of collaborative workplaces can be evaluated and the collaborative workplace constructed accordingly [20]. Recent research shows that it will be necessary to know the technological behaviour of the collaborating machine and, more importantly, its sociological impact on the co-worker [21]. The response that a co-worker may have to a collaborative workplace is complex and individual according to the employee's condition. More broadly, the impact of a collaborative workplace can significantly change production capacities and their efficiency. It should be emphasized that the collaborative workplace can be placed in different types of production systems, in different configurations, which represent an additional complexity of its optimization [22].

In our research work we want to answer the question of determining the collaborative workplace parameters (time study and financial norms) when introducing it into an existing production system. In doing so, we focus on the use of simulation modelling methods and the evaluation of a real-world collaborative workplace. Data from detailed time and costs analysis will enable the implementation and comparison of the broader impact of the collaborative workplace on the entire production system, where a comparison will be made between manual assembly and collaborative workplaces. The research is based on the study of the production system of assembly line and attempts to improve its limited production capacity.

2. Problem description

Optimizing an assembly production line system is a major challenge if the system is already at the minimum possible takt time and is no longer able to optimize assembly processing time for individual workplaces. Such an assembly line system, when orders increase, faces the inability to achieve the desired quantity of products with limited assembly capacities. In recent years, manual assembly workplaces have been automated and robotized, and such workplaces have some limitations as production capacity increases, investment costs increase, new equipment is introduced, and the size of such fully automated cells increases assembly line footprint. Given that the assembly line production system presented in Fig. 1 and the corresponding processing time data in Table 1 indicate assembly line constraints at manual assembly workplaces M_{as8} and M_{as9} , where the assembly processing time is equal to the line takt time. The question of the feasibility of introducing collaborative workplaces where the manual assembly is upgraded with the capacities of a collaborative robot, whose initial investment and introduction to an existing job is less demanding, is questionable.

2.1 Production system description

The research problem deals with the products assembly line with ten manual assembly workstations (M_{as}) and associated workstations processing times (work-element times) presented in Fig. 1 and Table 1 respectively. The assembly line production system has a certain line takt time of 54 s, a constant speed of the conveyor belt of 1.2 m/min, an additional mark-up coefficient of the conveyor belt length of 0.05. The assembly line is carried out in three shifts in five working days a week. Workers in the manual jobs of the assembly have a certain useful number of working hours in a shift, lasting 7.5 h. Transport to the initial station of the assembly line and shipment of finished products is carried out with the use of forklifts. Input semi-finished products and component assembly accessories are always available to the assembly workers.

Table 1 Assembly line manual workplaces processing times

| Workplace | M_{as1} | M_{as2} | M_{as3} | M_{as4} | M_{as5} | M_{as6} | M_{as7} | M_{as8} | M_{as9} | M_{as10} |
|---------------------|-----------|-----------|-----------|-----------|-----------|-----------|-----------|-----------|-----------|------------|
| Processing time (s) | 52 | 51 | 49 | 48 | 52 | 51 | 52 | 54 | 54 | 48 |

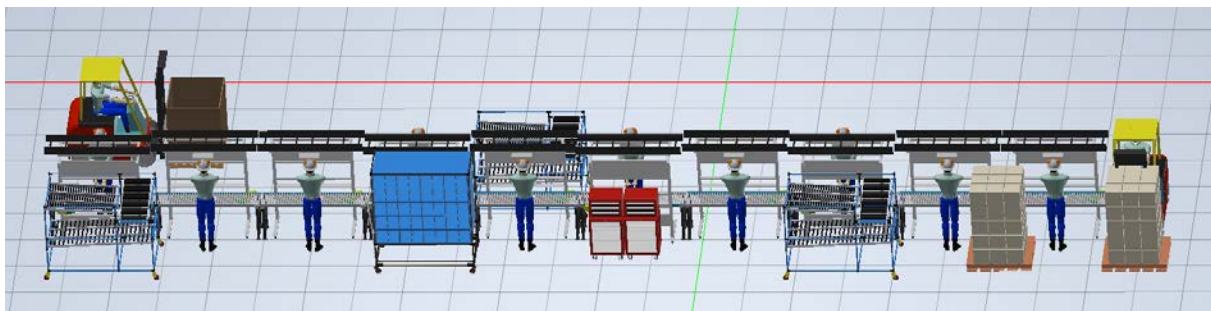


Fig. 1 Production system – manual assembly line with ten workplaces (3D model)

Eqs. 1 to 7 represent a numerical calculation of the assembly line characteristics. Numerically determined parameters are consistent with real-world production systems and serve as a basis for building a simulation model. For further calculations, next variables are defined:

| | |
|----------|---|
| $takt$ | Takt time |
| U_c | Useful capacity |
| n_c | Useful number of working hours in one shift |
| n_s | Number of shifts |
| η_c | Worktime efficiency coefficient |
| η_l | Line efficiency coefficient |
| Q_e | Quantitative efficiency |
| M_d | Number of workplaces |
| l_c | Conveyor length |
| k_l | Mark-up coefficient for the conveyor length |
| v_c | Conveyor speed |
| d_w | Distance between workplaces |
| d_p | Distance between products on the conveyor |
| t_f | Product's flow time |
| t_1 | Operation processing time |
| E | Additional number of products on the conveyor |

Eq. 1 defines useful capacity of the assembly line per working day, including three shifts working schedule, 7.5 h of useful working hours and worktime efficiency coefficient of 0.92. High worktime efficiency coefficient is used in relation to assembly line characteristics.

$$U_c = n_s \cdot n_c \cdot \eta_c = 3 \cdot 7.5 \cdot 0.92 = 20.7 \frac{\text{h}}{\text{day}} \text{ or } 1242 \frac{\text{min}}{\text{day}} \quad (1)$$

In correlation to defined takt time of 0.9 min, which is minimum possible takt time for presented operations in Table 1, and defined line's useful capacity, quantitative efficiency is defined as presented in Eq. 2.

$$Q_e = \frac{U_c}{takt} = \frac{1242}{0.9} = 1380 \frac{\text{pcs}}{\text{day}} \quad (2)$$

With the know number of workplaces ($M_d = 10$), takt time and total processing time the final assembly line theoretical efficiency is determined by Eq. 3.

$$\eta_l = \frac{\sum t_1}{M_d \cdot takt} = \frac{509}{10 \cdot 54} = 0.943 \text{ or } 94.3 \% \quad (3)$$

Defined number of workplaces, known distance between workplaces ($d_w = 2.16$ m) and proposed mark-up coefficient for the conveyor length ($k_l = 0.05$) the optimum conveyor length is defined by Eq. 4:

$$l_c = M_d \cdot d_w \cdot (1 + k_l) = 10 \cdot 2.16 \cdot (1 + 0.05) = 22.68 \text{ m} \quad (4)$$

Distance between products on the conveyor (d_p) is known when the speed of conveyor is defined ($v_c = 1.2$ m/min) and multiplied with the takt time of 0.9 min. Shown by the Eq. 5:

$$d_p = v_c \cdot takt = 1.2 \cdot 0.9 = 1.08 \text{ m} \quad (5)$$

An additional number of products on the conveyor is defined by the Eq. 6.

$$E = (M_d - 1) \cdot \frac{d_w}{d_p} = (10 - 1) \cdot \frac{2.16}{1.08} = 18 \quad (6)$$

Knowing the number of workplaces, additional number of products on the conveyor, distance between workplaces and distance between products on the conveyor products' flow time can be defined by Eq. 7.

$$t_f = (M_d + E) \cdot takt = (10 + 18) \cdot 0.9 = 25.2 \text{ min} \quad (7)$$

2.2 Collaborative workplace (CW_{as}) description

Our own designed flexible collaborative workplace, in Fig. 2, consist of a worktable (7), a collaborative robot UR3e (8), a collaborative gripper Robotiq 2F-85 (9), a pallet of semi-finished products (4), pallet of finished products (5), and three types of semi-finished products need to be assembled (type one yellow brick (1), type two green brick (2) and type three 4x2 brick (3)).

To run simulation models and study the capacity of the assembly line production system, it was necessary to determine the processing time of collaborative assembly operation between worker and collaborative robot. To determine the most accurate processing times, we carried out the time study evaluation with different speeds and accelerations of the collaborative robot (Table 2), evaluating different workers, in sitting and standing positions.

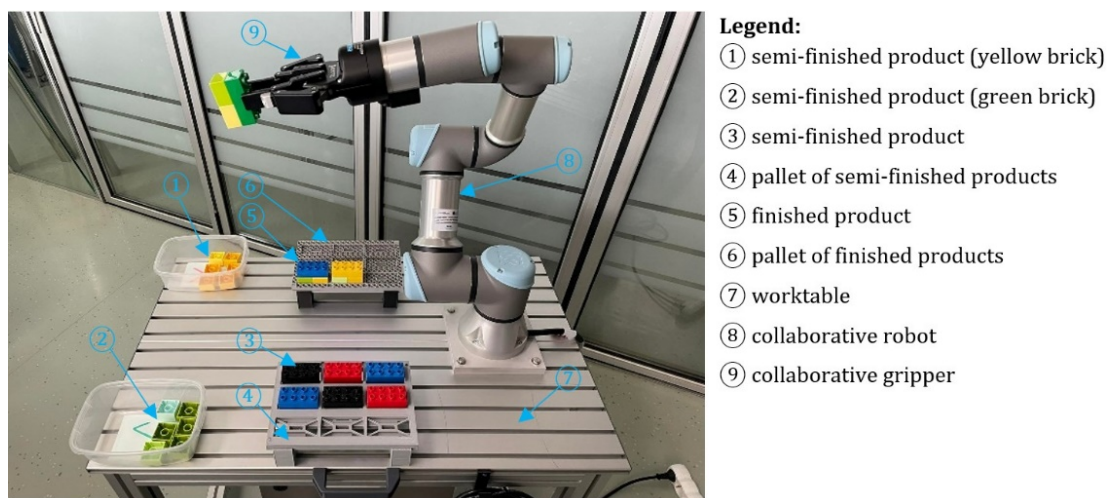


Fig. 2 Layout of a collaborative workplace

Table 2 Collaborative robot speeds and acceleration data

| Linear movement | | | | | Joint movement | | | |
|-----------------|--------|------------------|----------------------|-----|----------------|-------|------------------|---------------------|
| Speed (%) | (mm/s) | Acceleration (%) | (mm/s ²) | add | Speed (%) | (°/s) | Acceleration (%) | (°/s ²) |
| 100 | 750 | 100 | 2000 | | 100 | 180 | 100 | 360 |
| 80 | 600 | 80 | 1600 | | 80 | 144 | 80 | 288 |
| 60 | 450 | 60 | 1200 | | 60 | 108 | 60 | 216 |

By performing evaluation of the seventy-two iterations of the assembly operation, we were able to accurately determine the collaborative workplace's processing time, human operational time, optimal speed of the collaborative robot, and gain a better understanding of the collaborative robot influence on the worker.

The assembly operation consisted of simple assembling of three semi-finished products ①, ② and ③ into one finished product ⑤. In the initial stage, the collaborative robot picks up a semi-finished product ③ and move it to the assembly location (Fig. 2). At the assembly location, collaborative robot stops and waits for the worker to attach two semi-finished products ① and ②. At this stage of the assembly operation, the worker attaches two semi-finished products ① and ② to the semi-finished product ③, which is held in the collaborative gripper. The attachment position of the two semi-finished products ① and ② was determined, the green brick ① is always at the top, the yellow brick ② is always at the bottom, while the order of the composition is: first the yellow brick is attached followed by the green brick. After the three semi-finished products ①, ② and ③ were assembled into a finished product ⑤, the collaborative robot move and place the finished product on the pallet with the finished products. The working process is finished when the pallet of finished products ⑥ is filled. It should be noted that the work process was carried out in a laboratory environment, so the position of the semi-finished products pallet ④ was fixed, while in a real-world assembly line operation the pallet would be transported by a conveyor.

3. Simulation modelling

Given the presented line assembly production system and the problem of improving limited production system capacity by introducing collaborative workplaces, we used simulation modelling to build a simulation model of the assembly line production system and to analyse the collaborative workplace in detail. Initially, the input parameters of the assembly line production system presented in Section 2 were upgraded by numerical modelling of the manual and collaborative workplaces costs, further used to study individual workplaces financial justification.

For the simulation model, the workplaces cost calculation (M_{as} and worker-robot collaborative workplace CW_{as}) was performed. Table 3 presents the data and cost calculation of the workplaces provided for the results implementation into a discrete event simulation environment Simio. Obtained data provides the basis for the validation of the obtained results in Section 4.

Table 3 Workplaces cost calculation data

| Cost calculation parameter | M_{as} | CW_{as} |
|---|----------|-----------|
| Purchase value of the machine (€) | 11,666 | 35,000 |
| Machine power (kW) | 0.1 | 0.1 |
| Workplace area (m ²) | 6 | 6 |
| Depreciation period (year) | 7 | 7 |
| Useful capacity of the machine (h/year) | 5216 | 5670 |
| Machine write-off value (€/h) | 0.32 | 0.88 |
| Interest (€/h) | 0.01 | 0.03 |
| Maintenance costs (€/h) | 0.02 | 0.06 |
| Production system area costs (€/h) | 0.12 | 0.11 |
| Electrical energy consumption costs (€/h) | 0.02 | 0.02 |
| Machine operational costs (€/h) | 0.49 | 1.1 |
| Workplace total costs (€/h) | 11.54 | 12.76 |
| Workplace cost per item (€/piece) | 0.173 | 0.185 |

3.1 Production system modelling

The assembly line production system was modelled in the Simio software environment. The simulation model shown in Fig. 3 represents the assembly line, where all ten workplaces are devoted to manual assembly stations. The input parameters of the assembly line are the same as presented in Section 2, in addition, the parameters of workplaces costs evaluation according to mathematical modelling in Section 3 are added. The simulation model operates in three shifts, five working days a week. The model assumes that input materials and semi-finished products are always available, the system operates at 94.3 % efficiency rate. There are no unknown failures during the assembly operation. The main purpose of the simulation model is to evaluate the possibility of introducing collaborative workplaces to existing manual assembly workplaces with limited capacity.

In the intermediate graphic presentation (Fig. 3) we can observe that in the manual assembly jobs M_As8 and M_As9 bottlenecks of the production system appear, potentially these two manual assembly workplaces represent the final capacity of the evaluated assembly line. Since these two workplaces are about equalizing the time of the assembly cycle and the time of the assembly line takt time, it is advisable to optimize these two workplaces to raise production system capacity.

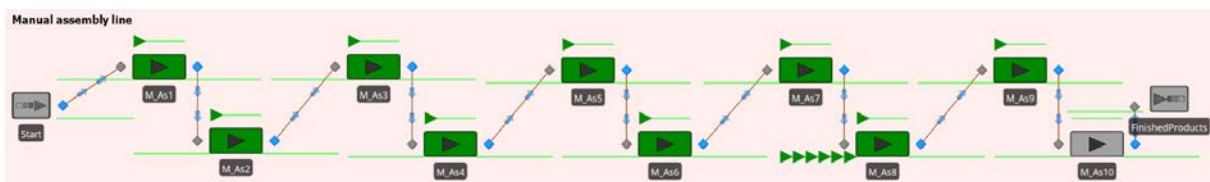


Fig. 3 Simulation model of the manual workplace's assembly line (2D model)

As a proposal to increase the production system capacity, the assembly line in Fig. 4 represents the introduction of one collaborative workplace, where one worker serves two collaborative robots. Fig. 4 shows this workplace with one AsCw1 worker workplace and two collaborative robots in AsCr1 and AsCr2 workplace. As shown, instead of ten workers in production, we now have only nine workers. In consideration, we have eight manual assembly workplaces and one collaborative workplace including worker and two robots. With the input parameters of the production system, all parameters of manual assembly workplaces remain unchanged. We added the input data for the collaborative workplace. The preliminary phase of graphic presentation of the simulation model shows the elimination of previous (Fig. 3) bottlenecks and the potential increase in the production system characteristics.

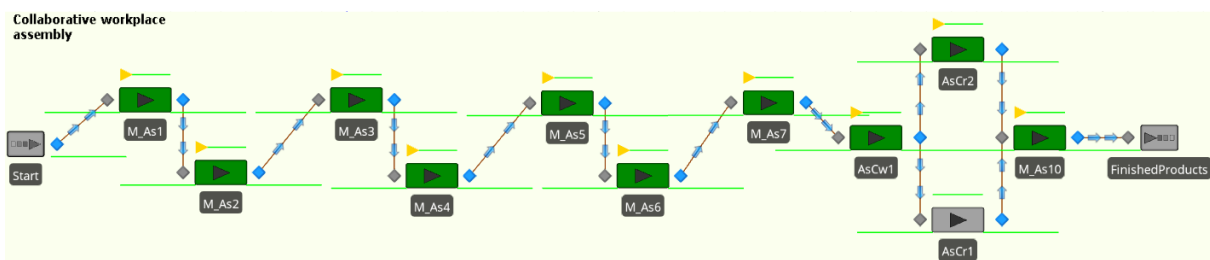


Fig. 4 Simulation model of the proposed collaborative workplaces assembly line

3.2 Collaborative workplace modelling

Collaborative workplace design and collaborative assembly operation were modelled in Siemens Process Simulate environment. The Process Simulate software environment allows us to model different systems or scenarios, simulate operations (machine or human), analyse human movements, optimize the production system, create robot programs, etc.

We have started by modelling the collaborative workplace and added all the necessary components for the collaborative work process, as shown in Fig. 5a. To perform the actual simulation, we first had to define the correct kinematics of the collaborative robot and the collaborative gripper. Properly defined kinematics is crucial to the functionality of the simulation model, as the same program of collaborative robot is running inside the simulation model as in the real-world

application. After defining the exact locations of components, we have started to create the program for collaborative robot. In the program, we adjusted the movement of collaborative robot according to the range, kinematics, speed, type of movement and human safety. After completing the program in Process Simulate environment, we have transferred the program from the virtual to the real-world collaborative robot, through an integrated interface, where we only checked proper functioning and safety of the program.

After ensuring the relevance of the collaborative robot and the human-robot collaboration, the collaborative operation was simulated (Fig. 5b). The goal of simulating human work was to compare the simulation processing time against a real-world study human processing time.

Table 4 shows the results of the real-world collaborative workplace time study evaluation, in which we conducted a time study of four workers with different ages (between 25 and 45 years). Workers were instructed for the correct assembly operation order and needed collaborative workplace knowledge. When performing time study, we have unknowingly changed the speed of the robot for the workers and automatically measured and recorded the assembly process processing time. We performed seventy-two iterations to study the time of the collaborative assembly operation. The results in Table 4 represent the average results of these iterations for an individual worker and total average assembly processing time with respect to the robot speed and acceleration. The total average processing time of collaborative assembly was used in both the simulation model of the production system, in Simio, and the collaborative workplace, in Process Simulate.

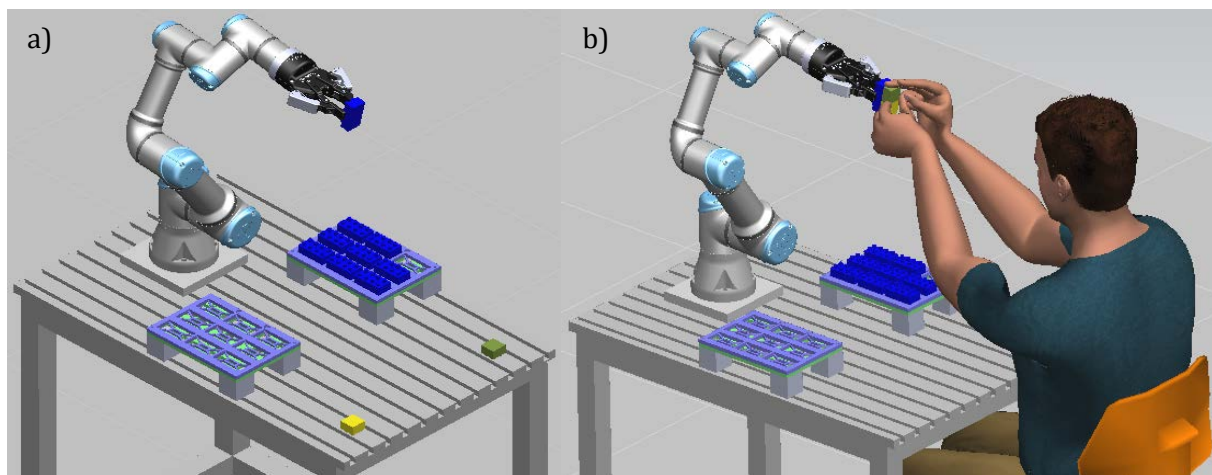


Fig. 5 Simulation model of human-robot collaboration

Table 4 Real-world evaluated workers (W_i) collaborative workplaces processing times

| Robot speed/acceleration (%) | Workers processing time (s) | | | | | Average |
|------------------------------|-----------------------------|--------|--------|--------|--|---------|
| | W_1 | W_2 | W_3 | W_4 | | |
| 60 | 90.146 | 89.796 | 86.950 | 86.566 | | 88.36 |
| 80 | 81.038 | 75.234 | 68.444 | 67.434 | | 73.04 |
| 100 | 64.544 | 62.108 | 59.286 | 63.318 | | 62.31 |

4. Results and discussion

The results in Table 5 show the simulation modelling results of the costs and the utilization rate of an individual manual assembly workplaces. The workplaces cost depends on the number of processed products in the simulation time of five working days, working in three shifts. According to the determination of the assembly line production cost per individual piece and the type of workplace (data presented in Table 3), we can see how the costs affect the number of production pieces on the assembly line. More important is the parameter of workplace utilization, for which the utilization of the first workplace M_{as1} is not relevant, since the simulation model assumes a constant supply of semi-finished products to the first assembly workplace. However, we can see that the highest utilization rate is in the workplaces M_{as5} , M_{as7} , M_{as8} and M_{as9} . Based on a detailed

analysis (throughput time, average time in station and number of entered/exited products) of the results, we find that the bottleneck of the production system is represented by the workplaces M_{as8} and M_{as9} , where the assembly processing time is equal to the assembly line takt time. Workplaces M_{as8} and M_{as9} are at the maximum of their capacity and prevent smooth flow of products through other workplaces. As we can see, the numerical results confirm the preliminary graphical representations of the simulation model and suggest the importance of optimizing these two workplaces.

When introducing a collaborative workplace (replacement of the M_{as8} and M_{as9}), which contains one CW_{as1} robot collaborative workplace and two CR_1 and CR_2 collaborative robots, the simulation results in Table 6 prove the feasibility of introducing such workplaces at evaluated assembly line. Table 6 shows the simulation results according to three different speed levels of collaborative robots. The results, as in Table 5, show the values of job costs according to the number of assembled products and associated to workplace utilization rate. As we can see, at 60 % of the robot's speed, the bottleneck in the assembly line workplace is already eliminated, in which case the collaborative worker and the robot are equally utilized (CW_{as1} : 92.2 %, CR_1 : 84.14 % and CR_2 : 85.45 %). The results of utilization rate prove a consistency of other manual assembly workplaces, which, however, approach the maximum capacity according to the results. Given the value of the cost per piece, we see a huge reduction in the cost of collaborative compared to manual assembly workplaces. Reducing costs is essential, as two collaborative robots represent significantly lower costs than one additional worker.

As the speed of the robots increases, their occupancy decreases (robots have more capacity to be used), but this does not significantly affect the rest of the assembly line workplaces, as the operator needs his/her time to properly assemble the parts on the collaborative robot. The cost of a collaborative workplace does not change, at all different speeds, the collaborative workplace enables the production of all available semi-finished products to be assembled. Based on the results, we can conclude that the production capacities are increased but the other workplaces' capacity is limited, potentially appearing new production line bottlenecks.

Table 5 Simulation model manual assembly line results

| WP type | M_{as1} | M_{as2} | M_{as3} | M_{as4} | M_{as5} | M_{as6} | M_{as7} | M_{as8} | M_{as9} | M_{as10} |
|-----------------|-----------|-----------|-----------|-----------|-----------|-----------|-----------|-----------|-----------|------------|
| Cost (€) | 939.39 | 939.23 | 939.06 | 939.06 | 938.74 | 938.57 | 938.41 | 903.48 | 903.31 | 903.15 |
| Utilization (%) | 100 | 98.06 | 94.2 | 92.26 | 99.93 | 97.99 | 99.9 | 99.88 | 99.86 | 88.75 |

Table 6 Simulation model collaborative workplace assembly line results

| CR ₁ and CR ₂ speed and acceleration 60% | | | | | | | | Average CW _{as1} processing time 88.36 s | | | |
|---|-----------|-----------|-----------|-----------|-----------|-----------|-----------|---|-----------------|-----------------|------------|
| WP type | M_{as1} | M_{as2} | M_{as3} | M_{as4} | M_{as5} | M_{as6} | M_{as7} | CW _{as1} | CR ₁ | CR ₂ | M_{as10} |
| Cost (€) | 939.39 | 939.23 | 939.06 | 939.06 | 938.9 | 938.57 | 938.41 | 938.244 | 29.78 | 30.25 | 937.26 |
| Utilization (%) | 100 | 98.06 | 94.2 | 92.26 | 99.93 | 97.99 | 99.9 | 92.2 | 84.14 | 85.45 | 92.1 |
| CR ₁ and CR ₂ speed and acceleration 80% | | | | | | | | Average CW _{as1} processing time 73.04 s | | | |
| WP type | M_{as1} | M_{as2} | M_{as3} | M_{as4} | M_{as5} | M_{as6} | M_{as7} | CW _{as1} | CR ₁ | CR ₂ | M_{as10} |
| Cost (€) | 939.39 | 939.23 | 939.06 | 939.06 | 938.74 | 938.57 | 938.41 | 938.24 | 29.78 | 30.27 | 937.75 |
| Utilization (%) | 100 | 98.06 | 94.2 | 92.26 | 99.93 | 97.99 | 99.9 | 92.2 | 69.55 | 70.7 | 92.14 |
| CR ₁ and CR ₂ speed and acceleration 100% | | | | | | | | Average CW _{as1} processing time 62.31 s | | | |
| WP type | M_{as1} | M_{as2} | M_{as3} | M_{as4} | M_{as5} | M_{as6} | M_{as7} | CW _{as1} | CR ₁ | CR ₂ | M_{as10} |
| Cost (€) | 939.39 | 939.23 | 939.06 | 938.9 | 938.74 | 938.57 | 938.41 | 938.24 | 29.78 | 30.28 | 937.91 |
| Utilization (%) | 100 | 98.06 | 94.2 | 92.26 | 99.93 | 97.99 | 99.9 | 92.2 | 59.33 | 60.33 | 92.16 |

Table 7 and Fig. 6 show the comparative average simulation results on which we find that the assembly line total cost in comparison with manual assembly workplace costs and the introduction of one collaborative workplace are reduced by 8.34 %. The reduction of the average workplaces utilization is minor, as collaborative robots are at any speed fully occupied. We can see that just one collaborative robot would be too few. In this case, the worker in the collaborative workplace would have to wait a long time for the next assembly operation to be performed, that time is significantly less justified in terms of cost and capacity than serving a pair of collaborative robots. Given the number of finished products, we can assume that the average number of finished products increases by 3.83 %, when introducing a collaborative workplace, at this state the number of finished products approaches the theoretical capacity of the production system. The theoretical assembly line capacity is limited by the longest processing time of the individual workplace.

In current state it is represented by the workplaces M_{as5} and M_{as7} , with a processing time of 52 s. An interesting fact is the number of unfinished products in the production system (remaining products in system RP_{is}), which represents the size of intermediate stocks. Considering that there were bottlenecks in the manual assembly line, we can see that this number is reduced by as much as 93.67 % in the introduction of the collaborative workplaces. This result demonstrates how the elimination of bottlenecks has a positive impact on production capacity and its justification.

Fig. 7 shows a simulation model of the product assembly process and time study of needed worker time to assembly one product. With the help of a simulation model, we can accurately determine the phases of assembly, the needs of the worker movement and the robot operations. The simulation model itself assumes the optimal speeds of such a collaborative workplace in correlation to the input parameters. Created simulation model assumes the assembly of one product, which includes three semi-finished products. The assembly phase is divided into five sub-phases (phase a – starting position, phase b – preparation of yellow and green semi-finished product, phase c – placement of yellow semi-finished product on a semi-finished product in robot gripper, phase d – placement of green semi-finished on a semi-finished product in robot gripper and phase e – final worker position). The initial assembly time is represented by the variable $t_s = 0$ s and the final time of the worker assembly phase by the variable t_f . The results prove that the simulation model predicted the working time of the worker assembly per product it would be 2.04 s, which is on average equivalent to 80 % of the robot speed criteria compared to the results in Table 8 where the four-worker real-world time study was performed.

Four evaluated workers have assembled nine consecutive products during the study. In Table 8, the results of the individual assembly processing times are captured between t_1 and t_9 . Workers assembled the product in a sitting position at three different robot speeds, unaware of the real speed of the robot. Presented results prove that different workers, and their working abilities can affect the assembly operation processing time, as shown in a simulation model, an average assembly processing time can be used for variety of workers. The results prove the expediency of evaluating the collaborative workplace in both real and simulation environments.

Table 7 Manual vs. collaborative workplace comparison results

| AL Type | M_{as} | CR speed 60 % | CR speed 80 % | CR speed 100 % |
|-------------------------|----------|---------------|---------------|----------------|
| Total AL costs (€) | 9282.4 | 8508.2 | 8508.5 | 8508.5 |
| Average utilization (%) | 97.1 | 94.2 | 91.5 | 89.7 |
| Throughputs (pcs) | 5507 | 5714 | 5717 | 5718 |
| RP_{is} (pcs) | 221 | 14 | 11 | 10 |

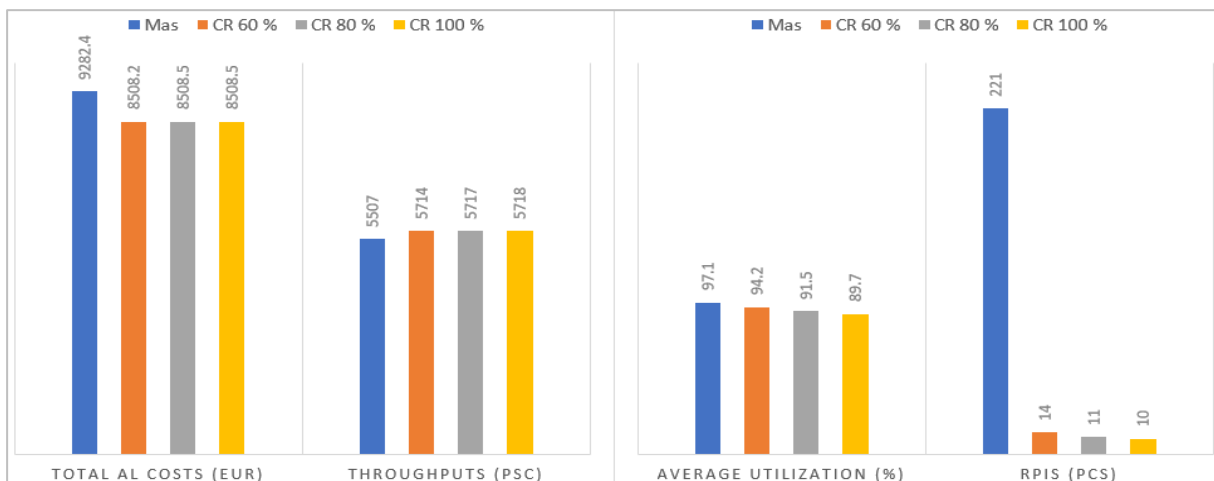


Fig. 6 Workplace comparison results

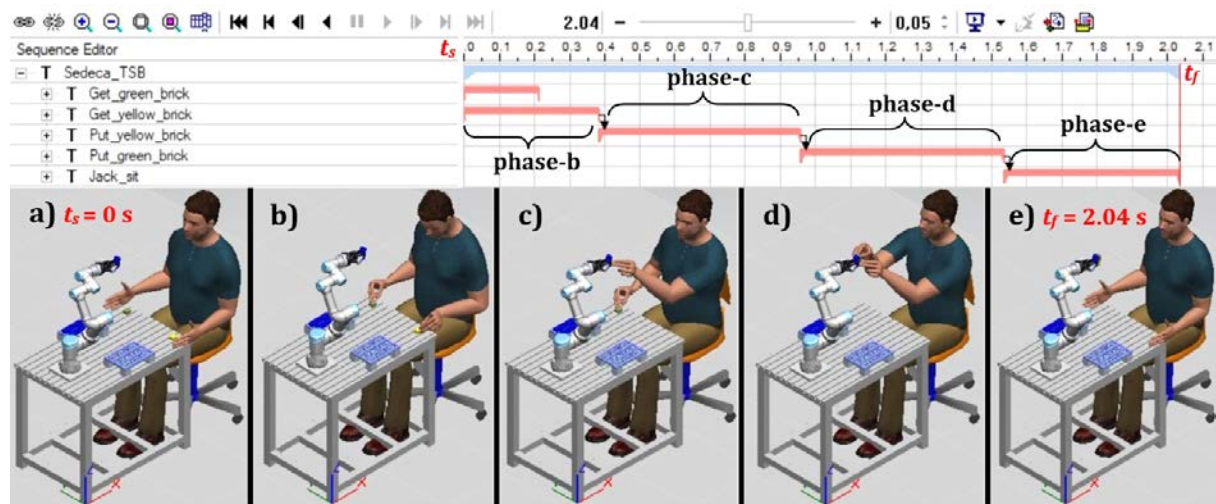


Fig. 7 Collaborative workplace simulation model – product assembly phases

Table 8 Real-world collaborative workplace worker product assembly processing time study

| Worker 1, age of 46 years | | | | | | | | | |
|---------------------------|---|-------|-------|-------|-------|-------|-------|-------|-------|
| CR speed (%) | Workers assembly processing time by product (s) | | | | | | | | |
| | t_1 | t_2 | t_3 | t_4 | t_5 | t_6 | t_7 | t_8 | t_9 |
| 60 | 1.956 | 2.056 | 2.008 | 1.900 | 2.536 | 2.264 | 3.122 | 2.082 | 2.616 |
| 80 | 1.898 | 2.184 | 2.124 | 1.982 | 1.084 | 2.076 | 1.830 | 1.922 | 1.944 |
| 100 | 2.044 | 2.192 | 2.012 | 1.958 | 2.460 | 1.940 | 2.338 | 1.754 | 2.356 |
| Worker 2, age of 27 years | | | | | | | | | |
| CR speed (%) | Workers assembly processing time by product (s) | | | | | | | | |
| | t_1 | t_2 | t_3 | t_4 | t_5 | t_6 | t_7 | t_8 | t_9 |
| 60 | 2.262 | 1.496 | 1.700 | 1.684 | 3.506 | 1.594 | 1.624 | 1.628 | 1.966 |
| 80 | 1.984 | 2.672 | 1.602 | 1.660 | 1.558 | 1.860 | 1.862 | 2.066 | 1.824 |
| 100 | 2.056 | 4.380 | 1.960 | 1.722 | 1.914 | 1.884 | 1.449 | 2.178 | 2.048 |
| Worker 3, age of 29 years | | | | | | | | | |
| CR speed (%) | Workers assembly processing time by product (s) | | | | | | | | |
| | t_1 | t_2 | t_3 | t_4 | t_5 | t_6 | t_7 | t_8 | t_9 |
| 60 | 1.674 | 1.474 | 1.358 | 1.254 | 1.230 | 1.454 | 1.118 | 1.370 | 1.184 |
| 80 | 1.416 | 1.460 | 1.366 | 1.330 | 1.350 | 1.758 | 1.306 | 1.454 | 1.288 |
| 100 | 1.400 | 1.314 | 1.414 | 1.406 | 1.468 | 1.226 | 1.422 | 1.448 | 1.118 |
| Worker 4, age of 25 years | | | | | | | | | |
| CR speed (%) | Workers assembly processing time by product (s) | | | | | | | | |
| | t_1 | t_2 | t_3 | t_4 | t_5 | t_6 | t_7 | t_8 | t_9 |
| 60 | 1.406 | 1.922 | 1.242 | 1.358 | 1.366 | 1.240 | 1.594 | 1.380 | 1.700 |
| 80 | 1.126 | 1.552 | 1.196 | 1.016 | 1.698 | 1.152 | 1.362 | 1.336 | 1.164 |
| 100 | 1.770 | 1.566 | 1.644 | 1.106 | 1.682 | 1.658 | 1.478 | 1.222 | 1.222 |

The obtained results prove the expediency of introducing collaborative workplaces in the positions of manual workplaces with limited capacities. The positive impact of collaborative workplaces is reflected in the entire production system capacity increase.

Presented simulation results of manual workplaces prove that they can identify bottlenecks in the production system, which need to be eliminated to achieve higher production capacities. Described graphical and numerical results accurately describe the place where the introduction of a collaborative workplaces is appropriate. In the present case, this is the M_{as8} and M_{as9} workplaces, where the workplaces processing time is equal to the line takt time.

With the help of simulation modelling, we have introduced a collaborative workplace to this assembly line station, where one worker serves two collaborative robots. The collaborative robot operates in three different modes of speed and acceleration. Based on the results, we find that the correct setting of the speed of the collaborative robot is key to achieving full utilization of capacities of the collaborative workplace. It should be noted that exceeding the optimal speed of a collaborating robot may have a negative impact on the worker, as excessive speed and acceleration cause discomfort to the worker and longer waiting times for the robot to proceed with the next

operation. At too high robot speeds and inability to achieve shorter assembly times on the side of the worker, congestion can occur due to poorly performed work of the worker. The correct choice of robot speed and the corresponding optimal process time of robot service is crucial, as evidenced by the simulation results of the collaborative workplace impact on the production system, where we see that the increasing robot speed beyond the robot service limit has no positive effect on the collaborative workplace production system. In general, we can see that elimination bottleneck in the manual assembly workstation can be eliminated by introducing collaborative workplace. In the evaluated case the costs of workplaces of entire production system have reduced by 8.34 %, the number of finished products has increased by 3.83 %, elimination of production system bottleneck decreased the remaining product in system by 93.67 %.

A detailed time study of the collaborative workplace confirms that all workers have an associated work rhythm that is not necessarily always the same for all workers. Since, we are talking about a collaborative workplace, where the robot cooperates directly with the workers, adjusting the processing time of the collaborative operation makes sense if this time is within the estimated time of the workplace, and it does not negatively affect the rest of the system utilization. It should be added that each worker has his own preferences regarding of the assembly position, both the worker and the robot (ergonomics and positions studies). Different workers feel more comfortable at different robot speeds. It makes sense to take all technological and sociological influences into account as much as possible when planning collaborative workplaces, thus ensuring maximum production system capacities.

5. Conclusion

In our research work, we have focused on presenting the impact of collaborative workplaces on the entire production process capacity, which is positive with the presented results. We presented various simulation models, both manual assembly workplaces, and the introduction and impact of collaborative workplaces on production capacity. A detailed time study of the assembly time impact of both the real-world collaborative workplace and the simulation model was presented. The presented results showed a positive degree of correlations and the specificity of the use of both approaches to achieve effective capacity planning. Of course, the results and findings, along with positive answers to the initial research question, raised many questions about how to optimally construct and prepare a collaborative workplace that could fully utilize both worker and robot capacities and effectively consider both technological and sociological aspects. In the future research work, we will focus on a detailed study of the technological and sociological aspects of collaborative workplaces and their correlation. Even though the presented research work deals with assembly line production, collaborative workplaces, with their great flexibility, can be used in different types of production at different workplaces. However, as can be seen from the results, their justification in relation to capacity utilization needs to be studied in detail in future.

Acknowledgement

The authors gratefully acknowledge the support of the Slovenian Research Agency (ARRS), Research Core Funding No. P2-0190. The authors acknowledge the use of research equipment system for development and testing cognitive production approaches in industry 4.0: Collaborative robots with equipment and Sensors, hardware and software for ergonomic analysis of a collaborative workplace, procured within the project "Upgrading national research infrastructures – RIUM", which was co-financed by the Republic of Slovenia, the Ministry of Education, Science and Sport and the European Union from the European Regional Development Fund.

References

- [1] Moniz, A.B., Krings, B.-J. (2016). Robots working with humans or humans working with robots? Searching for social dimensions in new human-robot interaction in industry, *Societies*, Vol. 6, No. 3, Article No. 23, doi: [10.3390/soc6030023](https://doi.org/10.3390/soc6030023).
- [2] Michalos, G., Makris, S., Tsarouchi, P., Guasch, T., Kontovrakis, D., Chryssoulouris, G. (2015). Design considerations for safe human-robot collaborative workplaces, *Procedia CIRP*, Vol. 37, 248-253, doi: [10.1016/j.procir.2015.08.014](https://doi.org/10.1016/j.procir.2015.08.014).

- [3] Nahavandi, S. (2019). Industry 5.0—A human-centric solution, *Sustainability*, Vol. 11, No. 16, Article No. 4371, doi: [10.3390/su11164371](https://doi.org/10.3390/su11164371).
- [4] Özdemir, V., Hekim, N. (2018). Birth of Industry 5.0: Making sense of big data with artificial intelligence, “The Internet of Things” and next-generation technology policy, *OMICS: A Journal of Integrative Biology*, Vol. 22, No. 1, 65-76, doi: [10.1089/omi.2017.0194](https://doi.org/10.1089/omi.2017.0194).
- [5] Gualtieri, L., Rauch, E., Vidoni, R. (2021). Emerging research fields in safety and ergonomics in industrial collaborative robotics: A systematic literature review, *Robotics and Computer-Integrated Manufacturing*, Vol. 67, Article No. 101998, doi: [10.1016/j.rcim.2020.101998](https://doi.org/10.1016/j.rcim.2020.101998).
- [6] Leber, M., Bastič, M., Moody, L., Schmidt Krajnc, M. (2018). A study of the impact of ergonomically designed workplaces on employee productivity, *Advances in Production Engineering & Management*, Vol. 13, No. 1, 107-117, doi: [10.14743/apem2018.1.277](https://doi.org/10.14743/apem2018.1.277).
- [7] Mateus, J.E.C., Claeys, D., Limère, V., Cottyn, J., Aghezaf, E.-H. (2019). Ergonomic and performance factors for Human-robot collaborative workplace design and evaluation, *IFAC-PapersOnLine*, Vol. 52, No. 13, 2550-2555, doi: [10.1016/j.ifacol.2019.11.590](https://doi.org/10.1016/j.ifacol.2019.11.590).
- [8] Lasota, A.M. (2020). A new approach to ergonomic physical risk evaluation in multi-purpose workplaces, *Tehnički Vjesnik – Technical Gazette*, Vol. 27, No. 2, 467-474, doi: [10.17559/TV-20180312131319](https://doi.org/10.17559/TV-20180312131319).
- [9] Ojstersek, R., Acko, B., Buchmeister, B. (2020). Simulation study of a flexible manufacturing system regarding sustainability, *International Journal of Simulation Modelling*, Vol. 19, No. 1, 65-76, doi: [10.2507/ijssimm19-1-502](https://doi.org/10.2507/ijssimm19-1-502).
- [10] Ojstersek, R., Buchmeister, B. (2020). Simulation modeling approach for collaborative workplaces’ assessment in sustainable manufacturing, *Sustainability*, Vol. 12, No. 10, Article No. 4103, 18 pages, doi: [10.3390/su12104103](https://doi.org/10.3390/su12104103).
- [11] Nikolakis, N., Maratos, V., Makris, S. (2019). A cyber physical system (CPS) approach for safe human-robot collaboration in a shared workplace, *Robotics and Computer-Integrated Manufacturing*, Vol. 56, 233-243, doi: [10.1016/j.rcim.2018.10.003](https://doi.org/10.1016/j.rcim.2018.10.003).
- [12] Koppenborg, M., Nickel, P., Naber, B., Lungfiel, A., Huelke, M. (2017). Effects of movement speed and predictability in human-robot collaboration, *Human Factors and Ergonomics in Manufacturing & Service Industries*, Vol. 27, No. 4, 197-209, doi: [10.1002/hfm.20703](https://doi.org/10.1002/hfm.20703).
- [13] Wang, Y., Cen, H.J., Yang, O. (2018). Optimal configuration for workshop manufacturing system under dual resource constraints, *International Journal of Simulation Modelling*, Vol. 17, No. 1, 180-189, doi: [10.2507/ijssimm17\(1\)co5](https://doi.org/10.2507/ijssimm17(1)co5).
- [14] Gualtieri, L., Rauch, E., Vidoni, R. (2021). Methodology for the definition of the optimal assembly cycle and calculation of the optimized assembly cycle time in human-robot collaborative assembly, *The International Journal of Advanced Manufacturing Technology*, Vol. 113, No. 7, 2369-2384, doi: [10.1007/s00170-021-06653-y](https://doi.org/10.1007/s00170-021-06653-y).
- [15] Ojstersek, R., Tang, M., Buchmeister, B. (2020). Due date optimization in multi-objective scheduling of flexible job shop production, *Advances in Production Engineering & Management*, Vol. 15, No. 4, 481-492, doi: [10.14743/apem2020.4.380](https://doi.org/10.14743/apem2020.4.380).
- [16] Trstenjak, M., Čosić, P., Antolić, D. (2019). Workpiece classification criteria in automated process planning, *Tehnički Vjesnik – Technical Gazette*, Vol. 26, No. 1, 256-262, doi: [10.17559/TV-20180215105405](https://doi.org/10.17559/TV-20180215105405).
- [17] Zheng, Z.L., Bao, X. (2019). The investment strategy and capacity portfolio optimization in the supply chain with spillover effect based on artificial fish swarm algorithm, *Advances in Production Engineering & Management*, Vol. 14, No. 2, 239-250, doi: [10.14743/apem2019.2.325](https://doi.org/10.14743/apem2019.2.325).
- [18] Katić, I., Berber, N., Slavić, A., Ivanišević, A. (2020). The relations between investment in employees’ development and organizational productivity and service quality, *Tehnički Vjesnik – Technical Gazette*, Vol. 27, No. 4, 1077-1083, doi: [10.17559/TV-20181121101314](https://doi.org/10.17559/TV-20181121101314).
- [19] Kungpeng, Y., Jiafu, S., Hui, H. (2017). Simulation of collaborative product development knowledge diffusion using a new cellular automata approach, *Advances in Production Engineering & Management*, Vol. 12, No. 3, 265-273, doi: [10.14743/apem2017.3.257](https://doi.org/10.14743/apem2017.3.257).
- [20] Fechter, M., Seeber, C., Chen, S. (2018). Integrated process planning and resource allocation for collaborative robot workplace design, *Procedia CIRP*, Vol. 72, 39-44, doi: [10.1016/j.procir.2018.03.179](https://doi.org/10.1016/j.procir.2018.03.179).
- [21] Rega, A., Vitolo, F., Di Marino, C., Patalano, S. (2021). A knowledge-based approach to the layout optimization of human-robot collaborative workplace, *International Journal on Interactive Design and Manufacturing*, Vol. 15, No. 1, 133-135, doi: [10.1007/s12008-020-00742-0](https://doi.org/10.1007/s12008-020-00742-0).
- [22] Mateus, J.C., Claeys, D., Limère, V., Cottyn, J., Aghezaf, E.-H. (2019). A structured methodology for the design of a human-robot collaborative assembly workplace, *The International Journal of Advanced Manufacturing Technology*, Vol. 102, No. 5, 2663-2681, doi: [10.1007/s00170-019-03356-3](https://doi.org/10.1007/s00170-019-03356-3).

A multi-criteria decision-making in turning process using the MAIRCA, EAMR, MARCOS and TOPSIS methods: A comparative study

Trung, D.D.^{a,*}, Tinh, H.X.^b

^aFaculty of mechanical engineering, Hanoi Univeristy of Industry, Vietnam

^bCenter for mechanical engineering, Hanoi Univeristy of Industry, Vietnam

ABSTRACT

Multi-criteria decision-making is important, and it affects the efficiency of a mechanical processing process as well as an operation in general. It is understood as determining the best alternative among many alternatives. In this study, the results of a multi-criteria decision-making study are presented. In which, sixteen experiments on turning process were carried out. The input parameters of the experiments are the cutting speed, the feed speed, and the depth of cut. After conducting the experiments, the surface roughness and the material removal rate (MRR) were determined. To determine which experiment guarantees the minimum surface roughness and maximum MRR simultaneously, four multi-criteria decision-making methods including the MAIRCA, the EAMR, the MARCOS, and the TOPSIS were used. Two methods the Entropy and the MEREC were used to determine the weights for the criteria. The combination of four multi-criteria making decision methods with two determination methods of the weights has created eight ranking solutions for the experiments, which is the novelty of this study. An amazing result was obtained that all eight solutions all determined the same best experiment. From the obtained results, a recommendation was proposed that the multi-criteria making decision methods and the weighting methods using in this study can also be used for multi-criteria making decision in other cases, other processes.

ARTICLE INFO

Keywords:

Turning;
Material removal rate (MRR);
Surface roughness;
Multi-criteria decision-making (MCDM);
Multi Attributive Ideal-Real Comparative Analysis (MAIRCA);
Evaluation by an Area-based Method of Ranking (EAMR);
Measurement of Alternatives and Ranking according to Compromise Solution (MARCOS);
Technique for Order of Preference by Similarity to Ideal Solution (TOPSIS);
Entropy;
Method based on the Removal Effects of Criteria (MEREC)

*Corresponding author:

doductrung@hau.edu.vn
(Trung, D.D.)

Article history:

Received 19 November 2021

Revised 8 December 2021

Accepted 9 December 2021



Content from this work may be used under the terms of the Creative Commons Attribution 4.0 International Licence (CC BY 4.0). Any further distribution of this work must maintain attribution to the author(s) and the title of the work, journal citation and DOI.

1. Introduction

Multi-criteria decision-making methods are used in many fields. These methods help to compare alternatives and find the best one [1]. For a mechanical machining process as well as a turning process, multi-criteria decision-making is very important. It can be said that because among

many input parameters to evaluate the turning process, sometimes there are parameters that the objective function sets for them are often opposite. For example, when high-speed turning to improve machining productivity, the tool wear rate is also large, causing the decrease of the tool life [2]. To increase the MRR, it is necessary to increase the feed rate and the depth of cut, but this increases the surface roughness [3]. Besides, to reduce the tool wear rate, it is necessary to increase the flow and the concentration of the coolant to reduce the cutting heat. However, doing that will not only increase the manufacturing cost but also affect the environment. In addition, increasing the machining productivity will often increase the cutting tool vibration, and lead to the reduction of the tool life and increase the surface roughness [4], etc. For the above reasons, many studies on multi-criteria decision-making for turning process have been carried out.

The TOPSIS is the most used method for multi-criteria decision-making in many different fields [5, 6]. This method has also been used for multi-criteria decision-making for turning processes in many studies. These studies usually focus on selecting optimal input process parameters to ensure multiple criteria at the same time such as: Ensuring the minimum surface roughness and the maximum MRR when processing Glass fiber reinforced polyester materials (GFRP) [7]; Ensuring all of six parameters of the surface roughness (including R_q , R_a , R_t , R_{ku} , R_z , R_{sm}) have the same minimum value when turning GFRP materials [8]; Ensure the minimum surface roughness (R_a and R_z) and the maximum MRR when turning EN19 steel [9]; Simultaneously ensuring the minimum surface roughness and tool wear rate, and the maximum MRR when turning 1030 steel [10]; Simultaneously ensuring the minimum surface roughness, the cutting force, the tool wear and the cutting heat, and the maximum MRR when turning pure Titanium [11]. Ensuring the minimum surface roughness, the cutting force and the tool wear when turning CP-Ti grade II material [12]; Simultaneously ensuring the minimum surface roughness, the cutting force, the tool wear and the cutting temperature when turning Ti-6Al-4V alloy [13]; Simultaneously ensuring the minimum surface roughness, and the maximum MRR when turning AISI D2 steel [14]; Simultaneously ensuring the minimum surface roughness, and the maximum MRR when turning Al 6351 alloy [15]; Simultaneously ensuring the minimum surface roughness, the minimum roundness deviation and the minimum tool wear when turning 9XC steel [16], etc. Recently, the TOPSIS method and six other methods including the SAW, the WASPAS, the VIKOR, the MOORA, the COPRAS, and the PIV, have been used in multi-criteria decision-making when turning 150Cr14 steel and the best option was received for all of methods [17].

In the last few years, scientists have also proposed new decision-making methods. Three of those methods are MAIRCA, EAMR, and MARCOS methods.

The MAIRCA method was first introduced in 2018 [18]. The outstanding advantage of this method over other methods is that the objectives can be in both qualitative and quantitative types. There have been several studies which applied this method to multi-criteria decision-making. For example, determining the most effective time (year) in mergers and acquisitions of companies in Turkey during the period 2015-2019 [19]; determining the best performing airline out of eleven emerging airlines from Turkey, Mexico, China, Indonesia and Brazil [20]; selecting a partner for a food company in Turkey [21]; preventing the Covid-19 epidemic to the sustainable development of OECD countries [22].

The EAMR method was discovered in 2016 [23]. This method has been used for a number of studies such as: selecting partners to hire for logistics [24]; selecting contract types of health care services [25]; deciding the order quantity for each supplier to ensure environmental criteria [26].

The MARCOS method was first used in 2019 [27]. This method has been applied in several studies such as: in the selection of intermediate modes of transport between countries in the Danube region [28]; for minimizing risks in the transportation [29], in selection of lifting equipment for services in warehouses [30]; for the selection of human resources for transportation companies [31], or for the cost selection in the construction [32].

Although the three methods MAIRCA, EAMR and MARCOS have been used in some studies as described above, so far there has been no research on the application of any of these methods for multi-criteria decision-making for the turning process. The combination of three methods

(MAIRCA, EAMR and MARCOS) with TOPSIS method is the basis for assessing the accuracy of the results obtained. This is the first reason for doing this study.

When performing multi-criteria decisions, an important task is to determine the weights for the criteria. This has a great influence on the ranking order of the alternatives [33]. If it is done by the decision maker, the accuracy achieved is not high because it depends on the knowledge as well as the subjective thoughts of that person. If it is determined by consulting the experts, its accuracy will depend on the experience of the experts as well as the way the questionnaires are presented, which is also very time consuming and high cost [34]. To overcome these limitations, it is necessary to determine the weights for the criteria based on mathematical models. In this way, the weight of the criteria is determined independent of the subjectivity of the decision maker. The Entropy is known as a method of determining weights with high accuracy, which has been used in many cases. When it is necessary to compare multi-criteria decision-making methods, the Entropy method is also recommended to use to determine the weights for the criteria [17].

MEREC is a weighting method which introduced in 2021 [35]. This method has been used to determine the weights for criteria such as: decision-making to determine the location of logistics distribution centers [36]; decision-making for documental classification [37]; etc. However, up to now this method has not been used to determine the weights for criteria in turning processes. The simultaneous use of two methods (the MEREC and the Entropy) to determine weights is the basis for evaluating stability when determining the best solution of multi-criteria decision-making methods. This is the second reason for doing this study.

Surface roughness and MRR are two commonly used parameters to evaluate turning processes. The reason is that the surface roughness has a great influence on the workability and durability of the products through the wear resistance, the chemical corrosion resistance, and the accuracy of the joint (for tight joints) [3], while MRR is an important factor to evaluate the cutting productivity [38]. Besides, determining the values of these parameters is also simpler than other that of parameters, such as the cutting force, the cutting temperature, or the vibration in the cutting process. This is the reason why this study will also use the surface roughness and *MRR* as two indicators to evaluate turning process.

This study presents the results of experimental research on turning process with two parameters to evaluate the turning process, namely surface roughness and MRR. In addition, the Entropy and the MEREC are two methods used to determine the weights for the criteria (surface roughness and MRR). Also, four methods including the MAIRCA, the EAMR, the MARCOS, and the TOPSIS will be used to make multi-criteria decision for turning process. The purpose of multi-criteria decision-making is to ensure simultaneous minimum surface roughness and maximum *MRR*.

2. Used methods of multi-criteria decision-making

2.1 The MAIRCA method

The steps to implement multi-criteria decision-making according to the MAIRCA method are as follows [18].

Step 1: Building the initial matrix according to the following equation:

$$X = \begin{bmatrix} x_{11} & \cdots & x_{1n} \\ x_{21} & \cdots & x_{2n} \\ \vdots & \cdots & \vdots \\ x_{m1} & \cdots & x_{mn} \end{bmatrix} \quad (1)$$

where m is the number of options; n is the number of criteria; x_{mn} is the value of the n criterion in m .

Step 2: Determining the priority for an indicator. When the decision maker is neutral, the role of the indicators is the same (no priority is given to any). Then the priority for the criteria is the same and is calculated as follows:

$$P_{A_j} = \frac{1}{m}, j = 1, 2, \dots, n \quad (2)$$

Step 3: Calculating the quantities $t_{p_{ij}}$ according to the equation:

$$t_{p_{ij}} = P_{A_j} \cdot w_j, i = 1, 2, \dots, m; j = 1, 2, \dots, n \quad (3)$$

where w_j is the weight of the j -th criterion.

Step 4: Calculating the quantities $t_{r_{ij}}$ according to the equations:

$$t_{r_{ij}} = t_{p_{ij}} \cdot \left(\frac{x_{ij} - x_i^-}{x_i^+ - x_i^-} \right) \text{ if } j \text{ is the criterion the bigger the better} \quad (4)$$

$$t_{r_{ij}} = t_{p_{ij}} \cdot \left(\frac{x_{ij} - x_i^+}{x_i^- - x_i^+} \right) \text{ if } j \text{ is the criterion as small as better} \quad (5)$$

Step 5: Calculating the quantities g_{ij} according to the equation:

$$g_{ij} = t_{p_{ij}} - t_{r_{ij}} \quad (6)$$

Step 6: Summing the g_j values according to the equation:

$$Q_i = \sum_{j=1}^m g_{ij} \quad (7)$$

Ranking the options according to the principle that the one with the smallest Q_i is the better.

2.2 The EAMR method

The steps according to the EAMR method are summarized as follows [23].

Step 1: Building a decision matrix:

$$X_d = \begin{bmatrix} x_{11}^d & \dots & x_{1n}^d \\ x_{21}^d & \dots & x_{2n}^d \\ \vdots & \dots & \vdots \\ x_{m1}^d & \dots & x_{mn}^d \end{bmatrix} \quad (8)$$

where $1 \leq d \leq k$, k is the number of decision makers; d is the index representing the decision maker d .

Step 2: Calculating the mean value of each alternative for each criterion according to the equation:

$$\bar{x}_{ij} = \frac{1}{k} (x_{ij}^1 + x_{ij}^2 + \dots + x_{ij}^k) \quad (9)$$

It should be noted that k is the index of the k decision maker, not the exponent.

Step 3: Determining the weights for the criteria. At this step, each decision maker can choose a different weighting method.

Step 4: Calculating the average weighted value for each criterion according to the equation:

$$\bar{w}_j = \frac{1}{k} (w_j^1 + w_j^2 + \dots + w_j^k) \quad (10)$$

Step 5: Calculating n_{ij} values according to the equation:

$$n_{ij} = \frac{\bar{x}_{ij}}{e_j} \tag{11}$$

in which, e_j is determined by the equation:

$$e_j = \max_{i \in \{1, \dots, m\}}(\bar{x}_{ij}) \tag{12}$$

Step 6: Calculating the normalized weight values according to the equation:

$$v_{ij} = n_{ij} \cdot \bar{w}_j \tag{13}$$

Step 7: Calculating the normalized score for the criteria:

$$G_i^+ = v_{i1}^+ + v_{i2}^+ + \dots + v_{im}^+ \quad \text{if } j \text{ is the criterion the bigger the better} \tag{14}$$

$$G_i^- = v_{i1}^- + v_{i2}^- + \dots + v_{im}^- \quad \text{if } j \text{ is the criterion as small as better} \tag{15}$$

Step 8: The rank of value (RV) is found based on G_i^+ and G_i^- .

Step 9: Calculating the evaluation score for the options according to the equation:

$$S_i = \frac{RV(G_i^+)}{RV(G_i^-)} \tag{16}$$

The solution with the largest S_i will be the best one, which is the ranking principle of the EAMR method.

2.3 The MARCOS method

The steps to implement multi-criteria decision-making according to the MARCOS method are as follows [27].

Step 1: Similar to step 1 of the MAIRCA method.

Step 2: Constructing an initial matrix that expands by adding an ideal solution (AI) and the opposite solution to the ideal solution (AAI) :

$$X = \begin{matrix} \text{AAI} \\ \text{A}_1 \\ \text{A}_2 \\ \vdots \\ \text{A}_m \\ \text{AI} \end{matrix} \begin{bmatrix} x_{aa1} & \dots & x_{aan} \\ x_{11} & \dots & x_{1n} \\ x_{21} & \dots & x_{2n} \\ \vdots & \vdots & \vdots \\ x_{m1} & \dots & x_{mn} \\ x_{ai1} & \dots & x_{ain} \end{bmatrix} \tag{17}$$

where:

$$\text{AAI} = \min(x_{ij}); i = 1, 2, \dots, m; j = 1, 2, \dots, n \quad \text{if } j \text{ is the criterion the bigger the better.}$$

$$\text{AAI} = \max(x_{ij}); i = 1, 2, \dots, m; j = 1, 2, \dots, n \quad \text{if } j \text{ is the criterion as small as better.}$$

$$\text{AI} = \max(x_{ij}); i = 1, 2, \dots, m; j = 1, 2, \dots, n \quad \text{if } j \text{ is the criterion the bigger the better.}$$

$$\text{AI} = \min(x_{ij}); i = 1, 2, \dots, m; j = 1, 2, \dots, n \quad \text{if } j \text{ is the criterion as small as better.}$$

Step 3: Calculating the normalized values according to the following equations:

$$u_{ij} = \frac{x_{AI}}{x_{ij}} \quad \text{if } j \text{ is the criterion as small as better} \tag{18}$$

$$u_{ij} = \frac{x_{ij}}{x_{AI}} \quad \text{if } j \text{ is the criterion the bigger the better} \tag{19}$$

Step 4: Calculating the weighted normalized values using the equation:

$$c_{ij} = u_{ij} \cdot w_j \tag{20}$$

where w_j is the weight of the criterion j .

Step 5: Calculating coefficients K_i^+ and K_i^- by the following equations:

$$K_i^- = \frac{S_i}{S_{AAI}} \tag{21}$$

$$K_i^+ = \frac{S_i}{S_{AI}} \tag{22}$$

where S_i , S_{AAI} and S_{AI} are the sum of the values of c_{ij} , x_{aai} and x_{ai} , respectively; with $i = 1, 2, \dots, m$.

Step 6: Calculating functions $f(K_i^+)$ and $f(K_i^-)$ by:

$$f(K_i^-) = \frac{K_i^+}{K_i^+ + K_i^-} \tag{23}$$

$$f(K_i^+) = \frac{K_i^-}{K_i^+ + K_i^-} \tag{24}$$

Step 7: Calculating function $f(K_i)$ according to the following equation and rank the alternatives:

$$f(K_i) = \frac{K_i^+ + K_i^-}{1 + \frac{1 - f(K_i^+)}{f(K_i^+)} + \frac{1 - f(K_i^-)}{f(K_i^-)}} \tag{25}$$

Ranking the solutions according to the best solution is the one with the largest value of the function $f(K_i)$.

2.4 The TOPSIS method

The steps performed in the TOPSIS method are described as follows [39, 40].

Step 1: Similar to step 1 of the MAIRCA method.

Step 2: Calculating the normalized values of k_{ij} according to the equation:

$$k_{ij} = \frac{x_{ij}}{\sqrt{\sum_{i=1}^m x_{ij}^2}} \tag{26}$$

Step 3: Calculating the weighted normalized values using the equation:

$$l_{ij} = w_j \times k_{ij} \tag{27}$$

Step 4: Determine the best solution A^+ and the worst solution A^- for the criteria according to the equations:

$$A^+ = \{l_1^+, l_2^+, \dots, l_j^+, \dots, l_n^+\} \tag{28}$$

$$A^- = \{l_1^-, l_2^-, \dots, l_j^-, \dots, l_n^-\} \tag{29}$$

wherein l_j^+ and l_j^- are the best and worst values of the j criterion, respectively.

Step 5: Calculating values S_i^+ and S_i^- by the following equations:

$$S_i^+ = \sqrt{\sum_{j=1}^n (l_{ij} - l_j^+)^2} \quad i = 1, 2, \dots, m \tag{30}$$

$$S_i^- = \sqrt{\sum_{j=1}^n (l_{ij} - l_j^-)^2} \quad i = 1, 2, \dots, m \tag{31}$$

Step 6: Calculating values C_i^* by:

$$C_i^* = \frac{S_i^-}{S_i^+ + S_i^-} \quad i = 1, 2, \dots, m; 0 \leq C_i^* \leq 1 \quad (32)$$

Step 7: Rank the alternatives according to the principle that the one with the largest C_i^* is the best one.

3. Used methods of determining the weight

3.1 The Entropy method

Determining the weights of the indicators by the Entropy method is performed according to the following steps [41].

Step 1: Determining the normalized values for the indicators:

$$p_{ij} = \frac{x_{ij}}{m + \sum_{i=1}^m x_{ij}^2} \quad (33)$$

Step 2: Calculating the value of the Entropy measure for each indicator:

$$me_j = - \sum_{i=1}^m [p_{ij} \times \ln(p_{ij})] - \left(1 - \sum_{i=1}^m p_{ij}\right) \times \ln\left(1 - \sum_{i=1}^m p_{ij}\right) \quad (34)$$

Step 3: Calculating the weight for each indicator:

$$w_j = \frac{1 - me_j}{\sum_{j=1}^m (1 - me_j)} \quad (35)$$

3.2 The MEREC method

The steps to determine the weights according to the MEREC method are as follows: [35]:

Step 1: Similar to step 1 of the MAIRCA method.

Step 2: Calculating the normalized values using the following equations:

$$h_{ij} = \frac{\min x_{ij}}{x_{ij}} \quad \text{if } j \text{ is the criterion the bigger the better} \quad (36)$$

$$h_{ij} = \frac{x_{ij}}{\max x_{ij}} \quad \text{if } j \text{ is the criterion as small as better} \quad (37)$$

Step 3: Calculating the overall efficiency of the alternatives by the following equation:

$$S_i = \ln \left[1 + \left(\frac{1}{n} \sum_j^n |\ln(h_{ij})| \right) \right] \quad (38)$$

Step 4: Calculating the efficiency of the alternatives according to the equation:

$$S'_{ij} = \ln \left[1 + \left(\frac{1}{n} \sum_{k, k \neq j}^n |\ln(h_{ik})| \right) \right] \quad (39)$$

Step 5: Calculating the absolute value of the deviations using the equation:

$$E_j = \sum_i^m |S'_{ij} - S_i| \quad (40)$$

Step 6: Calculating the weight for the criteria according to the equation:

$$w_j = \frac{E_j}{\sum_k^m E_k} \tag{41}$$

4. Used materials and execution of turning experiment

The experimental setup is described as follows: A conventional lathe ECOCA SJ460 (Taiwan) was used for the experiment. Besides, SKS3 steel samples with a diameter of 32 mm and a length of 260 mm were selected. In addition, three input parameters including cutting speed, feed rate and depth of cut were investigated. The Taguchi method was used to design an orthogonal matrix of 16 experimental runs (Table 1). After conducting the experiment, the MRR values were calculated according to the Eq. 42:

$$MRR = \frac{1}{60} \cdot n_w \cdot \pi \cdot d_w \cdot f_d \cdot a_p \text{ (mm}^3\text{/s)} \tag{42}$$

where n_w is the number of revolutions of the part per minute; d_w is the diameter of the work-piece; f_d is the feed rate, and a_p is the depth of cut (mm).

The surface roughness was also determined at each test using an SJ-201 equipment. Table 1 shows the obtained results of surface texture and *MRR*.

From Table 1, the minimum surface roughness is 0.455 μm in option A₁₃, but the maximum value of *MRR* is 362.046 mm³/s in option A₇. It is therefore necessary to define an alternative where the surface roughness is considered to be the “minimum” and the *MRR* is considered the “maximum”. This work can only be done by using mathematical methods in decision-making, and of course a mandatory job is also to determine the weights for the criteria. These two important contents will be presented in section 5 of this paper.

Table 1 Orthogonal experimental matrix L16 and the response

| Trial. | Actual value | | | Responses | |
|-----------------|-----------------|----------------|------------|------------------------|----------------------------|
| | n_w (rev/min) | f_d (mm/rev) | a_p (mm) | Ra (μm) | MRR (mm ³ /s) |
| A ₁ | 588 | 0.092 | 0.4 | 0.572 | 36.255 |
| A ₂ | 588 | 0.167 | 0.6 | 1.395 | 98.717 |
| A ₃ | 588 | 0.292 | 0.8 | 2.704 | 230.144 |
| A ₄ | 588 | 0.302 | 1.0 | 2.897 | 297.531 |
| A ₅ | 740 | 0.092 | 0.6 | 0.532 | 68.441 |
| A ₆ | 740 | 0.167 | 0.4 | 1.166 | 82.824 |
| A ₇ | 740 | 0.292 | 1.0 | 2.662 | 362.046 |
| A ₈ | 740 | 0.302 | 0.8 | 2.602 | 299.555 |
| A ₉ | 833 | 0.092 | 0.8 | 0.542 | 102.724 |
| A ₁₀ | 833 | 0.167 | 1.0 | 1.372 | 233.083 |
| A ₁₁ | 833 | 0.292 | 0.4 | 2.301 | 163.018 |
| A ₁₂ | 833 | 0.302 | 0.6 | 2.502 | 252.902 |
| A ₁₃ | 1050 | 0.092 | 1.0 | 0.455 | 161.855 |
| A ₁₄ | 1050 | 0.167 | 0.8 | 1.082 | 235.041 |
| A ₁₅ | 1050 | 0.292 | 0.6 | 2.221 | 308.228 |
| A ₁₆ | 1050 | 0.302 | 0.4 | 2.211 | 212.522 |

5. Results and discussion

5.1 Determining the weights for criteria

Eqs. 33 to 35 were used to determine the weights for the criteria according to the Entropy method. The weights of *Ra* and *MRR* are 0.6149 and 0.3851, respectively.

Eqs. 36 to 41 were applied to determine the weights for the criteria according to the MEREC method. The results have determined that the weights of *Ra* and *MRR* are 0.7042 and 0.2958, respectively.

5.2 Multi-criteria decision-making with the use of the entropy method for determining the weights of the criteria

Applying the MAIRCA method

Eq. 1 was used to build the initial matrix, which is the last two columns in Table 1.

Eq. 2 was applied to determine the priority P_{A_j} for the criteria. As the criteria are considered equal, that is, the decision maker does not give importance to one criterion over the other. Therefore, the priority for both criteria Ra and MRR is equal to $1/16 = 0.0625$.

Eq. 3 was applied to determine the value of parameter $t_{p_{ij}}$, with the weight of the criteria defined in section 5.1. The result has determined the value $t_{p_{ij}}$ of Ra and MRR are 0.0384 and 0.0241 respectively.

Eqs. 4 and 5 was used to calculate the values of $t_{r_{ij}}$; apply Eq. 6 to calculate g_{ij} ; apply Eq. 7 to calculate Q_i . All these values have been included in Table 2. The results of ranking options according to the value of Q_i have also been included in this table.

Table 2 Several MAIRCA parameters and ratings

| Trial. | $t_{r_{ij}}$ | | g_{ij} | | Q_i | Rank |
|-----------------|--------------|--------|----------|--------|--------|------|
| | Ra | MRR | Ra | MRR | | |
| A ₁ | 0.0366 | 0.0000 | 0.0018 | 0.0241 | 0.0259 | 6 |
| A ₂ | 0.0236 | 0.0046 | 0.0148 | 0.0195 | 0.0342 | 9 |
| A ₃ | 0.0030 | 0.0143 | 0.0354 | 0.0097 | 0.0451 | 16 |
| A ₄ | 0.0000 | 0.0193 | 0.0384 | 0.0048 | 0.0432 | 14 |
| A ₅ | 0.0372 | 0.0024 | 0.0012 | 0.0217 | 0.0229 | 4 |
| A ₆ | 0.0272 | 0.0034 | 0.0112 | 0.0206 | 0.0318 | 8 |
| A ₇ | 0.0037 | 0.0241 | 0.0347 | 0.0000 | 0.0347 | 10 |
| A ₈ | 0.0046 | 0.0195 | 0.0338 | 0.0046 | 0.0384 | 11 |
| A ₉ | 0.0371 | 0.0049 | 0.0014 | 0.0192 | 0.0205 | 3 |
| A ₁₀ | 0.0240 | 0.0145 | 0.0144 | 0.0095 | 0.0240 | 5 |
| A ₁₁ | 0.0094 | 0.0094 | 0.0291 | 0.0147 | 0.0438 | 15 |
| A ₁₂ | 0.0062 | 0.0160 | 0.0322 | 0.0081 | 0.0403 | 13 |
| A ₁₃ | 0.0384 | 0.0093 | 0.0000 | 0.0148 | 0.0148 | 1 |
| A ₁₄ | 0.0286 | 0.0147 | 0.0099 | 0.0094 | 0.0193 | 2 |
| A ₁₅ | 0.0106 | 0.0201 | 0.0278 | 0.0040 | 0.0318 | 7 |
| A ₁₆ | 0.0108 | 0.0130 | 0.0276 | 0.0110 | 0.0387 | 12 |

Applying the EAMR method

Eq. 8 was applied to build decision matrix. If the number of decision makers is k , then each person has a different decision matrix (possibly due to different experimental results). However, in this study, there is only one set of results shown in Table 1, i.e. k equals 1. Therefore, this step of *EAMR* method is similar to step 1 of *MAIRCA* method, which means that the main decision matrix is the last two columns in Table 1.

Eq. 9 was used to calculate the mean value of the alternatives for each criterion. For k equals 1, then $\bar{x}_{ij} = x_{ij}$.

Eq. 10 was applied to calculate the average weight for the criteria. Since k equals 1, so $\bar{w}_j = w_j$.

Eq. 11 was used to calculate n_{ij} values; apply Eq. 12 to calculate e_j values. Also, Eq. 13 was used to calculate v_{ij} .

Eqs. 14 and 15 were applied to calculate the respective values G_i .

Eq. 16 was used to calculate the S_i values.

The results of calculating these quantities are presented in Table 3. The results of ranking the alternatives according to the value of S_i have also been compiled into this table.

Table 3 EAMR parameters and ratings

| Trial. | n_{ij} | | v_{ij} | | G_i | | S_i | Rank |
|--------|----------|--------|----------|--------|--------|--------|--------|------|
| | Ra | MRR | Ra | MRR | Ra | MRR | | |
| A1 | 0.1974 | 0.1001 | 0.1214 | 0.0386 | 0.1214 | 0.0386 | 0.3176 | 16 |
| A2 | 0.4815 | 0.2727 | 0.2961 | 0.1050 | 0.2961 | 0.1050 | 0.3546 | 15 |
| A3 | 0.9334 | 0.6357 | 0.5739 | 0.2448 | 0.5739 | 0.2448 | 0.4265 | 12 |
| A4 | 1.0000 | 0.8218 | 0.6149 | 0.3165 | 0.6149 | 0.3165 | 0.5147 | 11 |
| A5 | 0.1836 | 0.1890 | 0.1129 | 0.0728 | 0.1129 | 0.0728 | 0.6447 | 9 |
| A6 | 0.4025 | 0.2288 | 0.2475 | 0.0881 | 0.2475 | 0.0881 | 0.3560 | 14 |
| A7 | 0.9189 | 1.0000 | 0.5650 | 0.3851 | 0.5650 | 0.3851 | 0.6816 | 7 |
| A8 | 0.8982 | 0.9719 | 0.5523 | 0.3743 | 0.5523 | 0.3743 | 0.6777 | 8 |
| A9 | 0.1871 | 0.3333 | 0.1150 | 0.1283 | 0.1150 | 0.1283 | 1.1156 | 3 |
| A10 | 0.4736 | 0.7562 | 0.2912 | 0.2912 | 0.2912 | 0.2912 | 1.0000 | 4 |
| A11 | 0.7943 | 0.5289 | 0.4884 | 0.2037 | 0.4884 | 0.2037 | 0.4170 | 13 |
| A12 | 0.8637 | 0.8205 | 0.5311 | 0.3160 | 0.5311 | 0.3160 | 0.5950 | 10 |
| A13 | 0.1571 | 0.5251 | 0.0966 | 0.2022 | 0.0966 | 0.2022 | 2.0939 | 1 |
| A14 | 0.3735 | 0.7626 | 0.2297 | 0.2937 | 0.2297 | 0.2937 | 1.2787 | 2 |
| A15 | 0.7667 | 1.0000 | 0.4714 | 0.3851 | 0.4714 | 0.3851 | 0.8169 | 6 |
| A16 | 0.7632 | 1.0000 | 0.4693 | 0.3851 | 0.4693 | 0.3851 | 0.8206 | 5 |

Applying the MARCOS method

Eq. 17 has been applied to determine the ideal solution (AI) and the opposite solution to the ideal solution (AAI). Accordingly, in the ideal solution, the values of Ra and MRR are $0.455 \mu\text{m}$ and $362.046 \text{ mm}^3/\text{min}$, respectively. At the opposite solution, the values of Ra and MRR are $2.897 \mu\text{m}$ and $36.255 \text{ mm}^3/\text{min}$, respectively.

Calculating the normalized values u_{ij} according to the Eqs. 18 and 19.

The normalized value considering the weight c_{ij} is calculated according to the Eq. 20.

The coefficients K_i^+ and K_i^- were calculated according to Eqs. 21 and 22.

The value of $f(K_i^+)$ that has been calculated by Eq. 23 is equal to 0.9025. Also, the value of $f(K_i^-)$ has been calculated by Eq. 24 is equal to 0.0975.

Eq. 25 has been applied to calculate the values of $f(K_i)$.

The results of calculating these quantities are presented in Table 4. The ranking results of the alternatives are also presented in this table.

Table 4 MARCOS parameters and ratings

| Trial. | u_{ij} | | c_{ij} | | K^+ | K^- | $f(K_i)$ | Rank |
|--------|----------|--------|----------|--------|---------|---------|----------|------|
| | Ra | MRR | Ra | MRR | | | | |
| A1 | 0.7955 | 0.1001 | 0.4891 | 0.0386 | 0.00146 | 0.01348 | 0.00144 | 4 |
| A2 | 0.3262 | 0.2727 | 0.2006 | 0.1050 | 0.00084 | 0.00780 | 0.00083 | 15 |
| A3 | 0.1683 | 0.6357 | 0.1035 | 0.2448 | 0.00096 | 0.00890 | 0.00095 | 13 |
| A4 | 0.1571 | 0.8218 | 0.0966 | 0.3165 | 0.00114 | 0.01055 | 0.00113 | 10 |
| A5 | 0.8553 | 0.1890 | 0.5259 | 0.0728 | 0.00165 | 0.01529 | 0.00163 | 3 |
| A6 | 0.3902 | 0.2288 | 0.2399 | 0.0881 | 0.00090 | 0.00838 | 0.00090 | 14 |
| A7 | 0.1709 | 1.0000 | 0.1051 | 0.3851 | 0.00135 | 0.01252 | 0.00134 | 6 |
| A8 | 0.1749 | 0.8274 | 0.1075 | 0.3186 | 0.00118 | 0.01088 | 0.00116 | 9 |
| A9 | 0.8395 | 0.2837 | 0.5162 | 0.1093 | 0.00173 | 0.01598 | 0.00171 | 2 |
| A10 | 0.3316 | 0.6438 | 0.2039 | 0.2479 | 0.00125 | 0.01154 | 0.00123 | 8 |
| A11 | 0.1977 | 0.4503 | 0.1216 | 0.1734 | 0.00081 | 0.00753 | 0.00081 | 16 |
| A12 | 0.1819 | 0.6985 | 0.1118 | 0.2690 | 0.00105 | 0.00973 | 0.00104 | 11 |
| A13 | 1.0000 | 0.4471 | 0.6149 | 0.1722 | 0.00217 | 0.02010 | 0.00215 | 1 |
| A14 | 0.4205 | 0.6492 | 0.2586 | 0.2500 | 0.00140 | 0.01299 | 0.00139 | 5 |
| A15 | 0.2049 | 0.8514 | 0.1260 | 0.3279 | 0.00125 | 0.01159 | 0.00124 | 7 |
| A16 | 0.2058 | 0.5870 | 0.1265 | 0.2261 | 0.00097 | 0.00901 | 0.00096 | 12 |

Applying the TOPSIS method

Eq. 26 was used to calculate the normalized values of k_{ij} . The normalized values taking into account the weight l_{ij} are calculated according to the Eq. 27.

The A^+ value of Ra and MRR has been determined by Eq. 28, with values of 0.0366 and 0.1597 respectively.

The A -value of Ra that MRR has also been determined by Eq. 29 is 0.2331 and 0.0160 respectively.

The values S_i^+ and S_i^- have been calculated according to the Eqs. 30 and 31, respectively.

The value C_i^* has been calculated by Eq. 32.

The results of calculating these quantities are presented in Table 5. The ranking results of the alternatives are also presented in this table.

Table 5 TOPSIS parameters and ratings

| Trial. | k_{ij} | | l_{ij} | | S_i^+ | S_i^- | C_i^* | Rank |
|--------|----------|--------|----------|--------|---------|---------|---------|------|
| | Ra | MRR | Ra | MRR | | | | |
| A1 | 0.0748 | 0.0415 | 0.0460 | 0.0160 | 0.1440 | 0.1871 | 0.5650 | 6 |
| A2 | 0.1825 | 0.1131 | 0.1122 | 0.0436 | 0.1386 | 0.1240 | 0.4721 | 9 |
| A3 | 0.3538 | 0.2637 | 0.2176 | 0.1015 | 0.1901 | 0.0869 | 0.3138 | 15 |
| A4 | 0.3791 | 0.3409 | 0.2331 | 0.1313 | 0.1985 | 0.1153 | 0.3673 | 14 |
| A5 | 0.0696 | 0.0784 | 0.0428 | 0.0302 | 0.1297 | 0.1908 | 0.5954 | 5 |
| A6 | 0.1526 | 0.0949 | 0.0938 | 0.0365 | 0.1358 | 0.1408 | 0.5090 | 7 |
| A7 | 0.3483 | 0.4148 | 0.2142 | 0.1597 | 0.1776 | 0.1450 | 0.4495 | 10 |
| A8 | 0.3405 | 0.3432 | 0.2094 | 0.1322 | 0.1749 | 0.1186 | 0.4040 | 11 |
| A9 | 0.0709 | 0.1177 | 0.0436 | 0.0453 | 0.1146 | 0.1917 | 0.6259 | 3 |
| A10 | 0.1795 | 0.2670 | 0.1104 | 0.1028 | 0.0932 | 0.1503 | 0.6174 | 4 |
| A11 | 0.3011 | 0.1868 | 0.1851 | 0.0719 | 0.1725 | 0.0737 | 0.2992 | 16 |
| A12 | 0.3274 | 0.2897 | 0.2013 | 0.1116 | 0.1716 | 0.1007 | 0.3699 | 13 |
| A13 | 0.0595 | 0.1854 | 0.0366 | 0.0714 | 0.0883 | 0.2041 | 0.6980 | 1 |
| A14 | 0.1416 | 0.2693 | 0.0871 | 0.1037 | 0.0754 | 0.1703 | 0.6932 | 2 |
| A15 | 0.2906 | 0.3531 | 0.1787 | 0.1360 | 0.1441 | 0.1317 | 0.4777 | 8 |
| A16 | 0.2893 | 0.2435 | 0.1779 | 0.0938 | 0.1559 | 0.0954 | 0.3795 | 12 |

5.3 Multi-criteria decision-making with the use of the MEREC method for determining the weights of the criteria

Doing the same as in section 5.2, the results of ranking options according to four multi-criteria decision-making methods (MAIRCA, EAMR, MARCOS and TOPSIS) when the weights are determined by the MEREC method (presented in section 5.1) are presented in Table 6. In addition, the ranking results of the alternatives when the weights are determined by the Entropy method (in Tables 2, 3, 4, 5) have also been summarized in Table 6.

Table 6 Ranking of alternatives by two methods of determining weight

| Trial. | Entropy weight | | | | MEREC weight | | | |
|--------|----------------|------|--------|--------|--------------|------|--------|--------|
| | MAIRCA | EAMR | MARCOS | TOPSIS | MAIRCA | EAMR | MARCOS | TOPSIS |
| A1 | 6 | 16 | 4 | 6 | 5 | 16 | 4 | 5 |
| A2 | 9 | 15 | 15 | 9 | 8 | 15 | 14 | 8 |
| A3 | 16 | 12 | 13 | 15 | 16 | 12 | 15 | 16 |
| A4 | 14 | 11 | 10 | 14 | 15 | 11 | 10 | 14 |
| A5 | 4 | 9 | 3 | 5 | 3 | 9 | 3 | 4 |
| A6 | 8 | 14 | 14 | 7 | 7 | 14 | 12 | 7 |
| A7 | 10 | 7 | 6 | 10 | 10 | 7 | 7 | 10 |
| A8 | 11 | 8 | 9 | 11 | 12 | 8 | 9 | 12 |
| A9 | 3 | 3 | 2 | 3 | 2 | 3 | 2 | 3 |
| A10 | 5 | 4 | 8 | 4 | 6 | 4 | 6 | 6 |
| A11 | 15 | 13 | 16 | 16 | 14 | 13 | 16 | 15 |
| A12 | 13 | 10 | 11 | 13 | 13 | 10 | 13 | 13 |
| A13 | 1 | 1 | 1 | 1 | 1 | 1 | 1 | 1 |
| A14 | 2 | 2 | 5 | 2 | 4 | 2 | 5 | 2 |
| A15 | 7 | 6 | 7 | 8 | 9 | 6 | 8 | 9 |
| A16 | 12 | 5 | 12 | 12 | 11 | 5 | 11 | 11 |

The ranking results of the options in Table 6 show that:

- With three methods MAIRCA, MARCOS, and TOPSIS: for different weighting methods, the ranking order of options is also different [33].
- All four multi-criteria decision-making methods identify A_{13} as the best option. This result is consistent when the weights of the criteria are determined by two different methods.
- The order of ranking the alternatives according to the EAMR method is completely the same when using two different weighting methods. This shows that the EAMR method has very high stability in ranking the alternatives.
- To ensure the "minimum" surface roughness and "maximum" MRR at the same time, the values of cutting speed, feed rate and cutting depth are 1050 rev/min, 0.092 mm/rev and 1.0 mm respectively.

6. Conclusion

This paper presents the results of an experimental study on the SKS3 steel turning process, with a total of 16 experiments designed according to the orthogonal matrix by the Taguchi method. Three cutting parameters were selected for the process input. Besides, surface roughness and MRR were selected as two parameters to evaluate turning process. Four methods including the MAIRCA, the EAMR, the MARCOS, and the TOPSIS were used for multi-criteria decision-making. The determination of the weights for the criteria was done by two methods Entropy and MEREC. From the results of the study, some conclusions are drawn as follows:

- For the first time, three methods including MAIRCA, EAMR, MARCOS are used to make multi-criteria decision for turning process. An excellent result has been obtained that all three methods as well as the TOPSIS method have consistently identified a best alternative.
- The MEREC method is applied for the first time in this study to determine the weights for the criteria of the turning process. The use of weights determined by the Entropy method or the MEREC method does not affect the determination of the best solution in all four cases where the different methods are used. Thus, with this study, determining the best solution when using four methods (MAIRCA, EAMR, MARCOS and TOPSIS) does not depend on the method of determining the weights.
- When using the Entropy method, for different multi-criteria decision-making methods, the same best solution can be determined [17]. In addition, when using two methods Entropy and MEREC, for different decision-making methods, the best solutions still only one option.
- To determine the best option when making a multi-criteria decision, the weighted method is Entropy and (or) MEREC should be used.
- The order of ranking the alternatives when using the EAMR method is completely the same when using two different weighting methods. This shows the use of the EAMR method to rank the alternatives for high stability. This can be explained that when applying this method, the weights of the criteria were normalized according to Eq. 13.
- The above conclusions are drawn based on the results of this study. To solidify them, there is a need for some more studies in which other weighting options are considered, in other machining processes.

References

- [1] Medić, N., Anišić, Z., Lalić, B., Marjanović, U., Brezočnik, M. (2019). Hybrid fuzzy multi attribute decision making model for evaluation of advanced digital technologies in manufacturing: Industry 4.0 perspective, *Advances in Production Engineering & Management*, Vol. 14, No. 4, 483-493, doi: [10.14743/apem2019.4.343](https://doi.org/10.14743/apem2019.4.343).
- [2] Ko, T.J., Kim, H.S. (2021). Surface integrity and machineability in intermittent hard turning, *International Journal of Advanced Manufacturing Technology*, Vol. 18, 168-175, doi: [10.1007/s001700170072](https://doi.org/10.1007/s001700170072).
- [3] Dich, T.V., Binh, N.T., Dat, N.T., Tiep, N.V., Viet, T.X. (2003). *Manufacturing technology*, Science and Technics Publishing House, Hanoi, Vietnam.

- [4] Özbek, O., Saruhan, H. (2020). The effect of vibration and cutting zone temperature on surface roughness and tool wear in eco-friendly MQL turning of AISI D2, *Journal of Materials Research and Technology*, Vol. 9, No. 3, 2762-2772, doi: [10.1016/j.jmrt.2020.01.010](https://doi.org/10.1016/j.jmrt.2020.01.010).
- [5] Aggarwal, A., Choudhary, C., Mehrotra, D. (2018). Evaluation of smartphones in Indian market using EDAS, *Procedia Computer Science*, Vol. 132, 236-243, doi: [10.1016/j.procs.2018.05.193](https://doi.org/10.1016/j.procs.2018.05.193).
- [6] Çelikkilek, Y., Tüysüz, F. (2020). An in-depth review of theory of the TOPSIS method: An experimental analysis, *Journal of Management Analytics*, Vol. 7, No. 2, 281-300, doi: [10.1080/23270012.2020.1748528](https://doi.org/10.1080/23270012.2020.1748528).
- [7] Parida, A.K., Routara, B.C. (2014). Multiresponse optimization of process parameters in turning of GFRP using TOPSIS method, *International Scholarly Research Notices*, Vol. 2014, Article ID 905828, doi: [10.1155/2014/905828](https://doi.org/10.1155/2014/905828).
- [8] Singh, A., Datta, S., Mahapatra, S.S. (2011). Application of TOPSIS in the Taguchi method for optimal machining parameter selection, *Journal for Manufacturing Science and Production*, Vol. 11, 49-60, doi: [10.1515/jmsp.2011.002](https://doi.org/10.1515/jmsp.2011.002).
- [9] Maheswara Rao, C., Jagadeeswara Rao, K., Laxmana Rao, K. (2016). Multi-objective optimization of MRR, Ra and Rz using TOPSIS, *International Journal of Engineering Sciences & Research Technology*, Vol. 5, No. 9, 376-384.
- [10] Prakash, D.B., Krishnaiah, G., Shankar, N.V.S. (2016). Optimization of process parameters adding AHP and TOPSIS when turning 1040 steel with coated tools, *International Journal of Mechanical Engineering and Technology*, Vol. 7, No. 6, 483-492.
- [11] Khan, A., Maity, K. (2017). Application of MCDM-based TOPSIS method for the selection of optimal process parameter in turning of pure titanium, *Benchmarking: An International Journal*, Vol. 24, No. 7, 2009-2021, doi: [10.1108/BIJ-01-2016-0004](https://doi.org/10.1108/BIJ-01-2016-0004).
- [12] Khan, A., Maity, K. (2019). Application potential of combined fuzzy-TOPSIS approach in minimization of surface roughness, cutting force and tool wear during machining of CP-Ti grade II, *Soft Computing*, Vol. 23, 6667-6678, doi: [10.1007/s00500-018-3322-7](https://doi.org/10.1007/s00500-018-3322-7).
- [13] Singh, R., Dureja, J.S., Dogra, M., Randhawa, J.S. (2019). Optimization of machining parameters under MQL turning of Ti-6Al-4V alloy with textured tool using multi-attribute decision-making methods, *World Journal of Engineering*, Vol. 16, No. 5, 648-659, doi: [10.1108/WJE-06-2019-0170](https://doi.org/10.1108/WJE-06-2019-0170).
- [14] Mane, S.S., Mulla, A.M. (2020). Relevant optimization method selection in turning of AISI D2 steel using cryogenic cooling, *International Journal of Creative Research Thoughts*, Vol. 8, No. 10, 803-812.
- [15] Rao, S.R., Jeelani, S.A.K., Swamulu, V. (2021). Multi-objective optimization using TOPSIS in turning of Al 6351 alloy, In: *Proceedings of Industry 4.0 Technologies in Civil and Mechanical Engineering (ICI4TCME 2020)*, Vol. 1112, Andhra Pradesh, India, Article No. 1112, doi: [10.1088/1757-899X/1112/1/012010](https://doi.org/10.1088/1757-899X/1112/1/012010).
- [16] Trung, D.D. (2021). Application of TOPSIS and PIV methods for multi - Criteria decision making in hard turning process, *Journal of Machine Engineering*, Vol. 21, No. 4, 57-71, doi: [10.36897/jme/142599](https://doi.org/10.36897/jme/142599).
- [17] Trung, D.D. (2021). A combination method for multi-criteria decision making problem in turning process, *Manufacturing Review*, Vol. 8, No. 26, Article No. 26, doi: [10.1051/mfreview/2021024](https://doi.org/10.1051/mfreview/2021024).
- [18] Pamucar, D.S., Pejčić Tarle, S., Parežanović, T. (2018). New hybrid multi-criteria decision-making DEMATEL - MAIRCA model: Sustainable selection of a location for the development of multimodal logistics centre, *Economic Research-Ekonomska Istraživanja* Vol. 31, No. 1, 1641-1665, doi: [10.1080/1331677X.2018.1506706](https://doi.org/10.1080/1331677X.2018.1506706).
- [19] Aksoy, E. (2021). An analysis on Turkey's merger and acquisition activities: MAIRCA method, *Gümüşhane Üniversitesi Sosyal Bilimler Dergisi*, Vol. 12, No. 1, 1-11.
- [20] Bakir, M., Akan, Ş., Kiraci, K., Karabasevic, D., Stanujkic, D., Popovic, G. (2020). Multiple-criteria approach of the operational performance evaluation in the airline industry: Evidence from the emerging markets, *Romanian Journal of Economic Forecasting*, Vol. 23, No. 2, 149-172.
- [21] Büyüközkan, G., Uztürk, D. (2022). A Novel 2-Tuple SAW-MAIRCA method for partner evaluation for circular economy, In: Kahraman, C., Cebi, S., Cevik Onar, S., Oztaysi, B., Tolga, A.C., Sari, I.U. (eds.), *Intelligent and Fuzzy Techniques for Emerging Conditions and Digital Transformation*, INFUS 2021, Lecture Notes in Networks and Systems, Vol 307, Springer, Cham.
- [22] Kayapınar Kaya, S. (2020). Evaluation of the effect of COVID-19 on countries' sustainable development level: A comparative MCDM framework, *Operational Research in Engineering Sciences: Theory and Applications*, Vol. 3, No. 3, 101-122, doi: [10.31181/oresta20303101k](https://doi.org/10.31181/oresta20303101k).
- [23] Keshavarz Ghorabae, M., Zavadskas, E.K., Amiri, M., Antucheviciene, J. (2016). Evaluation by an area-based method of ranking interval type-2 fuzzy sets (EAMRIT-2F) for multi-criteria group decision making, *Transformations in Business & Economics*, Vol. 15, No. 3, 76-95.
- [24] Yazdi, A.K., Hanne, T., Gómez, J.C.O., Alcaraz, J.L.G. (2018). Finding the best third-party logistics in the automobile industry: A hybrid approach, *Mathematical Problems in Engineering*, Vol. 2018, Article ID 5251261, doi: [10.1155/2018/5251261](https://doi.org/10.1155/2018/5251261).
- [25] Meidute-Kavaliauskiene, I., Ghorbani, S. (2021). Supply chain contract selection in the healthcare industry: A hybrid mcdm method in uncertainty environment, *Independent Journal of Management & Production*, Vol. 12, No. 4, 1160-1187, doi: [10.14807/ijmp.v12i4.1356](https://doi.org/10.14807/ijmp.v12i4.1356).
- [26] Keshavarz Ghorabae, M., Amiri, M., Zavadskas, E.K., Turskis, Z., Antucheviciene, J. (2017). A new multi-criteria model based on interval type-2 fuzzy sets and EDAS method for supplier evaluation and order allocation with environmental considerations, *Computers & Industrial Engineering*, Vol. 112, 156-174, doi: [10.1016/j.cie.2017.08.017](https://doi.org/10.1016/j.cie.2017.08.017).

- [27] Stević, Ž., Pamučar, D., Puška, A., Chatterjee, P. (2020). Sustainable supplier selection in healthcare industries using a new MCDM method: Measurement alternatives and ranking according to COmpromise solution (MARCOS), *Computers & Industrial Engineering*, Vol. 140, Article No. 106231, [doi: 10.1016/j.cie.2019.106231](https://doi.org/10.1016/j.cie.2019.106231).
- [28] Tadić, S., Kilibarda, M., Kovač, M., Zečević, S. (2021). The assessment of intermodal transport in countries of the Danube region, *International Journal for Traffic and Transport Engineering*, Vol. 11, No. 3, 375-391, [doi: 10.7708/ijtte2021.11\(3\).03](https://doi.org/10.7708/ijtte2021.11(3).03).
- [29] Stanković, M., Stević, Ž., Das, D.K., Subotić, M., Pamučar, D. (2020). A new fuzzy MARCOS method for road traffic risk analysis, *Mathematics*, Vol. 8, No. 3, Article No. 457, [doi: 10.3390/math8030457](https://doi.org/10.3390/math8030457).
- [30] Ulutaş, A., Karabasevic, D., Popovic, G., Stanujkic, D., Nguyen, P.T., Karaköy, Ç. (2020). Development of a novel integrated CCSD-ITARA-MARCOS decision-making approach for stackers selection in a logistics system, *Mathematics*, Vol. 8, No. 10, Article No. 1672, [doi: 10.3390/math8101672](https://doi.org/10.3390/math8101672).
- [31] Stević, Z., Brković, N. (2020). A novel integrated FUCOM-MARCOS model for evaluation of human resources in a transport company, *Logistics*, Vol. 4, No. 1, Article No. 4, [doi: 10.3390/logistics4010004](https://doi.org/10.3390/logistics4010004).
- [32] Anysz, H., Nicał, A., Stević, Ž., Grzegorzewski, M., Sikora, K. (2021). Pareto optimal decisions in multi-criteria decision making explained with construction cost cases, *Symmetry*, Vol. 13, No. 1, Article No. 46, [doi: 10.3390/sym13010046](https://doi.org/10.3390/sym13010046).
- [33] Gunantara, N. (2018). A review of multi-objective optimization: Methods and its applications, *Cogent Engineering*, Vol. 5, No. 1, Article No. 1502242, [doi: 10.1080/23311916.2018.1502242](https://doi.org/10.1080/23311916.2018.1502242).
- [34] Roszkowska, E. (2013). Rank ordering criteria weighting methods – A comparative overview, *Optimum. Economic Studies*, Vol. 5, No. 65, 14-33, [doi: 10.15290/OSE.2013.05.65.02](https://doi.org/10.15290/OSE.2013.05.65.02).
- [35] Keshavarz-Ghorabae, M., Amiri, M., Zavadskas, E.K., Turskis, Z., Antucheviciene, J. (2021). Determination of objective weights using a new method based on the removal effects of criteria (MERECE), *Symmetry*, Vol. 13, No. 4, Article No. 525, [doi: 10.3390/sym13040525](https://doi.org/10.3390/sym13040525).
- [36] Keshavarz-Ghorabae, M. (2021). Assessment of distribution center locations using a multi-expert subjective-objective decision-making approach, *Scientific Reports*, Vol. 11, Article No. 19461, [doi: 10.1038/s41598-021-98698-y](https://doi.org/10.1038/s41598-021-98698-y).
- [37] Sabaghian, K., Khamforoosh, K., Ghaderzadeh, A. (2021). Presentation of a new method based on modern multi-variate approaches for big data replication in distributed environments, *Plos One*, Vol. 16, No. 7, Article ID e0254210, [doi: 10.1371/journal.pone.0254210](https://doi.org/10.1371/journal.pone.0254210).
- [38] Lakshmi, V.V.K., Subbaiah, K.V., Kothapalli, A.V., Suresh K. (2020). Parametric optimization while turning Ti-6Al-4V alloy in mist-MQCL (green environment) using the DEAR method, *Manufacturing Review*, Vol. 7, Article No. 38, [doi: 10.1051/mfreview/2020034](https://doi.org/10.1051/mfreview/2020034).
- [39] Hwang, C.-L., Lai, Y.-J., Liu, T.-Y. (1993). A new approach for multiple objective decision making, *Computers & Operations Research*, Vol. 20, No. 8, 889-899, [doi: 10.1016/0305-0548\(93\)90109-V](https://doi.org/10.1016/0305-0548(93)90109-V).
- [40] Payal, H., Bharti, P.S., Maheshwari, S., Agarwal, D. (2020). Machining characteristics and parametric optimisation of Inconel 825 during electric discharge machining, *Tehnički Vjesnik – Technical Gazette*, Vol. 27, No. 3, 761-772, [doi: 10.17559/TV-20190214135509](https://doi.org/10.17559/TV-20190214135509).
- [41] Trung, D.D., Nguyen, N.-T., Van Duc, D. (2021). Study on multi-objective optimization of the turning process of EN 10503 steel by combination of Taguchi method and Moora technique, *EUREKA: Physics and Engineering*, Vol. 2021, No. 2, 52-65, [doi: 10.21303/2461-4262.2020.001414](https://doi.org/10.21303/2461-4262.2020.001414).

Molecular-dynamics study of multi-pulsed ultrafast laser interaction with copper

Yin, C.P.^a, Zhang, S.T.^a, Dong, Y.W.^{a,*}, Ye, Q.W.^a, Li, Q.^b

^aSchool of Aerospace Engineering, Xiamen University, Xiamen, P.R. China

^bENN Energy Power Technology (Shanghai) Co., Ltd, Shanghai, P.R. China

ABSTRACT

Ultrafast laser has an undeniable advantage in laser processing due to its extremely small pulse width and high peak energy. While the interaction of ultrafast laser and solid materials is an extremely non-equilibrium process in which the material undergoes phase transformation and even ablation in an extremely short time range. This is the coupling of the thermos elastic effect caused by the pressure wave and the superheated melting of the material lattice. To further explore the mechanism of the action of ultrafast laser and metal materials, the two-temperature model coupling with molecular dynamics method was used to simulate the interaction of the copper and laser energy. Firstly, the interaction of single-pulsed laser and copper film was reproduced, and the calculated two-temperature curve and the visualized atomic snapshots were used to investigate the influence of laser parameters on the ablation result. Then, by changing the size of the atomic system, the curve of ablation depth as a function of laser fluence was obtained. In this paper, the interaction of multi-pulsed laser and copper was calculated. Two-temperature curve and temperature contour of copper film after the irradiation of double-pulsed and multi-pulsed laser were obtained. And the factors which can make a difference to the incubation effect were analyzed. By calculating the ablation depth under the action of multi-pulsed laser, the influence of the incubation effect on ablation results was further explored. Finally, a more accurate numerical model of laser machining metal is established and verified by an ultra-short laser processing experiment, which provides a new calculation method and theoretical basis for ultra-fast laser machining of air film holes in aviation turbine blades, and has certain practical guiding significance for laser machining.

ARTICLE INFO

Keywords:

Ultrafast laser;
Multi-pulsed laser;
Ablation;
Copper;
Modelling and simulation;
Two-temperature model;
Molecular dynamics;
Laser machining

*Corresponding author:

yiweidong@xmu.edu.cn
(Dong, Y.W.)

Article history:

Received 22 September 2021

Revised 22 November 2021

Accepted 3 December 2021



Content from this work may be used under the terms of the Creative Commons Attribution 4.0 International Licence (CC BY 4.0). Any further distribution of this work must maintain attribution to the author(s) and the title of the work, journal citation and DOI.

1. Introduction

Ultrafast laser ablation, which uses ultrafast laser to remove the surface of solid materials, with processing accuracy ranging from micron to nanometer scale, which allows material processing with extremely high precision due to the relatively small heat affected zone from each pulse [1]. This feature makes the ultrafast laser have the advantage of ‘cold processing’ which means the thermal influence on the surrounding material is extremely small. The surrounding material is still in a ‘cold state’ while the electron temperature in the processed region reaches an extremely high level from the solid state to the plasma state, which ensures the processing edge is neat [2]. In addition, due to the distribution characteristics of the Gaussian laser, the size of the ultrafast laser processing can be smaller than the spot size of the laser to achieve microfabrication. In the process of ultrafast laser processing, the absorption of laser light by the material is multiphoton absorption [3], which is more dependent on the atomic properties of the material. This feature

makes the range of materials for femtosecond laser processing no longer limited. Ultrafast lasers have the above-mentioned significant advantages in the microfabrication process of materials, while the further improvement in processing technology and precision is limited by the complexity of its mechanism of action. In the process of ultrafast laser action, electronic excitation, internal heat transfer of materials and melting of materials are involved. Fig. 1 shows an overview of the physical phenomena involved in the time range considered.

The main methods used by domestic and foreign scholars of ultrafast laser ablation of solid materials can be divided into numerical simulation and experimental determination.

Numerical simulation is widely used because of its low cost, good reflection of physical processes, and ease of analysis. Annemie [4] *et al.* simulated atomic-scale material failures such as melting, vaporization and spallation by combining molecular dynamics (MD) and finite difference methods, derived the spatiotemporal evolution of density and pressure through the two-temperature model (TTM), then discussed the heat transfer of the special alloy with anisotropy, and calculated and verified the electron cooling time and ablation threshold. Ivanov [5] *et al.* presented an atomistic-to-continuum (AtC) computational model to investigate the dynamic microscopic mechanism of laser ablation of nickel and gold films. It is found that the interaction between the growth front of the melting front end of the film (liquid-crystal interface) and the uniform nucleation of the liquid phase inside the crystal is the reason that the laser fluence near the melting threshold causes the metal film to melt. At higher laser fluence, the high tensile stress generated inside the film is also a cause of cracking. Foumani [6] *et al.* used a TTM-MD method to investigate the response of copper film at different laser fluences. Based on the model, the dependence of the reflectivity of the copper film on the laser fluence and the evolution of density, electron temperature and lattice temperature with time were obtained. Porvanitsy [7] *et al.* used two different methods to simulate the laser ablation of aluminum bulks by changing the laser fluence. The first method is single-fluid two-temperature hydrodynamics (HD) completed with a two-temperature equation of state (EOS), the second approach is a combination of classical molecular dynamics and a continuum model of a free electron subsystem. After comparing the simulation results with the experiment, it is found that the HD and MD methods show good consistency in describing the phase explosion and cracking process. The TTM is a mainstream model for exploring the effects of metals and ultrafast lasers. The researchers have continuously improved and reduced the TTM [8] to apply to calculations in different materials and different media.

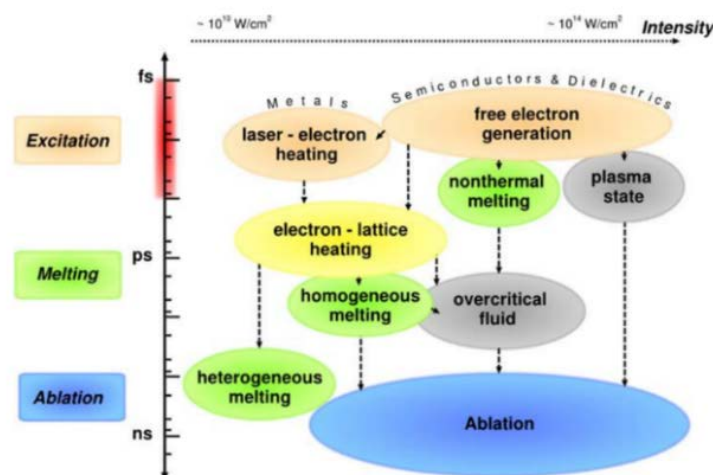


Fig. 1 Physical phenomena involved in the action of ultrafast lasers and solid materials [2]

In the field of multi-pulsed laser ablation, researchers often use experimental methods to study the changes of hole depth and hole morphology with incident laser parameters. Winter [9] *et al.* used the experimental method to ultra-fast measurement of the refractive index of copper. At the same time, the TTM and thermo-mechanical model with precise description of thermal and optical properties were used as theoretical support to explore the refractive index n and the extinction coefficient k in different time ranges. Wang [10] *et al.* used a double-pulsed femtosecond laser to

irradiate copper and aluminum films of 50 μm . It has been found that both the copper film and the aluminum film pore size decrease as the double pulse delay increases, but the diameters of the redeposited materials of the two films are different. Karim [11] *et al.* studied the interaction between short-pulsed lasers and metal surfaces with solid transparent coatings by combining experimental and atomic simulations and revealed the structural modification mechanism of the junction zone between metal and coating. Fokin [12] *et al.* used TTM-HD and TTM-MD method to clarify the reaction mechanism of metal targets on laser irradiation.

In this paper, the TTM-MD method is used to simulate the metal copper film irradiated by single-pulsed and multi-pulsed laser. We explored the factors that influence the ablation results and the ablation depth at different laser fluences under the action of a single pulsed laser. Then, the simulation of multi-pulsed laser ablation of metals reveals the existence of incubation effects and its effects on ablation depth.

2. Computational model

2.1 TTM-MD model for Cu target

When we describe the change of the metal after exposure to laser light, the energy transfer from the electron to the lattice is slow due to the large mass difference between the electron and the phonon [13]. Therefore, it is unreasonable to assume that the electron and the lattice temperature are the same when the duration of the laser pulse is no longer than the time at which the electron and the lattice reach equilibrium. The two-temperature model proposed by Anisimov [14] in 1973 is a good description of the time evolution of electron and lattice temperatures of metals under ultrafast laser irradiation. In recent years, TTM has become an effective model for studying the evolution of electron and lattice temperature with time under the action of ultrafast lasers. The two one-dimensional nonlinear differential equations are as follows:

$$c_e \frac{\partial T_e}{\partial t} = \frac{\partial}{\partial x} \left(k_e \frac{\partial T_e}{\partial x} \right) - g(T_e - T_i) + S(x, t) \quad (1)$$

$$c_i \frac{\partial T_i}{\partial t} = g(T_e - T_i) \quad (2)$$

Where T_e is the temperature of the electronic system and T_i is the temperature of the lattice system. The first term on the right side of Eq. 1 is the heat conduction term, the second term is the energy coupling term, and the third term is the laser source term. When using a Gaussian beam for numerical simulation, the source term can be rewritten as [15]:

$$S(x, t) = \frac{A\alpha F}{\sqrt{\pi/4 \ln(2)\tau_L}} \exp(-\alpha x) \cdot \exp[-4 \ln(2)(t/\tau_L - 2)^2] \quad (3)$$

Where A is the surface transmittance α , is the material absorption coefficient, F is the laser fluence, x is the depth from the calculated position to the surface of the material, and τ_L is the pulse width. When double-pulsed or multi-pulsed laser is used, the light source term can be rewritten as [16]:

$$S(x, t) = \frac{A\alpha F}{\sqrt{\pi/4 \ln(2)\tau_L}} \exp(-\alpha x) \cdot \exp[-4 \ln(2)(t/\tau_L - 2)^2 - 4 \ln(2)((t - dt_1)/\tau_L - 2)^2] \quad (4)$$

$$S(x, t) = \frac{A\alpha F}{\sqrt{\pi/4 \ln(2)\tau_L}} \exp(-\alpha x) \cdot \exp[-4 \ln(2)(t/\tau_L - 2)^2 - 4 \ln(2)((t - dt_1)/\tau_L - 2)^2 - 4 \ln(2)((t - dt_2)/\tau_L - 2)^2] \quad (5)$$

where dt_1 and dt_2 are the pulse interval time, respectively.

Although the two-temperature model is widely used to explore ablation mechanisms, predict ablation thresholds and many other research fields, there are still deficiencies. Especially in describing the phase transition of metal material continuum under high imbalance conditions, it often involves many assumptions and simplifications. There are many controversies about the phase transition mechanism under intense overheating, which requires TTM to be combined with other methods to perform more accurate simulations.

Therefore, we introduce molecular dynamics simulation. The significant advantage of molecular dynamics over hydrodynamic is that its priori includes nucleation kinetics and phase transitions without any assumptions about nucleation kinetics. This solves the shortcomings of the two-temperature model described before, so MD is suitable for the calculation of small scale fast unbalanced processes. The MD simulation assumes that all particles satisfy Newton's second law and are subject to the forces of other particles, this interaction satisfies the principle of superposition. The MD simulation process is to calculate the potential energy of the system under the given initial conditions, iteratively solve the motion equation to obtain the position information and spatial coordinates of the particles, and select the appropriate difference formula to calculate the potential energy. Then the spatial information of the particles will be newly calibrated by the constraint algorithm of temperature and pressure.

The classical molecular dynamics method only considers the lattice thermal conduction, but the electron conduction in the metal dominates, so it underestimates the total thermal conductivity of the metal, and cannot be directly used to simulate the interaction between metal and ultra-fast lasers without two-temperature model. The TTM-MD equations we used are shown as following [17]:

$$c_e(T_e) \frac{\partial T_e}{\partial t} = \frac{\partial}{\partial x} (k_e(T_e) \frac{\partial T_e}{\partial x}) - g(T_e - T_i) + S(x, t), \quad \text{TTM} \quad (6)$$

$$m_i \ddot{r}_i = F_i + \xi m_i V_i^T, \quad \text{MD} \quad (7)$$

$$\xi = \frac{1}{n} \sum_{k=1}^n g V_N(T_e^k - T_i) / \sum_i m_i (V_i^T)^2 \quad (8)$$

where m_i and r_i are the mass and position of the i th atom, respectively, F_i is produced by the interaction between atoms, that is, the force generated on the i th atom. The additional item $\xi m_i V_i^T$ in the equation is brought by electron-phonon coupling. The thermal motion velocity V_i^T in this term is different from the velocity V representing the atom in the whole system, which is generally a function of temperature. The lattice temperature and energy coupling coefficient ξ are determined by each unit cell and summed. The TTM-MD method not only explains the electron energy absorption, the energy exchange process between electrons and phonons, but also provides the possibility to describe the non-equilibrium ablation process when the lattice is overheated.

2.2 Calculation parameters

In this calculation we need to choose the appropriate potential function and set the periodic boundary conditions. The potential function between molecules represents the force of interaction between molecules, and the gradient of the potential function is the force function. In this calculation we use the metal potential function EAM (embedded-atom model), the mathematical expression [15] of the model is as follows:

$$u_{EAM} = \sum_{i=1}^N \sum_{j=i+1}^N u(r_{ij}) + \sum_{i=1}^N E(\rho_i) \quad (9)$$

The first term on the right side of Eq. 9 is the two-body potential between the nucleus, the second item is the mosaic energy of the nucleus, which is the result of multi-body action. According to the density functional theory (DFT), the nucleus is affected by other nuclei, and is also subjected to the multi-body effect in the background of the electron cloud, which is the second term of the equation.

Due to the limitation of computing resources, periodic boundary conditions are used in this calculation. Because of the existence of periodic boundary conditions, the particles can not only move in the central cell, but after the particles move out of one side boundary at a certain speed, they will enter the central cell at the same speed from the other side, to ensure a certain number of atoms and eliminate the boundary effect. The calculation model after applying periodic boundary conditions is shown in Fig. 2.

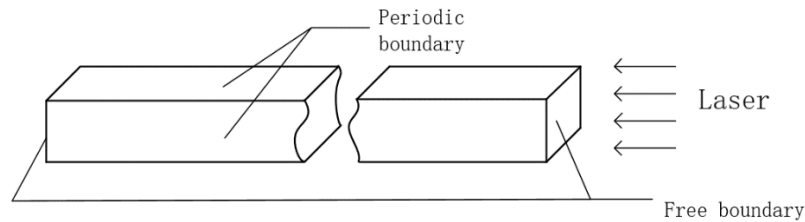


Fig. 2 Schematic diagram of boundary conditions of the model

In this paper, pure copper crystal is used for simulation of ultrafast laser ablation. When investigating the effect of pulse parameters on temperature changes and ablation results, the model size is $6a \times 6a \times 150a$, the lattice parameter of copper is $a = 0.3615$ nm, the copper crystal is a face-centered cubic structure, so the actual central cell model is 2.619 nm \times 2.619 nm \times 54.225 nm and the number of atoms is 21672. When calculating the ablation depth, in order to avoid the influence of thermal expansion caused by the system being too small, the model is expanded to 2.619 nm \times 2.619 nm \times 361.5 nm, and the number of atoms is expanded to 144072. The thermal property parameters of copper are derived from the 'Cu_ttm.mat' file in LAMMPS (LAMMPS Molecular Dynamics Simulator), in which the specific heat of the electron and the specific heat of the lattice are set to be constant, the electron-phonon coupling coefficient and the thermal conductivity of electrons and lattice are approximately linearly related to temperature.

Before the laser is incident during the simulation, the copper atoms in the system are relaxed and balanced at 300 K, and a total of 100,000 steps are performed in time step of 0.001 ps. In this way, the structural order parameters of the system are close to 1, and the atomic velocity distribution inside the system is Maxwell distribution at 300 K, which ensures the accuracy of the initial simulation system and the reliability of the calculation results.

3. Results and discussion

3.1 Interaction of single-pulsed laser with copper film

In this section, firstly we reproduced the simulated laser ablation process of single-pulsed laser with copper film, compared the results with existing literature [16] and further changed the parameters of laser to explore the mechanisms of ablation. Ablation depths under different laser fluences are also considerable for our research.

The comparison of the following temperature contours directly reflects the correctness and reliability of our simulation calculation. We selected the same laser parameters and potential function as the existing literature [16] in the calculation process. As shown in Figs. 3 and 4, the maximum electron temperatures are 16000 K both, the thermal influential area is 5 nm away from the incident surface of the laser, and the highest temperature can reach is more than 15000 K in the two pictures. Since the electron specific heat used in this paper is a fixed value and smaller than the linear relationship of $C_e = 96.6 T_e$ (J/m³·K) used in the comparison literature, the time it takes for the electron to reach the highest temperature is shorter.

Comparing Figs. 3 and 4, we found that since the electron-phonon coupling factor of this paper is slightly higher than 1×10^{17} (W/m³·K) used in the comparative literature [16], the lattice can reach its highest temperature faster. However, the thermal conductivity of the lattice is lower than the linear relationship simulated in the literature, so the highest temperature that the lattice can reach is lower than the comparative literature. In summary, this simulation is accurate and effective within the consideration of the selected parameters.

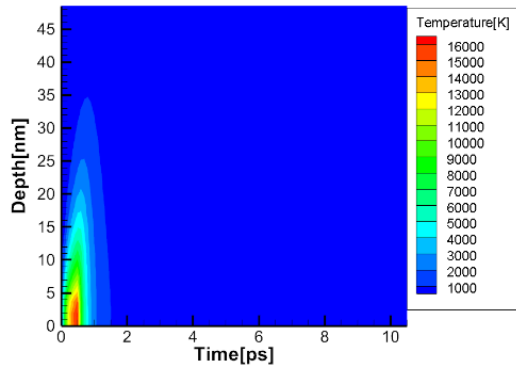


Fig. 3 Electron temperature contour with pulse width of 500 fs and laser fluence of 320 J/m²

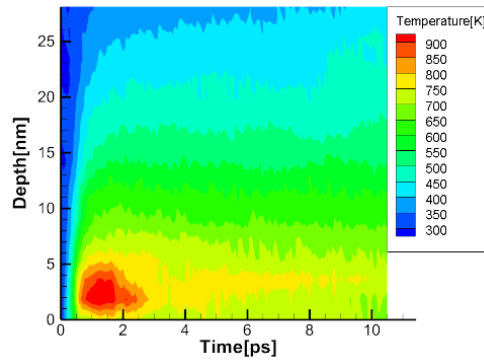


Fig. 4 lattice temperature contour with pulse width of 500 fs and laser fluence of 320 J/m²

Different influence factors for ablation results

Laser pulse width and laser fluence are two important factors affect the ablation results, to explore the mechanism of the action between laser and copper film, we changed these two parameters and make the laser source perpendicular to the $z = 0$ surface to obtain different two-temperature curves. In the first set of calculations, the fixed laser fluence is 1000 J/m², and the pulse width is selected to be 100 fs, 300 fs, and 500 fs, respectively.

The temperature shown in Figs. 5 to 8 are all refer to the average temperature. It can be seen in Fig. 5 that at 0.5 ps, the electron reached a maximum temperature of 6010 K, and then the energy obtained by electron transferred to the lattice by electro-phonon coupling, so the temperature of electron rapidly fell back. The lattice reached a peak temperature of 522 K at about 1.6 ps, after which the temperatures of the electron and the lattice tend to coincide. In Figs. 6 and 7, the electron reached peak temperature of 7642 K and 9767 K at 0.3 ps and 0.1 ps, respectively. And the process of electron-phonon coupling leading to a balance of electron and lattice temperature is highly consistent with the process shown in Fig. 5.

As can be seen from Fig. 8, the smaller the pulse width of the incident laser, the shorter the time required for the electron to reach the peak temperature, and the higher the peak temperature of the electron. This is because a small pulse width means a more concentrated pulse energy power, and the calculated electron and lattice equilibrium temperature for each calculation is constant because the laser fluence is a fixed value for the energy injected into the system.

Taking the calculation at pulse width 300 fs as an example, the electron and lattice temperature curves at the farthest end of the laser incident surface at $z = 54.225$ nm and the laser incident surface at $z = 0$ are analyzed, we obtain the two-temperature curves as shown in Figs. 9 and 10:

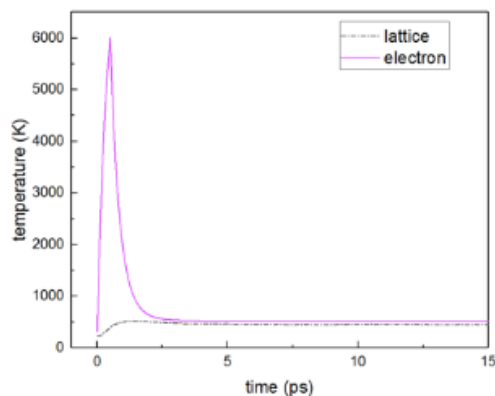


Fig. 5 Two-temperature curve with laser fluence of 1000 J/m² and pulse width of 500 fs

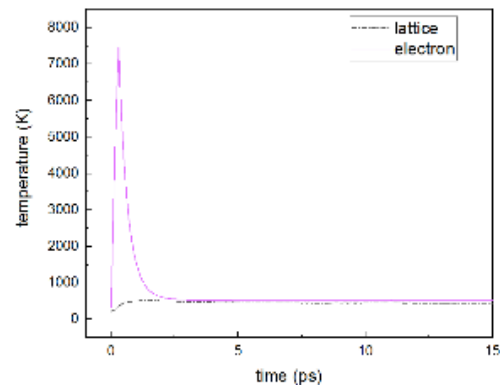


Fig. 6 Two-temperature curve with laser fluence of 1000 J/m² and pulse width of 300 fs

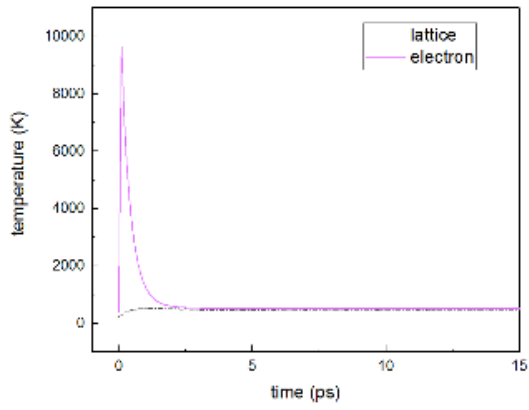


Fig. 7 Two-temperature curve with laser fluence of 1000 J/m^2 and pulse width of 100 fs

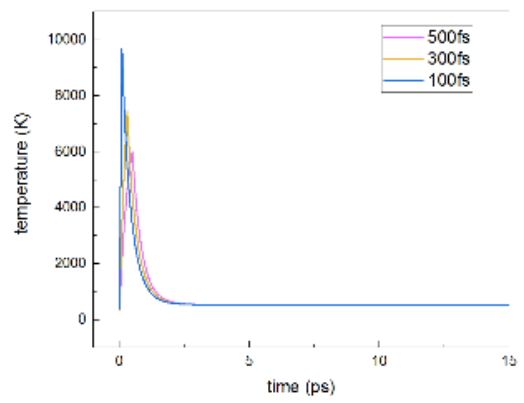


Fig. 8 Electron temperature curves with different pulse widths at laser fluence of 1000 J/m^2

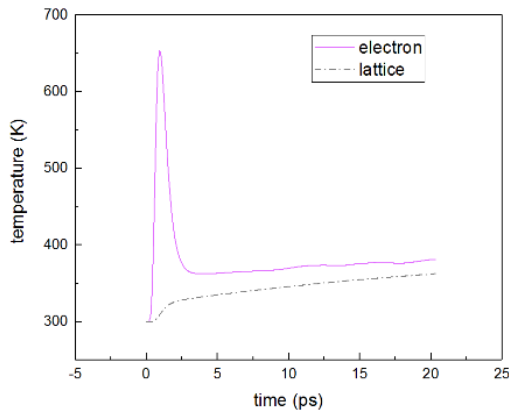


Fig. 9 Two-temperature curve at $z = 54.225 \text{ nm}$

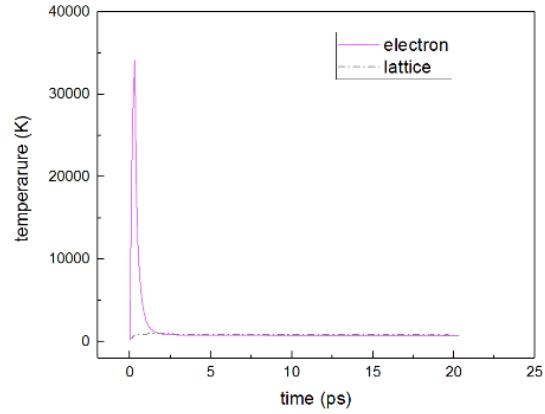


Fig. 10 Two-temperature curve at $z = 0$

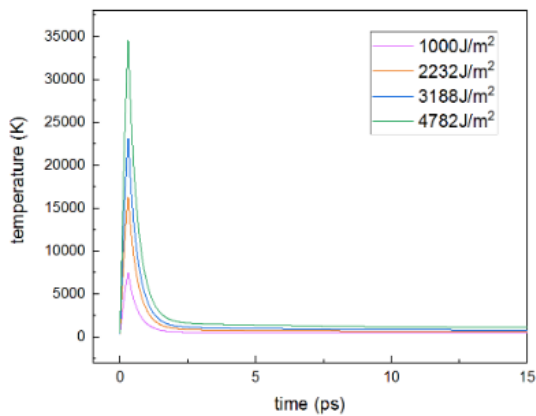


Fig. 11 Temperature change of electron

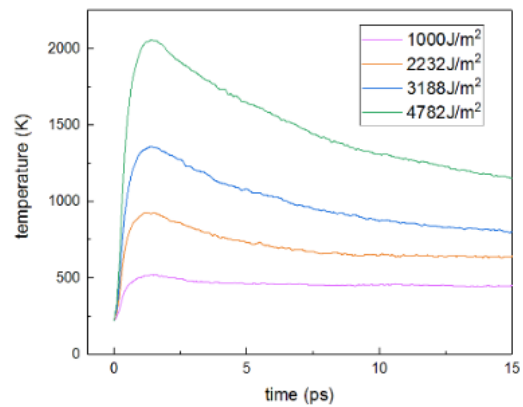


Fig. 12 Temperature change of lattice

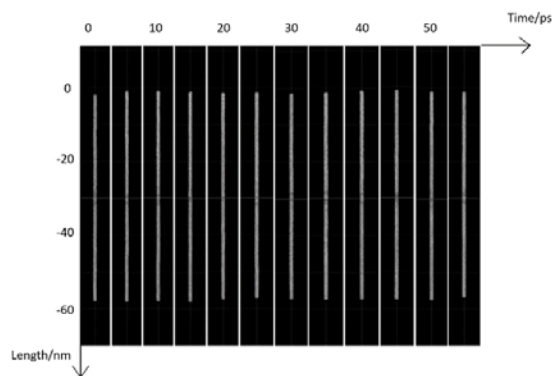


Fig. 13 Atomic snapshots at a laser fluence of 1000 J/m^2

The electron on the laser incident surface shown in Fig. 10 rapidly rose to 34147 K at 0.3 ps, and the lattice reached a maximum temperature of 1028 K at 1.4 ps. In the bottom region of the model, which is less affected by heat, the electron reached a maximum temperature of 653 K at 0.9 ps, after which the cooled electron and the lattice would keep the same rising trend of temperature due to the heat conduction from the front face. This is consistent with the change in the average temperature of the entire system.

In another set of calculations, we fixed the laser pulse width to 300 fs to obtain the two-temperature curves with different laser fluences of 1000 J/m², 2232 J/m², 3188 J/m² and 4782 J/m² as shown in the Figs. 11 to 12. It can be easily seen that an increase in laser fluence can cause an increase in electron and lattice temperature.

To clearly understand the ablation process, the trajectories of all atoms were imported into Visual Molecular Dynamics (VMD) for visualization. As shown in Fig. 13, when the laser fluence is small as 1000 J/m², no ablation occurs, and the energy is not enough to cause phase transformation of the material. However, it can be seen the film undergoes periodic elongation and shortening under the action of laser from the visualization results. The periodic expansion and contraction of the film under the action of internal stress waves is known as the 'film respiration' phenomenon [16]. The film was rapidly heated and expanded within 0-15 ps after being irradiated by the laser. During this time, since the heating time of the lattice is less than the time when the thermal expansion occurs, the compressive stress transmitted from the upper surface to the lower surface will be generated inside the film. After transmitting to the lower surface, a tensile stress wave of negative reflection was formed, then the tensile stress wave caused by thermal expansion and the tensile stress wave formed by negative reflection were superimposed on each other to promote expansion of the film during this period. The tensile stress wave would decrease as the film linear expansion value reached a maximum. At 15-30 ps, the tensile stress wave continued to weaken and the compressive stress wave was still forming, and the film began to shrink. After the film reached equilibrium at around 30 ps, it began to periodically expand and contract, and expanded to a maximum at 45 ps. Such a periodic action consumes the injected energy when the laser energy is insufficient to cause ablation.

As the laser fluence increases to 2232 J/m² shown in Fig 14, when the material is exposed to energy-concentrated ultrafast laser, an extremely non-equilibrium process occurs. The electrons were rapidly heated by the collision between the electrons after quickly absorbing a large amount of photon energy. At the same time, the lattice has not warmed up while its temperature was still close to room temperature. This will cause the unheated crystal lattice to be subjected to a strong force from the potential energy surface [17] (PES), which is usually affected by the effective potential of electrons acting on the ions. After the action of the force, the ions began to move and caused the material to be disordered rapidly. Usually, this ultra-fast disorder is considered to be a melting process. The front end of the material melts, some of the atoms are ablated from the surface of the material, and the material has a relatively obvious thermal expansion effect.

As the laser fluence becomes 3188 J/m², ablation is more severe as shown in Fig. 14, the atomic clusters began to break away from the system. Usually, the melting occurs at the disappearance of the heterogeneous nucleation barrier on the surface of the material and then propagates inside the material at a speed less than the speed of sound of hundreds of meters per second. In the case of sufficient overheating (overheating ratio greater than 1.5), it is also possible to produce a uniform nucleation melting phenomenon. The nucleation inside the material can be observed at -8 nm in Fig. 15. Further increase the laser fluence as Fig. 16 shown the more intense mechanical stress caused by thermal expansion and the melting generated inside the material cause the film to crack. Compared with the ablation at lower laser fluence in Fig. 15, the ablation depth increases and the linear expansion rate also increases significantly.

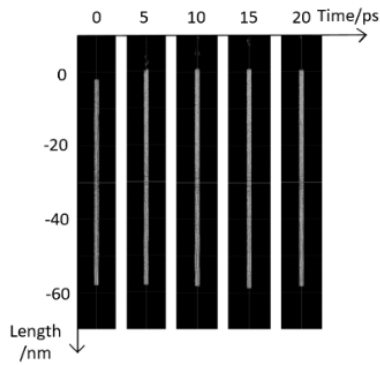


Fig. 14 Atomic snapshots at a laser fluence of 2232 J/m²

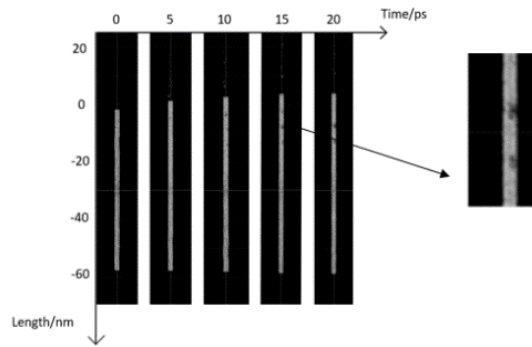


Fig. 15 Atomic snapshots at a laser fluence of 3188 J/m²

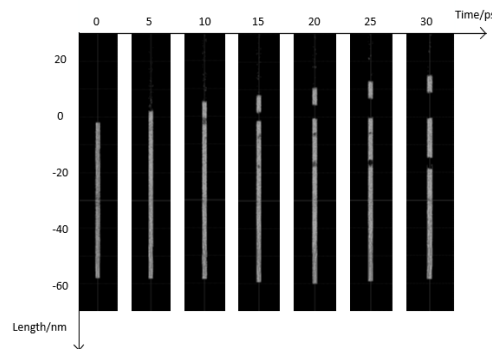


Fig. 16 Atomic snapshots at a laser fluence of 4782 J/m²

Ablation depths under different laser fluences

To understand the ablation process better, it is necessary to correlate the numerical simulation results with the actual drilling process and calculate the ablation depth. We increased the model size and the time step of the calculation to obtain more efficient simulation results. It's the way to ensure that the system is large enough to keep the atomic temperature of the bottom surface from being affected by heat at room temperature and make the simulation close to real processing conditions. We mainly explore the influence of the difference of laser fluence on the ablation depth of copper film, the pulse width for our simulation is a fixed value of 300 fs and the four parameters 3188 J/m², 4782 J/m², 6377 J/m², and 7971 J/m² are used to obtain the curve as shown as Fig. 17. The other curve in the figure is from the experimental data of the comparative literature [18]. The experimental curve obtained in the experiments of the literature [18] is shown in Fig. 18. Within the laser fluence range calculated in this paper, the ablation depth of the material exhibits an approximately linear relationship with the laser fluence. It can be seen that in the range of laser fluence simulated in this paper, the calculated value of the ablation depth is highly consistent with the experimental values in the comparative literature. Obviously, the ablation caused by single pulse is in the order of nanometers, and there is a certain gap with the actual processing needs in engineering. Therefore, it is necessary to carry out numerical simulation of multi-pulsed laser ablation of metal copper film.

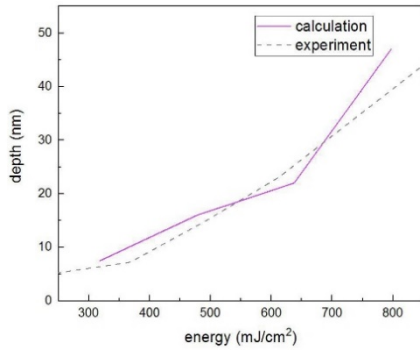


Fig. 17 Ablation depth changed by laser fluence

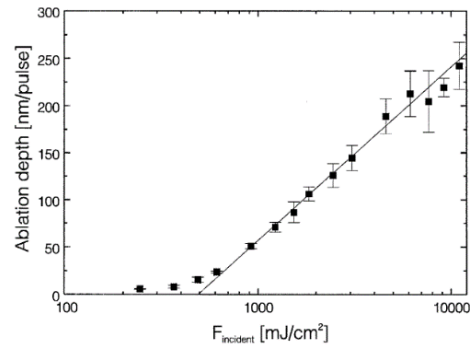


Fig. 18 Ablation depth changed by laser fluence [19]

3.2 Interaction of double-pulsed and multi-pulsed laser with copper film

In recent years, domestic and foreign scholars have done some research on the interaction of single-pulsed and double-pulsed with metal, while the field of multi-pulsed laser action on metal is less involved due to its extremely complex internal mechanism.

To explore the interaction of multi-pulsed laser and metal, we must explain the concept of ablation thresholds [19] firstly. The ablation threshold refers to the laser fluence required for the laser to irreversibly destroy the metal and remove the surface of the material during the ultrafast laser action of the metal. Usually, a certain value is obtained during the single-pulsed laser ablation of the metal, but as the number of pulses increases, the ablation threshold of the material will be inversely proportional to the number of pulses. The ablation process of the material can also be done with a small laser fluence, which is called the incubation effect [20], and its mathematical expression is:

$$F_{th}(N) = F_{th}(1) \cdot N_{S-1} \quad (10)$$

where N represents the number of pulses, $F_{th}(N)$ is the corresponding ablation threshold when the number of pulses is N , $F_{th}(1)$ is the ablation threshold corresponding to single pulse, and S is the coefficient of incubation effect. The laser source rewriting term in the two-temperature equation for simulating multi-pulsed laser has been described in Section 2.1.

Temperature analysis

Firstly, we would have a preliminary understanding of incubation effects by the temperature change of electron and lattice caused by the change of pulse number. The two-temperature curve of the material under the irradiation of single-pulsed, double-pulsed and multi-pulsed laser are as shown in Figs. 19 to 21, respectively. The laser fluence for each pulse is 1594 J/m^2 , the pulse τ_L width is 300 fs , and the pulse interval dt_1 is 1 ps .

As can be seen from Fig. 20, after the first pulse, the electron rapidly heated up to 11718 K after 0.3 ps , transferred energy to the lattice, and the lattice continued to heat up. The second pulse was irradiated after 1 ps , the electron has cooled to 1380 K before the laser action, and the lattice was still warming. The injection of the second pulse energy caused the electron to reach a maximum temperature of 12403 K at 1.6 ps , after which the electron continued to transfer the energy to the lattice that was not fully heated. Then the electron and the lattice tended to be balance with the same trend after 3 ps . The lattice temperature caused by the first pulse is about 487 K , after the second pulse, the lattice temperature rose 556 K to reach the highest temperature. Compared to the single pulse action, the lattice has a more conspicuous temperature drop before the electron-phonon relaxation. Analyzing the two-temperature curve as Fig. 21 shown under the action of multi-pulsed laser, we find that both the electron and the lattice underwent three temperature rises, and the peak temperature of the three temperature rises is increasing. Since the pulse width and the pulse interval have not changed, the temperature change of the electron and the lattice under the first two pulses are consistent with the two-temperature curve under the action of the double pulse. After the third pulse, the electron reached the highest temperature of 12812 K at 2.9

ps, and the energy was transferred to the lattice. The lattice was heated to 1838 K at 3.5 ps. After 3.5 ps, the temperature of the electron and the lattice decreased and tended to be consistent.

It can be seen from the atomic snapshots in Figs. 22 to 24 that the increase of the number of pulses not only further increases the temperature of the electron and the lattice, but also actually reduces the ablation threshold of the material. The copper film in Fig. 22 only produces ‘film respiration’ under the irradiation of laser pulse with laser fluence of 1594 J/m². Increasing the number of pulses, we can see the nucleation inside of the material in Fig. 23, in the Fig. 24, we can find that there is a crack occurring and the ablation becomes more severe.

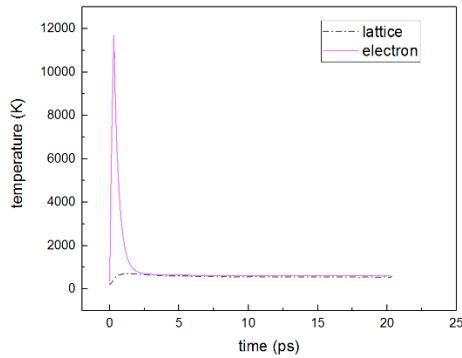


Fig. 19 Two-temperature curve under single-pulsed laser

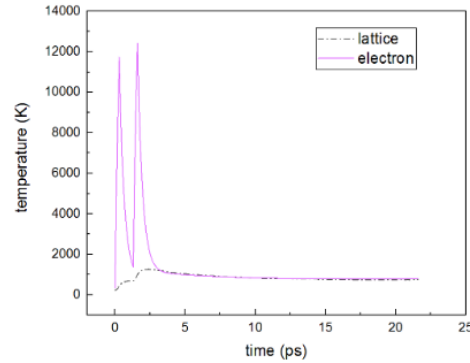


Fig. 20 Two-temperature curve under double-pulsed laser

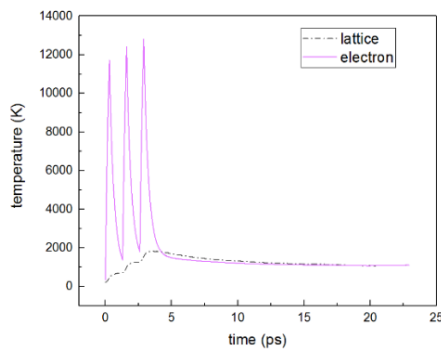


Fig. 21 Two-temperature curve under multi-pulsed laser

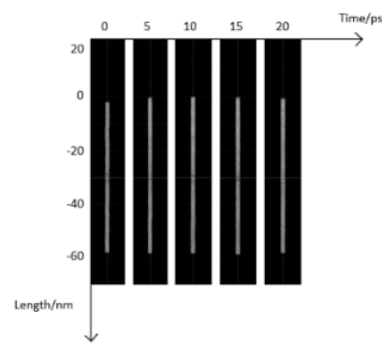


Fig. 22 Atomic snapshots under single-pulsed laser

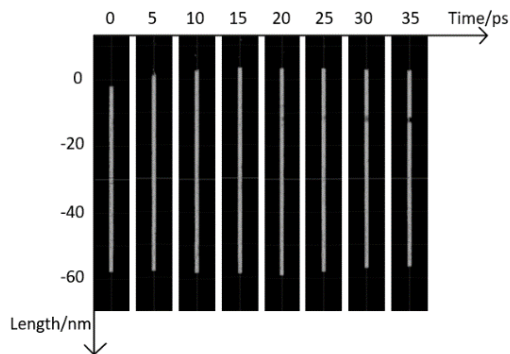


Fig. 23 Atomic snapshots under double-pulsed laser

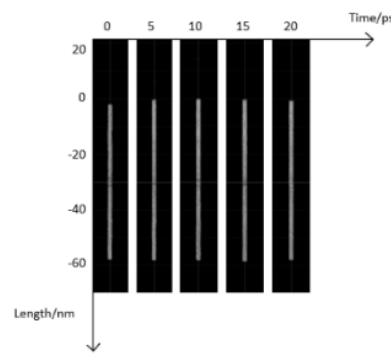


Fig. 24 Atomic snapshots under multi-pulsed laser

To further explore the temperature change of the electron and the lattice of each cross section of the material after the pulse action, we made a temperature contour with the time as the horizontal axis and the distance from the incident surface as the vertical axis as shown in Figs. 25 to 30.

Fig. 25 shows the electron temperature change of the internal sections of the metal material under the action of a single-pulsed laser. At 0.3 ps, the excitation made the electron 5 nm away from the incident surface rose to about 50000 K, the area with a large heat influence is 25 nm near the surface, which reached a maximum temperature of about 10000 K at 0.5 ps. Electron continuously transferred energy to the lattice through electron-phonon coupling. After 1 ps, the electron

temperature dropped below 5000 K. From Fig. 27, we can see that the electrons were excited twice, and the second laser was irradiated at 1.3 ps. At 1.6 ps, the electrons 5 nm from the front of the surface reached the highest temperature of about 55000 K, while the heat-affected zone was further expanded to 26.5 nm, and the electron temperature dropped back to 5000 K at around 2.2 ps. It can be seen from the temperature contour Fig. 29 that the highest temperature the electron could reach is 55000 K, which is the same as the highest temperature that can be achieved when the double-pulsed is applied. The difference is that the third pulse expands the heat-affected zone, and the electrons within 27 nm of the incident laser surface could be heated to more than 10000 K, and the thermal effect time of each pulse is also increased. As for the change of the lattice temperature, we can see from Fig. 26, Fig. 28 and Fig. 30 that the peak temperature of the lattice can be gradually increased due to the increase of the number of pulses, so as the heat-affected area.

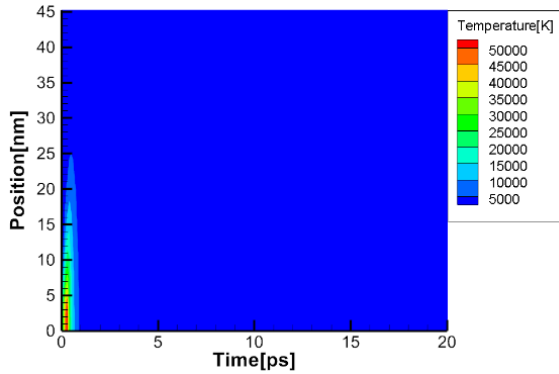


Fig. 25 Temperature contour of electron at laser fluence of 1594 J/m² under single-pulsed laser

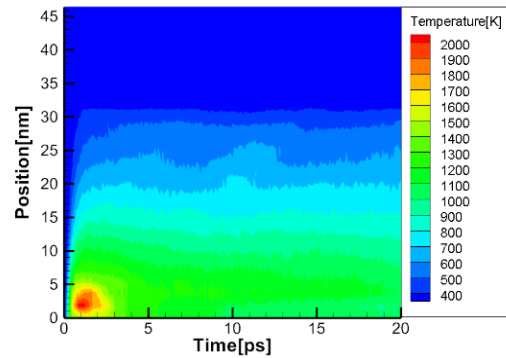


Fig. 26 Temperature contour of lattice at laser fluence of 1594 J/m² under single-pulsed laser

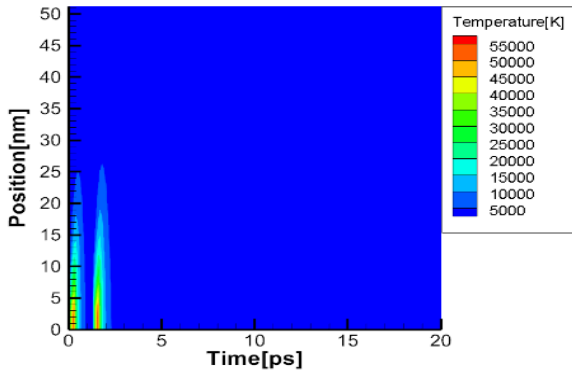


Fig. 27 Temperature contour of electron at laser fluence of 1594 J/m² under double-pulsed laser

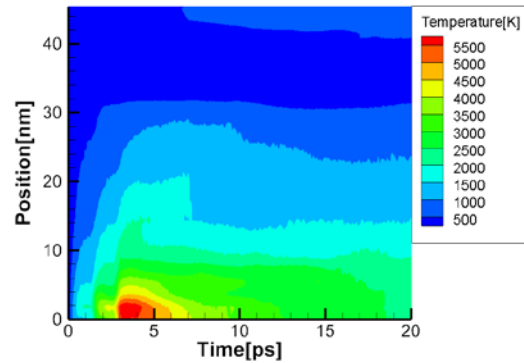


Fig. 28 Temperature contour of lattice at laser fluence of 1594 J/m² under double-pulsed laser

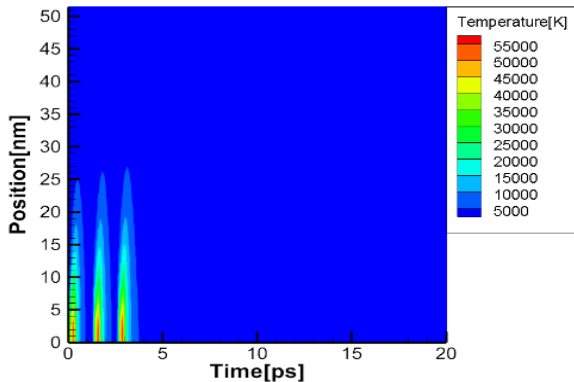


Fig. 29 Temperature contour of electron at laser fluence of 1594 J/m² under multi-pulsed laser

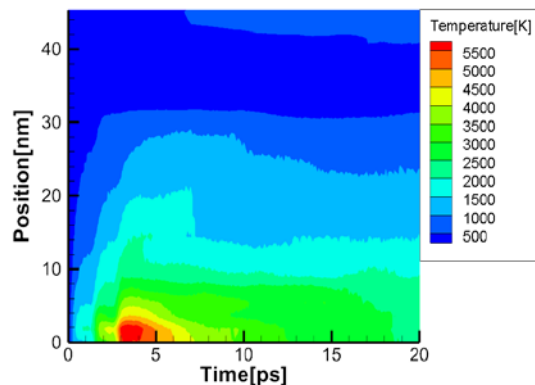


Fig. 30 Temperature contour of lattice at laser fluence of 1594 J/m² under multi-pulsed laser

Exploration of incubation effects

The existence of incubation effect causes the material to ablate at a single-pulse laser fluence that would otherwise not cause ablation, reducing the ablation threshold of the material. This is undoubtedly advantageous in engineering. However, in order to effectively remove the material, in addition to the research on the mechanism of action of multi-pulsed laser and metal, it is necessary to further explore the influencing factors of incubation effects. The greater the laser fluence, the more laser energy is injected into the system, and the ablation is more severe obviously.

In this section we would discuss the effect of pulse interval on the results of laser ablation of metals caused by multi-pulsed laser. Therefore, the fixed laser fluence and the pulse width τ_L are 4782 J/m^2 and 300 fs , the pulse intervals of three groups we chose for the calculation are $dt_1 = 1 \text{ ps}, dt_2 = 1 \text{ ps}$; $dt_1 = 0.3 \text{ ps}, dt_2 = 1 \text{ ps}$ and $dt_1 = 1 \text{ ps}, dt_2 = 3 \text{ ps}$, the calculated two-temperature curve are shown in Figs. 31 to 33.

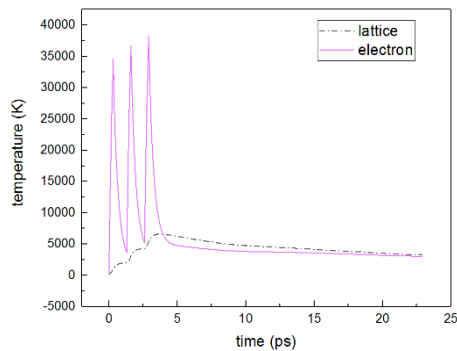


Fig. 31 Two-temperature curve when pulse interval are 1 ps, 1 ps

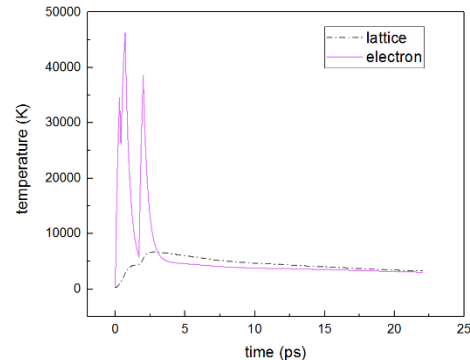


Fig. 32 Two-temperature curve when pulse interval are 0.3 ps, 1 ps

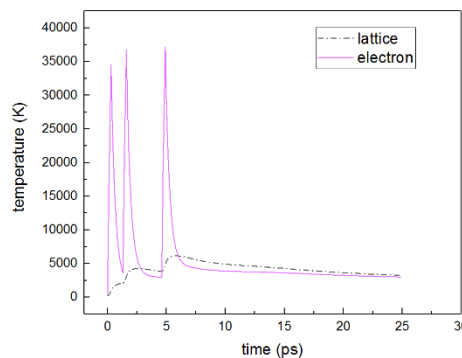


Fig. 33 Two-temperature curve when pulse interval are 1 ps, 3 ps

Analyzing the following three two-temperature curves Figs. 31 to 33, 1 ps is just about the approximate time required for the temperature to fall back after the electron rise to the peak temperature, which is roughly the time required for electron-phonon coupling. Therefore, when the pulse interval is 1 ps, the lattice temperature shows a steady upward trend. The highest lattice temperature appears at 3.7 ps, which is 6607 K, and the excited electron temperature can reach 21812 K.

When the first pulse interval is shortened to 0.3 ps, the electron temperature did not fall from the peak temperature completely when the second pulse irradiated. At the same time, the internal heat transfer of the electron and electron-phonon coupling was continuing, the thermal impact of the first pulse was still intense, the electron can be heated up to 46298 K, which is far greater than when the pulse interval of 1 ps. The energy obtained by the lattice is further increased, and the maximum temperature can reach 6697 K, which is also higher than the case when the pulse interval of 1 ps. Then we increase the second pulse interval to 3 ps, the temperature of the electron has dropped to 2955 K before the third pulse, and the peak temperature of the last pulse is only 37170 K, which is less than the above two cases.

According to the above analysis results, it can be found that the electron temperature, the lattice temperature, and the final equilibrium temperature are all improved when the pulse interval time is shortened to less than the electron-phonon coupling time. If the pulse interval time is longer than the electron-phonon coupling time, the inside of the material has already close to reaching the equilibrium state before the subsequent pulse action, and the effect of the energy of the subsequent pulse injection cannot be well exerted, which is not conducive to ablation. Therefore, the choice of pulse interval time is an important issue to improve the ablation efficiency. Shortening the pulse interval time is more conducive to energy accumulation.

Ablation depth is a visual representation of the pros and cons of processing results. In order to explore the influence of the important factor of the pulse interval on the ablation depth, the fixed pulse width is still 300 fs, and the first pulse interval is fixed at 1 ps. The second pulse interval for the four sets of calculations are 0.3 ps, 1 ps, 10 ps and 30 ps. To ensure the reliability of the calculation results, the visual result we obtain is shown in Fig. 34 by calculating 180,000 steps or 180 ps.

It can be seen from Fig. 34 that the ablation depth increases first and then decreases with the increase of the multi-pulsed laser time interval. Although the electron and the lattice can reach a higher temperature as shown in Fig. 31 at a pulse interval of 0.3 ps, the duration of the temperature above the ablation threshold is small compared to the case where the pulse time interval is close to the electron-phonon coupling time. Comparing the time when the first temperature rise of the electron reaches the peak to the start of the relaxation in Fig. 31 and Fig. 32, the pulse width is 3 ps at 0.3 ps, and the pulse width is about 5 ps at 1 ps. From this point of view, the pulse interval close to the electron-phonon coupling time allows the system to be maintained at a higher temperature for a longer time, resulting in an increase in the ablation depth. The shorter pulse interval makes the subsequent pulse and the pre-pulse to work together close to a single pulse, although a higher temperature is reached, but a shorter high temperature duration limits the increase in ablation depth. As the pulse interval is further increased to 10 ps and 30 ps, the thermal effect of the pre-pulse has been dissipated by the system, the lattice and electron temperatures have also fallen, and the ablation depth has gradually decreased. In summary, a pulse interval close to the electron-phonon coupling time of the material can complete a more efficient ablation of the material.

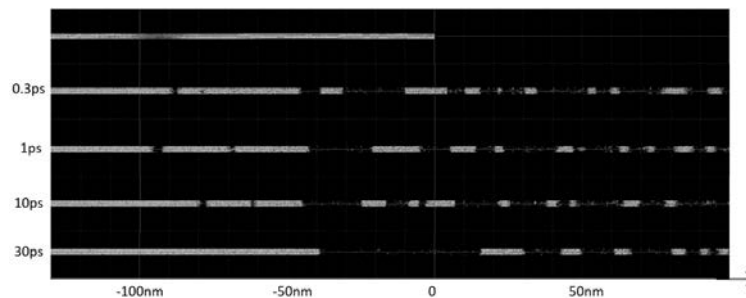


Fig. 34 Atomic snapshots of different pulse interval (at the moment of 180 ps)

4. Conclusion

The effect of ultrafast laser on metal is an extremely complex process with high imbalance, including the absorption of laser energy by electrons on the metal surface, the energy transfer from electron to the lattice through electron-phonon coupling and phonon collision, and the process of the lattice absorbs energy and causes the material to change phase. Finally, the surface of the material will be removed. To better describe the metal absorption process of laser ablates metallic materials, the researchers proposed a two-temperature model to describe the thermal conduction process of electrons and lattice systems of the material, while the two-temperature model is insufficient to explore the phase transition and ablation mechanism of metals during the unbalanced processes of laser processing. Therefore, molecular dynamics calculation is introduced to track the position and velocity of each atom by setting reasonable initial calculation conditions. We use

the EAM potential function and introduce periodic boundary conditions in the analysis of the interaction of metal and laser.

After establishing the appropriate size simulation system with the above method on the LAMMPS platform, we reproduced the ablation process of the single-pulsed laser to the metal and verified the correctness of our simulation. We firstly fixed the laser fluence and irradiated the surface of the copper film with lasers of different pulse widths. It was found that when the pulse width is reduced, the pulse energy is more concentrated, and the lattice and electrons inside the system can reach a higher peak temperature. Moreover, the smaller the pulse width, the faster the electron temperature rises. Then, the pulse width was set to a fixed value, the metal was irradiated with laser of different laser fluences, and the visualized atomic snapshots was analyzed. In the visualization results, the nucleation of voids when the laser fluence is small and the nucleation of bubbles inside the material when the laser fluence is large were observed. The larger laser fluence causes the layer cracking of the material, so that more materials are removed. After understanding the ablation mechanism, the calculation system was enlarged to eliminate the effect of thermal expansion. The laser ablation depth at different energy densities was calculated, the fitting curve was obtained, and compared with the literature.

Multi-pulsed laser ablation is not a simple superposition of single-pulsed laser. The process of interaction with metal is more complicated. In this paper, the multi-pulsed laser ablation was calculated by changing the light source term in the two-temperature equation. Comparing the temperature contour and atomic snapshots of multi-pulsed laser action and single-pulsed laser action, we found that the increase of the number of laser pulses reduces the ablation threshold of the material. The nucleation and phase change inside the material is more severe due to the increase of energy, the lattice disorder is more serious, and the ablation becomes faster. Then we discussed the influence of pulse interval time on the incubation effect of multi-pulsed laser. The pulse interval time is shorter than the electron-phonon coupling time, which makes the temperature of the system more intense. If the pulse interval is too long, the energy will be dissipated at the pulse interval. Therefore, the appropriate pulse interval should be selected during the laser processing.

It should be noted that although copper was chosen as the target material in this study due to the abundant research of its thermophysical properties, the method of molecular dynamic modeling and analysis can be applied to other metallic material as long as the detailed thermophysical parameters of the materials determined. The results obtained in this work can provide a new calculation method and theoretical basis for ultra-fast laser machining of air film holes in aviation turbine blades and has certain practical guiding significance for laser machining.

Acknowledgements

The material presented in this paper is based upon work supported by the National Natural Science Foundation of China (Grant Number 51705440), the Fundamental Research Funds for the Central Universities XMU (Grant Number 20720180072), the Aeronautical Science Foundation of China (Grant Number 20170368001), the Shenzhen Fundamental Research Program (Grant Number JCYJ20170818141303656), and the Natural Science Foundation of Fujian Province, China (Grant Number 2019J01044), National Science and Technology Major Project (J2019-III-0008), National Science and Technology Major Project (J2019-VII-0013-0153), Research Project (PZ2020016).

References

- [1] Mills, B., Heath, D.J., Grant-Jacob, J.A., Eason, R.W. (2018). Predictive capabilities for laser machining via a neural network, *Optics Express*, Vol. 26, No. 13, 17245-17253, doi: [10.1364/OE.26.017245](https://doi.org/10.1364/OE.26.017245).
- [2] Rethfeld, B., Ivanov, D.S., Garcia, M.E., Anisimov, S.I. (2017). Modelling ultrafast laser ablation, *Journal of Physics D: Applied Physics*, Vol. 50, No. 19, Article No. 193001, doi: [10.1088/1361-6463/50/19/193001](https://doi.org/10.1088/1361-6463/50/19/193001).
- [3] Templeton, J.A., Jones, R.E., Wagner, G.J. (2010). Application of a field-based method to spatially varying thermal transport problems in molecular dynamics, *Modelling and Simulation in Materials Science and Engineering*, Vol. 18, No. 8, Article No. 085007, doi: [10.1088/0965-0393/18/8/085007](https://doi.org/10.1088/0965-0393/18/8/085007).
- [4] Bogaerts, A., Aghaei, M., Autrique, D., Lindner, H., Chen, Z.Y., Wendelen, W. (2011). Computer simulations of laser ablation, plume expansion and plasma formation, *Advanced Materials Research*, Vol 227, 1-10, doi: [10.4028/www.scientific.net/AMR.227.1](https://doi.org/10.4028/www.scientific.net/AMR.227.1).
- [5] Ivanov, D.S., Zhigilei, L.V. (2003). Combined atomistic-continuum modeling of short-pulse laser melting and disintegration of metal films, *Physical Review B*, Vol. 68, No. 6, Article No. 064114, doi: [10.1103/PhysRevB.68.064114](https://doi.org/10.1103/PhysRevB.68.064114).

- [6] Amouye Foumani, A., Niknam, A.R. (2018). Atomistic simulation of femtosecond laser pulse interactions with a copper film: Effect of dependency of penetration depth and reflectivity on electron temperature, *Journal of Applied Physics*, Vol. 123, No. 4, 043106, doi: [10.1063/1.5009501](https://doi.org/10.1063/1.5009501).
- [7] Povarnitsyn, M.E., Fokin, V.B., Levashov, P.R. (2015). Microscopic and macroscopic modeling of femtosecond laser ablation of metals, *Applied Surface Science*, Vol. 357, Part A, 1150-1156, doi: [10.1016/j.apsusc.2015.09.131](https://doi.org/10.1016/j.apsusc.2015.09.131).
- [8] Liang, J.-G., Ni, X.-C., Yang, L., Wang, Q.-Y. (2005). Numerical simulation of the ablation on copper with ultrashort laser pulses, *China Laser*, Vol. 32, No. 9, 1291-1294, doi: [10.3321/j.issn:0258-7025.2005.09.029](https://doi.org/10.3321/j.issn:0258-7025.2005.09.029).
- [9] Winter, J., Rapp, S., Schmidt, M., Huber, H.P. (2017). Ultrafast laser processing of copper: A comparative study of experimental and simulated transient optical properties, *Applied Surface Science*, Vol. 417, 2-15, doi: [10.1016/j.apsusc.2017.02.070](https://doi.org/10.1016/j.apsusc.2017.02.070).
- [10] Wang, Q., Luo, S., Chen, Z., Qi, H., Deng, J., Hu, Z. (2016). Drilling of aluminum and copper films with femtosecond double-pulse laser, *Optics & Laser Technology*, Vol. 80, 116-124, doi: [10.1016/j.optlastec.2016.01.001](https://doi.org/10.1016/j.optlastec.2016.01.001).
- [11] Karim, E.T., Shugaev, M.V., Wu, C., Lin, Z., Matsumoto, H., Conneran, M., Kleinert, J., Hainsey, R.F., Zhigilei, L.V. (2016). Experimental characterization and atomistic modeling of interfacial void formation and detachment in short pulse laser processing of metal surfaces covered by solid transparent overlayers, *Applied Physics A*, Vol. 122, Article No. 407, doi: [10.1007/s00339-016-9944-7](https://doi.org/10.1007/s00339-016-9944-7).
- [12] Fokin, V.B., Povarnitsyn, M.E., Levashov, P.R. (2017). Simulation of ablation and plume dynamics under femtosecond double-pulse laser irradiation of aluminum: Comparison of atomistic and continual approaches, *Applied Surface Science*, Vol. 396, 1802-1807, doi: [10.1016/j.apsusc.2016.11.208](https://doi.org/10.1016/j.apsusc.2016.11.208).
- [13] Wu, Z., Dong, Y., Zhang, S., Liao, T., Yan, W., You, Y. (2021). Discussion on effect of laser parameters and trajectory in combined pulse laser drilling, *International Journal of Hydromechanics*, Vol. 4, No. 1, 43-54, doi: [10.1504/IJHM.2021.114175](https://doi.org/10.1504/IJHM.2021.114175).
- [14] Anisimov, S.I., Kapeliovich, B.L., Perelman, T.L. (1974). Electron emission from metal surfaces exposed to ultrashort laser pulses, *Soviet Journal of Experimental and Theoretical Physics*, Vol. 66, No. 2, 375-377.
- [15] Zhang, Z., Xu, Z., Wang, C., Liu, S., Yang, Z., Zhang, Q., Xu, W. (2021). Molecular dynamics-guided quality improvement in the femtosecond laser percussion drilling of microholes using a two-stage pulse energy process, *Optics & Laser Technology*, Vol. 139, Article No. 106968, doi: [10.1016/j.optlastec.2021.106968](https://doi.org/10.1016/j.optlastec.2021.106968).
- [16] Qui-lin, X., Li, Z., Xiao-geng, T. (2015). Ultrafast thermomechanical responses of a copper film under femtosecond laser trains: A molecular dynamics study, *Proceedings of the Royal Society A: Mathematical, Physical and Engineering Sciences*, Vol. 471, Article No. 20150614, doi: [10.1098/rspa.2015.0614](https://doi.org/10.1098/rspa.2015.0614).
- [17] Rethfeld, B., Ivanov, D.S., Garcia, M.E., Anisimov, S.I. (2017). Modelling ultrafast laser ablation, *Journal of Physics D: Applied Physics*, Vol. 50, No. 19, Article No. 193001, doi: [10.1088/1361-6463/50/19/193001](https://doi.org/10.1088/1361-6463/50/19/193001).
- [18] Momma, C., Nolte, S., Chichkov, B.N., Alvensleben, F.v., Tünnermann, A. (1997). Precise laser ablation with ultrashort pulses, *Applied Surface Science*, Vol. 109-110, 15-19, doi: [10.1016/S0169-4332\(96\)00613-7](https://doi.org/10.1016/S0169-4332(96)00613-7).
- [19] Zhang, Y.-F., Wang, L.-L., Gong, J.-L. (2016). Numerical simulation of femtosecond laser multi-pulse ablation of Ni-Ti alloy, *Journal of Photonics*, Vol. 45, No. 5, Article No. 0514002, doi: [10.3788/gzxb20164505.0514002](https://doi.org/10.3788/gzxb20164505.0514002).
- [20] Lasemi, N., Pacher, U., Zhigilei, L.V., Bomati-Miguel, O., Lahoz, R., Kautek, W. (2018). Pulsed laser ablation and incubation of nickel, iron and tungsten in liquids and air, *Applied Surface Science*, Vol. 433, 772-779, doi: [10.1016/j.apsusc.2017.10.082](https://doi.org/10.1016/j.apsusc.2017.10.082).

A comparative study of different pull control strategies in multi-product manufacturing systems using discrete event simulation

Xanthopoulos, A.S.^{a,*}, Koulouriotis, D.E.^b

^{a,b}Department of Production and Management Engineering, Democritus University of Thrace, V. Sofias 12, Xanthi, Greece

ABSTRACT

Pull production control strategies coordinate manufacturing operations based on actual demand. Up to now, relevant publications mostly examine manufacturing systems that produce a single type of a product. In this research, we examine the CONWIP, Base Stock, and CONWIP/Kanban Hybrid pull strategies in multi-product manufacturing systems. In a multi-product manufacturing system, several types of products are manufactured by utilizing the same resources. We develop queueing network models of multi-stage, multi-product manufacturing systems operating under the three aforementioned pull control strategies. Simulation models of the alternative production systems are implemented using an open-source software. A comparative evaluation of CONWIP, Base Stock and CONWIP/Kanban Hybrid in multi-product manufacturing is carried out in a series of simulation experiments with varying demand arrival rates, setup times and control parameters. The control strategies are compared based on average wait time of backordered demand, average finished products inventories, and average length of backorders queues. The Base Stock strategy excels when the manufacturing system is subjected to high demand arrival rates. The CONWIP strategy produced consistently the highest level of finished goods inventories. The CONWIP/Kanban Hybrid strategy is significantly affected by the workload that is imposed on the system.

ARTICLE INFO

Keywords:

Discrete event simulation (DES);
Open-source software;
JaamSim DES software;
Multi-product manufacturing;
Multi-stage production systems;
Pull-type production control strategies

*Corresponding author:

axanthop@pme.duth.gr
(Xanthopoulos, A.S.)

Article history:

Received 17 September 2021

Revised 30 November 2021

Accepted 3 December 2021



Content from this work may be used under the terms of the Creative Commons Attribution 4.0 International License (CC BY 4.0). Any further distribution of this work must maintain attribution to the author(s) and the title of the work, journal citation and DOI.

1. Introduction

According to a common definition of pull-type production control, a pull system is one in which production operations are coordinated based on actual demand occurrences and not on advance demand information or forecasts [1]. In a pull system production, operations are triggered by the arrival of demands for finished goods. Whereas in a push system production is scheduled based on forecasts of demand for goods, i.e. production operations are launched before the actual demand arrival. An excellent review of pull control methods and critical comparisons with alternative production control paradigms is given in [2].

Numerous pull control strategies (or policies) have been proposed in the relevant literature and a considerable number of papers have been devoted to the modeling, evaluation and comparison of alternative pull systems.

The reader is referred to [3] and Xanthopoulos and [4] for some indicative examples. A relatively recent trend in this research field pertains to the study of adaptive, pull control policies,

i.e. production control mechanisms that adapt to the current state of the demand and/or production processes [5].

Pull production control policies have been mostly studied in the context of single product type systems up to now. In recent years, a new research direction has emerged that examines multi-product systems [6, 7]. This paper advances the research on multi-product pull systems by examining the CONWIP, Base Stock and CONWIP/Kanban Hybrid strategies. The aforementioned systems are modeled as queueing network models with synchronization stations [4]. The models of the alternative manufacturing systems are implemented in the simulation software JaamSim [8]. The behavior of the examined control systems is studied in a series of simulation experiments.

The remainder of this paper is structured as follows. Section 2 contains a summary of relevant scholarly publications. The examined manufacturing system model is presented in section 3 together with the queueing network representations of the multi-product CONWIP, Base Stock and CONWIP/Kanban Hybrid systems. Section 4 contains the results of the simulation experiments together with their analysis. Finally, the paper is concluded in section 5, where some directions for future research are also provided.

2. Related work and contribution of research

In this section we offer a brief literature review of the most relevant published research to this article. Existing works on pull control strategies for systems that produce more than on part type can be classified based on the size of the underlying manufacturing system.

Single stage systems are studied in [9] and [10]. Multi-stage systems (typically consisting of 3 to 5 stages) are examined in the majority of relevant works [11-15]. A rather special case is the work of Krieg and Kuhn [16] who study a two-stage system analytically, i.e. by means of decomposition-based mathematical approximation methods.

With the exception of Krieg and Kuhn [16] who use the formalism of continuous-time Markov chains, the overwhelming majority of publications on multi-product, pull type production control systems uses simulation to model and analyze the manufacturing systems in question. Indicative software that are frequently employed for these purposes are Arena and ExtendSim (e.g. refer to [10] and [11]).

The relevant papers address either idealized, “synthetic” manufacturing systems [16, 9] or systems inspired by real-world applications. Case studies pertaining to the automotive industry are studied in [13] and [10]. Other, indicative, case studies are related to manufacturers of health-care products [12], drug process plants [11] and gear manufacturers [15].

Even though numerous pull production control strategies have been proposed in the literature, papers that focus on multi-product systems often address only a subset of them. For example, only the Kanban control approach is examined in [11], [16] and [9]. Existing comparative evaluations of alternative pull control policies typically involve two or three approaches (e.g. CONWIP, Kanban and Extended Kanban are compared in [15], Base Stock, Kanban and Extended Kanban are compared in [10] etc.). A noticeable exception is the work of Olaitan and Geraghty [12] where five alternative policies are compared (Kanban, CONWIP, Base Stock, Extended Kanban, Generalized Kanban).

Finally, and apart from the aforementioned categorizations, relevant published works are further differentiated in terms of several other features such as the existence of setups in the manufacturing system model, the performance metrics considered, and so forth.

The novelty and primary contribution of this research is the following:

- the queueing network models for the multi-stage, multi-product CONWIP, Base Stock and CONWIP/Kanban systems are developed,
- the alternative production control mechanisms are compared in a series of simulation experiments under the metrics of average number of backorders, average finished product inventories and average waiting time of backordered demand,

- insights on the behavior of the different pull production control methods are gained as well as the related managerial implications.

3. System description and production control policies

The system under investigation is comprised of several stages in tandem and manufactures a number of product types. In the remainder of this section, i and j will be used to denote an arbitrary production stage and product type, respectively.

Raw materials enter the system and are processed in all production stages starting from the first one and moving to the downstream stage. Finished products of type j are outputted by the last stage and stored in the respective finished goods inventory. Raw materials are assumed to be continuously available, i.e. the raw materials buffers are never empty. Demands for finished products arrive dynamically to the system and the times between successive demand arrivals are stochastic. Upon a demand arrival, one unit of type j product is requested instantly. If there are available finished products of type j , then the demand is satisfied immediately. If not, then the demand enters the, type j , backorders queue and waits until inventory is made available.

All production stages have a manufacturing facility that is composed of a single machine (with stochastic service times) and the associated input queue. A machine can process all product types; it processes products one-by-one and undergoes a setup when switching from one type to another. A type j product that completes its processing in the i -th stage is stored in output buffer i,j .

The flow of materials from one production stage to the next is coordinated by a pull-type production control policy. In broad terms, a production control policy determines when stage i should pull a type j part from the upstream output buffer in order to process it. In this paper, we examine the CONWIP, Base Stock and CONWIP/Kanban Hybrid policies for multi-product manufacturing. We develop the queueing network models of the respective systems in the following three sub-sections.

3.1 Multi-product CONWIP system

Fig. 1 shows a two-stage, two-product type CONWIP system (due to space limitations). Note that the properties of the CONWIP system presented here hold for any number of product types and production stages.

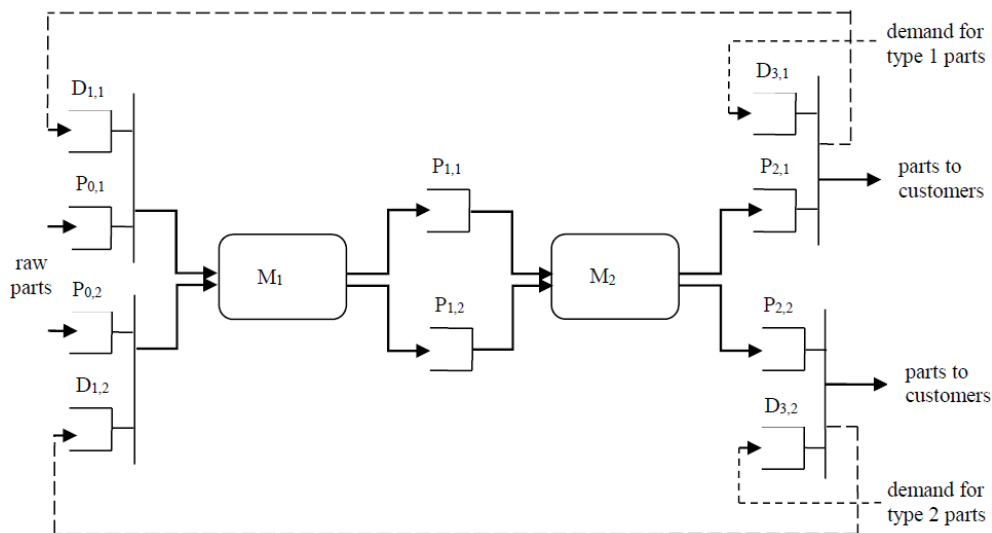


Fig. 1 A CONWIP system with two stages and two product types

In Fig. 1, M_i is the i -th manufacturing facility and $P_{0,j}$ is the raw materials buffer for product type j . The output buffer of stage i and type j is denoted as queue $P_{i,j}$ and queue $D_{3,j}$ contains demands for type j finished products. Finally, queue $D_{1,j}$ contains demands for stage – 1 products of type j . The discipline of all queues shown in Fig. 1 is First-Come-First-Served.

Initially, i.e. at time 0, all machines are idling and all queues are empty except $P_{0,j}$ (by definition) and $P_{i,j}$, for all i, j . At time 0, queue $P_{i,j}$ contains $S_{i,j}$ parts, where $S_{i,j}$ is the base stock (initial inventory) of stage- i and part- j products. The integers $S_{i,j}$, for all i, j , are the control parameters that characterize a multi-product CONWIP system. The sum of the $S_{i,j}$ parameters equals the constant number of parts that “circulate” in the manufacturing system.

The control logic of the CONWIP policy is the following. All stages except the first one are constantly authorized to produce. Consequently, it can be argued that production stages 2, 3, ... operate according to a push strategy. The first stage receives an authorization to process a new type- j part at the moment when a type- j finished product exits output buffer $D_{3,j}$ (transmission of information is assumed to be instantaneous).

3.2 Multi-product Base Stock system

Fig. 2 depicts a two-stage Base Stock system that manufactures two product types. It is noted that the control logic of Base Stock, as explained in this sub-section, can be straightforwardly extended to a system with an arbitrary number of stages and products.

In Fig. 2, M_i denotes the i -th manufacturing facility and $P_{0,j}$ symbolizes the raw materials inventory for product type j . Queue $P_{i,j}$ contains stage- i completed parts of type j . $D_{i,j}$ contains demands for type- j parts; e.g. an element of queue $D_{3,j}$ is a demand for a finished product of type j and an element of queue $D_{2,j}$ authorizes the production of a new stage-2 part of type j . All queues shown in Fig. 2 operate according to the First-Come-First-Served rule.

At time 0, all machines are idle and all queues are empty with the exception of $P_{0,j}$ and $P_{i,j}$, for all i, j . It is reiterated that an infinite supply of raw materials is assumed. Initially, queue $P_{i,j}$ contains $S_{i,j}$ parts. Similarly to CONWIP, the base stocks $S_{i,j}$, for all i, j , are the only control parameters of a multi-product Base Stock system. However, in a Base Stock system, there are no limits on the Work-In-Process and finished goods inventory levels.

The Base Stock system operates as follows. At the time when a demand for a type- j finished product arrives to the system, an analogous demand is transmitted to all queues $D_{i,j}$ authorizing the production of a new type- j , stage- i part, for all i . This way, the production of a new part can commence even if no finished goods inventory has been consumed, allowing for increased flexibility in following demand fluctuations.

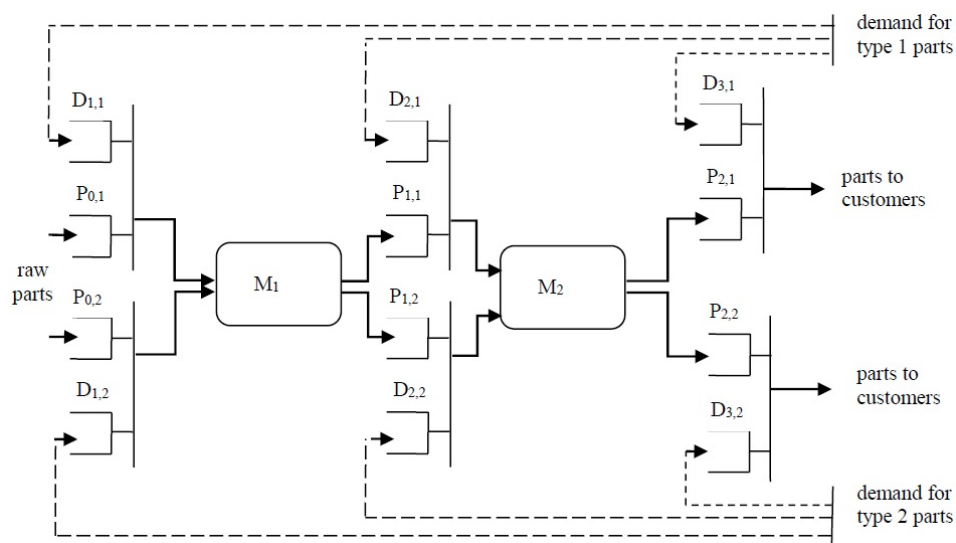


Fig. 2 A Base Stock system with two stages and two product types

3.3 Multi-product CONWIP/Kanban Hybrid system

The queueing network model of a two-stage, two-product CONWIP/Kanban Hybrid system is shown in Fig. 3. It is noted that the mechanics of this control policy, as illustrated in Fig. 3, also apply to systems with any number of stages and product types.

M_i symbolizes the manufacturing facility i and $P_{0,j}$ is the raw parts buffer for type j , in Fig. 3. Queue $PA_{i,j}$ contains stage- i , type- j completed parts with kanbans (production authorizations) attached on them. Queue $P_{2,j}$ has finished products of type j and queue $D_{3,j}$ contains demands for such products. CONWIP-type demands are held in queues D_1 and D_2 . Finally, queues $DA_{1,j}$ contain kanban/demand pairs for stage-1 parts of type j . The discipline of all queues in Fig. 3 is First-Come-First-Served.

Initially, all machines are idling and all queues are empty except for the raw parts buffers, which are always non-empty by definition, and queues $PA_{1,j}$ and $P_{2,j}$, for all j . The latter contain $K_{1,j}$ and $S_{2,j}$ parts, respectively. The number of stage-1, type- j kanbans $K_{1,j}$ and the base stocks $S_{2,j}$ are the control parameters of the system shown in Fig. 3.

The CONWIP/Kanban Hybrid system operates as follows. The last stage has a perpetual authorization to produce, similarly to the pure CONWIP policy. At the time when a type- j finished product is delivered to a customer, a relevant demand is sent to queue D_j at the beginning of manufacturing line. The first stage is authorized to produce a new type- j part if there is at least one element in each of the D_j and $DA_{1,j}$ queues. All other stages operate under a Kanban control policy (for additional details refer to [3]). The rationale behind the philosophy of the CONWIP/Kanban Hybrid policy is to combine the swift turnaround of the CONWIP system with the tight coordination between production stages offered by Kanban.

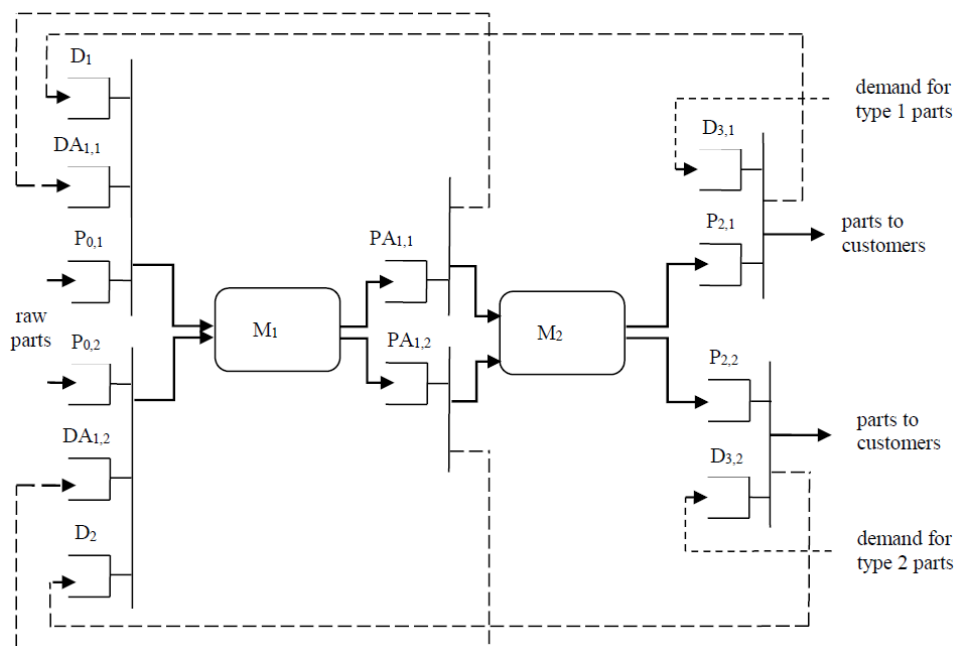


Fig. 3 A CONWIP/Kanban Hybrid system with two stages and two product types

4. Experimental results and discussion

The investigated control policies were compared in a series of simulation experiments that pertained to a manufacturing system with five stages and two product types. The simulation models that were developed for the purposes of this study can straightforwardly be extended to accommodate additional stages and/or product types. Nevertheless, this would increase substantially the effort for presenting/interpreting the results without necessarily providing additional insights on the behavior of the manufacturing systems. The implementation of the simulation models is outlined in the following section 4.1

4.1 Implementation of simulation models

All simulation models are built using the discrete event simulation [17-19] software JaamSim [8]. JaamSim is open-source and offers an intuitive GUI for building complex discrete event models with 3D graphics and animation as well as high execution speed of simulation experiments. These are some indicative reasons that resulted in the growing adoption of the JaamSim software by the community of simulation practitioners and researchers in recent years [20].

Indicatively, the 2D simulation models of the Base Stock, and CONWIP/Kanban hybrid systems with five production stages and two product types are shown in Figs. 4-5. Note that, due to the complexity of the models, their finest details cannot be displayed accurately. Figs. 4-5 are intended to give an overall impression of the structure of the simulation models in question.

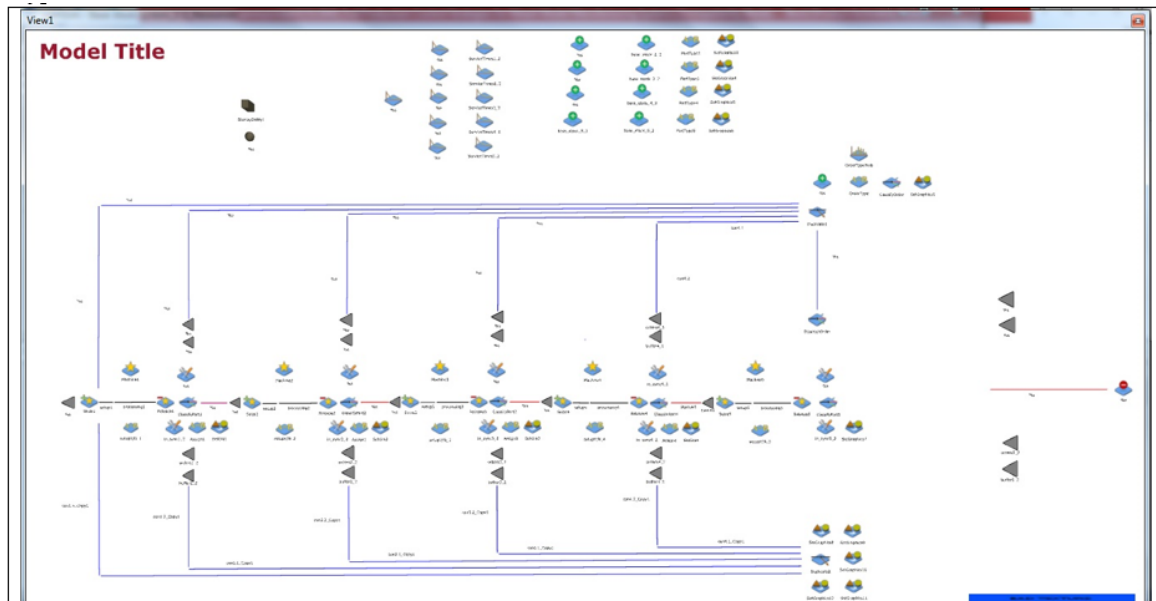


Fig. 4 JaamSim simulation model of Base Stock system with five production stages and two product types

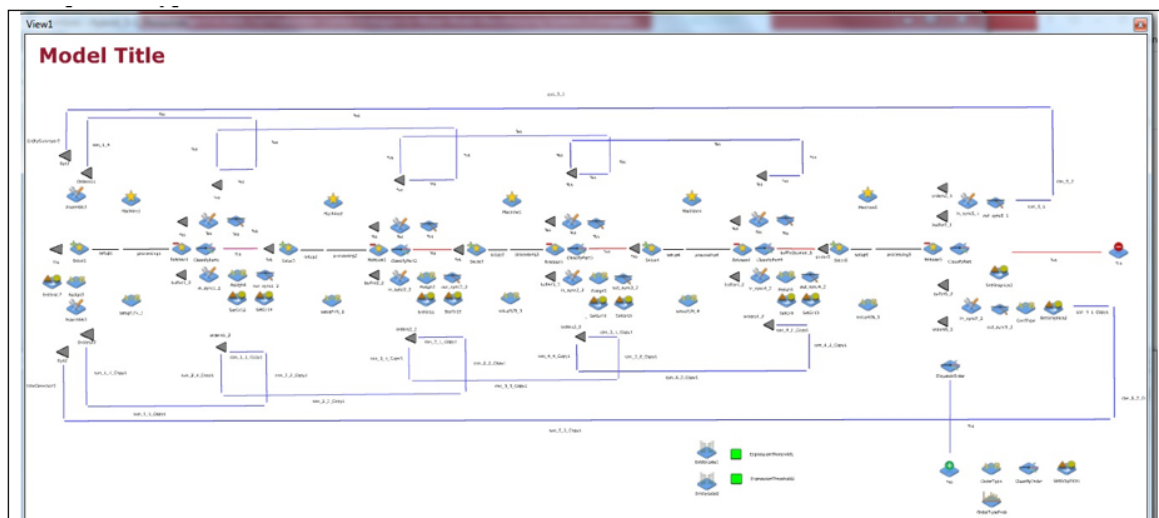


Fig. 5 Simulation model of CONWIP/Kanban Hybrid system with five production stages and two product types

4.2 Configuration of simulation experiments

We defined a base simulation case as the starting point of our analysis and then varied i) the average time between arrivals, ii) the setup time for switching from one product type to another, and iii) the policies' control parameters, in order to study the behavior of the alternative control mechanisms.

The base simulation case is defined as follows: times between arrivals are exponentially distributed with mean 1.26 time units. Upon a demand arrival, a type 1 (or type 2) finished product is requested with probability 0.5. The service times of all machines are exponential with mean 0.8 and 1.2 for type 1 and type 2 products, respectively. When a machine switches from one part type to another, a setup with duration 0.25 time units is incurred. The control parameters (i.e. base stocks and/or kanbans) for all policies, stages and products are set to the value of 5. For all simulation models, the length of a replication is set to 10000 time units and the number of independent replications for all models is 20.

In all simulation experiments we monitored the i) average finished product inventories, ii) the average number of backorders and iii) the average waiting time of backordered demands for each product type. The experimental results are presented in Figs. 6-8.

4.3 Comparing performance metrics of different product types

It is observed from Figs. 6-8 that the monitored performance metrics (i.e. average finished product inventory/average number of backorders/average waiting time of backordered demands for product type 1 and 2) do not vary substantially from one product type to another. E.g. for the CONWIP/Kanban Hybrid system with average time between arrivals equal to 1.38 the average finished product inventory is 14.11 and 13.97 for product type 1 and 2, respectively (refer to Fig. 6f).

This can be attributed to the following reasons. First, the incoming demand is “distributed” equally among the two product types (50 % for product type 1 and 50 % for type 2 as mentioned in section 4.2). Secondly, the number of kanbans/base stocks in each manufacturing stage for product type 1 is identical to that of product type 2. Finally, and most importantly, all parts are processed according to the FCFS queue discipline rule in all manufacturing facilities (M_i elements in Figs. 1-3) regardless of their type or required processing time.

The observed differences between the performance metrics for product type 1 and 2 are caused only by the different service times. Recall from section 4.2 that the mean service time of all machines for product type 1 and 2 is 0.8 and 1.2, respectively. As a result, the total processing time of a type 1 product is smaller than that of a type 2 product. Consequently, for all control policies and simulation cases, type 1 demands are serviced more quickly than type 2 demands, and this consistently leads to slightly higher finished product 1 inventories and smaller waiting times/backorders for type 1 (refer to Figs. 6-8).

An important observation that stems from this analysis is that the “sharing” of the production resources (manufacturing facilities) amongst multiple product types does not affect significantly the observed behavior of the various control policies (in contrast to the single product type case and under the aforementioned production system settings). However, this situation would probably change dramatically in the presence of batching or sequencing rules. For example, in our simulation case, the adoption of the SPT (Shortest Processing Time) rule for part sequencing would probably “favor” part 1 types (due to their smaller mean processing time) leading to a significant change in the performance metrics of product type 1 and 2. Nonetheless, this investigation is beyond the scope of this research.

4.4 Varying average arrival rate

Fig. 6 shows the performance metrics of each control policy for average time between arrivals that varies in the range [1.2, 1.38]. It is observed that the average waiting time of pending orders and the average lengths of the backorders queues are increasing functions of the arrival rate. On the contrary, the average finished product inventories are decreasing functions of the demand arrival rate. For relatively low arrival rates, it is observed that the performance of the alternative control policies is practically the same in respect to the average waiting time/number of backorders. However, for relatively high arrival rates the Base Stock (as well as the CONWIP) and the CONWIP/Kanban Hybrid policies are clearly the best and worst performing mechanisms in terms of the two aforementioned performance measures, respectively.

This can be attributed to the following qualitative characteristics of these control policies: the CONWIP/Kanban Hybrid system has a very tight coordination between the various production

stages whereas the Base Stock does not coordinate at all production operations at different stages. On the other hand, in a CONWIP system, parts flow without interruptions towards the downstream production stages. Consequently, the Base Stock and the CONWIP systems respond rapidly to demand fluctuations, compared to CONWIP/Kanban Hybrid.

From Figs. 6e and 6f, we observe that the CONWIP system causes the highest levels of finished goods inventories followed by the CONWIP/Kanban Hybrid mechanism. An interesting observation is the relative “insensitivity” of the Base Stock system regarding this performance metric and in relation to changes in the average time between arrivals.

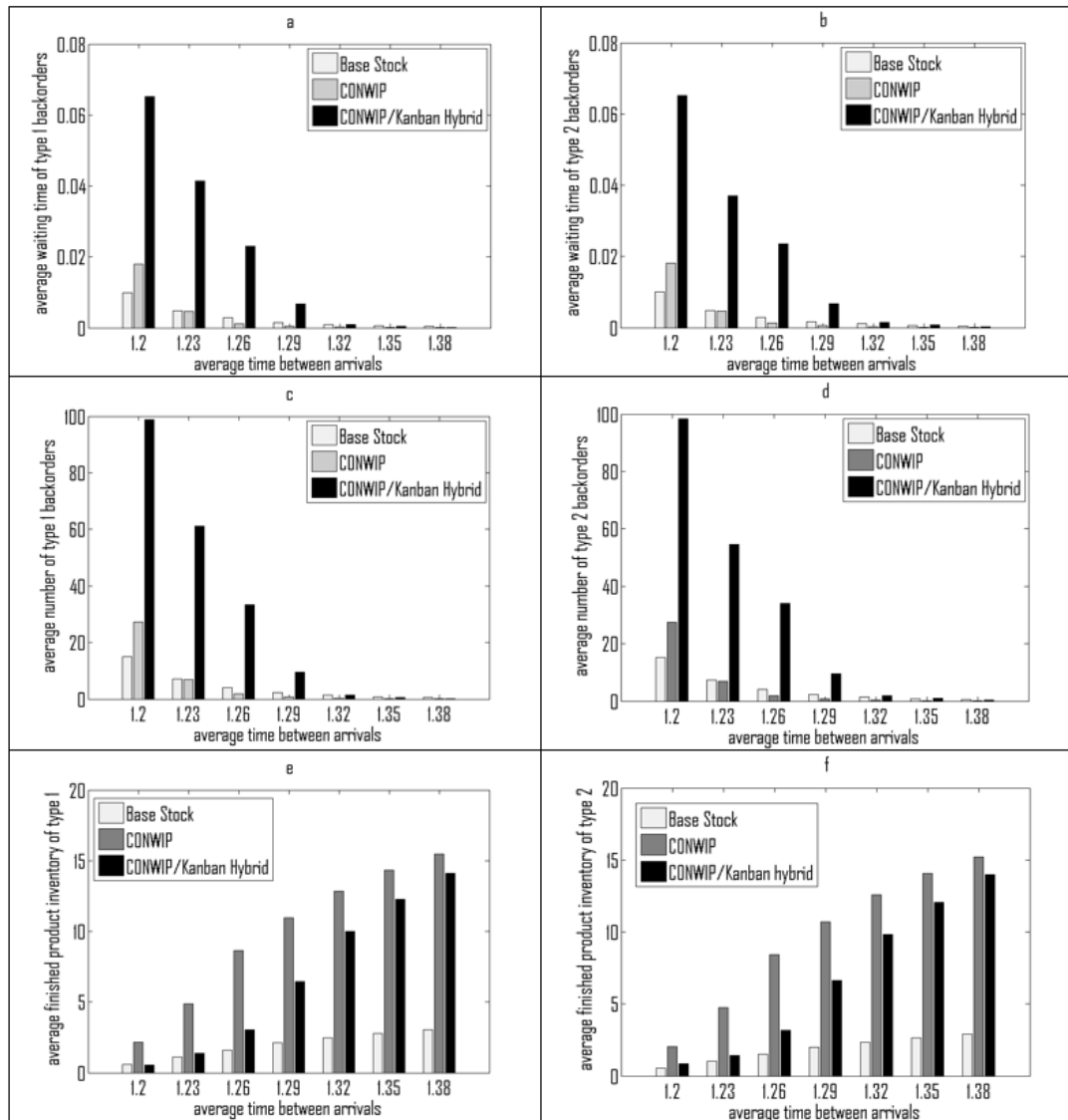


Fig. 6 Performance metrics of alternative production control policies for varying arrival rates. The time units of the y-axis in Figs. 7a-7f are multiplied by a factor of 3.6×10^3

4.5 Varying setup time

Fig. 7 shows the performance metrics of each control policy and product type for setup time equal to 0.1, 0.15, 0.2, 0.25, 0.3, 0.35 and 0.4 time units. It is seen that the average number/waiting time of backorders is an increasing function of the setup time. On the contrary, the average finished product inventories are decreasing functions of the setup time. Increasing the setup time has a similar effect to the system as increasing the arrival rate or decreasing the service rate, i.e. the workload imposed on the manufacturing system increases. However, note that this happens because the part sequencing in all manufacturing facilities is done by means of the FCFS rule and no special sequencing/batching takes place (refer to section 4.3 also).

Again, for relatively small setup times, the differences between the alternative control policies are rather negligible in respect to the average waiting time/number of backorders. For relatively large setup times the ranking of the policies is Base Stock, CONWIP, CONWIP/Kanban Hybrid for these two performance measures. The CONWIP system causes the highest levels of finished goods inventories followed by the CONWIP/Kanban Hybrid mechanism (refer to Figs. 7e-f). Overall, we can argue that CONWIP/Kanban Hybrid is significantly, and adversely, affected by the magnitude of the workload that is imposed on the system whereas the Base Stock system is relatively insensitive to changes in the workload. The Base Stock policy appears to be a good choice when the manufacturing system operates close to its capacity. Finally, an inherent characteristic of the CONWIP mechanism is that it consistently yields the highest finished goods inventories.

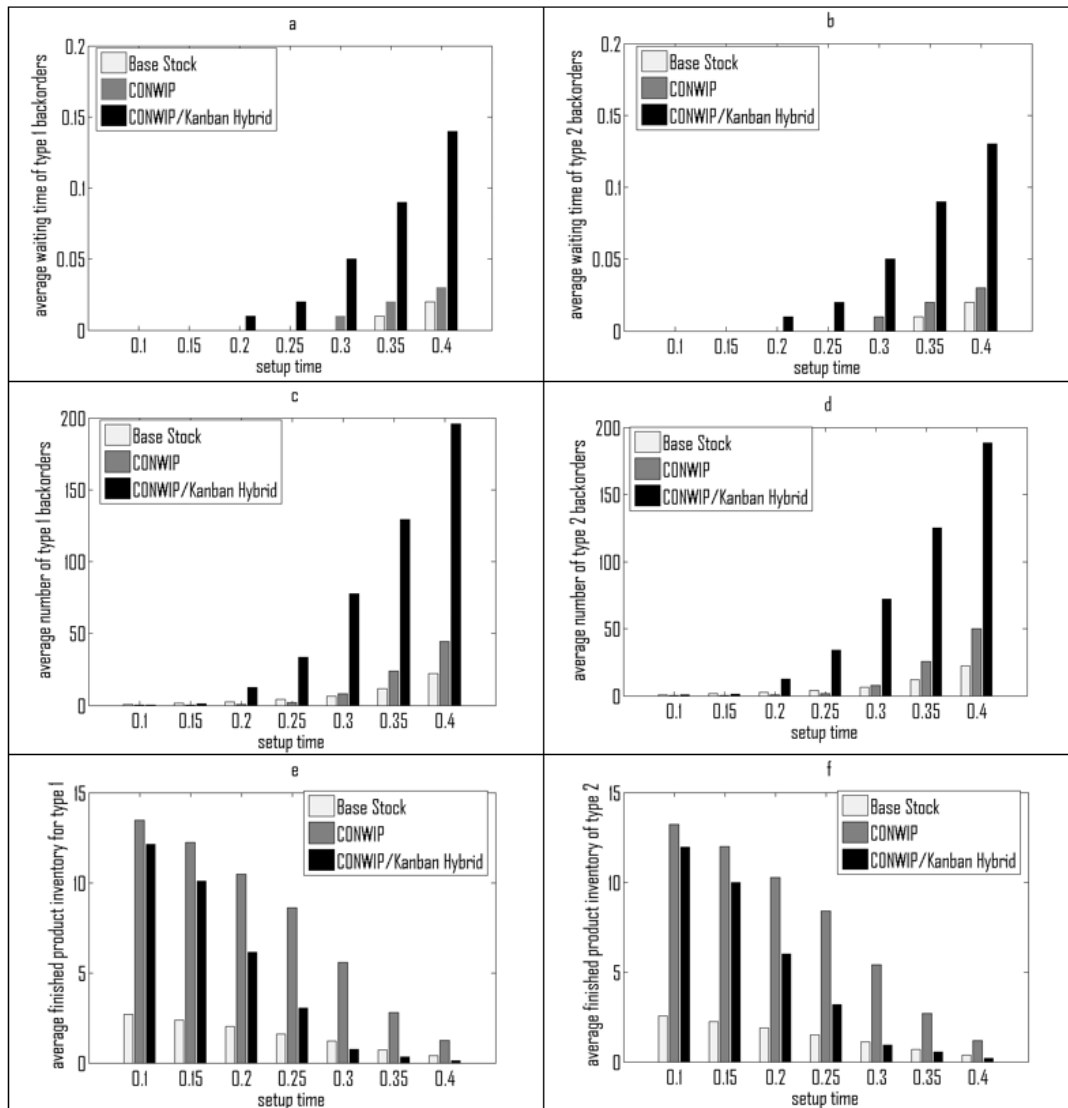


Fig. 7 Performance metrics of alternative production control policies for varying setup times. The time units of the y-axis in Figs. 8a-8f are multiplied by a factor of 3.6×10^3

4.6 Varying control parameters

To examine the effect of the control parameters to the performance of the investigated control mechanisms we used a fractional factorial design. The factors (parameters) of the experimental design are the base stocks or number of kanbans for each production stage and product type.

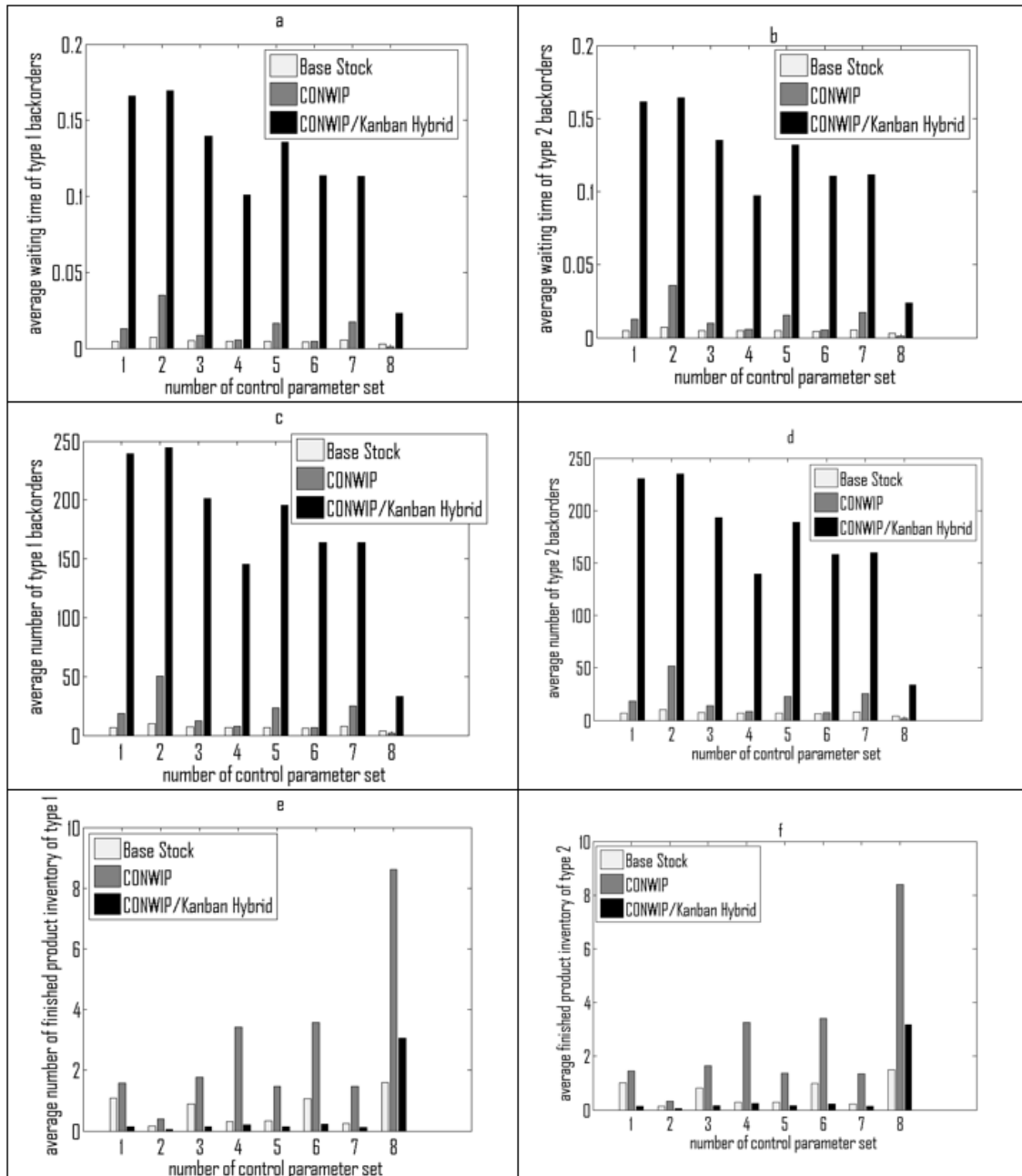


Fig. 8 Performance metrics of alternative production control policies for varying control parameters The time units of the y-axis in Figs. 9a-9f are multiplied by a factor of 3.6×10^3

The low and high level for all factors was set to 2 and 5 respectively. A 2^{4-1} fractional factorial design of resolution IV was generated [3] and it is presented in Table 1.

Fig. 8 shows the average waiting times/number of backorders and the average finished product inventories of all investigated manufacturing systems, for alternative control parameter sets. It is observed that, in order for the CONWIP/Kanban Hybrid system to be “competitive” or at least comparable to Base Stock and CONWIP, its control parameters need to be set to relatively high values. Fig. 8 shows that the CONWIP/Kanban Hybrid mechanism manages to satisfy incoming demand adequately only for the control parameter vector (5, 5, 5, 5, 5). It is observed that this hybrid policy is by far the most sensitive control strategy in respect to changes of parameters K_{ij}/S_{ij} ; for example refer to the difference in the average number of backorders between control parameter set 4 and 8.

Table 1 Examined sets of control parameters ($j = 1,2$). Parameters $K_{i,j}$ apply only to the Hybrid system

| Parameter set | $S_{1,j}(K_{1,j})$ | $S_{2,j}(K_{2,j})$ | $S_{3,j}(K_{3,j})$ | $S_{4,j}(K_{4,j})$ | $S_{5,j}$ |
|---------------|--------------------|--------------------|--------------------|--------------------|-----------|
| No 1 | 2 | 2 | 2 | 5 | 5 |
| No 2 | 5 | 2 | 2 | 2 | 2 |
| No 3 | 2 | 5 | 2 | 2 | 5 |
| No 4 | 5 | 5 | 2 | 5 | 2 |
| No 5 | 2 | 2 | 5 | 5 | 2 |
| No 6 | 5 | 2 | 5 | 2 | 5 |
| No 7 | 2 | 5 | 5 | 2 | 2 |
| No 8 | 5 | 5 | 5 | 5 | 5 |

An interesting characteristic of CONWIP and Base Stock regarding the relationship between their control parameters and the resulting finished product inventories is seen in Figs. 8e-f. The average finished goods inventories in a Base Stock system depend primarily on the base stocks of the last stage (parameter sets with $S_{5,j} = 5$ yield higher inventories compared to parameter sets with $S_{5,j} = 2$). However, in a CONWIP system the average inventories of finished products depend mostly to the sum of base stocks in all production stages. This clearly can be attributed to the fact that in a CONWIP system, Work-In-Process constantly flows without interruption to the last stage.

Finally, in respect to the metrics of average waiting time/number of backorders, the CONWIP system is found to be significantly more sensitive to changes in the control parameters compared to Base Stock.

5. Conclusion

We developed the queueing network models of the CONWIP, Base Stock and CONWIP/Kanban Hybrid control policies for multi-product manufacturing systems. The conversion from a single-type to a multi-type system is rather straightforward however, the model complexity increases dramatically for more than one product types.

The results of the simulation experiments indicated that the defining characteristics of the CONWIP, Base Stock and CONWIP/Kanban Hybrid policies for single-type systems are largely retained in multi-product type systems provided that all parts are processed according to the FCFS queue discipline rule in all manufacturing facilities. Our findings indicate that, when the system operates under a moderate workload, the performance differences between the alternative control policies are rather small.

The Base Stock control strategy offers a rather loose synchronization of the production operations in different stages and responds rapidly to demand fluctuations. These features render it to be a good choice when the manufacturing system is subjected to high demand arrival rates and operates close to its capacity. The behavior of the Base Stock mechanism was reported to be rather insensitive in respect to changes in the imposed workload and the control parameters. Finally, the average finished goods inventories in a Base Stock system were found to depend primarily on the initial stock of the last stage.

In a CONWIP system, parts flow without interruptions towards the downstream production stages. As a result, this control strategy responds rapidly to incoming demand, it is well-suited in situations with relatively high arrival rates and produces consistently the highest level of finished goods inventories. In a CONWIP system the average inventories of finished products depend mostly on the sum of base stocks in all production stages. The CONWIP system is found to be significantly more sensitive to changes in the control parameters compared to Base Stock.

The CONWIP/Kanban Hybrid system offers a very tight coordination between the various production stages compared to CONWIP and Base Stock. Consequently, and in this experimental trial, it was found to be the worst performing control mechanism in situations with high arrival rates. Its performance is significantly affected by the workload that is imposed on the system and by the values of the control parameters. For the CONWIP/Kanban Hybrid system to perform well, its control parameters need to be set to relatively high values, in comparison to CONWIP and Base Stock.

The managerial implications of this research pertain to the design and analysis of efficient production and material control approaches for complex manufacturing systems. This is particularly relevant in the modern and highly competitive manufacturing environment that dictates the elimination of waste in all production processes due to shortened product life cycles, diverse customer needs, and so forth.

There are several ways to extend this research. A straightforward extension is to consider additional pull control policies and conduct larger scale simulation experiments. An even more interesting extension would be to study the synergy of applying specific priority rules for Work-In-Process sequencing and production control policies in mixed-model systems.

References

- [1] Puchkova, A., Le Romancer, J., McFarlane, D. (2016). Balancing push and pull strategies within the production system, *IFAC-PapersOnLine*, Vol. 49, No. 2, 66-71, doi: [10.1016/j.ifacol.2016.03.012](https://doi.org/10.1016/j.ifacol.2016.03.012).
- [2] Liberopoulos, G. (2013). Production release control: Paced, WIP-based or demand driven? Revisiting the push/pull and make-to-order/make-to-stock distinctions, In: Smith, J., Tan, B. (eds.), *Handbook of stochastic models and analysis of manufacturing system operations*, International Series in Operations Research & Management Science, Vol. 192, Springer, New York, USA, 211-247, doi: [10.1007/978-1-4614-6777-9_7](https://doi.org/10.1007/978-1-4614-6777-9_7).
- [3] Koulouriotis, D.E., Xanthopoulos, A.S., Tourassis, V.D. (2010). Simulation optimization of pull control policies for serial manufacturing lines and assembly manufacturing systems using genetic algorithms, *International Journal of Production Research*, Vol. 48, No. 10, 2887-2912, doi: [10.1080/00207540802603759](https://doi.org/10.1080/00207540802603759).
- [4] Xanthopoulos, A.S., Koulouriotis, D.E. (2014). Multi-objective optimization of production control mechanisms for multi-stage serial manufacturing-inventory systems, *International Journal of Advanced Manufacturing Technology*, Vol. 74, 1507-1519, doi: [10.1007/s00170-014-6052-8](https://doi.org/10.1007/s00170-014-6052-8).
- [5] Xanthopoulos, A.S., Koulouriotis, D.E., Gasteratos, A. (2017). Adaptive card-based production control policies, *Computers & Industrial Engineering*, Vol. 103, 131-144, doi: [10.1016/j.cie.2016.11.019](https://doi.org/10.1016/j.cie.2016.11.019).
- [6] Onyeocha, C.E., Wang, J., Khoury, J., Geraghty, J. (2015). A comparison of HK-Conwip and BK-Conwip control strategies in a multi-product manufacturing system, *Operations Research Perspectives*, Vol. 2, 137-149, doi: [10.1016/j.orp.2015.07.001](https://doi.org/10.1016/j.orp.2015.07.001).
- [7] Renna, P. (2018). BK-Conwip adaptive control strategies in a multi-product manufacturing system, In: Khojasteh, Y. (ed.), *Production Management: Advanced Models, Tools, and Applications for Pull Systems*, CRC Press, Taylor & Francis Group, New York, USA, 45-62, doi: [10.1201/b21810-3](https://doi.org/10.1201/b21810-3).
- [8] King, D.H., Harrison, H.S. (2013). Open-source simulation software "JaamSim", In: *Proceedings of the 2013 Winter Simulation Conference (WSC)*, Washington, D.C., USA, 2163-2171, doi: [10.1109/WSC.2013.6721593](https://doi.org/10.1109/WSC.2013.6721593).
- [9] Murino, T., Naviglio, G., Romano, E., Zoppoli, P. (2009). Single stage multi product kanban system. Optimization and parametric analysis, In: *Proceedings of the 8th WSEAS International Conference on System Science and Simulation in Engineering*, Genova, Italy, 313-318.
- [10] Iplani, R., Ang, A.W.H. (2018). Performance comparison of multiple product kanban control systems, *International Journal of Production Research*, Vol. 56, No. 3, 1299-1312, doi: [10.1080/00207543.2017.1332436](https://doi.org/10.1080/00207543.2017.1332436).
- [11] Ezema, C.N., Okafor, E.C., Okezie, C.C. (2017). Kanban based scheduling in a multistage and multiproduct system, *Global Journal of Computer Science and Technology: C Software & Data Engineering*, Vol. 17, No. 1, Version 1, 6-13.
- [12] Olaitan, O.A., Geraghty, J. (2013). Evaluation of production control strategies for negligible-setup, multi-product, serial lines with consideration for robustness, *Journal of Manufacturing Technology Management*, Vol. 24, No. 3, 331-357, doi: [10.1108/17410381311318864](https://doi.org/10.1108/17410381311318864).
- [13] Onyeocha, C.E., Khoury, J., Geraghty, J. (2015). Evaluation of multi-product lean manufacturing systems with setup and erratic demand, *Computers & Industrial Engineering*, Vol. 87, 465-480, doi: [10.1016/j.cie.2015.05.029](https://doi.org/10.1016/j.cie.2015.05.029).
- [14] Onyeocha, C.E., Khoury, J., Geraghty, J. (2015). Robustness analysis of pull strategies in multi-product systems, *Journal of Industrial Engineering and Management*, Vol. 8, No. 4, 1125-1161, doi: [10.3926/jiem.1407](https://doi.org/10.3926/jiem.1407).
- [15] Sastry, G.G., Garg, R. (2017). Analysis of single flow line multi stage multi-product pull control systems, *Journal of Scientific & Industrial Research*, Vol. 76, 289-293.
- [16] Krieg, G.N., Kuhn, H. (2008). Performance evaluation of two-stage multi-product kanban systems, *IIE Transactions*, Vol. 40, No. 3, 265-283, doi: [10.1080/07408170701499554](https://doi.org/10.1080/07408170701499554).
- [17] Yang, S.L., Xu, Z.G., Li, G.Z., Wang, J.Y. (2020). Assembly transport optimization for a reconfigurable flow shop based on a discrete event simulation, *Advances in Production Engineering & Management*, Vol. 15, No. 1, 69-80, doi: [10.14743/apem2020.1.350](https://doi.org/10.14743/apem2020.1.350).
- [18] Li, G.Z., Xu, Z.G., Yang, S.L., Wang, H.Y., Bai, X.L., Ren, Z.H. (2020). Bottleneck identification and alleviation in a blocked serial production line with discrete event simulation: A case study, *Advances in Production Engineering & Management*, Vol. 15, No. 2, 125-136, doi: [10.14743/apem2020.2.353](https://doi.org/10.14743/apem2020.2.353).
- [19] Ištoković, D., Perinić, M., Borić, A. (2021). Determining the minimum waiting times in a hybrid flow shop using simulation-optimization approach, *Tehnički Vjesnik - Technical Gazette*, Vol. 28, No. 2, 568-575, doi: [10.17559/TV-20210216132702](https://doi.org/10.17559/TV-20210216132702).
- [20] Katsios, D., Xanthopoulos, A.S., Koulouriotis, D.E., Kiatipis, A. (2018). A simulation optimisation tool and its production/inventory control application, *International Journal of Simulation Modelling*, Vol. 17, No. 2, 257-270, doi: [10.2507/IJSIMM17\(2\)425](https://doi.org/10.2507/IJSIMM17(2)425).

Latent class analysis for identification of occupational accident casualty profiles in the selected Polish manufacturing sector

Nowakowska, M.^{a,*}, Pajęcki, M.^b

^aFaculty of Management and Computer Modelling, Kielce University of Technology, Poland

^bFaculty of Management and Computer Modelling, Kielce University of Technology, Poland

ABSTRACT

The objective of the analysis is identifying profiles of occupational accident casualties as regards production companies to provide the necessary knowledge to facilitate the preparation and management of a safe work environment. Qualitative data characterizing employees injured in accidents registered in Polish wood processing plants over a period of 10 years were the subject of the research. The latent class analysis (LCA) method was employed in the investigation. This statistical modelling technique, based on the values of selected indicators (observed variables) divides the data set into separate groups, called latent classes, which enable the definition of patterns. A procedure which supports the decision as regards the number of classes was presented. The procedure considers the quality of the LCA model and the distinguishability of the classes. Moreover, a method of assessing the importance of indicators in the patterns description was proposed. Seven latent classes were obtained and illustrated by the heat map, which enabled the profiles identification. They were labelled as follows: very serious, serious, moderate, minor (three latent classes), slight. Some recommendations were made regarding the circumstances of occupational accidents with the most severe consequences for the casualties.

ARTICLE INFO

Keywords:
Manufacturing industry;
Occupational accidents;
Accident profiles identification;
Modelling;
Latent class analysis (LCA);
Cluster analysis;
Model selection

**Corresponding author:*
spimm@tu.kielce.pl
(Nowakowska, M.)

Article history:
Received 24 June 2021
Revised 5 December 2021
Accepted 6 December 2021



Content from this work may be used under the terms of the Creative Commons Attribution 4.0 International Licence (CC BY 4.0). Any further distribution of this work must maintain attribution to the author(s) and the title of the work, journal citation and DOI.

1. Introduction

Occupational accidents play an important role in the functioning of a society. They influence the costs of social security as well as the operating costs of both organizations and individuals. The accidents also affect the productivity, competitiveness and image of enterprises, and contribute to material and moral losses of casualties and their families. Work safety is a crucial issue tackled in various aspects. In general, it can concern ergonomics, in which the increase of effectiveness is indicated by designing workplaces or adapting work along with eliminating (among others) threats that increase the risk of developing employees' illnesses and injuries [1]. It is also included as an element of occupational health and safety in risk assessment in enterprises [2]. In a more detailed aspect, work safety is concentrated on the analysis of occupational accidents and their casualties, trying to discover the circumstances and causes of the events. To reduce accidents at work, mitigate their consequences, and shape a safe work environment, not only sys-

temic actions and countermeasures resulting from the regulations but also various scientific studies are undertaken.

In the scientific literature, the subject has been considered for many years and it includes the analysis of accidents: (1) for specific cases (such as investigations of individual accidents or accidents at specific workplaces in a company, (2) in a variety of spatial aspects (region, country or group of countries), (3) having a certain profile, for example, of the same type or severity, (4) in connection with a specific sector of the economy, for example, construction or mining.

A significant part of the publication is devoted to the analyses of occupational accidents in the construction sector, and both the subject of the research and applied methods are very diverse. Müngen and Gürcanli [3], based on road construction fatal accidents data in Turkey from 1969-1999, using mainly the frequency analysis, indicated a significant share of fatal accidents in road accidents occurring in the road works zones. The authors drew attention to the fact that it was difficult to access the national level data. Rivas *et al.* [4] found that using traditional statistical methods in the investigation does not always allow the identification of actual cause-and-effect relationships as regards accidents at work, recommending the use of advanced analytical techniques, such as: decision rules, Bayesian networks, support vector machines and classification trees. They identified the most important causes of accidents and developed certain predictive models for accidents at work in construction (and additionally mining) companies. Cheng *et al.* [5], investigated the data set of 1,546 observations from 2000-2007 and indicated which factors are particularly responsible for the occurrence of occupational accidents in small construction companies in Taiwan. They used descriptive statistics, correlation analysis and ANOVA. Alizadehi *et al.* [6], in the set of 6722 records, identified 48 groups of workers suffering from accidents at construction workplaces in Iran. Using the Bayes' theorem, they estimated the posterior probability of the severity of the events under consideration. From a literature review, the authors concluded that in similar works on the construction industry, methods such as descriptive statistics, fuzzy inference and fuzzy logic, fuzzy sets, Bayesian analysis or ANOVA were used. Szóstak [7] obtained from the National Labour Inspectorate, 361 individual data records on accidents at work in five voivodships in the Polish construction sector, for 2008-2014. Using non-hierarchical *k*-means cluster analysis, he defined profiles of occupational accident casualties characterized by qualitative and quantitative variables. Drozd [8], on the basis of one country region data from 2014-2016, analysed accidents in the Polish construction sector using the market basket analysis and defined typical association rules for such events. In turn, Berglund *et al.* [9] analysed and characterized accidents in the Swedish construction industry in 2016, calculating selected accident rates for individual trades. Ayhan and Tokdemir [10] undertook a task of developing a method for forecasting the consequences of accidents at work in the construction industry. They proposed a hybrid model combining the LCA cluster analysis and a supervised artificial neural network. The study was based on the collection of 4109 cases anonymously provided by construction companies located in the Euro-Asia region. Lee *et al.* [11] pointed out that various data mining methods are very often used in the analysis of data on occupational accidents in the construction industry. The authors proposed a research procedure for data pre-processing as well as supervised and unsupervised modelling of relationships between the characteristics of occupational accidents in the discussed economic sector. They used, among others: cluster analysis, chi-square test, V-Cramer test, support vector machine, and decision-tree-based ensembles. The elaborated tool was applied to analyse the set of 963 records from a large construction company in Korea. The possibility of using text mining techniques to analyse reports on occupational accidents in the construction sector was noted by Zhang *et al.* [12]. They examined and labelled (by the causes of the accident) 1954 documents describing events from 2003-2010. Keywords were extracted from the documents, which, together with the label, defined the data structure. This data set was the basis for building the accident cause classification models. A variety of mining techniques were used: support vector machine, *k*-nearest neighbours method, decision trees, logistic regression, and naive Bayesian classifier.

Similar methods of analyses are used in works devoted to scientific studies of occupational accidents in sectors other than construction. Palamara *et al.* [13] used a two-level approach involving Kohonen's SOM maps and *k*-means algorithm to identify the most common accident se-

quences leading to accidents in the Italian wood processing industry; data from 2002-2004 were analysed. The same SKM method (SOM and *k*-means) in the research of accidents in the same sector (based on the set of 1247 records) was used by Comberti *et al.* [14], however, focusing on the dynamics of accidents. The authors continued their work for the following years, for a larger data set [15] and in the aspect of a sensitivity analysis [16]. Moura *et al.* [17, 18] used unsupervised neural networks (including Kohonen's SOM) for the analysis of 238 serious accidents from technologically advanced industries (such as: aviation, chemical industry, refineries, petrochemical industry). In their opinion, the use of the proposed tools made it possible to reveal typical patterns and present them in the form of a graphic map, even though accidents are quite complex events, difficult to predict, and in which many different interactions take place. Verma *et al.* [19] analysed 843 occupational accidents registered in steel mills in India and identified patterns of such incidents using the association analysis. Ghousi [20], operating on the set of 1954 records from 2003-2010 and using *k*-means clustering method and the association analysis, investigated occupational accidents in production and industrial units in Iran to create a decision supporting system for managers. Sanmiquel *et al.* [21] identified the main factors influencing accidents at work in the Spanish mining industry. The authors analysed the set of 56,034 accident data records from 2005-2015, identifying association rules that define the causes of accidents based on a specific set of input variables. Farina *et al.* [22] used "learning by mistakes" and latent class analysis (LCA) methods to detect patterns of fatal occupational accidents in the injury dynamics aspect. They used data describing 354 events in enterprises of various industries in one of the regions of Italy (Piedmont) in 2005-2014. The LCA method was also used by Davoudi Kakhki *et al.* [23]. They identified occupational risk groups on the basis of the analysis of 1,031 serious injury events recorded in the Midwest US agribusiness industry in 2008-2016.

The researchers' focus on the construction sector may arise from the opinion that it has the most dangerous workplaces, although this judgment may be determined by a country specificity. However, work on a production line in wood processing companies also generates significant threats to the life and health of employees, since it involves the performing many dangerous actions, such as sawing, mechanical working, planning, cutting, laminating, whittling, and gluing. Nevertheless, work safety issues in the wood processing sector are discussed occasionally. In Poland, it is characterized by one of the highest risk indicators related to a work process. Hence, in the presented research, profiles of casualties of occupational accidents in production plants of the sector in question were identified. A qualitative data analysis tool was used, which is the LCA method. The presented work is the continuation and development of the authors' pilot study discussed as regards a chosen Polish region [24].

The work is an added value to a comparatively limited knowledge about occupational accidents in the wood processing industry. The most important elements for a scientific contribution are:

- determining the specificity of threats in manufacturing companies in the industry on a national scale, taking into account data from a long time horizon (10 years),
- proposing measures that support the assessment of the LCA model quality and proposing a method for the LCA model selection considering these measures,
- development of the discriminating ability index for the observed variables of the LCA model.

The article consists of five parts. After reviewing the selected literature in this chapter, the theoretical foundations of the latent class method are presented. Then, the data for the analyses are characterized and the preparation process for data modelling is described. The next chapter discusses the preliminary results, which are a set of models differing in the number of classes (clusters), and proposes a method of selecting the best one taking into account various criteria. In the next part, the latent classes of the selected model are described according to the observed variables characterizing occupational accident casualties, considering the importance of these variables. Finally, a summary and conclusions are presented.

2. Theoretical fundamentals of latent class analysis

Latent class analysis (LCA) is one of the cluster analysis methods used in the investigation of categorical variables in multivariate data. In the LCA model, a certain abstract qualitative variable LV , called a construct or a latent variable, is not directly observed (is hidden) but it reveals (manifests) its presence and intensity through other qualitative variables $X_j, j = 1, \dots, J$, whose values can be observed. These observed variables are symptoms or indicators of the construct [25]. The purpose of the method is to identify disjoint homogeneous subsets (groups, clusters) in the data set. They are called latent classes and represent the values of the LV latent variable.

In each latent class $K_c, c = 1, \dots, C$, each observation z in the Z multivariate data set has a value for the j -th observed variable. Assuming the independence of the observed variables within the classes, the probability of the product of the corresponding events is the product of the probabilities of these events. Therefore, the probability of occurrence in the class K_c of observation z , for which the vector of values of the observed variables $r(z)$ takes the value q , is the product of the probabilities of the occurrence of individual components of the vector q . Taking into consideration the above statement, the following form of the LCA model can be defined, which estimates the probability that in the z observation the $r(z)$ vector, representing the combination of values of the indicators X_1, \dots, X_j , has the value equal to q [25]:

$$P(r(z) = q) = \sum_{c=1}^C \gamma_c \cdot \prod_{j=1}^J P(r_j(z) = q_j | z \in K_c) = \sum_{c=1}^C \gamma_c \cdot \prod_{j=1}^J \rho_{q_j|c} \tag{1}$$

where: K_c is c -th latent class, $c = 1, \dots, C$; C is the number of latent classes; γ_c is the probability of the c -th latent class, which is the probability of belongings of an observation to the K_c latent class: $\gamma_c = P(K_c) = P(z \in K_c), c = 1, \dots, C (\sum_{c=1}^C \gamma_c = 1)$; $\rho_{q_j|c}$ is the conditional probability, that j -th observed variable has the value of q_j in the K_c latent class: $\rho_{q_j|c} = P(q_j|c) = P(r_j(z) = q_j | z \in K_c)$; q_j is the value of j -th observed variable, $q_j \in R_j$; R_j is the set of values of j -th observed variable, $j = 1, \dots, J$.

Non-zero probabilities $P(r(z) = q)$ are usually estimated by the optimization of the $V(Z)$ negative log likelihood. The optimization for the model Eq. 1 is finding such values of γ_c and $P(r_j(z) = q_j | z \in K_c) (= \rho_{q_j|c})$ estimators that the $V(Z)$ function of the form:

$$V(Z) = - \sum_{q \in R} N(q) \cdot \ln \left(\sum_{c=1}^C \gamma_c \cdot P(r(z) = q | z \in K_c) \right) \tag{2}$$

takes the smallest value with the following constraints:

$$\sum_{c=1}^C \gamma_c = 1 \tag{3}$$

$$\bigwedge_{c=1, \dots, C} 0 < \gamma_c \leq 1 \tag{4}$$

$$\bigwedge_{j=1, \dots, J} \bigwedge_{c=1, \dots, C} \sum_{q_j \in R_j} P(r_j(z) = q_j | z \in K_c) = 1 \tag{5}$$

$$\bigwedge_{j=1, \dots, J} \bigwedge_{c=1, \dots, C} \bigwedge_{q_j \in R_j} P(r_j(z) = q_j | z \in K_c) \in [0, 1] \tag{6}$$

where: $R = R_1 \times \dots \times R_j$; $q = (q_1, \dots, q_j)$; $N(q)$ is the empirical frequency in a contingency table cell defined by the q vector of values for the observed variables (in other words: the number of ob-

servations in the Z data set for which the vector of the observed variables $X = (X_1, \dots, X_j)$ has values of the q vector).

The G^2 statistic is used to assess the quality of the estimated latent classes model [25]:

$$G^2 = 2 \sum_{q \in R} N(q) \cdot \ln \left(\frac{N(q)}{\hat{N}(q)} \right) \quad (7)$$

where: N is the Z data set size (number of observations); $\hat{N}(q)$ is theoretical (expected) frequency in a contingency table cell defined by the q vector of values: $\hat{N}(q) = N \cdot P(r(z) = q)$, $P(r(z) = q)$ is given by the relationship Eq. 1.

To compare the models differing in the number of latent classes, information criteria are used, in particular considering the size of the data set (N) and the complexity of the model (M) [26, 27, 28]:

- $CAIC = G^2 + M \cdot (\ln(N) + 1)$ – Consistent Akaike Information Criterion,
- $BIC = G^2 + M \cdot \ln(N)$ – Bayes Information Criterion,
- $ABIC = G^2 + M \cdot \ln((N + 2)/24)$ – Adjusted Bayes Information Criterion.

In the above formulas, M is the number of the estimated parameters of the model Eq. 1 equal to:

$$M = (C - 1) + C \cdot \sum_{j=1}^J (|R_j| - 1) \quad (8)$$

where: $|R_j|$ is the number of values of the X_j variable.

The smaller the values of the measures are, the better the assessment of the model is. With a small sample size, the importance of complex models (with a large number of latent classes and a large contingency table) is greatly reduced.

To build the LCA model in this work, the authors used the *Proc LCA* procedure of the SAS system [29] and their own calculations elaborated in the MS Excel environment.

3. Data for analysis

In Poland, data on occupational accidents for all professional activities, systematized according to the PKD section – Polish Classification of Activities (economic activity), are collected by the Central Statistical Office (GUS). Due to the function of supervising and controlling regulations as regards work health and safety, the National Labour Inspectorate (PIP) also collects information on occupational accidents investigated by PIP inspectors. This refers obligatorily to severe, fatal and group accidents. The GUS registers are digital and their structure complies with the structure of the national statistical accident card (defined by the regulation of the Minister of Labour and Social Policy of January 7, 2009 [30], amended in 2019 by the regulation of the Minister of Family, Labour and Social Policy of June 4, 2019 [31]). Each card contains details on a person injured in an accident, described by 29 features. Most of these features are descriptive, which implies the need to use qualitative data analysis methods.

The subject of the presented research are individual data records on accidents at work for 2008-2017, registered in production plants in Poland, that is in enterprises included in the C section according to the Polish Classification of Activities, obtained from the Central Statistical Office. Out of 24 branches of the C section, branch 16 was selected for the investigation. This is *Manufacture of wood and cork products, excluding furniture; manufacture of articles of straw and plaiting materials*. The companies in this branch produce such elements as: plywood, sawmill products, floor coverings, wooden packaging, veneer, and other carpentry articles. The nature of work of people employed in the production process generates very high accident risks [32]. In comparison with other branches of the C section, the accident rate (number of injured persons per 1000 employees per year), equal to 15.24, placed branch 16 above the 0.8 quantile. The accident casualty severity rate (the number of people injured in serious and fatal accidents per 10,000 employees per year), equal to 36.09, was the highest for this branch. Taking into account

the above, the research was focused on the production process. In the collection of the data on accidents at work for branch 16, a subset that met the following criteria (the wordings in italics are taken from the statistical accident card) was selected:

- people injured in accidents at work: *Industrial workers and craftsmen, Operators and assemblers of machines and devices, and Employees doing simple works,*
- accident location: *Industrial production sites,*
- work process: *Production, processing, storage.*

For the need of calculations in the work, features characterizing the accidents casualties are marked with the symbol *Pxx*, where *xx* stands for the number of an item from the statistical accident card (for example, *P02* means the age of the injured person). In a data pre-processing step, variables (indicators) were selected for the LCA model creation and outliers and observations that did not provide significant information were removed (for example, *P09 – Injured body part = Unknown or undefined, P21 – Activity performed at accident time = No information available*). Data transformation was proposed, mainly values or variables aggregation, which helped to solve the problem of rare categories. The resulting data set consisted of nine indicators and 13,750 observations. The characteristics of the set are presented in Table 1. Modifications made to the data are marked in italics. The numerical codes of the values (consecutive positive integers) and distributions for each observed variable are given.

Table 1 Characteristics of the research data

| Indicators and their descriptive values | Value code | (%) |
|--|------------|-------|
| P02 – Casualty age | | |
| Up to 24 years old | 1 | 17.30 |
| 25-34 years old | 2 | 30.23 |
| 35-44 years old | 3 | 25.43 |
| 45-54 years old | 4 | 18.65 |
| Over 54 years <i>Aggregation of original values: (55-59 years) + (over 59 years)</i> | 5 | 8.38 |
| P05 – Casualty occupation | | |
| Industrial workers, craftsmen, and employees doing simple works <i>Aggregation of original values: (Industrial workers and craftsmen), (Employees doing simple works)</i> | 1 | 67.83 |
| Operators and assemblers of machines and devices | 2 | 32.17 |
| P06 – Enterprise job seniority | | |
| Up to 5 years | 1 | 67.64 |
| 6-10 years | 2 | 15.97 |
| Over 10 years <i>Aggregation of original values: (11-15), (16-20), (21-30), (Over 30 years)</i> | 3 | 16.39 |
| P08 – Injury type | | |
| Wounds and superficial injuries | 1 | 55.96 |
| Bone fractures | 2 | 16.23 |
| Displacements, dislocations, sprains and strains | 3 | 11.19 |
| Traumatic amputations (loss of body parts) | 4 | 7.24 |
| Various other injuries <i>Aggregation of original values: (Unknown or undefined), (Internal injuries), (Burns, frost-bites), (Poisoning, infections), (Drowning, suffocating from lack of oxygen), (Effects of sounds, vibrations and pressure), (Effects of extreme temperatures, lighting and radiation), (Shocks), (Multiple injuries), (Another injury)</i> | 5 | 9.39 |
| P09 – Injured body part | | |
| Head, neck <i>Aggregation of original values: (Head), (Neck with cervical spine)</i> | 1 | 7.01 |
| Body <i>Aggregation of original values: (Thoracic and lumbar spine), (Torso and internal organs), (Whole body and its various parts), (Other body part)</i> | 2 | 4.84 |
| Upper limbs | 3 | 67.31 |
| Lower limbs | 4 | 20.84 |

Table 1 Characteristics of the research data (continuation)

| P21 – Activity performed at accident time | | (%) |
|---|---|-------|
| Operating machinery | 1 | 46.92 |
| Working with tools and objects | 2 | 29.20 |
| <i>Aggregation of original values: (Working with hand tools), (Handling objects)</i> | | |
| Transport at workplace | 3 | 14.63 |
| <i>Aggregation of original values: (Driving means of transport / operation of moving machines and other devices), (Manual transporting)</i> | | |
| Being at accident scene | 4 | 9.26 |
| <i>Aggregation of original values: (Moving about), (Presence)</i> | | |
| P26 – Material factor as injury source | | |
| Buildings, structures, surfaces | 1 | 6.83 |
| <i>Objects as above and their elements including positions: (At ground level), (Below ground level), (Above ground level)</i> | | |
| Another factor | 2 | 9.43 |
| <i>Aggregation of original values: (There is no material factor), (Supply, distribution and discharge systems for gases, liquids and solids, pipe networks, installations), (Equipment for the generation, processing, storage, transmission and distribution of energy), (Road vehicles), (Other transport vehicles), (Chemical, radioactive, explosive, biological substances), (Safety related devices and equipment), (Office equipment, personal equipment, sports equipment, weapons), (People and other living organisms), (Waste), (Physical phenomena and elements of the natural environment), (Another factor)</i> | | |
| Hand tools | 3 | 9.32 |
| <i>Aggregation of original values: (Non-powered hand tools), (Hand-held or hand guided mechanized tools)</i> | | |
| Machines and devices | 4 | 39.99 |
| <i>Aggregation of original values: (Portable or mobile machines and equipment), (Stationary machines, devices and equipment), (Machines, devices and equipment for lifting, carrying and storage)</i> | | |
| Materials, objects, products, machine parts | 5 | 34.43 |
| P27 – Main accident cause | | |
| Defect of material factor | 1 | 16.38 |
| <i>Aggregation of original values: (Design defects or inappropriate technical and ergonomic solutions of material factor), (Improper manufacturing of material factor), (Material defects of material factor)</i> | | |
| Misuse of material factor | 2 | 13.98 |
| <i>Aggregation of original values: (Inappropriate exploitation of material factor), (Employee's non-use or inappropriate handling of material factor)</i> | | |
| Inappropriate work organization | 3 | 11.67 |
| <i>Aggregation of original: (Inadequate overall organization of work), (Inappropriate organization of a workplace), (Employee's failure to use protective equipment)</i> | | |
| Safety neglect | 4 | 57.97 |
| <i>Aggregation of original values: (Employee's psychophysical state, not ensuring safe work performance), (Employee's inappropriate arbitrary behaviour), (Employee's misconduct)</i> | | |
| P289 – Casualty injury severity; a new variable, defined on the basis of the variables: P28 (accident consequence) and P29 (inability to work) | | |
| Minor accident resulting in inability to work for 0-29 days (up to a month) | 1 | 46.41 |
| <i>Aggregation of original values: (Minor accident resulting in inability to work for 0-13 days), (Minor accident resulting in inability to work for 14-29 days)</i> | | |
| Minor accident resulting in inability to work for 30-89 days (from one to three months) | 2 | 37.97 |
| Serious accident | 3 | 15.61 |
| <i>Aggregation of original values: (Severe or fatal accident), (Minor accident causing inability to work for more than 90 days)</i> | | |

4. Selection of the LCA model

As in every cluster analysis method, also in the case of the LCA model, the decision on the number of latent classes is the key element. The following aspects were considered:

- relatively low values of information criteria, such as: *CAIC*, *BIC*, and *ABIC*,

- acceptable probability values of latent classes (which are weights determining classes support) – these values cannot be too low,
- the number of classes must not be too small to prevent the loss of information relevant to the definition of patterns,
- the number of classes must not be too large for the identified patterns to be distinguishable.

The decision on all the criteria is subjective and requires balancing, which means that a trade-off between fit and practical usability of the model should be considered. The latter aspect is related to the interpretability of the model – its suitability for distinguishing between classes. To facilitate the decision-making process, two measures were defined: the model balance ratio and the measure of the discriminating ability of the observed variable.

If, according to the assumption of the LCA model, the latent classes K_c and their probabilities γ_c define the distribution of the LV latent random variable that has C values (latent classes), then the entropy H of this variable is given by the relationship [33]:

$$H = - \sum_{c=1}^C \gamma_c \cdot \ln(\gamma_c) \quad (9)$$

Entropy has the greatest value when all probabilities are the same. In this case, H equals $\ln(C)$ and means that the importance of all latent classes is the same, which is considered to balance the model. The HB balance ratio is proposed as the quotient of the entropy H of the estimated LCA model and the entropy of the corresponding balanced model, taking into account the number of classes:

$$HB = \frac{H}{\ln(C)} \quad (10)$$

The closer to unity the value of HB is, the smaller the number of trivial latent classes (with small values of probabilities) are. The HB indicator, when combined with other measures, may support the selection of the LCA model.

The paper also proposes an index of the discriminating ability AR of the X_j observed variable. It is defined on the basis of the range of conditional probabilities of the X_j variable:

$$AR(X_j) = \frac{1}{|R_j|} \sum_{q_j \in R_j} Range(q_j|\{c\}) \quad (11)$$

where: $Range(q_j|\{c\}) = \max_{c=1, \dots, C} \{\rho_{q_j|c}\} - \min_{c=1, \dots, C} \{\rho_{q_j|c}\}$.

The algorithm leading to obtaining the AR value can be described as follows:

- the range of conditional probabilities assigned to the q_j value of the variable X_j with regard to the classes of the LCA model is calculated (there are as many probabilities as the latent classes for one q_j),
- the average of all the range values (there are as many ranges as the X_j variable values) obtained for the X_j variable creates the $AR(X_j)$ index.

The discriminating ability of an observed variable, valued with the AR measure, can be interpreted as an assessment of the distinction possibility of latent classes with respect to this variable. The maximum value of any range from formula Eq. 11 is equal to 1. It occurs when the conditional probability of the variable category in one class is 0 and in another class is 1. It means that in the case of perfect distinguishability of at least two classes, the AR measure is equal to 1. The AR value belongs to the interval $[0, 1]$. The nature of the measure indicates that the closer to unity its value is, the stronger the discriminating ability of the observed variable becomes. In this aspect, the AR measure can also be used as an importance weight of the observed variable in defining profiles as regards the phenomenon under investigation. Extreme cases, when $AR = 0$ or $AR = 1$, for real data almost never occur. In the work, it is assumed that an observed variable has a good discriminating ability if its AR exceeds 0.5.

A series of experiments with a different number of latent classes, from 1 to 16, was performed to determine an acceptable model. Considering that numerical methods are used in the calculations, for each model with a given number of classes, 20 estimates with different initial values for the iterative process were carried out. In the set of C -class models obtained in this way, a representative was selected – the model for which the function Eq. 2 had the lowest value. The final model was selected from among 16 representatives, using the previously described measures. The plots of values of $CAIC$, BIC , and $ABIC$ information criteria, the HB balance ratio, and the $AR(X_i)$, $i = 1, \dots, 9$ measures by each model (with a certain number of classes $C = 1, \dots, 16$) are shown in Fig. 1, Fig. 2, and Fig. 3 respectively. The numbers of latent classes in the LCA model are marked on the horizontal axes (they also indicate the model numbers).

Fig. 1 was elaborated as a scree plot. It shows that the decline in the value of information criteria is relatively gentle, starting with the 7-class or 8-class model. It can be seen that increasing the number of latent classes above eight does not disrupt the linear trend almost parallel to the horizontal axis for all the three measures. The HB ratio graph is very diverse (Fig. 2), although the range of values is relatively small – it varies within the interval (0.9, 0.99). The three distinctive points on the polygonal chain suggest a very good balance for the LCA models with the number of latent classes equal to: 3, 7, and 8. According to Fig. 3, five observed variables form the group that plays the greatest role in distinguishing between latent classes: *Activity performed at accident time* (P21), *Injury type* (P08), *Injured body part* (P09), *Material factor as injury source* (P26), and *Casualty injury severity* (P289). Beginning with the 7-class model, all these variables have the AR value greater than 0.5. The following features are characterized by a worse discriminating ability: *Casualty age* (P02), *Casualty occupation* (P05) and *Main accident cause* (P27). They have the AR value less than 0.3 for the first eight models. The *Enterprise job seniority* (P06) observed variable is located between these two groups, starting from the 6-class model, and the discriminating ability of this indicator can be both high ($AR = 0.63$) and small ($AR = 0.37$), depending on the number of classes. Similar chart layouts characterize 6-class to 9-class models. Taking into account all the considered measures and, additionally, the insight into the estimated parameters, finally allowed selecting a 7-class model for further analysis, the qualitative assessment of which was better than that of other models. This model is identified by the $LCA-7$ symbol further in the study.

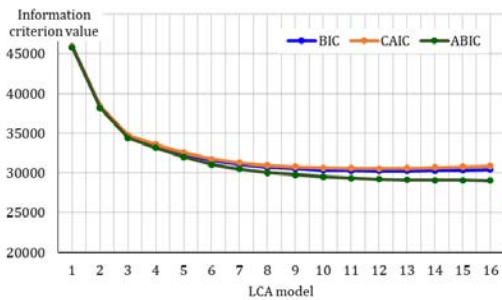


Fig. 1 Information criteria values by the number of classes in the LCA model

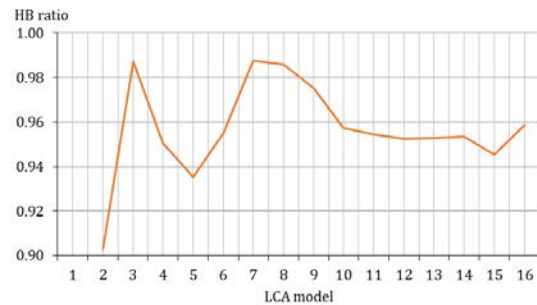


Fig. 2 HB balance ratio values by the number of classes in the LCA model

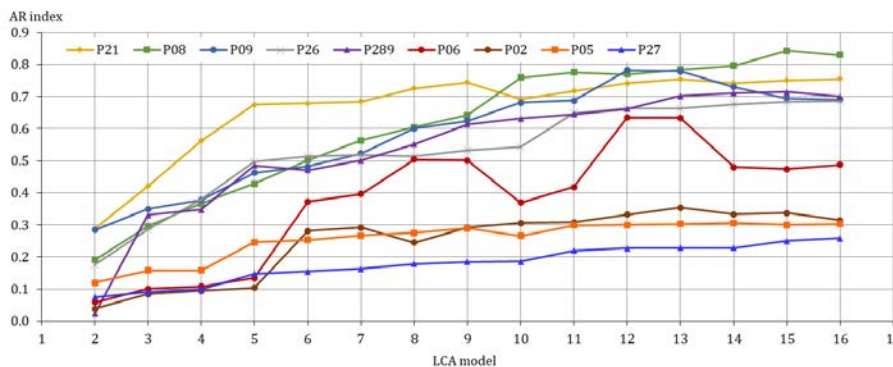


Fig. 3 AR index of observed variables by the number of classes in the LCA model

Table 2 presents the estimated statistics for the latent classes of the *LCA-7* model. Classes support is quite satisfactory. In each case, the number of observations exceeds 1000, which means that, on average, during a year there are over 100 casualties of accidents at work characterized by the profile of a given cluster.

Table 2 Support for latent classes of the *LCA-7* model

| Latent class identifier | Class K ₁ | Class K ₂ | Class K ₃ | Class K ₄ | Class K ₅ | Class K ₆ | Class K ₇ |
|--------------------------|----------------------|----------------------|----------------------|----------------------|----------------------|----------------------|----------------------|
| Latent class probability | 0.13 | 0.17 | 0.12 | 0.18 | 0.09 | 0.14 | 0.17 |
| Latent class size | 1727 | 2381 | 1668 | 2480 | 1226 | 1956 | 2312 |

5. Results

A synthetic summary on the selected *LCA-7* model is shown in Fig. 4. The resulting latent classes are illustrated in the form of a heat map. The map layout is defined according to the ordering of the analysed observed variables by their importance (assessed by discriminating ability), starting from the indicator with the highest value of the *AR* measure. The heat map column in front of the vertical line shows the distribution of the corresponding variables for the whole data set and it is the reference for the rest of the map. The cells behind the vertical line reflect the estimated conditional probabilities that the indicator (*P21*, *P08*, etc.) takes a certain value, provided that the observation (accident casualty) it characterizes belongs to a given latent class c ($c = K_1, \dots, K_7$).

| Indicator value | Whole data set | Class K ₁ | Class K ₂ | Class K ₃ | Class K ₄ | Class K ₅ | Class K ₆ | Class K ₇ |
|--|----------------|----------------------|----------------------|----------------------|----------------------|----------------------|----------------------|----------------------|
| <i>P21</i> - Activity performed at accident time; $AR(P21) = 0.6847$ | | | | | | | | |
| Operating machinery | 0.47 | 0.30 | 0.86 | 0.00 | 0.62 | 0.10 | 0.28 | 0.72 |
| Working with tools and objects | 0.29 | 0.31 | 0.13 | 0.99 | 0.20 | 0.06 | 0.25 | 0.20 |
| Transport at workplace | 0.15 | 0.33 | 0.01 | 0.01 | 0.15 | 0.22 | 0.30 | 0.08 |
| Being at accident scene | 0.09 | 0.06 | 0.01 | 0.00 | 0.02 | 0.62 | 0.17 | 0.00 |
| <i>P08</i> - Injury type; $AR(P08) = 0.5633$ | | | | | | | | |
| Wounds and superficial injuries | 0.56 | 0.04 | 0.39 | 0.86 | 0.80 | 0.12 | 0.56 | 0.87 |
| Bone fractures | 0.16 | 0.69 | 0.16 | 0.05 | 0.07 | 0.21 | 0.01 | 0.06 |
| Displacements, dislocations ... | 0.11 | 0.18 | 0.01 | 0.02 | 0.07 | 0.62 | 0.08 | 0.02 |
| Traumatic amputations ... | 0.07 | 0.03 | 0.37 | 0.01 | 0.00 | 0.00 | 0.00 | 0.02 |
| Various other injuries | 0.09 | 0.05 | 0.08 | 0.06 | 0.06 | 0.04 | 0.35 | 0.03 |
| <i>P09</i> - Injured body part; $AR(P09) = 0.5226$ | | | | | | | | |
| Head, neck | 0.07 | 0.01 | 0.00 | 0.09 | 0.04 | 0.01 | 0.27 | 0.06 |
| Body | 0.05 | 0.06 | 0.01 | 0.01 | 0.01 | 0.03 | 0.24 | 0.00 |
| Upper limbs | 0.67 | 0.58 | 0.96 | 0.80 | 0.81 | 0.16 | 0.20 | 0.86 |
| Lower limbs | 0.21 | 0.35 | 0.02 | 0.10 | 0.14 | 0.80 | 0.28 | 0.07 |
| <i>P26</i> - Material factor as injury source; $AR(P26) = 0.5173$ | | | | | | | | |
| Buildings, structures, surfaces | 0.07 | 0.08 | 0.00 | 0.03 | 0.01 | 0.48 | 0.07 | 0.00 |
| Another factor | 0.09 | 0.10 | 0.03 | 0.05 | 0.06 | 0.24 | 0.20 | 0.06 |
| Hand tools | 0.09 | 0.04 | 0.03 | 0.56 | 0.02 | 0.00 | 0.03 | 0.03 |
| Machines and devices | 0.40 | 0.18 | 0.82 | 0.00 | 0.53 | 0.18 | 0.19 | 0.58 |
| Materials, objects, products, machine parts | 0.34 | 0.60 | 0.11 | 0.37 | 0.38 | 0.09 | 0.52 | 0.33 |
| <i>P289</i> - Casualty injury severity; $AR(P289) = 0.5012$ | | | | | | | | |
| Minor accident, inability to work for 0-29 days | 0.46 | 0.10 | 0.09 | 0.77 | 0.67 | 0.36 | 0.68 | 0.55 |
| Minor accident, inability to work for 30-89 days | 0.38 | 0.62 | 0.51 | 0.19 | 0.32 | 0.44 | 0.20 | 0.38 |
| Serious accident | 0.16 | 0.28 | 0.40 | 0.03 | 0.01 | 0.20 | 0.12 | 0.07 |
| <i>P06</i> - Enterprise job seniority; $AR(P06) = 0.3962$ | | | | | | | | |
| Up to 5 years | 0.68 | 0.63 | 0.74 | 0.75 | 0.97 | 0.55 | 0.63 | 0.38 |
| 6 - 10 years | 0.16 | 0.17 | 0.15 | 0.14 | 0.03 | 0.19 | 0.19 | 0.28 |
| Over 10 years | 0.16 | 0.20 | 0.12 | 0.10 | 0.00 | 0.26 | 0.18 | 0.34 |
| <i>P02</i> - Casualty age; $AR(P02) = 0.29123$ | | | | | | | | |
| Up to 24 years old | 0.17 | 0.09 | 0.17 | 0.25 | 0.44 | 0.08 | 0.11 | 0.00 |
| 25 - 34 years old | 0.30 | 0.28 | 0.29 | 0.36 | 0.45 | 0.29 | 0.28 | 0.16 |
| 35 - 44 years old | 0.25 | 0.27 | 0.25 | 0.23 | 0.09 | 0.30 | 0.30 | 0.38 |
| 45 - 54 years old | 0.19 | 0.25 | 0.20 | 0.12 | 0.02 | 0.23 | 0.21 | 0.32 |
| Over 54 years | 0.08 | 0.11 | 0.10 | 0.04 | 0.00 | 0.10 | 0.10 | 0.15 |
| <i>P05</i> - Casualty occupation; $AR(P05) = 0.2667$ | | | | | | | | |
| Industrial workers, craftsmen ... | 0.68 | 0.68 | 0.78 | 0.67 | 0.69 | 0.52 | 0.61 | 0.71 |
| Operators and assemblers of machines ... | 0.32 | 0.32 | 0.22 | 0.33 | 0.31 | 0.48 | 0.39 | 0.29 |
| <i>P27</i> - Main accident cause; $AR(P27) = 0.1632$ | | | | | | | | |
| The defect of material factor | 0.16 | 0.12 | 0.25 | 0.12 | 0.12 | 0.08 | 0.17 | 0.23 |
| Misuse of material factor | 0.14 | 0.19 | 0.15 | 0.19 | 0.15 | 0.03 | 0.10 | 0.14 |
| Inappropriate work organization | 0.12 | 0.15 | 0.07 | 0.08 | 0.10 | 0.17 | 0.20 | 0.08 |
| Safety neglect | 0.58 | 0.54 | 0.53 | 0.61 | 0.62 | 0.73 | 0.54 | 0.56 |

Fig. 4 The heat map of occupational accident casualty profiles for the *LCA-7* model

6. Discussion

The individual profiles of the *LCA-7* model were characterized on the basis of the obtained conditional probabilities and they are presented in Table 3. Descriptions are given according to the importance of the observed variables. If, for important indicators, the differentiation between the classes is small (like for the K_4 and K_7 classes), then the characteristics are completed according to other (less important) variables (in the case of the K_4 and K_7 classes, the difference is noticeable for the variables: $P06$, *Enterprise job seniority*, and $P02$, *Casualty age*).

Table 3 Occupational accident casualty profiles

| Class K_1 – Major limb injuries during manufacturing process or its service | |
|---|---|
| P21 | Any activity related to a production process or service of this process (transport) performed during the occurrence of an accident is almost equally possible: $P(P21 = 1 \text{ or } P21 = 2 \text{ or } P21 = 3 K_1) = 0.30 + 0.31 + 0.33 = 0.94$. |
| P08 | Bone fractures is the most common type of injury: $P(P08 = 2 K_1) = 0.69$. |
| P09 | Injuries affect limbs; more often the upper ones, less often the lower ones: $P(P09 = 3 \text{ or } P09 = 4 K_1) = 0.58 + 0.35 = 0.93$. |
| P26 | Most injuries are caused by materials, objects, products, or machine parts: $P(P26 = 5 K_1) = 0.60$. |
| P289 | Accidents result in long or very long absence from work but also in serious or fatal injuries $P(P289 = 2 \text{ or } P289 = 3 K_1) = 0.62 + 0.28 = 0.90$. |
| P06 | Mostly employees with the lowest job seniority are involved in accidents – up to 5 years: $P(P06 = 1 K_1) = 0.63$. |
| Class K_2 – Major upper limb injuries when operating machinery | |
| P21 | An activity performed by an employee is related to operating machinery: $P(P21 = 1 K_2) = 0.86$. |
| P08 | Body injuries on the one hand include wounds and superficial injuries ($P(P08 = 1 K_2) = 0.39$), on the other hand – traumatic amputations (loss of body parts) ($P(P08 = 4 K_2) = 0.37$). |
| P09 | Upper limbs are injured: $P(P09 = 3 K_2) = 0.96$. |
| P26 | Machines and devices are the source of injuries: $P(P26 = 2 K_2) = 0.82$. |
| P289 | An accident leads to a serious injury or death of a casualty: $P(P289 = 2 \text{ or } P289 = 3 K_2) = 0.51 + 0.40 = 0.91$. |
| P06 | In nearly three quarters of the cases, employees with the lowest job seniority are involved in accidents – up to 5 years: $P(P06 = 1 K_2) = 0.74$. |
| Class K_3 – Slight upper limbs injuries when working with tools or objects | |
| P21 | An activity performed by an employee is related to the use of tools and objects: $P(P21 = 2 K_3) = 0.99$. |
| P08 | Suffered harms refer to wounds and superficial injuries: $P(P08 = 1 K_3) = 0.86$. |
| P09 | Injuries affect mainly upper limbs: $P(P09 = 3 K_3) = 0.80$. |
| P26 | In most cases, injuries are caused by hand tools, less often – by materials, objects, products, or machine parts, possibly involving the work of hands: $P(P26 = 3 \text{ or } P26 = 5 K_3) = 0.56 + 0.37 = 0.93$. |
| P289 | Accidents are minor, resulting in inability to work for no more than a month: $P(P289 = 1 K_3) = 0.77$. There are almost no serious incidents. |
| P06 | Mostly employees with the lowest job seniority are involved in accidents – up to 5 years: $P(P06 = 1 K_3) = 0.67$. |
| Class K_4 – Minor upper limbs injuries to people professionally inexperienced during production process | |
| P21 | An activity performed by an employee is directly related to a production process; operating machinery or working with tools or objects: $P(P21 = 1 \text{ or } P21 = 2 K_4) = 0.62 + 0.20 = 0.82$. |
| P08 | Suffered harms refer to wounds and superficial injuries: $P(P08 = 1 K_4) = 0.80$. |
| P09 | Injuries affect mainly upper limbs: $P(P09 = 3 K_4) = 0.81$. |
| P26 | In most cases, the injuries are caused by machines and devices, less often – by materials, objects, products, or machine parts, possibly involving the work of hands: $P(P26 = 4 \text{ or } P26 = 5 K_4) = 0.53 + 0.38 = 0.91$. |
| P289 | Accidents are minor, resulting in inability to work for no more than three months: $P(P289 = 1 \text{ or } P289 = 2 K_4) = 0.67 + 0.32 = 0.99$. There are no serious incidents. |
| P06 | Almost all casualties of accidents are employees with the lowest job seniority – up to 5 years: $P(P06 = 1 K_4) = 0.97$. |
| P02 | These are very young (up to 24 years old) and young (from 24 to 34 years old) people: $P(P02 = 1 \text{ or } P02 = 2 K_4) = 0.44 + 0.45 = 0.89$. |

Table 3 Occupational accident casualty profiles (continuation)

| Class K_5 – Lower limb injuries of varying severity not directly related to production process | |
|--|---|
| P21 | An activity performed by a casualty during an accident is not directly related to a production process; most often this is being at the accident scene: $P(P21 = 4 K_5) = 0.62$. |
| P08 | Displacements, dislocations, sprains and strains are the main injuries: $P(P08 = 3 K_5) = 0.62$. |
| P09 | Injuries affect mainly lower limbs: $P(P09 = 4 K_5) = 0.80$. |
| P26 | In nearly half of the cases, the factors behind the injuries relate to buildings, structures or surfaces: $P(P26 = 1 K_5) = 0.48$. |
| P289 | Accidents vary in severity (minor and serious), most often resulting in inability to work from 1 to 3 months: $P(P289 = 2 K_5) = 0.44$. |
| P06 | Slightly more than half of the casualties are employees with the lowest job seniority: $P(P06 = 1 K_5) = 0.55$, albeit there is one quarter of people with the highest work experience – more than 10 years: $P(P06 = 3 K_5) = 0.26$. |
| P05 | Compared to others, in class K_5 , operators or assemblers of machines or devices constitute a significant share of the injured: $P(P05 = 2 K_5) = 0.48$ (nearly half of the observations). |
| P27 | Work safety neglect is the main cause of an accident: $P(P27 = 4 K_5) = 0.73$. |
| Class K_6 – Minor injuries of various causes | |
| P21 | An activity performed by an employee during the occurrence of the event related to a production process or a service of this process (transportation) is roughly equally possible: $P(P21 = 1 \text{ or } P21 = 2 \text{ or } P21 = 3 K_6) = 0.28 + 0.25 + 0.30 = 0.83$. |
| P08 | Most frequent harms refer to wounds and superficial injuries: $P(P08 = 1 K_6) = 0.56$, secondly – various injuries (heterogeneous category – see Table 1): $P(P08 = 5 K_6) = 0.35$. |
| P09 | Any part of the body can be injured. |
| P26 | In slightly more than half of the cases, injuries are caused by materials, objects, products, or machine parts: $P(P26 = 5 K_6) = 0.52$. |
| P289 | Accidents are minor, resulting in inability to work for no more than a month: $P(P289 = 1 K_6) = 0.68$. |
| P06 | Mostly employees with the lowest job seniority are involved in accidents – up to 5 years: $P(P06 = 1 K_6) = 0.63$. |
| Class K_7 – Minor upper limbs injuries to people professionally experienced when operating machinery | |
| P21 | An activity performed by an employee is usually related to operating machinery: $P(P21 = 1 K_7) = 0.72$. |
| P08 | Suffered harms refer to wounds and superficial injuries: $P(P08 = 1 K_7) = 0.87$. |
| P09 | Injuries affect mainly upper limbs: $P(P09 = 3 K_7) = 0.86$. |
| P26 | In most cases, injuries are caused by machines and devices, less often – by materials, objects, products, or machine parts, possibly involving the work of hands: $P(P26 = 4 \text{ or } P26 = 5 K_7) = 0.58 + 0.33 = 0.91$. |
| P289 | Accidents are minor, resulting in inability to work for no more than three months: $P(P289 = 1 \text{ or } P289 = 2 K_7) = 0.55 + 0.38 = 0.93$. |
| P06 | Job seniority in an enterprise is very diverse, the majority of which is over 5 years: $P(P06 = 2 \text{ or } P06 = 3 K_7) = 0.28 + 0.34 = 0.62$. In the K_7 latent class, employees with the lowest job seniority occur sporadically. |
| P02 | Very young casualties are absent, and the young ones are rare: $P(P02 = 1 \text{ or } P02 = 2 K_7) = 0.00 + 0.16 = 0.16$. |

The most serious accidents relate to operating machinery (class K_2). The weak link in this case may be the failure of machinery or equipment as well as the safety neglect by the employee. This means that the workstation at the machine, both due to the possible technical defects of the equipment and possibly the incorrect way the employee performs their work, may be under insufficient supervision. Therefore, special attention should be paid to provide adequate training regarding the workstation and the machine operated by the employee. Considering serious accidents (class K_1), the work organisation should be under special concern. In particular, it is important to carve appropriate transport routes, to provide a proper storage system, and to adapt a suitable efficient in-house transport equipment. In the case of these two most severe profiles of work accident casualties, it would be reasonable to introduce additional covers or other technical solutions as well as to use more effective ergonomic personal protective equipment to improve the protection of limbs.

As mentioned in the introduction section, there is a small number of publications concerning the analysis of occupational accidents in wood industry, particularly with the use of data mining methods. The four publications cited earlier concern Italy. Palamara *et al.* [13] and Comberti *et al.* [14] considered *the industry of manufacturing of furniture and building elements* that is a different production area from the one studied in this article. In both works, the same data set was used. Contrary to the research presented in this study, the Italian data did not contain information about fatal casualties. Clusters were identified considering sequences of events causing

accidents defined by the *Activity*, *Deviation* and *Contact* variables. In the first work, “*The purpose is to discover the most common sequences of events leading to accidents for devising preventive actions*”. Fourteen clusters containing sequences were identified. However, the authors did not discuss any profiles. They only stated that the most critical sequences are the loss of control and the incorrect movements during the work with manual tools. They considered working with machinery to be a less critical situation – this is different from the characteristics described in Table 3. The main purpose of [13] seems not to identify patterns but to analyze the effectiveness of the proposed clustering method. Comberti *et al.* [14] presented the same approach; they identified several clusters, but the discussion was concentrated on a coupled clustering methodology (SKM – SOM and *k*-means method). The purpose of the article by Comberti *et al.* [15] was the validation of the SKM method. Data from the wood processing industry and related to a selected region of Italy were used. They were described by six variables: *Activity*, *Deviation*, *Material of deviation*, *Contact*, *Injured body part*, *Age of worker involved*. The research resulted in obtaining 21 clusters of different dynamics (*Activity-Deviation-Contact*). However, the clusters were not discussed further on (that was beyond the scope of the study). The *Risk index* was defined for the evaluation of the clusters. Only two most critical clusters, according to the risk assessment, related to “manual work with hand-tools” and to “to falls during manual transport or movements”, were indicated. In [16], Comberti *et al.* focused on improving the previously used methods. The description of obtained clusters was not given as the research had a methodological aspect (see the introduction section).

7. Final remarks and conclusions

Accidents at work constitute a significant social and economic problem, often causing serious bodily injuries or even death of a casualty. The identification of accident patterns may help in the development of effective tools leading to the improvement of work safety. The research was undertaken to identify patterns and describe profiles of people who suffered accidents at work. The analysis relates to accidents that occurred in connection with production processes in enterprises in Poland in 2008-2017 in the economic activity of branch 16 – *Manufacture of wood and cork products, excluding furniture; manufacture of articles of straw and plaiting materials* – of section C called *Industrial processing* (according to Polish Classification of Activities).

The LCA method, which divides the data set into groups called latent classes, was used enabling the definition of patterns of occupational accident casualties. With the exception of one, in all groups, accident casualties are primarily workers professionally inexperienced in a given job position; their percentage in individual patterns varies from 55 % to 97 %. One pattern relates to *very serious* cases (class K_2), including disability or death. It relates to upper limb injuries and concerns workers operating machinery. The second pattern describes *serious* accidents (class K_1) with long-term consequences. Accidents can arise at various stages of a production process or its service, be generated by various objects (things) of these processes and various activities of employees, and result in limb injuries. The *moderate* accident pattern (class K_5) includes workers not performing a production activity, who due to neglect of work safety (inattention, carelessness), suffered lower limb injuries. The pattern of *minor* accidents (class K_4) characterizes young people with the lowest job seniority, who operate machinery, devices or tools, and suffer from upper limb injuries. There is also a pattern of *minor* accidents (class K_6) difficult to characterize due to its heterogeneity; it includes various activities performed by an injured person, various injuries (not fractures, dislocations and amputations), and injury of any casualty body part. The *slight* accident pattern (class K_3) applies to people using hand tools. Upper limb injuries predominate, leading to a short absence from work. In one pattern (class K_7), professionally inexperienced employees are the least frequent and the youngest ones are absent. Here, wounds and superficial injuries are machine-driven, *minor*, and relate to upper limbs.

During the research, some tools supporting analytical work were proposed. A method was presented to facilitate the decision-making process as regards the number of classes of the LCA model so that the model quality and class distinguishability could be taken into account. A meth-

od of assessing the importance of the observed variables in the pattern description was also developed.

It is planned to expand the research scope in various aspects of identifying patterns of occupational accident casualties, considering an enterprise geographical location (a country region) and an industrial plant size. Developing the method of a systematic selection of indicators for the characterization of latent classes is also intended to include it to the whole analysis process.

References

- [1] Leber, M., Bastič, M., Moody, L., Schmidt Krajnc, M. (2018). A study of the impact of ergonomically designed workplaces on employee productivity, *Advances in Production Engineering & Management*, Vol. 13, No. 1, 107-117, doi: [10.14743/apem2018.1.277](https://doi.org/10.14743/apem2018.1.277).
- [2] Vulanović, S., Deliđ, M., Kamberović, B., Beker, I., Lalić, B. (2020). Integrated management systems based on risk assessment: Methodology development and case studies, *Advances in Production Engineering & Management*, Vol. 15, No. 1, 93-106, doi: [10.14743/apem2020.1.352](https://doi.org/10.14743/apem2020.1.352).
- [3] Müngen, U., Gürcanli, G.E. (2005). Fatal traffic accidents in the Turkish construction industry, *Safety Science*, Vol. 43, No. 5-6, 299-322, doi: [10.1016/j.ssci.2005.06.002](https://doi.org/10.1016/j.ssci.2005.06.002).
- [4] Rivas, T., Paz, M., Martín, J.E., Matías, J.M., García, J.F., Taboada, J. (2011). Explaining and predicting workplace accidents using data-mining techniques, *Reliability Engineering & System Safety*, Vol. 96, No. 7, 739-747, doi: [10.1016/j.res.2011.03.006](https://doi.org/10.1016/j.res.2011.03.006).
- [5] Cheng, C.-W., Leu, S.-S., Lin, C.-C., Fan, C. (2010). Characteristic analysis of occupational accidents at small construction enterprises, *Safety Science*, Vol. 48, No. 6, 698-707, doi: [10.1016/j.ssci.2010.02.001](https://doi.org/10.1016/j.ssci.2010.02.001).
- [6] Alizadeh, S.S., Mortazavi, S.B., Sepehri, M.M. (2015). Assessment of accident severity in the construction industry using the Bayesian theorem, *International Journal of Occupational Safety and Ergonomics*, Vol. 21, No. 4, 551-557, doi: [10.1080/10803548.2015.1095546](https://doi.org/10.1080/10803548.2015.1095546).
- [7] Szóstak, M. (2018). The application of cluster analysis to identify the occupational profile of people injured in accidents in the Polish construction industry, In: *Proceedings of VII International Symposium Actual Problems of Computational Simulation in Civil Engineering*, Vol. 456, Novosibirsk, Russian Federation, Article No. 012027, doi: [10.1088/1757-899X/456/1/012027](https://doi.org/10.1088/1757-899X/456/1/012027).
- [8] Drozd, W. (2017). Identifying and profiling the patterns of construction accidents using affinity analysis, *Technical Transactions / Czasopismo Techniczne*, Vol. 5, 15-24, doi: [10.4467/2353737XCT.17.065.6422](https://doi.org/10.4467/2353737XCT.17.065.6422).
- [9] Berglund, L., Johansson, M., Nygren, M., Samuelson, B., Stenberg, M., Johansson, J. (2021). Occupational accidents in Swedish construction trades, *International Journal of Occupational Safety and Ergonomics*, Vol. 27, No. 2, 552-561, doi: [10.1080/10803548.2019.1598123](https://doi.org/10.1080/10803548.2019.1598123).
- [10] Ayhan, B.U., Tokdemir, O.B. (2020). Accident analysis for construction safety using latent class clustering and artificial neural networks, *Journal of Construction Engineering and Management*, Vol. 146, No. 3, Article No. 04019114, doi: [10.1061/\(ASCE\)CO.1943-7862.0001762](https://doi.org/10.1061/(ASCE)CO.1943-7862.0001762).
- [11] Lee, J.Y., Yoon, Y.G., Oh, T.K., Park, S., Ryu, S.I. (2020). A study on data pre-processing and accident prediction modelling for occupational accident analysis in the construction industry, *Applied Sciences*, Vol. 10, No. 21, Article No. 7949, doi: [10.3390/app10217949](https://doi.org/10.3390/app10217949).
- [12] Zhang, F., Fleyeh, H., Wang, X., Lu, M. (2019). Construction site accident analysis using text mining and natural language processing techniques, *Automation in Construction*, Vol. 99, 238-248, doi: [10.1016/j.autcon.2018.12.016](https://doi.org/10.1016/j.autcon.2018.12.016).
- [13] Palamara, F., Piglione, F., Piccinini, N. (2011). Self-organizing map and clustering algorithms for the analysis of occupational accident databases, *Safety Science*, Vol. 49, No. 8-9, 1215-1230, doi: [10.1016/j.ssci.2011.04.003](https://doi.org/10.1016/j.ssci.2011.04.003).
- [14] Comberti, L., Baldissone, G., Demichela, M. (2015). Workplace accidents analysis with a coupled clustering methods: S.O.M. and K-means algorithms, *Chemical Engineering Transactions*, Vol. 43, 1261-1266, doi: [10.3303/CET1543211](https://doi.org/10.3303/CET1543211).
- [15] Comberti, L., Demichela, M., Baldissone, G., Fois, G., Luzzi, R. (2018). Large occupational accidents data analysis with a coupled unsupervised algorithm: The S.O.M. K-means method. An application to the wood industry, *Safety*, Vol. 4, No. 4, Article No. 51, doi: [10.3390/safety4040051](https://doi.org/10.3390/safety4040051).
- [16] Comberti, L., Demichela, M., Baldissone, G. (2018). A combined approach for the analysis of large occupational accident databases to support accident-prevention decision making, *Safety Science*, Vol. 106, 191-202, doi: [10.1016/j.ssci.2018.03.014](https://doi.org/10.1016/j.ssci.2018.03.014).
- [17] Moura, R., Beer, M., Patelli, E., Lewis, J., Knoll, F. (2017). Learning from accidents: Interactions between human factors, technology and organisations as a central element to validate risk studies, *Safety Science*, Vol. 99, Part B, 196-214, doi: [10.1016/j.ssci.2017.05.001](https://doi.org/10.1016/j.ssci.2017.05.001).
- [18] Moura, R., Beer, M., Patelli, E., Lewis, J. (2017). Learning from major accidents: Graphical representation and analysis of multi-attribute events to enhance risk communication, *Safety Science*, Vol. 99, Part A, 58-70, doi: [10.1016/j.ssci.2017.03.005](https://doi.org/10.1016/j.ssci.2017.03.005).
- [19] Verma, A., Khan, S.D., Maiti, J., Krishna, O.B. (2014). Identifying patterns of safety related incidents in a steel plant using association rule mining of incident investigation reports, *Safety Science*, Vol. 70, 89-98, doi: [10.1016/j.ssci.2014.05.007](https://doi.org/10.1016/j.ssci.2014.05.007).

- [20] Ghousi, R. (2015). Applying a decision support system for accident analysis by using data mining approach: A case study on one of the Iranian manufactures, *Journal of Industrial and Systems Engineering*, Vol. 8, No. 3, 59-76.
- [21] Sanmiquel, L., Bascompta, M., Rossell, J.M., Anticoi, H.F., Guash, E. (2018). Analysis of occupational accidents in underground and surface mining in Spain using data-mining techniques, *International Journal of Environmental Research and Public Health*, Vol. 15, No. 3, Article No. 462, doi: [10.3390/ijerph15030462](https://doi.org/10.3390/ijerph15030462).
- [22] Farina, E., Bianco, S., Bena, A., Pasqualini, O. (2019). Finding causation in occupational fatalities: A latent class analysis, *American Journal of Industrial Medicine*, Vol. 62, No. 2, 123-130, doi: [10.1002/ajim.22936](https://doi.org/10.1002/ajim.22936).
- [23] Davoudi Kakhki, F., Freeman, S.A., Mosher, G.A. (2019). Segmentation of severe occupational incidents in agribusiness industries using latent class clustering, *Applied Sciences*, Vol. 9, No. 18, Article No. 3641, doi: [10.3390/app9183641](https://doi.org/10.3390/app9183641).
- [24] Nowakowska, M., Pajęcki, M. (2020). Applying latent class analysis in the identification of occupational accident patterns, *Scientific Papers of Silesian University of Technology – Organization & Management*, No. 146, 339-355, doi: [10.29119/1641-3466.2020.146.25](https://doi.org/10.29119/1641-3466.2020.146.25).
- [25] Collins, L.M., Lanza, S.T. (2010). *Latent class and latent transaction analysis: With applications in the social, behavioral, and health sciences*, John Wiley & Sons, New Jersey, USA, doi: [10.1002/9780470567333](https://doi.org/10.1002/9780470567333).
- [26] Kim, S-Y. (2014). Determining the number of latent classes in single- and multiphase growth mixture models, *Structural Equation Modeling: A Multidisciplinary Journal*, Vol. 21, No. 2, 263-279, doi: [10.1080/10705511.2014.882690](https://doi.org/10.1080/10705511.2014.882690).
- [27] Lin, T.H., Dayton, C.M. (1997). Model selection information criteria for non-nested latent class models, *Journal of Educational and Behavioral Statistics*, Vol. 22, No. 3, 249-264, doi: [10.3102/10769986022003249](https://doi.org/10.3102/10769986022003249).
- [28] Nylund, K.L., Asparouhov, T., Muthén, B.O. (2007). Deciding on the number of classes in latent class analysis and growth mixture modeling: A Monte Carlo simulation study, *Structural Equation Modeling: A Multidisciplinary Journal*, Vol. 14, No. 4, 535-569, doi: [10.1080/10705510701575396](https://doi.org/10.1080/10705510701575396).
- [29] Lanza, S.T., Dziak, J.J., Huang, L., Wagner, A.T., Collins, L.M. (2015). Proc LCA & Proc LTA Users' Guide (Version 1.3.2), University Park: The Methodology Center, Penn State, from <https://www.methodology.psu.edu/>, accessed April 10, 2021.
- [30] Ordinance of the Minister of Labour and Social Policy of 7 January 2009 on a statistical accident card at work, *Journal of Laws of 2009*, No. 14, item 80, as amended, from <http://isap.sejm.gov.pl/isap.nsf/download.xsp/WDU20090140080/O/D20090080.pdf>, accessed June 24, 2021.
- [31] Regulation of the Minister of Family, Labour and Social Policy of 4 June 2019 amending the regulation on a statistical accident card at work, *Journal of Laws of 2019*, item 1106, as amended, from <http://isap.sejm.gov.pl/isap.nsf/download.xsp/WDU20190001106/O/D20191106.pdf>, accessed June 24, 2021.
- [32] Pajęcki, M. (2020) Bezpieczeństwo pracy w sekcji przetwórstwa przemysłowego w Polsce – stan wypadkowości, In: Knosala, R. (ed.), *Inżynieria zarządzania. Cyfryzacja produkcji. Aktualności badawcze 3*, PWE, Poland, 1223-1232.
- [33] Chakrabarti, C.G., Chakrabarty, I. (2005). Shannon entropy: Axiomatic characterization and application, *International Journal of Mathematics and Mathematical Sciences*, Vol. 2005, Article ID 234590, doi: [10.1155/IJMMS.2005.2847](https://doi.org/10.1155/IJMMS.2005.2847).

Impact of Industry 4.0 on decision-making in an operational context

Rosin, F.^{a,*}, Forget, P.^b, Lamouri, S.^c, Pellerin, R.^d

^aLAMIH UMR CNRS 8201, Arts et Métiers, Aix-en-Provence, France

^bDepartment of Industrial Engineering, Université du Québec à Trois-Rivières, Trois-Rivières, Canada

^cLAMIH UMR CNRS 8201, Arts et Métiers, Paris, France

^dDepartment of Mathematics and Industrial Engineering, Polytechnique Montréal, Montréal, Canada

ABSTRACT

The implementation of Industry 4.0 technologies suggests significant impacts on production systems productivity and decision-making process improvements. However, many manufacturers have difficulty determining to what extent these various technologies can reinforce the autonomy of teams and operational systems. This article addresses this issue by proposing a model describing different types of autonomy and the contribution of 4.0 technologies in the various steps of the decision-making processes. The model was confronted with a set of application cases from the literature. It emerges that new technologies' improvements are significant from a decision-making point of view and may eventually favor implementing new modes of autonomy. Decision-makers can rely on the proposed model to better understand the opportunities linked to the fusion of cybernetic, physical, and social spaces made possible by Industry 4.0.

ARTICLE INFO

Keywords:

Industry 4.0;
Decision-making;
Decision types;
Autonomous production system;
Cyber-physical production systems (CPPS);
Human;
Human cyber-physical system (HCPS);
Lean;
Problem solving

*Corresponding author:

frederic.rosin@ensam.eu
(Rosin, F.)

Article history:

Received 26 February 2021

Revised 7 December 2021

Accepted 8 December 2021



Content from this work may be used under the terms of the Creative Commons Attribution 4.0 International Licence (CC BY 4.0). Any further distribution of this work must maintain attribution to the author(s) and the title of the work, journal citation and DOI.

1. Introduction

Many researchers have described the potential benefits of Industry 4.0 technologies to improve production systems' productivity and profitability [1-3]. In this sense, there is a close link between Lean and Industry 4.0 as many companies have already partially or fully implemented principles and tools from the Lean management approach [4]. However, previous studies have shown that the principles associated with problem-solving and employees and teamwork currently seem to be little or not improved by Industry 4.0 technologies [5]. However, implementing these high-level principles of Lean and Toyota Production System, as described in the 4 P model proposed by J. Liker [6], is based on a singular decision-making process. Indeed, problem-solving as an element

of continuous improvement and learning, is based on decisions taken on the ground (Gemba decisions) in a consensual manner by carefully examining all the options (Nemawashi) before a rapid implementation of the actions resulting from the decisions taken [6]. In the context of the search for complementarities between Lean and Industry 4.0, the impact and role of Industry 4.0 technologies on the decision-making process is of particular interest.

Sari *et al.* [7] point out that the implementation level of Industry 4.0 technologies increases as the manufacturing firms' size increases. While ERP system, Supply Chain Management (SCM) and near real-time production control system can play a vital role for manufacturers in the context of Industry 4.0 especially in transition countries, future research needs to consider the full range of technologies that are considered facilitators of Industry 4.0 [8]. These technologies are numerous. Many authors present different lists of 4.0 technologies [2, 9-13]. They all agree on their capability to enhance communication, flexibility, real-time feedback, and improve how humans make decisions to solve problems in a production context.

Indeed, improving decision-making processes is a recurring focus and a primary objective in deploying these technologies [14-17]. Several research studies focus on production data-based decision-making for process design, scheduling, planning, and control [17]. Different types of autonomy of the production system are possible and are determined by which steps of the decision-making process are (or are not) enhanced. The difficulty of detecting abnormal situations or opportunities for improvements of the current system depends on the complexity of the information being integrated, the number of possible solutions, and the managers' interest in empowering the production systems.

As such, no previous research clearly illustrates how 4.0 technologies can enhance a decision-making process and how it may affect the autonomy of the resources involved. This article addresses this issue by analyzing the impact of Industry 4.0 technologies on decision-making in production systems at the work center level and by proposing a decision-making process model describing different types of autonomy.

The remainder of the paper is structured as follows. The following section presents a literature review on the decision-making process in an operational context. In Section 3, the proposed decision-making process applied to the operational context is described and the different types of autonomy levels. The proposed model is then validated in Section 4, based on a comparison with a set of case studies from the literature. Section 5 presents future works and a conclusion.

2. Literature review

Highlighting the difficulty for manufacturing firms to establish a deployment strategy for industry 4.0 technologies, Osterrieder *et al.* [17] proposed an intelligent factory model around 8 eight distinct thematic perspectives. The authors note that problems related to decision-making are common to several of these categories but stress the need to make it a research focus in its own right to analyze and develop concepts for data-based decision-making situations in manufacturing, using the different technologies of Industry 4.0.

On the other hand, the human decision-making process has been studied in many fields, including psychology and management. It has been analyzed and described by numerous research studies in various operational [18], strategic [19], or crisis contexts [20]. Intuitive and analytical strategies were also investigated in laboratory experiments or field observations to study judgments and decision-making under complex conditions [21-23].

Simon [24] was one of the first to propose a formal decision-making model called IDC. According to this model, a decision goes through three phases: Investigation, Design, and Selection. The Investigation phase consists of formulating the problem and identifying a gap between the current situation and the desired situation. In the Design phase, the subject develops possible actions to resolve the situation and tries to predict these different actions' impact on their environment. In the Selection phase, the different actions are compared, ranked, and selected.

Mintzberg [19] took up ideas from Simon's model but sought to list all the approaches to human decision-making in a specific context, namely strategic corporate decisions. By analyzing 25 decisions from different companies, he proposed a decision-making model that includes all the

possibilities that were enumerated. The proposed phases by Mintzberg [19] are similar to Simon [24], but he describes them in terms of seven central “routines”: Recognition, Diagnosis, Search, Screen, Design, Evaluation-Choice, Authorisation. Also, he notes three sets of routines that support the central phases, decision control, communication, and political. Mintzberg [19] attempted to present the processes used in human decision-making and not an ideal decision-making process. His model also predicts possible interruptions in the process and the jumps in routines that companies have made.

This interest in describing the actual decision-making process has been followed by a trend towards Naturalistic Decision Making (NDM) [25]. Following this trend, authors have focused on the biases and limitations of human decision-making, particularly in situations of time constraints [26] or crisis [25, 27]. The body of knowledge associated with the NDM that emerged in the 1980s changed the approach to decision-making. There was a shift from “normative” models that describe how rational decisions should be made to models that describe the decisions that are actually made [28]. Some work has highlighted the particularities of decision-making in naturalistic contexts [29] and the unrealistic nature of some of the assumptions underlying rational choice theory [25]. In an operational context, agents are subject to constraints that do not allow them to analyze a large amount of information and consider all of the available choices or make complex calculations to evaluate different options and their potential impacts. Other researchers have described models of decision-making that do not necessarily lead to an optimal decision, but where the decision-making process activities are carried out by humans or through automation [30, 31]. However, this work does not connect or acknowledge various technologies that can be employed. In contrast, other authors have proposed perfect decision-making models, particularly in the literature related to the development of artificial intelligence and intelligent agents, including BDI (Beliefs-Desire-Intention) models [32, 33]. This type of model, inspired by human decision-making models, is then used to design artificial decision-making systems. However, these models rely on targeted technologies, including simulation techniques, massive data analysis, and artificial intelligence. However, none of these models link to the full range of technologies associated with Industry 4.0 by analyzing the opportunities offered by the joint contribution of various technologies.

The DMN (Decision Model and Notation) standard was recently developed by the Object Management Group (OMG) [34] to model decisions in an understandable way and has been adopted by both industry and academia. This standard aims to form a bridge between business process models and decision logic models by introducing a Decision Requirements Diagram that defines the decisions to be made in business processes, their interrelationships, and their requirements for decision logic. It can be used for modeling human decision-making, the requirements for automated decision-making, or for implementing automated decision-making. Group decision-making is always better than individual decisions [35], and DMN models can describe collaborative organizational decisions, their governance, and the business knowledge required for them. This standard is rather dedicated to operational decisions taken as part of daily operational processes, rather than strategic decision-making for which there are fewer rules and representations. This standard defines the word “decision” as the act of choosing among multiple possible options or the option that is chosen. Hasic *et al.* [36] point out that DMN was only studied and implemented in a static fashion despite the dynamic nature of modern knowledge-intensive systems. Decision schema change patterns have not received any attention so far. Therefore, this type of model still seems unsuitable for operational decisions taken in a changing and uncertain environment for which the decision rules, input data, and business knowledge are not pre-established at least in advance. Besides, some articles attempt to link with Decision Support System (DSS) research or show how certain technologies can facilitate the implementation of this standard. Still, none of them encompass the possibilities offered by the full range of technologies in industry 4.0.

The literature associated with Industry 4.0 proposes real-time decision-making in a decentralized but coordinated manner at a global level, with people and machines working together. These developments promote the flexibility and agility of systems at the operational level by increasing their responsiveness and autonomy [10]. However, the research work currently being carried out in this model does not go into the decision-making process’s details. It has been largely described

by analyzing human decision-making. Still, the questioning of these models and their limits by the introduction of all Industry 4.0 technologies has not yet been studied. Therefore, it seems that no current model studies the reinforcement using 4.0 technologies in the different decision-making process stages, which, in an operational context, can be carried out by an individual or a group to define standard or tailor-made solutions in an increasingly changing and uncertain production environment. This paper, therefore, aims to propose different types of operational decision-making processes based on the use of various technologies.

3. Decision-making model in Industry 4.0 operational context

3.1 Decision-making process

Based on Mintzberg's [19] model described earlier, we propose the following decision-making process in an operational context (Fig. 1).

Like Mintzberg's [19] model, this process consists of 3 phases: Problem or opportunity validation, Solution validation, and Implementation validation. The Problem or Opportunity Validation phase includes the Capture-Measure and Gap recognition steps. The Capture-Measure step consists of collecting information in real-time in the production system. The second step, Gap recognition, consists of recognizing an abnormal situation, i.e., a discrepancy between the current situation and the desired situation that requires a reaction from the production center.

For the Solution validation phase, the Diagnosis, Search, Design, and Selection steps are used. The Diagnosis step corresponds to the Diagnosis step of Mintzberg's [19] model, i.e., understanding cause and effect relationships in the situation under study. Subsequently, depending on whether or not solutions are known to address the identified problem, a choice will be made between the Search or Design steps. If solutions are known, the Search step is used to look among the possible solutions to find those that offer an adequate response to the problem. If no solution is known, the Design step is preferred where it is necessary to design a new solution to the problem or modify a known solution. Afterward, if the Selection step allows, we look to eliminate inappropriate solutions to limit the number of solutions to be evaluated. Then, the Evaluation step allows us to compare the solutions and ensure that the selected solution will solve the situation. Finally, the third phase includes a single step: Authorize. Here, an authorization is issued either by the production center itself (the operator or the machine) or a higher hierarchical entity (a team leader, a manager, or a centralized computer system).

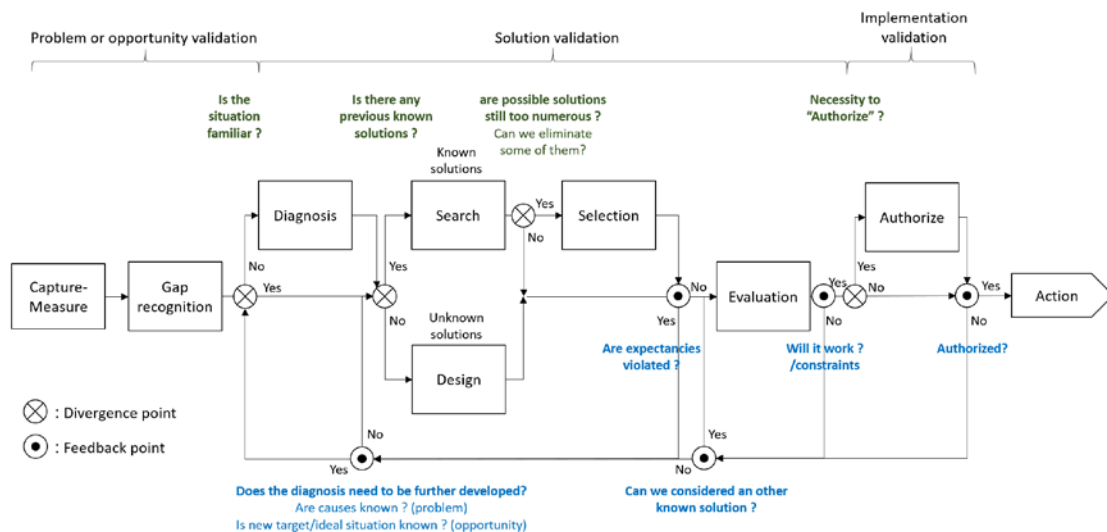


Fig. 1 Proposed decision-making process in an operational context

This decision-making model is non-sequential, and several types of feedback are possible. This is particularly the case when the Selection step leads to eliminating all known solutions identified in the Search step. If the understanding of the situation allows it, the Design step can then be engaged directly to identify a tailor-made solution. Otherwise, the Diagnosis step is undertaken to identify the root causes of the problem, define the target situation precisely, and analyze the conditions for reducing the current situation gap. This same type of feedback can occur if the Evaluation step leads to the rejection of all known or custom-designed solutions or if the Authorize step does not lead to approval for implementing the selected and proposed solution. Shorter feedback can be used to evaluate only solutions that have already been identified but were not evaluated or retained in the first instance.

3.2 Industry 4.0 decision-making support model

Technologies from Industry 4.0 can help operators and/or machines to carry out one or more steps of the decision-making process. Depending on the company's needs and the specific characteristics of the production center, more or fewer steps in the decision-making process may be supported and enhanced by one or more Industry 4.0 technologies.

Porter and Heppelmann [1] propose a model of the various uses of Industry 4.0 technologies but from the perspective of intelligent and connected products rather than a manufacturing production context. More specifically, they propose four levels called capacity levels. These levels are incremental, and each builds on the previous one. These capacity levels are: 1- Monitoring, 2- Control, 3-Optimization, and 4-Autonomy. A few authors have taken these levels, including [2] and [10]. Comparing this highly structured model designed for intelligent products with the decision-making model described above has revealed certain limitations. The Porter and Heppelmann [1] model does not cover some scenarios in complex decision-making processes that generally involve humans. For example, the implementation of the solution Evaluation step differs between standard and custom solutions. The type of enhancement provided by 4.0 technologies is not the same in these two cases. The treatment around the authorization step is also not specified. While this step can be bypassed for decisions made locally on a relatively small perimeter and often of limited complexity, this is not the case when integrating the high levels of autonomy targeted by Industry 4.0. The extended scope of responsibility given to operational teams or systems requires that decisions taken in a decentralized manner remain consistent with optimizing the overall system. New technologies can be mobilized to facilitate and strengthen horizontal, vertical, or end-to-end information exchanges. Depending on the type of decision and the level of autonomy targeted, it is possible to make decision-making more collaborative while maintaining a high level of responsiveness of the operational system.

Inspired by the four capability levels of Porter and Heppelmann's [1] products, seven types of decision-making autonomy are proposed based on Industry 4.0 technologies for manufacturing systems (Fig. 2). For every operational context, a specific type of autonomy should be targeted while considering the more or less stable and predictable nature of the operating environment, the nature and complexity of the decisions to be made, their importance and impact, the skill level and scope of responsibility of the operational teams, the managerial model, and the corporate culture. These seven types of autonomy are therefore not incremental. They are not mutually inclusive and do not present a gradation in terms of intelligence and autonomy. Rather, they respond to different needs for decision-making assistance and enhancement depending on the help needed and whether the solutions are known or not. The seven types of autonomy based on Industry 4.0 technologies in a manufacturing context are as follows: 1) Cyber Monitoring, 2) Cyber Search, 3) Standard Decision Support, 4) Cyber Control, 5) Cyber Design, 6) Customized Decision Support and 7) Cyber Autonomy. These types of autonomy are distinguished according to the possible quantity of solutions sought and according to the specific steps enhanced or supported by the 4.0 technology involved.

| | | | | |
|----------------------|--|--|--|--|
| Customized solutions | 1. Cyber monitoring - Enhanced data capture and measure - Enhanced gap recognition - Enhanced diagnosis (if necessary) | 5. Cyber Design - Enhanced data capture and measure - Enhanced gap recognition - Enhanced diagnosis (if necessary) - Optional reinforcement of search, selection, evaluation or authorize, but only for standard solutions (possible anteriority but design required in the end) - Enhanced solution design because no known solutions | 6. Customized Decision Support - Enhanced data capture and measure - Enhanced gap recognition - Enhanced diagnosis (if necessary) - Optional reinforcement of search, selection, evaluation or authorize only for standard solutions - Enhanced solution design because no known solutions possible - Enhanced evaluation | 7. Cyber Autonomy - Enhanced data capture and measure - Enhanced gap recognition - Enhanced diagnosis (if necessary) - Enhanced solution search & selection (possible anteriority but design required) - Enhanced solution design because no known solutions possible - Enhanced evaluation - Enhanced authorization |
| | 2. Cyber Search - Enhanced data capture and measure - Enhanced gap recognition - Enhanced diagnosis (if necessary) - Enhanced solution search among pre-established known solutions | 3. Standard Decision Support - Enhanced data capture and measure - Enhanced gap recognition - Enhanced diagnosis (if necessary) - Enhanced solution search & selection or design - Enhanced evaluation | 4. Cyber Control - Enhanced data capture and measure - Enhanced gap recognition - Enhanced diagnosis (if necessary) - Enhanced solution search among pre-established known solutions - Enhanced selection (if too many solutions) - Enhanced evaluation - Enhanced authorization | |
| Standard solutions | Enhanced data collection | Enhanced solution search | Enhanced solution search & evaluation | Enhanced solution search & evaluation & authorization |

Fig. 2 Model of types of autonomy: an Industry 4.0 decision-making support model

The following figures highlight each type of autonomy, the steps of the decision-making process that can be enhanced, optionally or not, by the different Industry 4.0 technologies. Some types of autonomy do not mobilize certain steps, which then appear as hatched. The main questions managed at divergence points appear in green and those conditioning the crossing of the feedback points appear in blue.

The Cyber Monitoring type corresponds to the enhancement of the Capture and Measure and Gap recognition steps. Here, we allow for an improvement in the collection of production data and analyzing this data to detect an abnormal situation or an opportunity for improvement. Any technology does not enhance the search for solutions in Industry 4.0, and the other steps of the decision-making process are left to humans. However, in some cases, the Diagnostic step can be enhanced to prepare better the steps dedicated to searching for standard or customized solutions. Fig. 3 shows the application of Cyber Monitoring to the proposed decision-making process.

The Cyber Search type corresponds, like the Cyber Monitoring type, to enhance the Capture-Measure and Gap recognition steps using 4.0 technologies, but adding optional support for the Diagnostic step if the reasons behind the observed deviation are not immediately recognized. Also, if the system knows solutions to resolve the situation, the Search step is enhanced to find the possible solution(s) to be applied. A human user provides the following steps. Fig. 4 shows the application of the Cyber Search type to the proposed decision-making process.

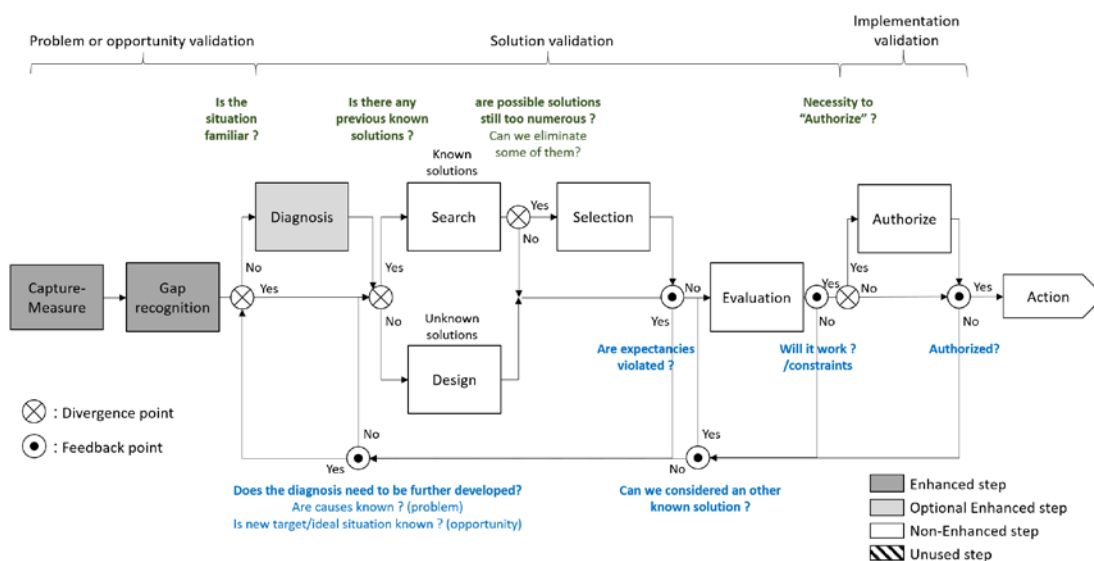


Fig. 3 Enhanced steps in the Cyber Monitoring type

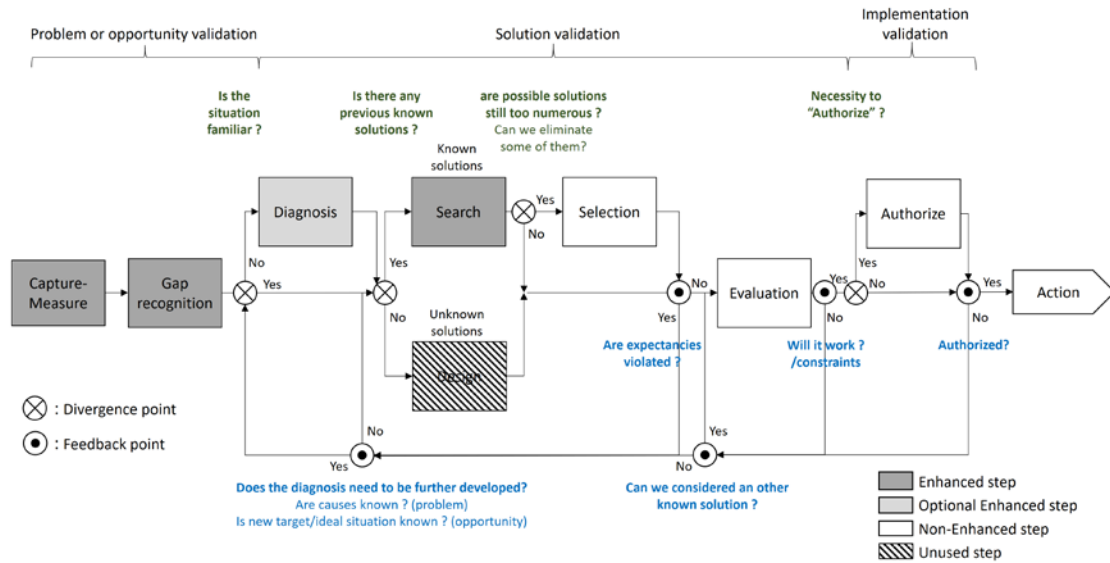


Fig. 4 Enhanced steps in the Cyber Search type

The Standard Decision Support type shown in Fig. 5 is similar to the Cyber Search type and subsequently supports the Selection and Evaluation decision-making steps. Thus, for a situation where solutions are known, a search for solutions (Search step) is carried out. The Selection step follows this if more than one solution is possible. This step aims to limit the number of solutions that will then be evaluated by eliminating what is unfeasible. The Evaluation step is also enhanced to determine the most appropriate solution, notably by anticipating the consequences of implementing the solutions identified in the Search step and filtered by the Selection step.

The Cyber Control type assists in all of the decision-making steps if solutions are known. The final step, authorizing the action, is also enhanced to facilitate the action's commitment when it has to be approved at a level other than the perimeter from which the chosen solution emanates. Fig. 6 shows the application of Cyber Control to the proposed decision-making process.

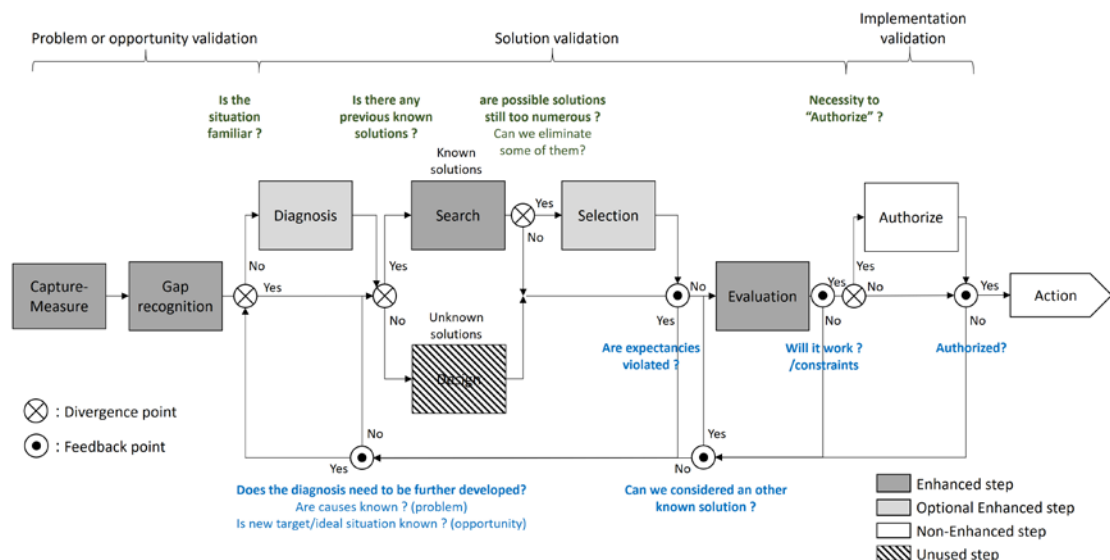


Fig. 5 Enhanced steps in the Standard Decision Support type

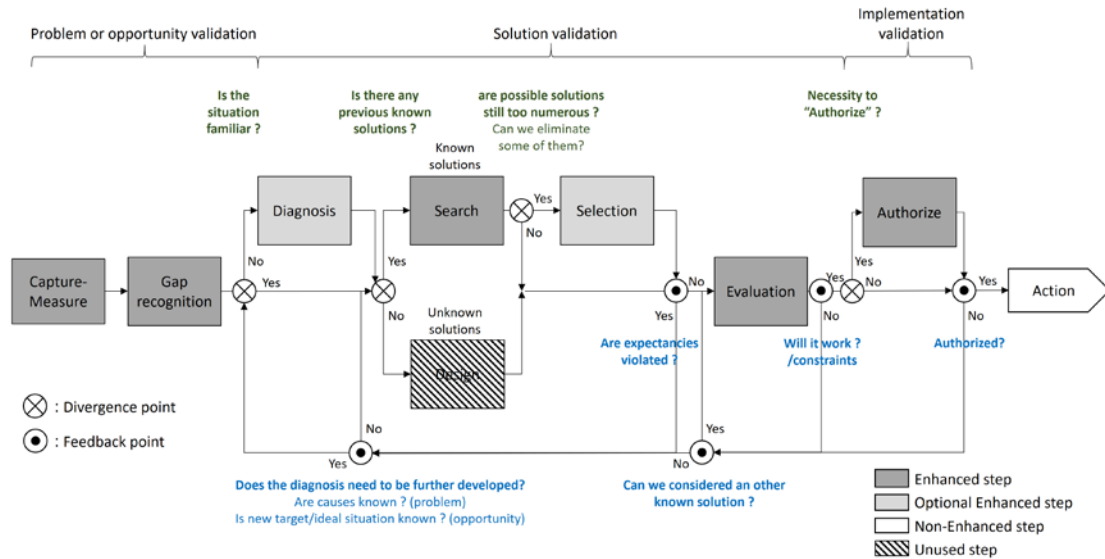


Fig. 6 Enhanced steps in the Cyber Control type

The Cyber Design type is similar to the Cyber Search type, but in a situation where no possible solution is known. Here, it is the Design step that is enhanced to design a tailor-made solution. The search for a standard solution based on the optional enhancement of the Search, Selection, Evaluation, and Authorize steps may sometimes have preceded the design step's mobilization but without success. The preferred technologies 4.0 must build a new solution that would reduce the gap in the production system. The steps that follow the Design step are then left to the human's responsibility without any special assistance. Fig. 7 shows the application of the Cyber Design type to the proposed decision-making process.

The Customized Decision Support type is similar to the Cyber Design type, with the addition of the Evaluation step enhancement. The Search and Selection steps could have been activated beforehand to identify known solutions that proved to be either unsuitable or ineffective. Feedback then leads to a search for a tailor-made solution at the Design step. The evaluation step's enhancement is more complex than in the Standard Decision Support type because this process must evaluate tailor-made solutions that are not known beforehand. The Authorization step remains the only one that is the responsibility of the human without any assistance. Fig. 8 shows the application of the Customized Decision Support type to the proposed decision-making process.

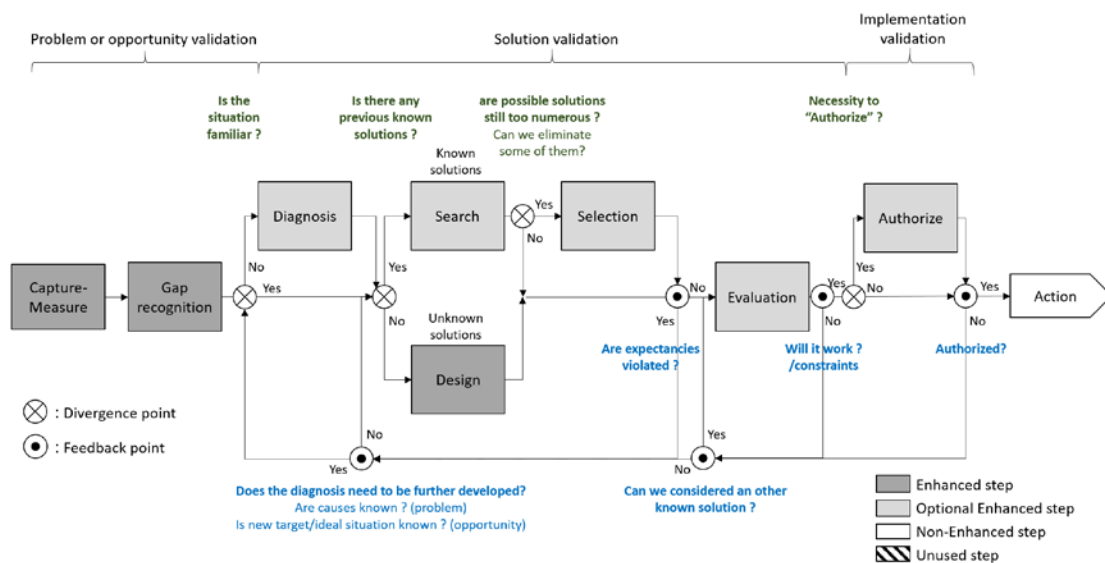


Fig. 7 Enhanced steps in the Cyber Design type

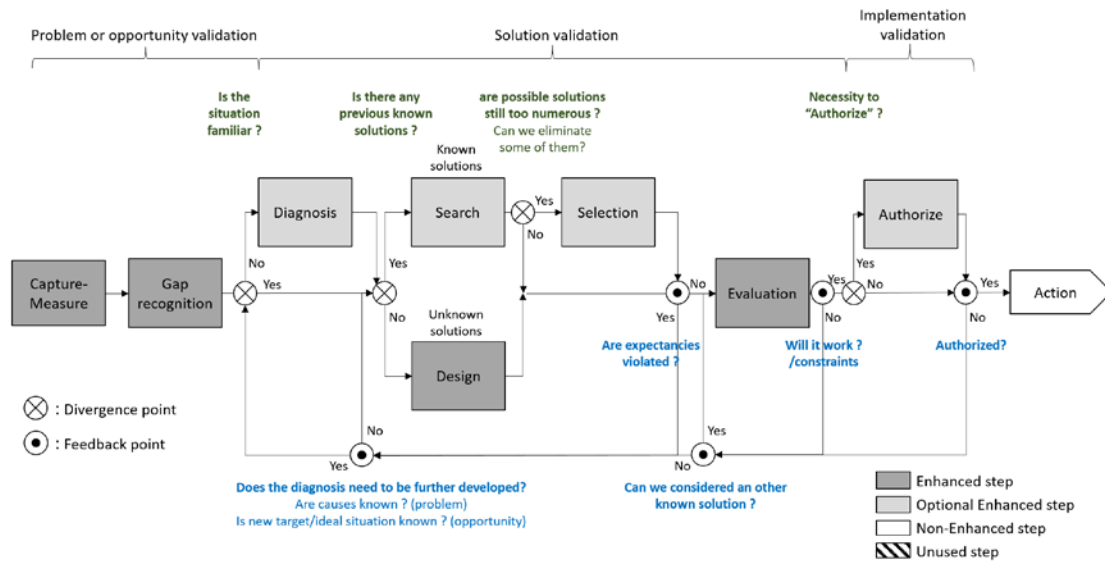


Fig. 8 Enhanced steps in the Customized Decision Support type

Finally, the Cyber Autonomy type is based on the Customized Decision Support type, with the addition of the Authorize step's enhancement. In this case, as with the Cyber Control type, no step is performed by human users without assistance. However, any type of situation corresponding to problems or opportunities associated with known or unknown solutions can be handled autonomously throughout the operational teams' decision-making process. Fig. 9 shows the application of the Cyber Autonomy type to the proposed decision-making process.

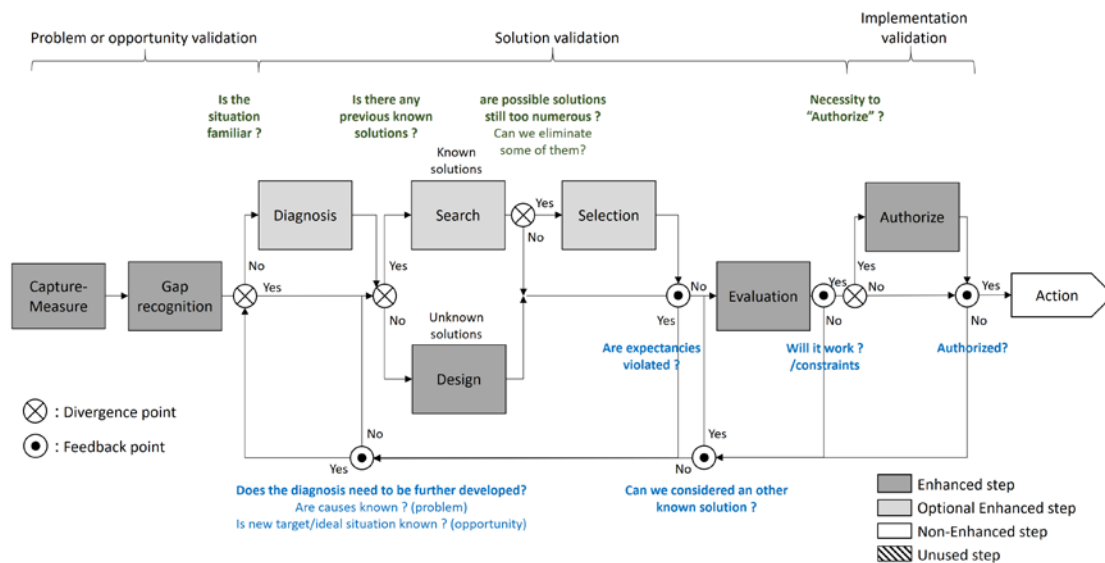


Fig. 9 Enhanced steps in the Cyber Autonomy type

4. Model validation

For validation purposes, the model was compared with case studies found in the literature. These cases were targeted using the keywords "industry 4.0" OR "industry 4.0" AND "use case" OR "case study" in the SCOPUS database. By focusing on articles related to the theme "Decision Sciences", we were able to identify 180 papers, over a third (69) of which were related to engineering and production. An analysis of these articles led to the exclusion of 37 articles for the following reasons:

- the use cases were associated with the technical validation of the implementation of one or more technologies of the industry 4.0 and not how they are used to support or control an operational system,
- the use cases did not make a direct link to identify decision-making in an operational context,
- the use cases did not sufficiently detail the use of industry 4.0 technologies or were not sufficiently described.

The remaining 32 articles identified 41 cases in which the application of technologies from Industry 4.0 could be linked to one of the seven types of autonomy based on the technologies proposed in our model. It should be noted that very few application cases are dated before 2017, and their number has been increasing since then. Their connection to the different types of autonomy has been achieved by an in-depth reading of the articles and a systematic questioning in relation to the conditions of activation of the steps and branches specific to each type of autonomy of the model. Another researcher carried out a double analysis to verify the reproducibility of the proposed linkage. Table 1 presents the result of this analysis, making it possible to confirm that the proposed model can cover all of the described application cases.

It has emerged from this analysis that 2 out of every 3 cases today correspond to Cyber monitoring. Conversely, some types of autonomy still seem very far from being mature. For example, no application case could be linked to the Standard decision support type. This may seem surprising at first glance because operational excellence and continuous improvement approaches, already widely used in operational contexts, encourage capitalizing on the solutions identified during problem resolution to turn them into reaction standards. Although cases of Cyber search applications have been identified to enhance the search for already known standard solutions, the evaluation of these solutions is still mainly carried out by humans.

Several cases correspond to Cyber control but relate to decisions that are still relatively uncomplicated or related to a still limited scope of responsibility. We have found articles that foresee future developments corresponding to the Cyber design type but without any real implementation at the moment. For example, some applications concern the feedback and analysis of information from the field to continually readjust the design of highly customized products or continuously adapt the rules applied by a maintenance department to monitor equipment. This implies a strengthening of interoperability between different information systems, which in many cases is still a major technological barrier. The Customized support decision type always seems to be reserved for applications in process industries. This is probably explained by the need to have already a large database and the high level of complexity and cost associated with implementing this type of autonomy.

We find cases of Cyber autonomy for applications realized in an experimental framework and the realization of precise actions for which the choice of the chosen solution depends on clearly identified and measurable parameters. As the possibility of achieving this level of autonomy is often evoked in the literature, we did not find any already functional application cases for more complex decisions for which the interdependencies between data and variables are either unknown or uncertain or when the data, constraints, objectives or knowledge are non-explicit.

The distribution of application cases across the different types of autonomy is now very unbalanced. The dominant weight of Cyber monitoring marks the fact that the priority today is to enhance the detection of problems and opportunities to start the decision-making process as early as possible. It also marks the potential for further progress in deploying new technologies to enhance the entire decision-making process. The mass of data that many companies are currently building up through the implementation of Cyber monitoring is a capital that is still poorly valued. It seems to us that this will inevitably call for an extension of the digitization approaches already undertaken to aim for types of autonomy that would cover a greater part of the steps in the decision-making process. However, the complexity of implementing certain types of autonomy, the associated risks, particularly in terms of cybersecurity, the related costs, a sometimes low ROI, the repercussions at the managerial and social levels, and the consideration of environmental issues are all reasons that may not necessarily justify enhancing all steps of the decision-making process.

Therefore, we can expect to gradually migrate towards a more balanced distribution of the application cases over the different types of autonomy in the years to come, without necessarily converging towards types of autonomy such as Cyber control or Cyber autonomy.

Table 1 Distribution of the use cases on the different types of autonomy

| | 1. Cyber monitoring | 2. Cyber Search | 3. Standard Decision Support | 4. Cyber Control | 5. Cyber Design | 6. Customized Decision Support | 7. Cyber Autonomy |
|---|---------------------|-----------------|------------------------------|------------------|-----------------|--------------------------------|-------------------|
| Soic R., Vukovic M., Skocir P., Jezic G. (2020) [37] | X | | | | | | |
| Aliev K., Antonelli D., Awouda A., Chiabert P. (2019) [38] | X | | | | | | |
| Antón S.D., Schotten H.D. (2019) [39] | X | | | | | | |
| Bakakeu J., Brossog M., Zeitler J., Franke J., Tolksdorf S., Klos H., Peschke J. (2019) [40] | X | | | | | | X |
| Burow K., Franke M., Thoben K.-D. (2019) [41] | X | | | | | | |
| Chiacchio F., D'Urso D., Compagno L., Chiarenza M., Velardita L. (2019) [42] | X | | | | | | |
| Conzon D., Rashid M.R.A., Tao X., Soriano A., Nicholson R., Ferrera E. (2019) [43] | | | | | | | X |
| Giehl A., Schneider P., Busch M., Schnoes F., Kleinwort R., Zaeh M.F. (2019) [44] | X | | | | | | |
| Loske M., Rothe L., Gertler D.G. (2019) [45] | X | | | | | | |
| Miehle D., Meyer M.M., Luckow A., Bruegge B., Essig M. (2019) [46] | | | | X | | | |
| Pusch A., Noël F. (2019) [47] | X | X | | | | | |
| Rabelo R.J., Zambiasi S.P., Romero D. (2019) [48] | X | X | | | | X | |
| Sala R., Pirola F., Dovero E., Cavalieri S. (2019) [49] | X | | | | | | |
| Subramanian D., Murali P., Zhou N., Ma X., Cesar Da Silva G., Pavuluri R., Kalagnanam J. (2019) [50] | | | | | | X | |
| Cagnin R.L., Guilherme I.R., Queiroz J., Paulo B., Neto M.F.O. (2018) [51] | | | | X | | | |
| Freitag M., Wiesner S. (2018) [52] | X | | | | | | |
| Luetkehoff B., Blum M., Schroeter M. (2018) [53] | X | | | | | | |
| Mittal S., Romero D., Wuest T. (2018) [54] | X | | | | | | |
| Molka-Danielsen J., Engelseth P., Wang H. (2018) [55] | X | | | | | | |
| Monizza G. P., Rojas R.A., Rauch E., Garcia M.A.R., Matt D.T. (2018) [56] | | | | | | | X |
| Nesi P., Pantaleo G., Paolucci M., Zaza I. (2018) [57] | X | | | | | | |
| Roda I., Macchi M., Fumagalli L. (2018) [58] | X | | | | | | |
| Serrano D. C., Chavarría-Barrientos D., Ortega A., Falcón B., Mitre L., Correa R., Moreno J., Funes R., Gutiérrez A. M. (2018) [59] | X | | | | | | |
| Badarinath R., Prabhu V.V. (2017) [60] | X | | | X | | | |
| Dragičević N., Ullrich A., Tsui E., Gronau N. (2017) [61] | X | | | X | | | |
| Durão L.F.C.S., Haag S., Anderl R., Schützer K., Zancul E. (2017) [62] | X | | | | | | |
| Innerbichler J., Gonul S., Damjanovic-Behrendt V., Mandler B., Strohmeier F. (2017) [63] | X | | | | | | |
| Lall M., Torvatn H., Seim E.A. (2017) [64] | X | | | | | | |
| Saldivar A.A.F., Goh C., Li Y., Yu H., Chen Y. (2017) [65] | X | | | | | | |
| Sandor H., Genge B., Haller P., Graur F. (2017) [66] | X | | | | | | |
| Tedeschi S., Emmanouilidis C., Farnsworth M., Mehnen J., Roy R. (2017) [67] | X | | | | | | |
| Adeyeri M.K., Mpofu K., Adenuga Olukorede T. (2015) [68] | X | X | | X | | | X |
| | 27 | 3 | 0 | 5 | 0 | 2 | 4 |

5. Conclusion and future developments

A model of seven types of autonomy associated with the decision-making process in an operational context and based on Industry 4.0 technologies for manufacturing systems was proposed. The model contributes to the current literature on Industry 4.0 by clearly demonstrating how 4.0 technologies can enhance decision-making processes and how they affect the autonomy of the resources involved at an operational level.

From a practical point of view, this model can help industrial establish a structured and coherent roadmap for the deployment of Industry 4.0 technologies. Decision-makers can rely on this model to target the type of autonomy they wish to see entrusted to operational teams to improve the production system's responsiveness to the problems and opportunities encountered in the field. This implies drawing up an initial list of critical decisions that the operational teams must or should manage and the main obstacles and errors usually encountered.

It should be noted that the proposed model is not adapted to respond to large-scale and complex unexpected disruptions such as health or financial crisis. Indeed, such cases involve a set of decisions taken at different strategic, tactical, and operational levels, whereas the proposed model is limited to an operational scope. However, the coupling of this model with other types of models such as DMN (Decision Model and Notation) models could constitute an answer to this type of situation. In this respect, it seems that this could constitute a new and particularly promising research axis in the future.

In the next step of this research, we will study the contribution of Industry 4.0 technologies to the implementation of these different types of autonomy through the enhancement of the various steps of the decision-making process. It is important to note that the proposed model was developed as part of a larger study to investigate the integration of Industry 4.0 technologies into Lean production systems. In this regard, an earlier study on the linkages between Industry 4.0 and Lean approaches showed that some Lean principles currently appear to show little or no improvement by Industry 4.0 technologies. This is particularly the case for Lean principles related to employees and teamwork, continuous improvement, stable and standardized processes, and the Toyota model philosophy [5]. Among future research, a practical case is being formalized to test the proposed model of autonomy types and to study the conditions of acceptance of Industry 4.0 technologies that contribute to reinforcing the decision-making process. It is based on a learning factory and uses existing Lean management training modules designed in partnership with several manufacturers. Various Industry 4.0 technologies such as IoT, cloud computing, Big data analysis, machine learning, simulation, augmented reality, and data visualization will be progressively deployed. Within this framework, the different types of empowerments of operational teams in decision-making will be tested to manage the production problems encountered in real-time. This will constitute the next step in validating our model before implementing it in a real production unit.

Among other issues that must be addressed within the proposed approach, the impact of change resistance toward Industry 4.0 technologies needs further study. As stated by Klein [69], decision support systems are generally not well received by those who are supposed to use them, as they are not necessarily aware of certain cognitive biases or do not perceive any real interest in being assisted. Anchoring these technologies' deployment within continuous improvement approaches and training teams in people-centered use of these new technologies is essential. This implies a more detailed analysis of the physical, sensing, cognitive, and collaborative capabilities that Industry 4.0 technologies can reinforce at the operational level to compare them with the needs that can be perceived or expressed by operators 4.0 and team 4.0.

References

- [1] Porter, M.E., Heppelmann, J.E. (2015). How smart, connected products are transforming companies, *Harvard Business Review*, Vol. 93, No. 10, 96-114.
- [2] Moeuf, A., Pellerin, R., Lamouri, S., Tamayo-Giraldo, S., Barbaray, R. (2017). The industrial management of SMEs in the era of Industry 4.0, *International Journal of Production Research*, Vol 56, No. 3, 1118-1136, doi: [10.1080/00207543.2017.1372647](https://doi.org/10.1080/00207543.2017.1372647).
- [3] Pacchini, A.P.T., Lucato, W.C., Facchini, F., Mummolo, G. (2019). The degree of readiness for the implementation of Industry 4.0, *Computers in Industry*, Vol. 113, Article No 103125, doi: [10.1016/j.compind.2019.103125](https://doi.org/10.1016/j.compind.2019.103125).
- [4] Buer, S.-V., Strandhagen, J.O., Chan, F.T.S. (2018). The link between Industry 4.0 and lean manufacturing: Mapping current research and establishing a research agenda, *International Journal of Production Research*, Vol. 56, No. 8, 2924-2940, doi: [10.1080/00207543.2018.1442945](https://doi.org/10.1080/00207543.2018.1442945).
- [5] Rosin, F., Forget, P., Lamouri, S., Pellerin, R. (2019). Impacts of Industry 4.0 technologies on lean principles, *International Journal of Production Research*, Vol. 58, No. 6, 1644-1661, doi: [10.1080/00207543.2019.1672902](https://doi.org/10.1080/00207543.2019.1672902).
- [6] Liker, J.K. (2004). *The Toyota way: 14 management principles from the world's greatest manufacturer*, McGraw-Hill Education, New York, USA.

- [7] Sari, T., Güleş, H.K., Yiğitöl, B. (2020). Awareness and readiness of Industry 4.0: The case of Turkish manufacturing industry, *Advances in Production Engineering & Management*, Vol. 15, No. 1, 57-68, doi: [10.14743/apem2020.1.349](https://doi.org/10.14743/apem2020.1.349).
- [8] Medić, N., Anišić, Z., Lalić, B., Marjanović, U., Brezocnik, M. (2019). Hybrid fuzzy multi-attribute decision-making model for evaluation of advanced digital technologies in manufacturing: Industry 4.0 perspective, *Advances in Production Engineering & Management*, Vol. 14, No. 4, 483-493, doi: [10.14743/apem2019.4.343](https://doi.org/10.14743/apem2019.4.343).
- [9] Boston Consulting Group (2015). Industry 4.0: The future of productivity and growth in manufacturing industries, from https://image-src.bcg.com/Images/Industry_40_Future_of_Productivity_April_2015_tcm9-61694.pdf, accessed December 7, 2021.
- [10] CEFRIO (2016). Prendre part à la révolution manufacturière? Du rattrapage technologique à l'Industrie 4.0 chez les PME, from <https://espace2.etsmtl.ca/id/eprint/14578/1/Prendre-part-%C3%A0-la-r%C3%A9volution-manufacturi%C3%A8re-Du-rattrapage-technologique-%C3%A0-l%E2%80%99Industrie-4.0-chez-les-PME.pdf>, accessed December 7, 2021.
- [11] Mayr, A., Weigelt, M., Kühl, A., Grimm, S., Erll, A., Potzel, M., Franke, J. (2018). Lean 4.0 – A conceptual conjunction of lean management and Industry 4.0, *Procedia CIRP*, Vol. 72, 622-628, doi: [10.1016/j.procir.2018.03.292](https://doi.org/10.1016/j.procir.2018.03.292).
- [12] Sanders, A., Elangeswaran, C., Wulfsberg, J. (2016). Industry 4.0 implies lean manufacturing: Research activities in Industry 4.0 function as enablers for lean manufacturing, *Journal of Industrial Engineering and Management*, Vol. 9, No. 3, 811-833, doi: [10.3926/jiem.1940](https://doi.org/10.3926/jiem.1940).
- [13] Wagner, T., Herrmann, C., Thiede, S. (2017). Industry 4.0 impacts on lean production systems, *Procedia CIRP*, Vol. 63, 125-131, doi: [10.1016/j.procir.2017.02.041](https://doi.org/10.1016/j.procir.2017.02.041).
- [14] Lu, Y., Morris, K.C., Frechette, S. (2016). Current standards landscape for smart manufacturing systems, *National Institute of Standards and Technology, NISTIR*, Vol. 8107, 39, doi: [10.6028/NIST.IR.8107](https://doi.org/10.6028/NIST.IR.8107).
- [15] Jardim-Goncalves, R., Romero, D., Grilo, A. (2017). Factories of the future: Challenges and leading innovations in intelligent manufacturing, *International Journal of Computer Integrated Manufacturing*, Vol. 30, No. 1, 4-14.
- [16] Zhou, J., Li, P., Zhou, Y., Wang, B., Zang, J., Meng, L. (2018). Toward new-generation intelligent manufacturing, *Engineering*, Vol. 4, No. 1, 11-20, doi: [10.1016/j.eng.2018.01.002](https://doi.org/10.1016/j.eng.2018.01.002).
- [17] Osterrieder, P., Budde, L., Friedli, T. (2019). The smart factory as a key construct of Industry 4.0: A systematic literature review, *International Journal of Production Economics*, Vol. 221, Article No. 107476, doi: [10.1016/j.ijpe.2019.08.011](https://doi.org/10.1016/j.ijpe.2019.08.011).
- [18] Klein, G.A., Orasanu, J., Calderwood, R., Zsombok, C.E. (1993). *Decision making in action: Models and methods*, Ablex Publishing Corporation, Norwood, USA.
- [19] Mintzberg, H., Raisinghani, D., Théorêt, A. (1976). The structure of “unstructured” decision processes, *Administrative Science Quarterly*, Vol 21, No. 2, 246-275, doi: [10.2307/2392045](https://doi.org/10.2307/2392045).
- [20] Cannon-Bowers, J.A., Salas, E. (1998). *Making decisions under stress: Implications for individual and team training*, American Psychological Association, Washington, USA, doi: [10.1037/10278-000](https://doi.org/10.1037/10278-000).
- [21] Hammond, K.R., Hamm, R.M., Grassia, J., Pearson, T. (1987). Direct comparison of the efficacy of intuitive and analytical cognition in expert judgment, *IEEE Transactions on Systems, Man, and Cybernetics*, Vol. 17, No. 5, 753-770, doi: [10.1109/TSMC.1987.6499282](https://doi.org/10.1109/TSMC.1987.6499282).
- [22] Kahneman, D., Klein, G. (2009). Conditions for intuitive expertise: A failure to disagree, *American Psychologist*, Vol. 64, No. 6, 515-526, doi: [10.1037/a0016755](https://doi.org/10.1037/a0016755).
- [23] Gigerenzer, G., Gaissmaier, W. (2011). Heuristic decision making, *Annual Review of Psychology*, Vol. 62, 451-482, doi: [10.1146/annurev-psych-120709-145346](https://doi.org/10.1146/annurev-psych-120709-145346).
- [24] Simon, H.A. (1960). *The new science of management decision*, Harper & Brothers, New York, USA, doi: [10.1037/13978-000](https://doi.org/10.1037/13978-000).
- [25] Klein, G. (2008). Naturalistic decision making, *Human Factors: The Journal of the Human Factors and Ergonomics Society*, Vol. 50, No. 3, 456-460, doi: [10.1518/001872008X288385](https://doi.org/10.1518/001872008X288385).
- [26] Power, D.J., Cyphert, D., Roth, R.M. (2019). Analytics, bias, and evidence: The quest for rational decision-making, *Journal of Decision Systems*, Vol. 28, No. 2, 120-137, doi: [10.1080/12460125.2019.1623534](https://doi.org/10.1080/12460125.2019.1623534).
- [27] Okoli, J., Watt, J. (2018). Crisis decision-making: The overlap between intuitive and analytical strategies, *Management Decision*, Vol. 56, No. 5, 1122-1134, doi: [10.1108/MD-04-2017-0333](https://doi.org/10.1108/MD-04-2017-0333).
- [28] Schraagen, J.M. (2018). Naturalistic decision-making, In: Ball, L.J., Thompson, V.A. (eds.), *The Routledge international handbook of thinking and reasoning*, Routledge/Taylor & Francis Group, New York, USA, 487-501.
- [29] Orasanu, J., Connolly, T. (1993). The reinvention of decision-making, In: Klein, G.A., Orasanu, J., Calderwood, R., Zsombok, C.E. (eds.), *Decision making in action: Models and methods*, Ablex Publishing Corporation, Norwood, USA, 3-20.
- [30] Rasmussen, J., Goodstein, L.P. (1987). Decision support in supervisory control of high-risk industrial systems, *Automatica*, Vol. 23, No. 5, 663-671, doi: [10.1016/0005-1098\(87\)90064-1](https://doi.org/10.1016/0005-1098(87)90064-1).
- [31] Naikar, N. (2010). A comparison of the decision ladder template and the recognition-primed decision model, Defence science and technology organization, Australian Government, Department of Defence, Victoria, Australia.
- [32] Rao, A.S., Georgeff, M.P. (1995). BDI agents: From theory to practice, In: *Proceedings of the First International Conference on Multiagent Systems, ICMAS 1995*, California, USA, 312-319.
- [33] Kinny, D., Georgeff, M., Rao, A. (1996). A methodology and modelling technique for systems of BDI agents, In: Van de Velde, W., Perram, J.W. (eds.), *Agents breaking away. MAAMAW 1996, Lecture notes in computer science (Lecture notes in artificial intelligence)*, Vol. 1038, Springer, Berlin, Heidelberg, 56-71, doi: [10.1007/BFb0031846](https://doi.org/10.1007/BFb0031846).
- [34] Object Management Group. Decision Model and Notation, from <https://www.omg.org/spec/DMN>, accessed December 7, 2021.

- [35] Chakraborty, P.S., Sarkar, B., Majumdar, G. (2013). Group decision making for a manufacturing organization considering intensity of preference, *Advances in Production Engineering & Management*, Vol. 8, No. 3, 149-156, [doi: 10.14743/apem2013.3.162](https://doi.org/10.14743/apem2013.3.162).
- [36] Hasić, F., Corea, C., Blatt, J., Delfmann, P., Serral, E. (2020). Decision model change patterns for dynamic system evolution, *Knowledge and Information Systems*, Vol. 62, No. 9, 3665-3696, [doi: 10.1007/s10115-020-01469-w](https://doi.org/10.1007/s10115-020-01469-w).
- [37] Soic, R., Vukovic, M., Skocir, P., Jezic, G. (2020). Context-aware service orchestration in smart environments, In: Jezic, G., Chen-Burger, Y.H., Kusek, M., Šperka, R., Howlett, R., Jain, L. (eds.), *Agents and multi-agent systems: Technologies and applications 2019. Smart innovation, systems and technologies*, Vol 148. Springer, Singapore, [doi: 10.1007/978-981-13-8679-4_3](https://doi.org/10.1007/978-981-13-8679-4_3).
- [38] Aliev, K., Antonelli, D., Awouda, A., Chiabert, P. (2019). Key performance indicators integrating collaborative and mobile robots in the factory networks, In: Camarinha-Matos, L., Afsarmanesh, H., Antonelli, D. (eds.), *Collaborative networks and digital transformation. PRO-VE 2019. IFIP advances in information and communication technology*, Vol. 568, Springer, Cham, Switzerland, 635-642, [doi: 10.1007/978-3-030-28464-0_56](https://doi.org/10.1007/978-3-030-28464-0_56).
- [39] Antón, S.D.D., Schotten, H.D. (2019). Putting together the pieces: A concept for holistic industrial intrusion detection, *Computer Science, Cryptography and Security*, Cornell University, <https://arxiv.org/abs/1905.11701v1>.
- [40] Bakakeu, J., Brossog, M., Zeitler, J., Franke, J., Tolksdorf, S., Klos, H., Peschke, J. (2019). Automated reasoning and knowledge inference on OPC UA information models, In: *Proceedings of 2019 IEEE International Conference on Industrial Cyber Physical Systems (ICPS)*, Taipei, Taiwan, 53-60, [doi: 10.1109/ICPHYS.2019.8780114](https://doi.org/10.1109/ICPHYS.2019.8780114).
- [41] Burow, K., Franke, M., Thoben, K.D. (2019). 5G-ready in the industrial IoT-environment, In: Ameri, F., Stecke, K., von Cieminski, G., Kiritsis, D. (eds.), *Advances in production management systems. Production management for the factory of the future. APMS 2019. IFIP advances in information and communication technology*, Vol. 566, Springer, Cham, Switzerland, 408-413, [doi: 10.1007/978-3-030-30000-5_51](https://doi.org/10.1007/978-3-030-30000-5_51).
- [42] Chiacchio, F., D'urso, D., Compagno, L., Chiarenza, M., Velardita, L. (2019). Towards a blockchain based traceability process: A case study from pharma industry, In: Ameri, F., Stecke, K., von Cieminski, G., Kiritsis, D. (eds.), *Advances in production management systems. Production management for the factory of the future. APMS 2019. IFIP advances in information and communication technology*, Vol. 566, Springer, Cham, Switzerland, 451-457, [doi: 10.1007/978-3-030-30000-5_56](https://doi.org/10.1007/978-3-030-30000-5_56).
- [43] Conzon, D., Rashid, M.R.A., Tao, X., Soriano, A., Nicholson, R., Ferrera, E. (2019). BRAIN-IoT: Model-based framework for dependable sensing and actuation in intelligent decentralized IoT systems, In: *Proceedings of 2019 4th International Conference on Computing, Communications and Security (ICCS)*, Rome, Italy, 1-8, [doi: 10.1109/ICCS.2019.8888136](https://doi.org/10.1109/ICCS.2019.8888136).
- [44] Giehl, A., Schneider, P., Busch, M., Schnoes, F., Kleinwort, R., Zaeh, M.F. (2019). Edge-computing enhanced privacy protection for industrial ecosystems in the context of SMEs, In: *Proceedings of 2019 12th CMI Conference on Cybersecurity and Privacy (CMI)*, Copenhagen, Denmark, 1-6, [doi: 10.1109/CMI48017.2019.8962138](https://doi.org/10.1109/CMI48017.2019.8962138).
- [45] Loske, M., Rothe, L., Gertler, D.G. (2019). Context-aware authentication: State-of-the-art evaluation and adaption to the IIoT, In: *Proceedings of 2019 5th World Forum on Internet of Things (WF-IoT)*, Limerick, Ireland, 64-69, [doi: 10.1109/WF-IoT.2019.8767327](https://doi.org/10.1109/WF-IoT.2019.8767327).
- [46] Miehle, D., Meyer, M.M., Luckow, A., Bruegge, B., Essig, M. (2019). Toward a decentralized marketplace for self-maintaining machines, In: *Proceedings of 2019 IEEE International Conference on Blockchain (Blockchain)*, Atlanta, USA, 431-438, [doi: 10.1109/Blockchain.2019.00066](https://doi.org/10.1109/Blockchain.2019.00066).
- [47] Pusch, A., Noël, F. (2019). Augmented reality for operator training on industrial workplaces – Comparing the Microsoft hololens vs. small and big screen tactile devices, In: Fortin, C., Rivest, L., Bernard, A., Bouras, A. (eds.), *Product lifecycle management in the digital twin era. PLM 2019. IFIP advances in information and communication technology*, Vol. 565. Springer, Cham, Switzerland, 3-13, [doi: 10.1007/978-3-030-42250-9_1](https://doi.org/10.1007/978-3-030-42250-9_1).
- [48] Rabelo, R.J., Zambiasi, S.P., Romero, D. (2019). Collaborative softbots: Enhancing operational excellence in systems of cyber-physical systems, In: Camarinha-Matos, L., Afsarmanesh, H., Antonelli, D. (eds.), *Collaborative networks and digital transformation. PRO-VE 2019. IFIP advances in information and communication technology*, Vol. 568, Springer, Cham, Switzerland, 55-68, [doi: 10.1007/978-3-030-28464-0_6](https://doi.org/10.1007/978-3-030-28464-0_6).
- [49] Sala, R., Pirola, F., Dovere, E., Cavalieri, S. (2019). A dual perspective workflow to improve data collection for maintenance delivery: An industrial case study, In: Ameri, F., Stecke, K., von Cieminski, G., Kiritsis, D. (eds.), *Advances in production management systems. Production management for the factory of the future. APMS 2019. IFIP advances in information and communication technology*, Vol. 566, Springer, Cham, Switzerland, 485-492, [doi: 10.1007/978-3-030-30000-5_60](https://doi.org/10.1007/978-3-030-30000-5_60).
- [50] Subramanian, D., Murali, P., Zhou, N., Ma, X., Da Silva, G.C., Pavuluri, R., Kalagnanam, J. (2019). A prediction-optimization framework for site-wide process optimization, In: *Proceedings of 2019 IEEE International Congress on Internet of Things (ICIOT)*, Milan, Italy, 125-132, [doi: 10.1109/ICIOT.2019.00031](https://doi.org/10.1109/ICIOT.2019.00031).
- [51] Cagnin, R.L., Guilherme, I.R., Queiroz, J., Paulo, B., Neto, M.F.O. (2018). A multi-agent system approach for management of industrial IoT devices in manufacturing processes, In: *Proceedings of 2018 IEEE 16th International Conference on Industrial Informatics (INDIN)*, Porto, Portugal, 31-36, [doi: 10.1109/INDIN.2018.8471926](https://doi.org/10.1109/INDIN.2018.8471926).
- [52] Freitag, M., Wiesner, S. (2018). Smart service lifecycle management: A framework and use case, In: Moon, I., Lee, G., Park, J., Kiritsis, D., von Cieminski, G. (eds.), *Advances in production management systems. Smart manufacturing for Industry 4.0. APMS 2018. IFIP advances in information and communication technology*, Vol. 536, Springer, Cham, Switzerland, 97-104, [doi: 10.1007/978-3-319-99707-0_13](https://doi.org/10.1007/978-3-319-99707-0_13).
- [53] Luetkehoff, B., Blum, M., Schroeter, M. (2018). Development of a collaborative platform for closed loop production control, In: Camarinha-Matos, L., Afsarmanesh, H., Rezgui, Y. (eds.), *Collaborative networks of cognitive systems*.

- PRO-VE 2018. IFIP advances in information and communication technology*, Vol. 534, Springer, Cham, Switzerland, 278-285, doi: [10.1007/978-3-319-99127-6_24](https://doi.org/10.1007/978-3-319-99127-6_24).
- [54] Mittal, S., Romero, D., Wuest, T. (2018). Towards a smart manufacturing toolkit for SMEs, In: Chiabert, P., Bouras, A., Noël, F., Ríos, J. (eds.), *Product lifecycle management to support Industry 4.0. PLM 2018. IFIP advances in information and communication technology*, Vol. 540, Springer, Cham, Switzerland, 476-487, doi: [10.1007/978-3-030-01614-2_44](https://doi.org/10.1007/978-3-030-01614-2_44).
- [55] Molka-Danielsen, J., Engelseth, P., Wang, H. (2018). Large scale integration of wireless sensor network technologies for air quality monitoring at a logistics shipping base, *Journal of Industrial Information Integration*, Vol. 10, 20-28, doi: [10.1016/j.jii.2018.02.001](https://doi.org/10.1016/j.jii.2018.02.001).
- [56] Pasetti Monizza, G., Rojas, R.A., Rauch, E., Garcia, M.A.R., Matt, D.T. (2018). A case study in learning factories for real-time reconfiguration of assembly systems through computational design and cyber-physical systems, In: Chiabert, P., Bouras, A., Noël, F., Ríos, J. (eds.), *Product lifecycle management to support Industry 4.0. PLM 2018. IFIP advances in information and communication technology*, Vol. 540, Springer, Cham, Switzerland, 227-237, doi: [10.1007/978-3-030-01614-2_21](https://doi.org/10.1007/978-3-030-01614-2_21).
- [57] Nesi, P., Pantaleo, G., Paolucci, M., Zaza, I. (2018). Auditing and assessment of data traffic flows in an IoT architecture, In: *Proceedings of 2018 IEEE 4th International Conference on Collaboration and Internet Computing (CIC)*, Philadelphia, USA, 388-391, doi: [10.1109/CIC.2018.00058](https://doi.org/10.1109/CIC.2018.00058).
- [58] Roda, I., Macchi, M., Fumagalli, L. (2018). The future of maintenance within Industry 4.0: An empirical research in manufacturing, In: Moon, I., Lee, G., Park, J., Kiritsis, D., von Cieminski, G. (eds.), *Advances in production management systems. Smart manufacturing for Industry 4.0. APMS 2018. IFIP advances in information and communication technology*, Vol. 536, Springer, Cham, Switzerland, 39-46, doi: [10.1007/978-3-319-99707-0_6](https://doi.org/10.1007/978-3-319-99707-0_6).
- [59] Cortés Serrano, D., Chavarría-Barrientos, D., Ortega, A., Falcón, B., Mitre, L., Correa, R., Moreno, J., Funes, R., Molina Gutiérrez, A. (2018). A framework to support Industry 4.0: Chemical company case study, In: Camarinha-Matos, L., Afsarmanesh, H., Rezgui, Y. (eds.), *Collaborative networks of cognitive systems. PRO-VE 2018. IFIP advances in information and communication technology*, Vol. 534, Springer, Cham, Switzerland, 387-395, doi: [10.1007/978-3-319-99127-6_33](https://doi.org/10.1007/978-3-319-99127-6_33).
- [60] Badarinath, R., Prabhu, V.V. (2017). Advances in internet of things (IoT) in manufacturing, In: Lödding, H., Riedel, R., Thoben, K.D., von Cieminski, G., Kiritsis, D. (eds.), *Advances in production management systems. The path to intelligent, collaborative and sustainable manufacturing. APMS 2017. IFIP advances in information and communication technology*, Vol. 513, Springer, Cham, Switzerland, 111-118, doi: [10.1007/978-3-319-66923-6_13](https://doi.org/10.1007/978-3-319-66923-6_13).
- [61] Dragičević, N., Ullrich, A., Tsui, Y.H.E., Gronau, N. (2017). Modelling knowledge dynamics in Industry 4.0: A smart grid scenario, In: *Proceedings of the 18th European Conference on Knowledge Management, ECKM 2017*, Vol. 1, Academic Conferences Limited, Barcelona, Spain, 267-274.
- [62] Durão, L.F.C.S., Haag, S., Anderl, R., Schützer, K., Zancul, E. (2017). Development of a smart assembly data model, In: Ríos, J., Bernard, A., Bouras, A., Foufou, S. (eds.), *Product lifecycle management and the industry of the future. PLM 2017. IFIP advances in information and communication technology*, Vol. 517, Springer, Cham, Switzerland, 655-666, doi: [10.1007/978-3-319-72905-3_58](https://doi.org/10.1007/978-3-319-72905-3_58).
- [63] Innerbichler, J., Gonul, S., Damjanovic-Behrendt, V., Mandler, B., Strohmeier, F. (2017). NIMBLE collaborative platform: Microservice architectural approach to federated IoT, In: *Proceedings of 2017 Global Internet of Things Summit (GIoTS)*, Geneva, Switzerland, 1-6, doi: [10.1109/GIoTTS.2017.8016216](https://doi.org/10.1109/GIoTTS.2017.8016216).
- [64] Lall, M., Torvatn, H., Seim, E.A. (2017). Towards Industry 4.0: Increased need for situational awareness on the shop floor, In: Lödding, H., Riedel, R., Thoben, K.D., von Cieminski, G., Kiritsis, D. (eds.), *Advances in production management systems. The path to intelligent, collaborative and sustainable manufacturing. APMS 2017. IFIP advances in information and communication technology*, Vol. 513, Springer, Cham, Switzerland, 322-329, doi: [10.1007/978-3-319-66923-6_38](https://doi.org/10.1007/978-3-319-66923-6_38).
- [65] Saldívar, A.A.F., Goh, C., Li, Y., Yu, H., Chen, Y. (2016). Attribute identification and predictive customisation using fuzzy clustering and genetic search for Industry 4.0 environments, In: *Proceedings of 2016 10th International Conference on Software, Knowledge, Information Management & Applications (SKIMA)*, Chengdu, China, 79-86, doi: [10.1109/SKIMA.2016.7916201](https://doi.org/10.1109/SKIMA.2016.7916201).
- [66] Sandor, H., Genge, B., Haller, P., Graur, F. (2017). Software defined response and network reconfiguration for industrial control systems, In: Rice, M., Sheno, S. (eds.), *Critical infrastructure protection XI. ICCIP 2017. IFIP advances in information and communication technology*, Vol. 512, Springer, Cham, Switzerland, 157-173, doi: [10.1007/978-3-319-70395-4_9](https://doi.org/10.1007/978-3-319-70395-4_9).
- [67] Tedeschi, S., Emmanouilidis, C., Farnsworth, M., Mehnen, J., Roy, R. (2017). New threats for old manufacturing problems: Secure IoT-enabled monitoring of legacy production machinery, In: Lödding, H., Riedel, R., Thoben, K.D., von Cieminski, G., Kiritsis, D. (eds.), *Advances in production management systems. The path to intelligent, collaborative and sustainable manufacturing. APMS 2017. IFIP advances in information and communication technology*, Vol. 513, Springer, Cham, Switzerland, 391-398, doi: [10.1007/978-3-319-66923-6_46](https://doi.org/10.1007/978-3-319-66923-6_46).
- [68] Adeyeri, M.K., Mpofu, K., Adenuga Olukorede, T. (2015). Integration of agent technology into manufacturing enterprise: A review and platform for industry 4.0, In: *Proceedings of 2015 International Conference on Industrial Engineering and Operations Management (IEOM)*, Dubai, United Arab Emirates, 1-10, doi: [10.1109/IEOM.2015.7093910](https://doi.org/10.1109/IEOM.2015.7093910).
- [69] Klein, G.A. (2009). *Streetlights and shadows: Searching for the keys to adaptive decision making*, MIT Press, Cambridge, Massachusetts, USA, doi: [10.7551/mitpress/8369.001.0001](https://doi.org/10.7551/mitpress/8369.001.0001).

Calendar of events

- 6th International Conference on Manufacturing Technologies, January 22-24, 2022, Singapore.
- 11th International Conference on Operations Research and Enterprise Systems, February 3-5, 2022, Vienna, Austria.
- The 5th International Conference on Materials Engineering and Applications, February 12-14, 2022, Nha Trang, Vietnam.
- 9th International Engine Congress 2022, February 22-23, Baden-Baden, Germany, (hybrid event).
- 7th International Conference on Manufacturing, Material and Metallurgical Engineering, March 18-20, 2022, Osaka, Japan.
- The 10th IIAE International Conference on Industrial Application Engineering, March 26-30, 2022, Matsue, Japan (hybrid event).
- 50th SME North American Manufacturing Research Conference, June 27 to July 1, 2022, West Lafayette, USA.
- 16th International Conference on Micromachining Technology, October 17-18, 2022, Dubai, United Arab Emirates.

This page intentionally left blank.

Notes for contributors

General

Articles submitted to the *APEM journal* should be original and unpublished contributions and should not be under consideration for any other publication at the same time. Manuscript should be written in English. Responsibility for the contents of the paper rests upon the authors and not upon the editors or the publisher. The content from published paper in the *APEM journal* may be used under the terms of the Creative Commons Attribution 4.0 International Licence (CC BY 4.0). For most up-to-date information please see the APEM journal homepage apem-journal.org.

Submission of papers

A submission must include the corresponding author's complete name, affiliation, address, phone and fax numbers, and e-mail address. All papers for consideration by *Advances in Production Engineering & Management* should be submitted by e-mail to the journal Editor-in-Chief:

Miran Brezocnik, Editor-in-Chief
UNIVERSITY OF MARIBOR
Faculty of Mechanical Engineering
Chair of Production Engineering
Smetanova ulica 17, SI – 2000 Maribor
Slovenia, European Union
E-mail: editor@apem-journal.org

Manuscript preparation

Manuscript should be prepared in *Microsoft Word 2010* (or higher version) word processor. *Word .docx* format is required. Papers on A4 format, single-spaced, typed in one column, using body text font size of 11 pt, should not exceed 12 pages, including abstract, keywords, body text, figures, tables, acknowledgements (if any), references, and appendices (if any). The title of the paper, authors' names, affiliations and headings of the body text should be in *Calibri* font. Body text, figures and tables captions have to be written in *Cambria* font. Mathematical equations and expressions must be set in *Microsoft Word Equation Editor* and written in *Cambria Math* font. For detail instructions on manuscript preparation please see instruction for authors in the *APEM journal* homepage apem-journal.org.

The review process

Every manuscript submitted for possible publication in the *APEM journal* is first briefly reviewed by the editor for general suitability for the journal. Notification of successful submission is sent. After initial screening, and checking by a special plagiarism detection tool, the manuscript is passed on to at least two referees. A double-blind peer review process ensures the content's validity and relevance. Optionally, authors are invited to suggest up to three well-respected experts in the field discussed in the article who might act as reviewers. The review process can take up to eight weeks on average. Based on the comments of the referees, the editor will take a decision about the paper. The following decisions can be made: accepting the paper, reconsidering the paper after changes, or rejecting the paper. Accepted papers may not be offered elsewhere for publication. The editor may, in some circumstances, vary this process at his discretion.

Proofs

Proofs will be sent to the corresponding author and should be returned within 3 days of receipt. Corrections should be restricted to typesetting errors and minor changes.

Offprints

An e-offprint, i.e., a PDF version of the published article, will be sent by e-mail to the corresponding author. Additionally, one complete copy of the journal will be sent free of charge to the corresponding author of the published article.

APEM

journal

Advances in Production Engineering & Management

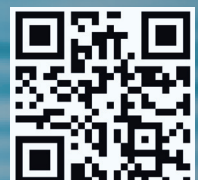
Chair of Production Engineering (CPE)
University of Maribor
APEM homepage: apem-journal.org

Volume 16 | Number 4 | December 2021 | pp 389-518

Contents

| | |
|---|-----|
| Scope and topics | 392 |
| A deep learning-based worker assistance system for error prevention: Case study in a real-world manual assembly Riedel, A.; Gerlach, J.; Dietsch, M.; Herbst, S.; Engelmann, F.; Brehm, N.; Pfeifroth, T. | 393 |
| Optimal path planning of a disinfection mobile robot against COVID-19 in a ROS-based research platform Banjanović-Mehmedović, L.; Karabegović, I.; Jahić, J.; Omerčić, M. | 405 |
| Using augmented reality devices for remote support in manufacturing: A case study and analysis Buń, P.; Grajewski, D.; Górski, F. | 418 |
| The impact of the collaborative workplace on the production system capacity: Simulation modelling vs. real-world application approach Ojstersek, R.; Javernik, A.; Buchmeister, B. | 431 |
| A multi-criteria decision-making in turning process using the MAIRCA, EAMR, MARCOS and TOPSIS methods: A comparative study Trung, D.D.; Thinh, H.X. | 443 |
| Molecular-dynamics study of multi-pulsed ultrafast laser interaction with copper Yin, C.P.; Zhang, S.T.; Dong, Y.W.; Ye, Q.W.; Li, Q. | 457 |
| A comparative study of different pull control strategies in multi-product manufacturing systems using discrete event simulation Xanthopoulos, A.S.; Koulouriotis, D.E. | 473 |
| Latent class analysis for identification of occupational accident casualty profiles in the selected Polish manufacturing sector Nowakowska, M.; Pajęcki, M. | 485 |
| Impact of Industry 4.0 on decision-making in an operational context Rosin, F.; Forget, P.; Lamouri, S.; Pellerin, R. | 500 |
| Calendar of events | 515 |
| Notes for contributors | 517 |

Published by CPE, University of Maribor



apem-journal.org